



**NTNU – Trondheim**  
Norwegian University of  
Science and Technology

# Development and Construction of Vehicle for Participation in the Shell Eco-marathon Competition

**Aslak Brage Espeland**  
**Håkon Johan Seiness**  
**Petter Thorrud Larsen**  
**Hans Gudvangen**

Product Design and Manufacturing  
Submission date: June 2012  
Supervisor: Knut Einar Aasland, IPM

Norwegian University of Science and Technology  
Department of Engineering Design and Materials



# PREFACE

This project would not have been possible without the help of our supervisors, sponsors, families and friends. The team would like to sincerely thank all of the student who have helped us during the project. We would specially like to thank:

Bjarne Stolpnæssæter, Knut Einar Aasland, Børge Holen, Iver Johnsen and Per Øystein Nordtug at the institute of product development and materials.

Eker Design and Paal Fediuk at High Performance Composites in Fredrikstad for helping us produce the monocoque. Gylling Teknikk for making a second battery pack on very short notice, just in time for the competition. SmartMotor for exceptional help with the motor controller. We would like to thank the rest of the team for all the good times and great experiences.

Finally we would like to thank our main sponsor Det Norske Veritas (DNV) and Kristina Dahlberg for their continued support of the NTNU Shell Eco-marathon team.

Trondhiem, June 2012



Aslak Brage Espeland



Hans Gudvangen



Håkon Johan Seiness



Petter Thorrud Larsen



# ABSTRACT

A team of 13 NTNU students have developed and built a car to compete in the Shell Eco-Marathon 2012 competition. This master project is a continuation of the specialization project done in the autumn semester 2011. Production started in February and the car was ready on the start line the 18th of May. Out of 22 competing teams in the battery-electric category, the DNVFuelfigher2 came in 5th place. The best result achieved was 163km/kWh which can be calculated into an equivalent of 1581km/liter of gasoline. This report includes the design and production process of all sub systems. In addition project management, system engineering, media and the race itself is described.

# SAMMENDRAG

Et team bestående av 13 NTNU-studenter har utviklet og bygget en bil for å konkurrere i studentkonkurransen Shell Eco-Marathon Europe 2012. Dette master prosjektet er en videreføring av fordypningsprosjekt gjennomført høstsemesteret 2011. Produksjonen startet i februar og bilen sto klar på startstreken 18. mai. Ut av 22 konkurrerende lag i batteriklassen, kom DNVFuelfigher2 på femte plass. Det beste resultatet ble 163km/kWh som kan omregnes til en ekvivalent på 1581km/liter bensin. Denne rapporten omfatter design og produksjonen av alle delsystemer. I tillegg er prosjektledelse, system engineering, media og selve løpet beskrevet.

NORGES TEKNISK-  
NATURVITENSKAPELIGE UNIVERSITET  
INSTITUTT FOR PRODUKTUTVIKLING  
OG MATERIALER

**MASTEROPPGAVE VÅR 2012**  
**FOR**  
**STUD.TECHN. PETTER T. LARSEN,**  
**HÅKON JOHAN SEINESS,**  
**ITXASO YUGUERO GARMENDIA,**  
**HANS GUDVANGEN OG**  
**ASLAK ESPELAND**

**UTVIKLING OG BYGGING AV BIL FOR DELTAKELSE I ECO-MARATHON-  
KONKURRANSEN**

**Development and construction of car for eco-marathon for participation in competition**

I høstsemesteret har prosjektgruppa gjort en spesifikasjon av en ny Eco-marathon-bil, basert på undersøkelse av fjorårets Eco-marathon-bil og de nye reglene og rammebetingelsene for 2012. De første fasene av et prosjekt fram mot en ny bil er dermed gjennomført. Nå skal de gjenstående fasene fram mot et kjøretøy som skal delta i Shell Eco-marathon i Nederland i mai 2012 gjennomføres. Et godt grunnlag er lagt, og masteroppgaven bygger på resultatene fra prosjektoppgaven.

Arbeidet i masteroppgaven foregår på fire nivå:

- Prosjektet i sin helhet inklusive offentlighetsarbeid, prosjektstyring og sponsorarbeid
- Selve bilen som et samspill av alle sine enkeltsystemer
- Enkeltsystemene med tilhørende interface
- Nødvendige eksterne tekniske og organisatoriske støttesystemer knyttet til bygging, testing og gjennomføring

Alt må selvsagt gjøres innenfor reglene som gjelder for Eco-marathon. Kandidaten må bidra på tvers av alle 4 nivå og samtidig ta et helhetlig ansvar for definerte deloppgaver som må defineres i prosjektplanen.

Arbeidet bedømmes både med hensyn til helheten og med hensyn til kandidatens deloppgaver. Bedømmelsen tar hensyn til både sluttresultatene og dokumentasjonen i utviklingsarbeidet. Dette aspektet er spesielt viktig med hensyn til fremtidig deltakelse i Eco-marathon. Det presiseres at det er kjempebra å "vinne", men det er hverken tilstrekkelig eller nødvendig for en god bedømmelse.

Leveransen fra prosjektet er i henhold til det fire nivå:

- Prosjektrapport inklusive informasjonsmateriell som er utviklet
- Selve bilen samt teknisk produktutviklingsrapport inklusive evaluering og forbedringsforslag
- Hvert enkeltsystem samt teknisk produktutviklingsrapport inklusive evaluering og forbedringsforslag
- Alle tekniske og organisatoriske støttesystemer samt utviklingsrapport inklusive evaluering og forbedringsforslag

Besvarelsen skal ha med signert oppgavetekst, og redigeres mest mulig som en forskningsrapport med et sammendrag på norsk og engelsk, konklusjon, litteraturliste, innholdsfortegnelse, etc. Ved utarbeidelse av teksten skal kandidaten legge vekt på å gjøre teksten oversiktlig og velskrevet. Med henblikk på lesning av besvarelsen er det viktig at de nødvendige henvisninger for korresponderende steder i tekst, tabeller og figurer anføres på begge steder. Ved bedømmelse legges det stor vekt på at resultater er grundig bearbeidet, at de oppstilles tabellarisk og/eller grafisk på en oversiktlig måte og diskuteres utførlig.

Som et vedlegg til rapporten skal det leveres en PU-journal. Denne skal være uredigert og inneholde alle de notater og idéer man har vært inne på undervegs i arbeidet. Fortrinnsvis skal den være i instituttets A3-format.

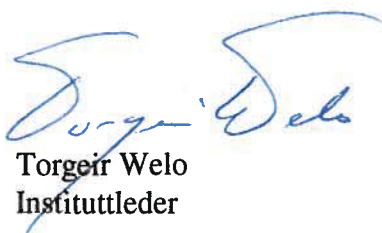
Senest 3 uker etter oppgavestart skal et A3 ark som illustrerer arbeidet leveres inn. En mal for dette arket finnes på instituttets hjemmeside under menyen undervisning. Arket skal også oppdateres ved innlevering av masteroppgaven.

Besvarelsen skal leveres i elektronisk format via DAIM, NTNUs system for Digital arkivering og innlevering av masteroppgaver.

Kontaktperson hos AS Norske Shell: Lillian Aasheim

Kontaktperson hos DNV: Kristina Dahlberg

Ressurspersoner ved NTNU/SINTEF: Nils Petter Vedvik, Terje Rølvåg, Detlef Blankenburg



Torgeir Welo  
Instituttleder



NTNU  
Norges teknisk-  
naturvitenskapelige universitet

Institutt for produktutvikling  
og materialer



Knut Aasland  
Faglærer

# TABLE OF CONTENTS

<b>1</b>	<b>INTRODUCTION</b>	<b>8</b>		
1.1	Shell Eco-marathon	10		
1.2	The Team	12		
<b>2</b>	<b>NON-TECHNICAL</b>	<b>14</b>		
<b>2.1</b>	<b>Project Management</b>	<b>16</b>		
<b>2.1.1</b>	<b>Planning</b>	<b>18</b>		
2.1.1.1	Individual Management Plans	19		
2.1.1.2	Creating WBS	22		
2.1.1.3	Scheduling Project	22		
2.1.1.4	Budgeting	27		
2.1.1.5	Risk Identification and Assessment	28		
2.1.1.6	Risk Identification and Assessment Challenges	30		
<b>2.2</b>	<b>Systems Engineering</b>	<b>32</b>		
<b>2.2.1</b>	<b>Knowledge Management</b>	<b>34</b>		
2.2.1.1	Capturing Knowledge with LEAN Techniques	36		
2.2.1.2	Storing and Sharing Knowledge with Model-Based SE	40		
<b>2.2.2</b>	<b>Visual Workflow Management</b>	<b>41</b>		
2.2.2.1	Stand-Up Meetings and Visual Project Board	41		
2.2.2.2	Visualizing Project Progress	42		
2.2.2.3	Average Risk Level as a Tool for Tracking Progress	42		
2.2.2.4	The Timeline	43		
2.2.2.5	Project Progress in a Micro-Level	44		
<b>2.2.3</b>	<b>Verification, Validation and Testing Activities of the DNVFF2</b>	<b>44</b>		
2.2.3.1	Unit Testing			
2.2.3.2	Assembly Testing	44		
2.2.3.3	Performance Test	46		
<b>2.3</b>	<b>Promotion</b>	<b>48</b>		
<b>2.4</b>	<b>Rotterdam</b>	<b>56</b>		
<b>2.4.1</b>	<b>Shell Eco-marathon</b>	<b>58</b>		
2.4.1.1	Track	58		
2.4.1.2	Technical Inspection	60		
2.4.1.3	Testing	64		
2.4.1.4	Race	65		
<b>3</b>	<b>TECHNICAL</b>	<b>66</b>		
<b>3.1</b>	<b>Exterior</b>	<b>68</b>		
<b>3.1.1</b>	<b>Introduction</b>	<b>70</b>		
<b>3.1.2</b>	<b>Strength Analysis</b>	<b>72</b>		
3.1.2.1	Boundary Conditions	72		
3.1.2.2	Layup	73		
3.1.2.3	Results	75		
3.1.2.4	Conclusion	76		
<b>3.1.3</b>	<b>Designing the Molds</b>	<b>78</b>		
<b>3.1.4</b>	<b>Production</b>	<b>80</b>		
3.1.4.1	Milling	80		
3.1.4.2	Layup	86		
3.1.4.3	Doors	92		
3.1.4.4	Firewall	92		
3.1.4.5	Wheel Well Covers	94		
<b>3.1.4</b>	<b>Assembly</b>	<b>96</b>		
3.1.4.1	Monocoque	96		
3.1.4.2	Wheel Well Covers	98		
3.1.4.3	Doors	102		
3.1.4.4	Surface Finish	104		
<b>3.1.5</b>	<b>Windows</b>	<b>106</b>		
3.1.5.1	Molds	108		
3.1.5.2	Vacuum Table	110		
3.2.5.3	Production	110		
3.1.5.4	Assembly	111		
<b>3.1.6</b>	<b>Lights</b>	<b>112</b>		
3.1.6.1	Former Lights	112		
3.1.6.2	Interfaces	113		
3.1.6.3	List of Requirements	113		
3.1.6.4	Materials and Technology	114		
3.1.6.5	Concept Development	115		
3.1.6.6	Final Concept	116		
3.1.6.7	Production	117		
<b>3.1.7</b>	<b>Details</b>	<b>118</b>		
3.1.7.1	Door Details	119		
3.1.7.2	Wiper	124		
3.1.7.3	Back Hatch Mounting	129		
3.1.7.4	Side Cover Mounting	130		
3.1.7.5	Towing Hook	132		
<b>3.1.8</b>	<b>Foil</b>	<b>134</b>		
3.1.8.1	Paint VS Foil	134		
3.1.8.2	Inspiration	135		
3.1.8.2	Production and Mounting	138		
<b>3.1.9</b>	<b>Wind Tunnel Testing</b>	<b>140</b>		
3.1.9.1	Wind Tunnel	141		
3.1.9.2	Experimental Setup	142		
3.1.9.3	Results	143		
3.1.9.4	Conclusion	144		
<b>3.2</b>	<b>Interior</b>	<b>146</b>		
<b>3.2.1</b>	<b>Introduction</b>	<b>148</b>		
<b>3.2.2</b>	<b>Dashboard</b>	<b>150</b>		
3.2.2.1	Last Cars Dashboard	150		
3.2.2.2	Interfaces	151		
3.2.2.3	Ergonomics	152		
3.2.2.4	Analysis of Functions	153		



3.2.2.5	List of Requirements	154	3.4.1.2	Tie Rod Mount	236
3.2.2.6	Cooperation with Other Students	155	3.4.1.3	Cable Mount	237
3.2.2.7	Concept Development	156	3.4.1.4	Additional Drag Link Parts	237
3.2.2.8	Final Concept	157	<b>3.4.2 Steering Column</b>		<b>237</b>
3.2.2.9	Placement of Buttons and Display	158	3.4.2.1	Analysis	238
<b>3.2.3 Steering Wheel</b>		<b>160</b>	<b>3.4.3 Pulleys and Kevlar Cable</b>		<b>238</b>
3.2.3.1	Last Cars Steering Wheel	160	<b>3.4.4 Assembly and Testing</b>		<b>240</b>
3.2.3.2	Necessary Functions	161	<b>3.4.5 Race and Conclusion</b>		<b>241</b>
3.2.3.3	Production Methods	162			
3.2.3.4	Inspiration	163	<b>3.5 Brakes</b>		<b>244</b>
3.2.3.5	List of Requirements	164	<b>3.5.1 Brake Pedal</b>		<b>247</b>
3.2.3.6	Idea Generation	166	3.5.1.1	Pedal Arm	247
3.2.3.7	Ergonomic Testing	166	3.5.1.2	Brake Pedal Box	249
3.2.3.8	Three Different Concepts	168	3.5.1.3	Master Cylinders	250
3.2.3.9	Production	172	<b>3.5.2 Other Brake Circuit Parts</b>		<b>250</b>
<b>3.2.4 Seat</b>		<b>174</b>	<b>3.5.3 Assembly and Testing</b>		<b>252</b>
3.2.4.1	Former Seat	174	<b>3.5.4 Race and Conclusion</b>		<b>253</b>
3.2.4.2	Inspiration	175			
3.2.4.3	Possible Materials	176	<b>3.6 Wheels</b>		<b>254</b>
3.2.4.4	Interfaces	177	<b>3.6.1 Strenght Analysis</b>		<b>256</b>
3.2.4.5	Basic Ergonomics	178	<b>3.6.2 Production</b>		<b>257</b>
3.2.4.6	List of Requirements	179	<b>3.6.3 Performance</b>		<b>259</b>
3.2.4.7	Idea Generation	180	<b>3.6.4 Further Recommendations</b>		<b>259</b>
3.2.4.8	Three Ideas	182			
3.2.4.9	Selecting Ideas	185	<b>3.7 Propulsion</b>		<b>260</b>
3.2.4.10	Detailing of the Final Concept	186	<b>3.7.1 Motor Design</b>		<b>262</b>
3.2.4.11	Production	187	3.7.1.1	Requirements	262
<b>3.2.5 Rear View Mirrors</b>		<b>188</b>	3.7.1.2	Concept Description	262
3.2.5.1	Mirrors on DNVFF	188	3.7.1.3	Hubs and Axle	262
3.2.5.2	Inspiration	189	3.7.1.4	Rotors	265
3.2.5.3	List of Requirements	190	3.7.1.5	Rim Adapter	265
3.2.5.3	Idea Generation	191	3.7.1.6	Test Rig and SM-Adapter	266
3.2.5.4	Different Concepts	192	<b>3.7.2 Motor Development</b>		<b>268</b>
3.2.5.5	Production and Finished Product	193	3.7.2.1	Rotor	268
			3.7.2.2	Stator Production	271
<b>3.3 Suspension</b>		<b>194</b>	3.7.2.3	Mold Production	271
<b>3.3.1 Front Suspension</b>		<b>196</b>	3.7.2.4	Open Casting	271
3.3.1.1	Hubs	204	3.7.2.5	Vacuum Casting	272
3.3.1.2	Axles	205	3.7.2.6	Spacer Ring	272
3.3.1.3	Steering Knuckles	206	3.7.2.7	Assembly of the Motor	273
3.3.1.4	Linkages	210	3.7.2.8	Problems Regarding the Construction	273
3.3.1.5	Mounting Points	214	3.7.2.9	Testing the Existing Motor	276
3.3.1.6	Conclusion	215	3.7.2.10	Conclusion	278
<b>3.3.2 Rear Suspension</b>		<b>216</b>			
3.3.2.1	Introduction	216	<b>2.8 Control System</b>		<b>280</b>
3.3.2.2	Knuckle	216	<b>2.8.1 Car Control System</b>		<b>282</b>
3.3.2.3	Lower A-arm Connector	222	2.8.1.1	Characteristics	282
3.3.2.4	Coilover	224	2.8.1.2	Changes to the Car Control System	282
3.3.2.5	Toe Link Extension	227	<b>2.8.2 Propulsional Control System</b>		<b>284</b>
3.3.2.6	Rods and Rod Ends	228	2.8.2.1	Characteristics	284
3.3.2.7	Assembly	228	2.8.2.2	Changes in the Car Control System	284
3.3.2.8	Further Recommendations	230			
			<b>4 CONCLUSION</b>		<b>286</b>
<b>3.4 Steering</b>		<b>232</b>			
<b>3.4.1 Drag Link</b>		<b>235</b>	<b>5 REFERENCES</b>		<b>290</b>
3.4.1.1	Length Adjustment	235			



**NORWEGIAN  
UNIVERSITY OF  
SCIENCE AND  
TECHNOLOGY**

TEAM NAME  
NTNU  
CAR MODEL  
DNV FUEL FIGHTER 2

RACE NUMBER

**724**

**1**

**IN**

WAAR KOMT EEN  
GEWELDIG IDEE VANDAAN?  
WHAT'S YOUR  
BEST IDEA?



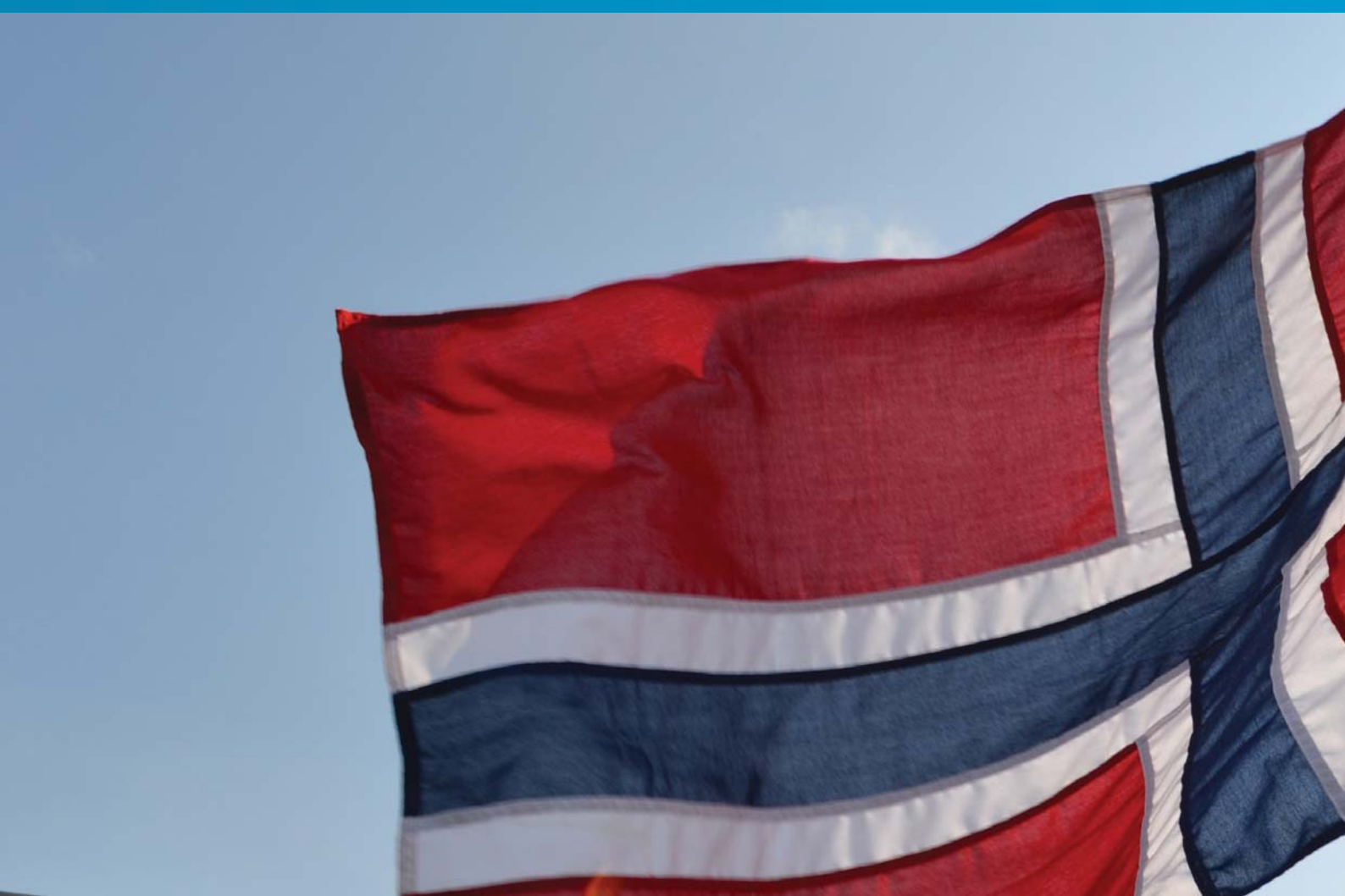
LEARN  
SHARE  
EXPERIENCE



- 1 REGISTRATION
- 2 THE Paddock
- 3 TECHNICAL INSPECTION
- 4 FAN ZONE
- 5 START-FINISH

# TRODUCTION

HERBYT? OIT



# 1.1 SHELL ECO-MARATHON

The Shell Eco-marathon (SEM) challenges high school and college student teams from around the world to design, build and test energy efficient vehicles. With annual events in the Americas, Europe and Asia, the winners are the teams that go the farthest distance using the least amount of energy.

The competition is divided into different vehicle and energy categories:

- **Prototype:** Vehicles in this category aim to build the most aerodynamic and fuel-efficient vehicle possible. The rules for this class impose few limitations and allows for very radical designs.
- **UrbanConcept:** The UrbanConcept category offers participants an opportunity to design and build fuel-economy vehicles that are close in appearance to today's passenger cars.

The vehicles may use one of the following fuel or energy types:

- Gasoline
- Diesel
- Biofuels
- Ethanol
- Natural gas
- Hydrogen
- Solar
- Battery

In 2012 the competition was held in an urban environment for the first time in Shell Eco-marathon Europe's history. This was a way of showcasing the exciting student innovations and futuristic vehicles on a more realistic stage.

Shell selected Rotterdam in the Netherlands to provide this urban stage given it is centrally located in Europe. Shell Eco-marathon Europe 2012 ran from 17-19 May on the Ahoy track in the middle of Rotterdam. The competition was a huge success with many spectators and great racing happening on track.



The story of NTNU's participation in the Shell Eco-marathon started in the fall of 2007. During the first 4 years NTNU participated with the DNV Fuel Fighter (DNVFF). This car used a hydrogen fuel cell as a energy source to power its electric motor. Many prizes and awards were achieved with this car, including two second prizes and a world record in its class.

The 2012 team decided to build a brand new vehicle to continue competing in the Urban concept class, but this time using plug-in battery technology. The new urban setting for the competition demanded a more robust car and a well made suspension system. Experiences gained throughout the years from the DNVFF meant that improvements could be made within every sub system.

DNV was willing to continue the role as main sponsor for 2012. The car was appropriately named the DNV Fuel Fighter 2 (DNVFF2) as a continuation of NTNU and DNV's cooperation in this project. Transnova, a Norwegian governmental organisation promoting environmentally friendly transportation, sponsored the team with additional fundings. Several other important sponsors helped make

the car a reality, supporting the team with materials, knowledge and production facilities. The team designed, built, assembled and tested the car in just 9 months, making it ready for the competition in May.

When the car arrived in Rotterdam it was immediately recognized as an eye catcher. Several teams, spectators and tv-crews wanted to have a look at the car. The team was very happy to see their hard work being appreciated by the crowd. Due to extensive testing in Trondheim the car only needed minor adjustments before it was fully ready for the race. A total of three long distance runs were completed; one test run and two race attempts (ny record for ntnu?). The best result achieved was 163 km/kWh in a near perfect run. The competition level in the battery class was very high and the team ended up in 5th place.



# 1.2 THE TEAM

The 2012 team consists of 13 master students from the Norwegian University of Science and Technology

*Fariborz A. Heidarloo*  
Industrial Engineering, Project Management, 2-year master  
Project manager

Benjamin Gutjahr  
Engineering Cybernetics, 5-year master  
Control system

*Fredrik V. Endresen*  
Energy and Environmental Engineering, 5-year  
Motor

*Aksel Qviller*  
Engineering Science & ICT, 5-year master  
Suspension

*Petter Thorrud Larsen*  
Mechanical Engineering, 2-year master  
Exterior

*Aslak Brage Espeland*  
Mechanical Engineering, 2-year master  
Exterior

*Mats Herding Solberg*  
Industrial design, 5-year master  
Design

*Silje Kristine Skogbrann*  
Media Communication and Information Technology, 5-year  
master  
PR and media



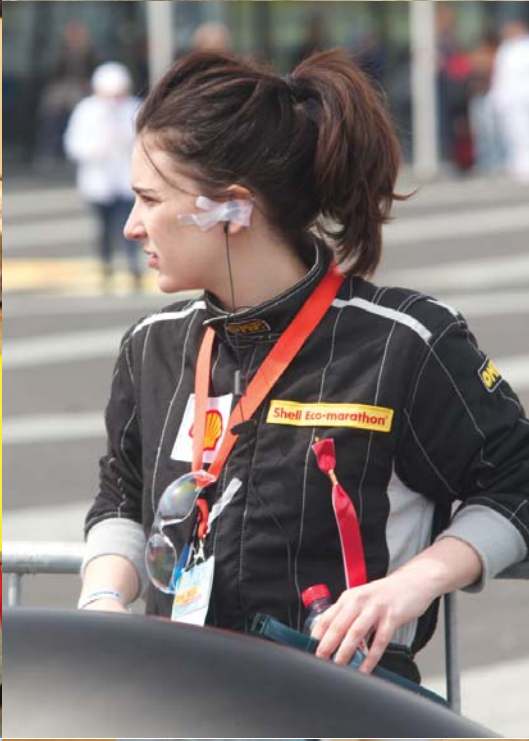
*Itsaso Yuguero Garmendia*  
Mechanical Engineering, 5-year master  
System engineering

*Hans Gudvangen*  
Mechanical Engineering, 2-year master  
Suspension & rims

*Oluf Tønning*  
Engineering Science & ICT, 5-year master  
System engineering

*Eivind Sæter*  
Industrial design, 5-year master  
Design

*Håkon Johan Seiness*  
Engineering Science & ICT, 5-year master  
Steering and Brakes





# SHELL ECO-MARATHON

Rotterdam 16. - 19. mai 2012

# SHELL ECO-MARATHON

Rotterdam 16. - 19. mai 2012



mai 2012



ON YOUR MARK.  
GET SET.  
LET'S GO.

# 2





**NON-  
TECHNICAL**

FUEL FIGHT  
QR CODES





# 2.1 PROJECT MANAGEMENT



## 2.1 PROJECT MANAGEMENT

Shell Eco-marathon 2012 was a New Product Development (NPD) project. One of the distinct characteristics of this type of projects is significant uncertainty. According to Tatikonda & Rosenthal (2000) technology novelty and project complexity are sources of uncertainty while a team tries to make new product that can be brand new or result of improvements on its precedent. Comparing to regular NPD projects, Shell Eco-marathon 2012 has unique feature which is not having marketing perspective. In high level, the goal of project is learning through executing a project and challenge students' knowledge in practical case. High level of uncertainty on the one hand and a project team that is formed by non professional members (students) on the other hand makes planning stage of the project very prominent. Therefore, the focus of project management chapter in this report is on planning Shell Eco-marathon project.

### 2.1.1 PLANNING

The planning stage comprises those course of actions executed to found the scope of the project, clarify the goals, and develop the processes needed to achieve those goals.

According to Verganti (1997) two planning styles may be utilized for new product development projects, feedback planning or reactive approach and feed-forward planning or proactive approach. Choosing how the project is going to be planned in early phase in order to save time and money is another challenge. By using reactive approach, project team does not spend significant time on solving uncertainties and gathering information for accomplishing tasks. This method which is based on the notion of uncertainty reduction during project advancement, doesn't need substantial financial resource and it is not



time consuming but it increases the risk of facing late changes during execution phase that puts sizeable financial burden on project. Unlike this, by following proactive approach, project team shall allocate considerable time to think about what may go wrong during project development and come up with solution for each opportunities or constraints. Performing this method is expensive as processing data and having experts for anticipating uncertain information need substantial financial support and the danger of losing track of time due to drowning into analyzing details. Project manager shall choose suitable technique for planning based on project characteristics. In Shell Eco-marathon 2012 project both feedback and feed forward approaches were used. During initiating phase Table 2.1.1 was prepared which illustrates the improvement points in developing new vehicle systems based on study performed on status of various systems of precedent car DNVFF.

This table helped project manager to know which type of planning approach is suitable for various parts or systems of the future vehicle. If the scope of change is not huge, then feedback

planning but if complete change is expected feed-forward planning was used.

For accomplishing this stage through Shell Eco-marathon 2012 project, following processes were carried out: developing individual management plans, creating work break down structure, scheduling project, budgeting and risk identification and management.

#### **2.1.1.1 Individual Management Plans**

Why previous leaders of NTNU's Shell Eco-marathon team were not totally successful for handling all project management knowledge areas? Why same level of management was not applied on various knowledge areas? The answer for these questions can be inferred from project reports of prior teams as following:

- Absence of management plans.
- Unsuccessful efforts to properly implement management plans during project lifecycle due to lack of experience.

Lack of experience is not an avoidable factor since team members including project manager

are chosen among master students who are not experts. According to available project reports, preceding team leaders preferred to decide upon the way of managing different processes right before their executing time. This approach caused various troubles for team leaders such as losing track of time, inefficient data distribution and communication. Avoiding similar difficulties, project manager needs to think about strategies to manage and control different knowledge areas (scope, time, cost, communication...) before starting with course of actions. Not only experience is an important factor to develop strategies (individual management plans), also stakeholders' opinion and comments, lessoned learned from preceding projects and university's policies are key factor to build a basis. Project manager shall not consider planning processes as one time task while request changes from stakeholders or project team, unexpected events and feedbacks from executing and monitoring stages make reviewing and revising plans repetitively critical. Precluding lack of enough time to proceed with other project's stages, it is important to spend sufficient time on planning processes. Therefore, based on importance of project and required level of management, project manager needs to think how detailed the initial plans should be. By taking progressive elaboration into account, making a comprehensive and perfect plan on inception steps which demands a lot of information is misleading point of view about planning project. Following individual plans were generated for Shell Eco-marathon 2012 project, after few modifications:

#### Time Management Plan

Team members have to read previous project reports and choose their role in project within two weeks after introductory session. Next two weeks should be assigned to think about master

plan of different systems of vehicle and project's goal needs to be defined during this time. A week after by taking team members' individual plans into account, team leader has to propose an initial schedule. Project schedule should be realistic; meaning using large leads, lags or slack is not approvable. Proposal may be reviewed and modified by team during group sessions and be finalized (baseline) in one week. Shell Eco-marathon 2012 will have deterministic weighted schedule. The schedule shall contain work breakdown structure in two levels (excluding level 0), estimated duration of each work package, relations among them, their weight factor and list of important milestones. Preventing complexity and delivering an easy to understand schedule, resource allocation will not be considered in schedule's network calculations. For accurate and realistic result out of project schedule. Updating work packages have to be weighted. Project manager is responsible for breaking the weight factors and assigning them to project schedule elements. Microsoft Project 2012 is going to be used as time management tool. For tracking time, each week team members have to send a summary to project manager that includes 'what they have done' and 'what they will do'. Project schedule will be updated and be compared with baseline based on received summaries. Among with different updating approaches available in Microsoft Project 2012 software, recording elapsed actual duration will be used. Results of weekly evaluation have to be communicated with authorized stakeholders. These weekly reports shall cover the status of project, roots of variance and forecasts to be illustrated with tables, charts and especially S-curves. This plan can be altered by any change request confirmed by project manager.

#### Cost Management Plan

Name of part	Major Improvement Points	Scope of Change	Impact on Making New Car
Chassis	More complete shape and better aerodynamics, Use of lighter materials, increase aerodynamics	Complete change	High
Control System	Software: Two-way communication with the SMC, possibly using CAN-bus!	Complete change	Mid
Engine Plates	Weight reduction	Slight change	Low

Table 2.1.1: Improvement points for developing a new vehicle

Project team is responsible for developing list of activities in order to estimate demanded financial resources. Proposed budget for securing sponsors shall be calculated by bottom-up approach. Rough estimations from team members have to be aggregated to calculate required funds for higher work packages. Contingency reserve has to be considered in final approximation of proposed budget. This reserved will be evaluated for each level 1 work package. If project team is not successful to gather enough funds as as proposed budget, project manager is responsible to do top-down budgeting based on available money after securing sponsors. Project manager has to have a categorization for different costs within project to have better control over them. Spent amount of money on each system of vehicle needs to be communicated with project manager by weekly summary. Project manager is in charge of generating clear report of financial status of project that includes comparison of actual expenses and baseline (budget) for each work package. Any purchase that values less than 1500 NOK can be carried on without project manager confirmation. Project manager has authority to block further procurement and money transaction of work package if associated budget has reached its limit. As reviewing money transactions and tracking expenses is essential, project team members must preserve procurement documents appropriately.

#### *Communication Management Plan*

Apart from any communication which includes technical data, team leader shall be the hub for any external communication and responsible to distribute information to right person in team. Due to the fact that reviewing history of communications may be necessary any time in future, project team has to avoid relying on exchanging information via telephone or any other methods that they are not traceable. Using same email address (e.g. NTNU's) for any communication is imperative. In case of sharing information with whole team, individuals can use either shared project calendar on Google or use project mailing list. Precluding misunderstanding, interchangeable information must be clear and easy to understand. Language of all different types of communication (verbal and non-verbal) should be English. This plan can be altered by any change request confirmed by project manager.

#### *Risk Management Plan*

Project manager and system engineer are responsible persons to handle project risks. System

engineer may define risks in different systems of the vehicle by involvement of other team members to prepare risk register. Project manager has responsibility to assure that not only technical risks but also organizational risks are considered. Preventing confusion, only qualitative risk analysis will be performed to determine the likelihood and impact of each risk. With help of other members, system engineer is in charge of preparing preventive or mitigation actions. Reviewing risk register has to be done each two weeks to ensure proper monitoring. All team members are in charge of reporting emergence of new risk by weekly summary. If required, both project manager and system engineer have to make sure risk response is applied completely. Risk register may be updated anytime during project planning and executing by anyone in the team. In order to communicate status of project risk, online shared spreadsheet on Google Document platform will be made to simplify data gathering and distribution. This plan can be altered by any change request confirmed by project manager. Although these plans were improved and detailed by passing time but due to lack of enough information at start-up to create comprehensive framework, above mentioned plans sufficed to make a foundation for managing different knowledge areas. Collecting individual plans result in cohesive structure that is called "project management plan" Project management plan is endorsed, confirmed, live document that defines project requirements, determine expected outcome, and lead project execution and control. This document is integral point of team leader's responsibility and s/he needs to receive the approval from key stakeholders and the commitment of team members on its content to solve further conflicts as it becomes project control reference.

#### *Individual Plans Challenges*

By defining individual management plans, team leader determines what have to be done during project life cycle. By this mean, she/he specifies a framework which team members are expected to perform in. Apart from feature of the plans, strict or easy to deal, detailed or abridged, project manager shall not assume all of team members will accept management style right away. The point about Shell Eco-marathon project that should not be neglected is how individuals form the team, voluntarily. Therefore project manager cannot impose own preferred style of management plans to team members because it might

have negative impact on team performance or in the worst case may result in disbanding of one or more members which put the project in huge danger. Confusion, rejection or not having same comprehension of project management plans, from team members was one of the challenges during planning stage of Shell Eco-marathon 2012 project. Due to facing rigid deadlines, responsibilities and clear expectation from project manager, team felt limited and tried to bring comments in order to alter the content of plans and make them easy to deal which mostly result into less structured arrangement. Although some opinions were considered project manager put endeavor to give the understanding that individual plans are required and essential to handle project in integrate manner. If it is required one-on-one meeting with each team member should be held to ensure same level of comprehension is shared among them. Not following same path for reaching goal or working out of project scope are possible outcomes if team does not work in predefined frame. Important rules and deadlines shall be printed and put on the wall or a place where everyone can easily see them as oral communication is not reliable method for conveying important information that need to be last till end of project.

### 2.1.1.2 Creating Work Breakdown Structure

Work breakdown structure (WBS), (figure 2.1.1) is a hierarchical arrangement which shows how the project work is decomposed to manageable and understandable pieces. This structure visualizes the project scope; meaning it defines what is and is not going to be done and delivered during project life cycle. As all of required steps to accomplish project has to be determined in WBS, missing a work package may cause unfavorable consequences. Depending on project manager's preference and the purpose of executing project, WBS may be created in several ways. García-Fornieles et al. (2003) have introduced following approaches (classifications) for making WBS: product oriented, process or functional, organizational, project life cycle, geographic location of people. Suitable WBS is not only a tool for understanding scope; also it is useful to estimate time and budget. Furthermore, work breakdown structure provides holistic view of project to stakeholders which help them to comprehend what project team is going to do. Jung and Woo (2004) stated that the WBS provides a common view toward project for involved parties and it provides shared project language. Based on importance of project, manager has to decide upon

proper level of detailing in WBS. Level of detail has influence on how project cost, duration and technical complications will be taken care of. In another word, it deals with the manageability of WBS segments. Reaching the smallest (lowest) elements of WBS makes more information available but it also has to be considered that it requires more data processing and calculation. Sticking to high level work packages makes the road of achieving goal vague and less comprehensible. Based on project goal, functional work breakdown structure was chosen for Shell Eco-marathon 2012 project. Different systems of final deliverable (vehicle) were assumed as high level work packages and almost the same logic was considered for decomposing them: specifying reusable parts from previous vehicle if it is possible, making a list of general requirement for the system, conceptual designing, finalizing design of system, production and/or purchasing of parts. Avoiding confusion, WBS was detailed down to two levels (excluding level 0) and supporting efforts such as PR and media activities or team building sessions cannot be found in WBS because this type of efforts did not have influence on scope of final deliverable but they are considered in project schedule as milestones. More levels were prepared by team members to not miss any single task for delivering a system, but including them in work break down structure was totally unnecessary as they could make time tracking, budgeting and resource planning complicated. In presence of other team members bottom-up assessment was done to assure all deliverables and tasks were involved. Tasks related to work breakdown structure of Shell Eco-marathon 2012 project was created as following. Due to lack of information regarding time and place of testing the vehicle as integrated whole, this task is not mentioned in WBS and considered as milestone in project schedule.

### 2.1.1.3 Scheduling Project

"Develop schedule is the process of analyzing activity sequences, durations, resource requirements and schedule constraints to create project schedule" (PMI, 2008). Project schedule has different types of elements which may be used based on scheduler's choice, but following components are essential:

- Activities: Lowest level of work breakdown structure also known as operation or tasks which are steps to accomplish work packages. Time, budget and resource can be allocated to this element.



- Milestones: A milestone is a principal event that mostly indicates completion of a deliverable or a major step during project execution.
- Precedence relations: This element shows in what sequence activities or milestones shall be to reach the goal. Four precedence relations in scheduling are: Finish to Start (FS), Finish to Finish (FF), Start to start (SS) and Start to Finish (SF).

Before start with scheduling, project manager needs to decide upon the approach for generating the framework. Generally, two approaches exist:

- Deterministic: Assuming fixed duration for project schedule's elements is fundamental of this approach. Two methods are widely used in this class: Critical Path Method (CPM) and Program Evaluation and Review Technique (PERT). By using CPM, duration of task or work package will be a single number which is derived from past similar projects or technical opinion of experts. In PERT, three numbers, optimistic (minimum) time, most likely time and pessimistic (maximum) time, are generated for estimating duration. As

this method uses predefined probability distribution (beta) that results into definite value, it is classified in deterministic approach.

- Probabilistic (stochastic): in this approach, a unique statistical distribution curve is assigned to each activity or work package which determines the duration by generating a random number from defined curve.

Each approach has advantages and disadvantages. Deterministic approach is easy to do and understand. It needs less time and knowledge compared to probabilistic approach. But according to Pohl and Chapman (1987) deterministic scheduling is unable to take uncertainty into account and it leaves no opportunity for project manager to handle it. Although stochastic scheduling aims at considering uncertainty of activity or work package, but this approach needs considerable experience and knowledge and it takes more time to make a framework compared to deterministic one.

Project manager has to put enough time to prepare a flexible schedule that covers entire scope of project, nothing more or less. Project schedule is a framework to include essential elements that

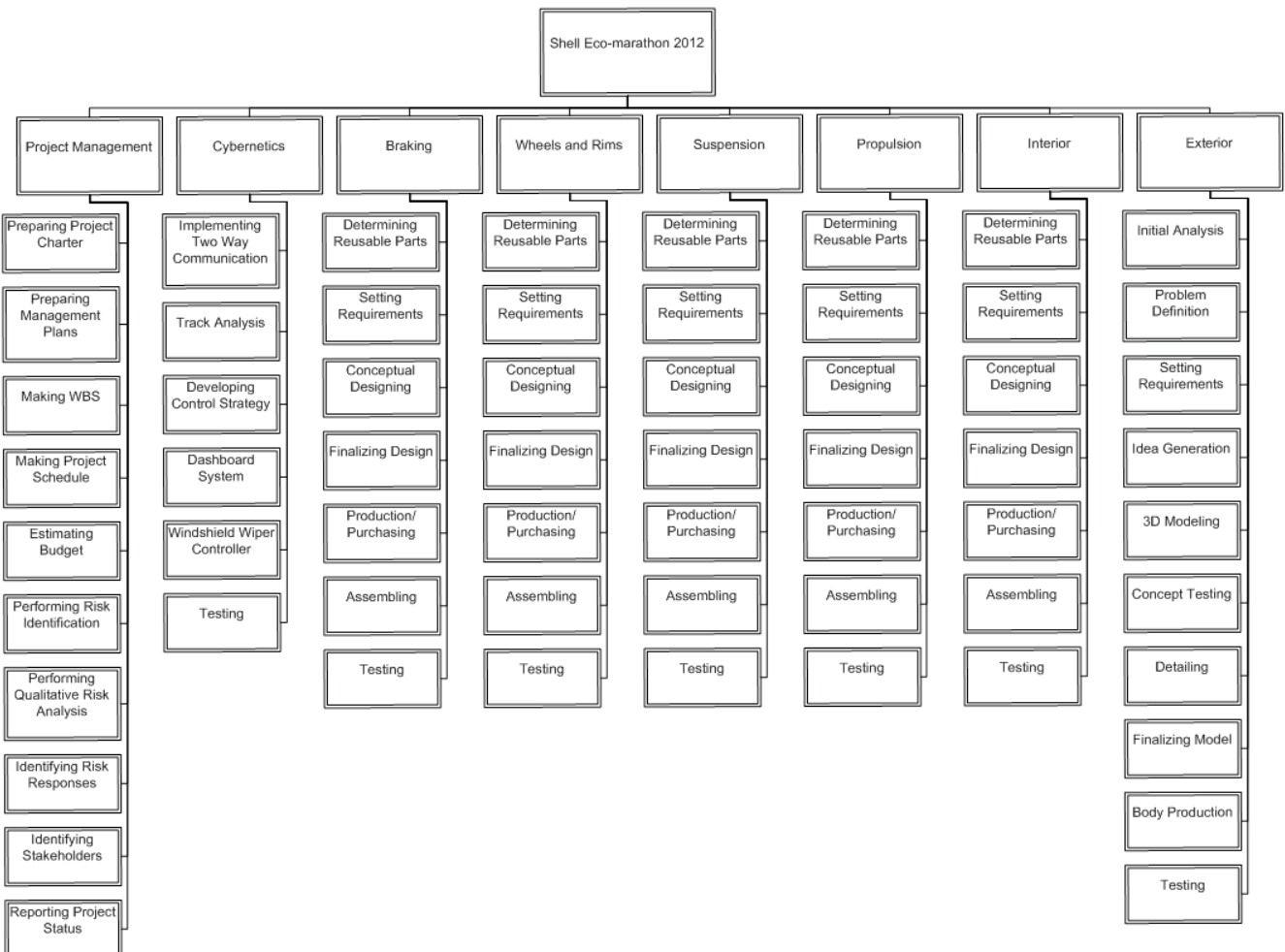


Figure 2.1.1: Work breakdown structure

without them the objective is not attainable. This framework shall contain tasks or work packages which estimating time, cost and required resources for them is feasible. Supporting tasks such as public relation and media activities is recommended to not be taken into account during scheduling because they are not dependant on specific duration, and mostly not schedulable. Activities with this attribute are called Level of Effort (LOE). Project schedule components have to have unique and clear name. This makes it more understandable for anyone and also it helps the project manager in time of filtering or grouping segments.

According to PMI (2008) three types of dependencies may be used during scheduling. Dependencies determine precedence relations:

- **Mandatory:** Mandatory dependencies are constraints which are forced by nature of work.
- **Discretionary:** Discretionary dependency, called soft logic, is restriction applied based on scheduler's logic in order to handle elements better.
- **External:** External dependency is limitation from outside of project team such as stakeholders that might influence the schedule.

In time of defining precedence relations, all activities and milestones have to have successor and predecessor expect. First one which does not need predecessor and last one which doesn't need successor. So, it is logical to say that all activities and milestones should have at least on FS or SS relation with predecessor(s) and at least one FS or FF relation with its successor(s). It is the project manager's responsibility to review all relations in order to ensure that none of the elements is dangled. Independent elements cause inaccurate tracking over schedule in time of updating it. Misusing leads and lags for compressing or giving float without any strategy will decrease the authenticity of the schedule as it will not show the real condition.

Assigning resources makes schedule more professional but it should not be always an option as it also makes the schedule more complicated and hard to comprehend. Therefore, for preventing bafflement, if resource management is not important, resource allocation is better not to be done in project schedule. Kolisch and Padman (2001) have defined two categories for project resources: renewable and nonrenewable. Renewable resources are available within specific period

e.g. manpower. Nonrenewable resources without time restriction are accessible as long as project runs e.g. project budget.

Shell Eco-marathon 2012 had deterministic schedule. CPM method was used to determine work packages duration. This option was chosen due to short available time for making schedule and build easy to understand framework for involved parties. Estimating time was done for level two work packages. Based on detailed breakdown that each team member possessed for related system, approximate duration for each work package was appraised. Summation of rough numbers from team members and reserved slack time for each work package was considered as project duration. Project manager should be aware that team members mostly try to assume the best condition in time of generating values. So, it is up to him/her to think about time safety margin for each component or whole project to avoid lack of time because of and to have buffer in order to respond risks or deal with uncertainties. Milestones were used in two situations: For significant steps through project such as "body mold is available" and when team had no control over task's duration and it was totally dependent on external entity such as sponsor. Figure 2.1.2 shows how milestones were arranged in schedule.

Based on experience and information from interviews with team members that provided more technical insight, project manager defined the relations among work packages. All three types of dependencies were considered during scheduling. The most influential dependency was external one from DNV (main sponsor) and Shell (competition holder) that imposed strict deadlines on project. SF relation was not use at all and maximum duration for leads or lags was 4 days. Before proposing the schedule, all work packages and milestones were checked to not be dangled. To have accurate and realistic result from upgrading the schedule, Shell Eco-marathon 2012 had weighted timing framework in which, each work package was given a value, according to its importance and duration. The total of weight factors shall be 1 or 100. Table 2.1.2 shows how weight was distributed among different elements of schedule. Important milestones has the most weight, as very important elements such testing the vehicle is included in it.

Group session was held with entire team to review project schedule and ensure all relations

within a systems and among systems of the vehicle have correctly set. The outcome of this meeting was the baseline. S-curve related to baseline was sketched afterwards in order to be a tool to compare actual performance with planned one. According to time management plan, Microsoft Project (MSP) 2012 software was chosen to implement the framework. For sketching planned S-curve which shows expected cumulative progress, two new columns were defined in MSP file, 'Weight Factor' and 'Weighted %Complete'. Following formula was set for Weighted %Complete column:

$$[\% \text{ Complete}] * [\text{Weight Factor}] / 100$$

By updating the project schedule weekly in software (moving status date), MSP calculates %Complete column (cumulative progress) based on proportion of elapsed duration to total duration. But this does not count the importance of element into account. That is why weighted %Complete is more realistic value to rely on. Planned S-curve of Shell Eco-marathon 2012 project including weight factors was sketched as shown in Figure 2.1.3.

As it is shown, no progress is expected between weeks 14 to 17 due to Christmas break. The slope of S-curve is considerably increased between weeks 24 to 30 because the work packages with huge weight factor had to be accomplished in this period.

### Scheduling Challenges

How can the best fitted schedule for project be developed? Answering this question is a challenge for project manager during scheduling. Scheduling a project should be done by considering its resource, activities and performance measure characteristics. If project manager does not put enough thought on identifying what is the status of three mentioned factors, she/he might have a result that is not realistic. Herroelen et al. (1997) have mentioned that for dealing with complexities during scheduling, knowing its three features is essential. According to them, three elements shall be assumed for resources to analyze them properly:

1. Number of resource type that can be zero, one or more than one.
2. Whether the resources are renewable or non renewable and their accessibility time period, if it is for whole project duration or specific one.
3. Availability of renewable resources if it is in constant amounts or in variable amounts.

Six elements are recommended for understanding the activities' attributes:

1. If activities can be resumed in time of interruption or not.
2. Constraints between activities that can be mandatory, external or discretionary
3. The network of activities is probabilistic or deterministic.

84	2.9	☐ Finish Milestones	64.75 days	Wed 28/09/11	Mon 30/01/12	
85	2.9.1	☐ Technical	25 days	Wed 30/11/11	Mon 30/01/12	
86	2.9.1.1	Ordering Carbon Fiber	0 days	Wed 30/11/11	Wed 30/11/11	42,10,31,36
87	2.9.1.2	Carbon fiber available	0 days	Mon 30/01/12	Mon 30/01/12	86FS+5 wks
88	2.9.1.3	Order mold material	0 days	Mon 23/01/12	Mon 23/01/12	12FS+3 wks
89	2.9.1.4	Mold material available	0 days	Thu 15/12/11	Thu 15/12/11	13FS+1 wk
90	2.9.1.5	Odering body mold	0 days	Thu 15/12/11	Thu 15/12/11	13,12,89
91	2.9.1.6	Body mold available	0 days	Mon 23/01/12	Mon 23/01/12	90FS+2 wks
92	2.9.2	☐ Managerial	39.38 days	Wed 28/09/11	Wed 30/11/11	
93	2.9.2.1	Initial contacting-old sponsors	0 days	Wed 28/09/11	Wed 28/09/11	
94	2.9.2.2	Meeting withold sponsors / Finding new sponsors	0 days	Mon 31/10/11	Mon 31/10/11	
95	2.9.2.3	Finalizing contact with sponsors	0 days	Wed 30/11/11	Wed 30/11/11	
96	2.9.2.4	Finalizing Recruitment	0 days	Tue 15/11/11	Tue 15/11/11	
97	2.9.2.5	Finalizing contract with main sponsor	0 days	Mon 31/10/11	Mon 31/10/11	

Figure 2.1.2: Milestones arranged in the schedule

4. Activities duration that can be random integer number, or random continuous duration or all tasks have same duration equal to  $T_d$ .
5. Project deadline which means if there is no deadline, there is deadline imposed on activities and there is deadline on project.
6. If cash flows are considered with activities or not. Both amount and timing of cash flows can be arbitrary or predetermined numbers.

Regarding performance measures, project manager shall know if penalty functions for delivering the final product, result or service in due time exist or not. Former condition is called regular and latter is named non-regular measure. Minimizing the project delay is an example for regular measures and maximizing quality of the project is an instance for non-regular measure.

Analysis of Shell Eco-marathon 2012 project schedule by considering resources, activities and performance measure characteristics are as below:

- Resources: project had two types of resources, work and material. Both renewable and nonrenewable (with variable amount availability) resources were accessible for limited and specific period of time.
- Activities: Shell Eco-marathon 2012 project had deterministic schedule. Both resumable (testing a system) and non-resumable (producing monocoque) activities were taken into account. Project manager thought over three types of constraints in time of defining relations among tasks. All of activities had integer number as duration which were not random as they were calculated based on members' judgement and historical data. Non of tasks had specified deadline but pro-

Name of Work Package	Weight
Exterior	14
Interior	9
Propulsion	11
Suspension	12
Wheels and Rims	9
Braking and Steering	9
Cybernetics	11
Project Management	8
Important Milestones	27
Total	100

Table 2.1.2: Weighting of different elements

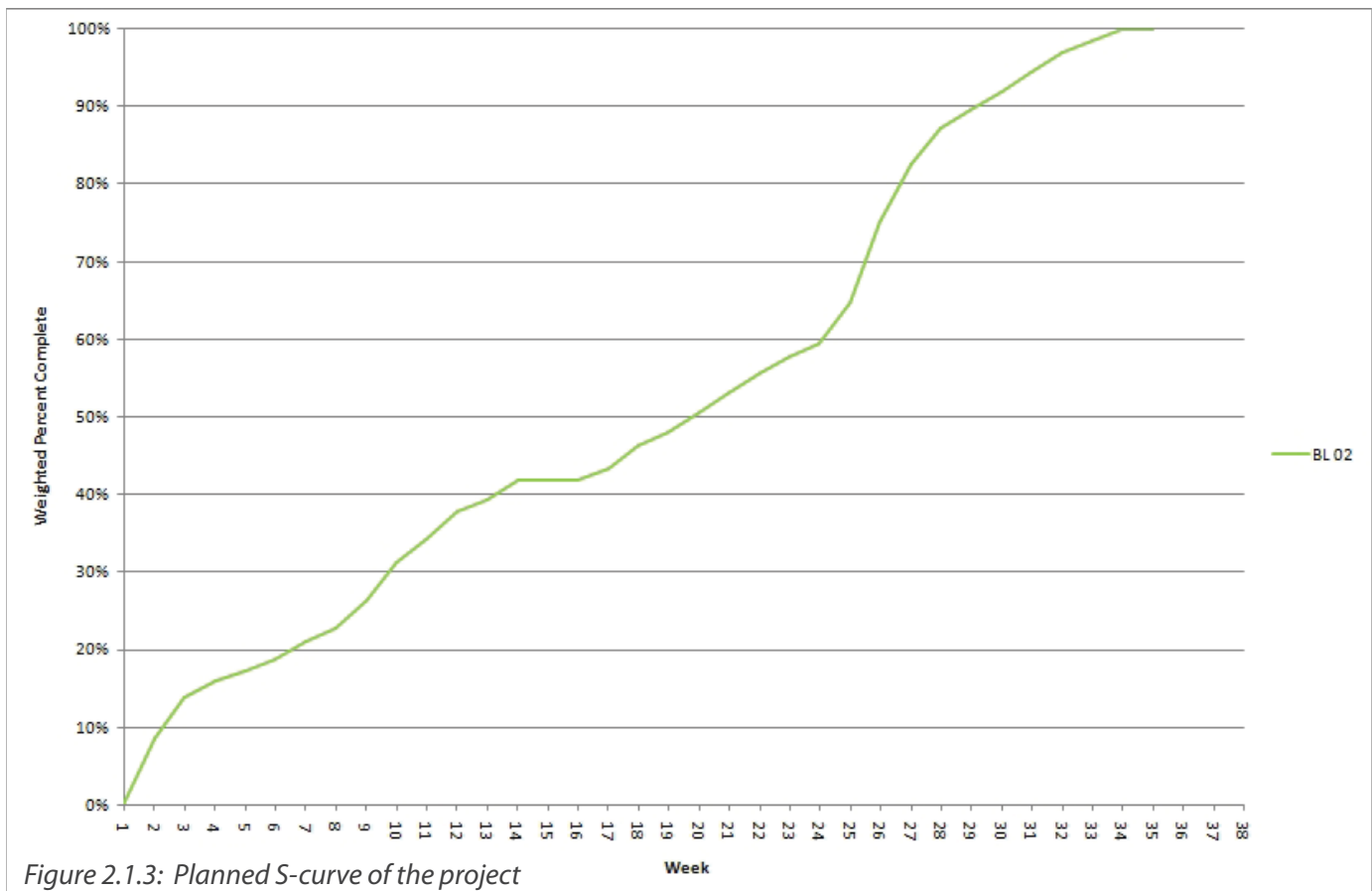


Figure 2.1.3: Planned S-curve of the project

ject had strict deadline of May 17, 2012 for competing in the race.

- Performance measure: Schedule of project were developed based regular measure, minimizing the project tardiness.

#### 2.1.1.4 Budgeting

According to Huang and Xu (1998) best solution for financing projects with high uncertainty is external subsidization. This is exactly how Shell Eco-marathon project is financed every year. It is up to project team to find sponsors for project and university plays no role in supporting project financially. Kamien and Schwartz (1978) indicated two main difficulties with external financing compared to self-financing for project associated with high uncertainty:

1. Finding external sponsor may be hard in such endeavors because if the project fails, few tangible assets will be left which lender can make claim on them.
2. Receiver of the fund may reveal some information about project which might be valuable for existing or new rivals of lender's business.

For attracting external sponsor(s), project team has to calculate proposed budget which will be the basis of financial negotiations in further steps.

An estimate should be calculated for all project works or any element of project schedule that needs financial resource to be taken care of. This estimation that has to be approved by key stakeholders is the budget. Taking all project costs into account is essential for budgeting. Project manager has to classify costs in order to not miss any and have better control over them. There is no single categorization logic for grouping them and suitable approach may be chosen depending on project condition.

As unexpected events which burden extra costs on project happen during execution, contingency reserve shall also be included in budgeting process. Contingency reserve is critical financial resources to reduce the risk of cost overrun. For estimate the reserve, project manager needs to go through the result of qualitative or quantitative analysis of risks. By considering the risks that have significant financial impact on budget, required fund can be estimated.

There are two approaches for calculating de-

manded money to finish project work: "Bottom-Up" and "Top-Down" In bottom-up approach, cost estimation has to be done for the lowest level components of work breakdown structure. Then estimation of activities which are related to same work package shall be summed. By continuing this, essential fund for the highest level of WBS can be calculated. This approach has following advantages:

- The most important advantage of this method according to Venkataraman and Pinto (2008), is forcing project team to make detailed breakdown structure at planning stage
- Within this approach, as the knowledge of all involved persons in project, even those who are responsible for the lowest level activities will be used for such important process; motivation of team members will be increased due to feeling of involvement with project.

But this method also has a down side:

- By applying this method, the role of project manager (or top management) in such critical task will be reduced at first steps as team members in lower level of hierarchy who has the responsibility of activities shall estimate the costs and project manager has no control over the process till analysis are presented.
- The chance of overestimating within bottom-up approach is higher compared to top-down because project team members might tend to exaggerate the cost in order to increase the flexibility.
- By considering before mentioned characteristics, repetitive adjustments to have best estimation is expected and this makes bottom-up approach time consuming.

In bottom-up approach, demanded financial resources is calculated and then provided but in top-down approach, project team has to deal with predefined amount of money that has been allocated to project by upper managers and try to proportion it appropriately among high level work packages and this process continues to the lowest level of WBS. Top-down method has following advantages:

- "The advantage of top-down budgeting is that top management's estimate of project costs, in aggregate terms, often tend to be quite accurate" (Venkataraman & Pinto, 2008).
- On contrary to bottom-up approach, project

manager has full control over disaggregating the budget to work packages, which results in more accurate estimations and cost control.

Disadvantages of this method are as following:

- Project costs might be underestimated due to cost saving.
- Experience is essential to perform this method. If project manager doesn't have enough knowledge or understanding about work packages and related activities, improper fund allocation is largely possible.

Shell Eco-marathon 2012 project costs were classified into followings:

- Direct costs that are particularly related to activities on project. Following items are included in this category:
  - Human resource costs: this includes salary of two team members that had to be paid because of their student assistant contract with department.
  - Material Costs
  - Operational Costs
- Indirect costs which do not have direct impact on the work of project. Mostly, administrative expenses are put in this category.

Budgeting this project requires both bottom-up and to-down budgeting approaches. First for negotiating with sponsors, project team needed to come up with proposed budget. In this order based on historical data from previous project reports and team members' judgments, rough calculations were done for WBS work packages. Using bottom-up approach, the proposed budget was estimated at 1.095.000 NOK including contingency reserve. Table 2.1.3 shows more detail about it.

Lots of effort were put by project team and manager to secure sponsors in order to decrease the amount of demanded money in different items of the budget. Beside, by gaining more information about structure and design of various systems, team found overestimations in some items which was expected after utilizing bottom-up approach because for not facing any trouble individual's assessments were associated with high uncertainty. At last, NTNU's team could receive financial contribution from Det Norske Veritas (DNV) of 600.000 (main sponsor) and Transnova of 150.000 NOK. As taken fund was less than

what team planned for, budget was revised by top-down approach by project manager. Practicing this method, available fund was distributed among high level work packages which resulted in following figure (cost baseline).

#### 2.1.1.5 Risk Identification and Assessment

An undetermined event with either positive or negative impact on project is called risk. One of the critical responsibilities of project manager is ensuring that project's risk are identified and assessed. Registering risks and their characteristics should be performed as first step. Involving project manager, project team and stakeholders in this step is crucial. Team members' participation is important as they have to take responsibility of determined risks and their responses. Involvement of stakeholders is critical as they provide supplemental goal information. Identifying risks and making associated plans to respond them for whole project life cycle at planning stage is not possible as new risks emerge during project advancement. Because of this, project management team should analyze the status of project iteratively in order to be sure that all kinds of risks are considered. Project feature (low/high uncertainty) defines how often such analysis shall be done. According to PMBOK (2008) five processes can be accomplished in planning stage to follow best practices in risk management area:

1. Plan risk management: Within this process, project manager define how risks are going to be handled through project life cycle. Importance of making this plan is having an accepted basis among team members to evaluate undetermined events. Risk management plan is explained in section.
2. Identify risks: Result of finishing this process is a list of categorized risks. Chapman (2002) has stated that although present models and methods in project management make valuable tools available but still experts' judgments are the key input for identifying project risks. This process is fundamental for all of risk management efforts; therefore accuracy is very important. Various methods are available for gathering such inputs. Chapman R. J. (1998) has classified all methods into three groups:
  - Identification managed by one risks analyst e.g. reconsidering historical data.
  - Identification performed by analyst interviewing project's key players.
  - Identification conducted by presence of

Budget item	Planned Cost (NOK)	Contingency Reserve (NOK)
Propulsion	150.000	20.000
Exterior	300.000	50.000
Wheels and Rims	55.000	5.000
Suspension	110.000	20.000
Braking and Steering	15.000	5.000
Interior	10.000	5,000
Cybernetics	50.000	10.000
Shipments	40.000	10.000
Trip to Rotterdam	142.000	8.000
Misc	40.000	0
Safety Margin		50.000
<b>Total</b>	<b>912.000</b>	<b>183.000</b>

Table 2.1.3: Detailed budget

all key players in form of group sessions that is led by analyst e.g. brainstorming.

From above mentioned classes, first and third were used in Shell Eco-marathon 2012 project. First, different engineers based on historical data from previous years' reports and their experience, tried to list risks associated to systems that they were responsible for. Afterwards, by using scenario building (analysis) technique in group sessions led by project engineer and supervised by project manager, risks related to system interfaces were determined. By using this technique various possible events and their outcomes were identified. While scenario building, one does not count historical data and does not include them into assessment; but it provides a picture of future which is linked to past. Beside technical (low level) risks, team members and project manager identified managerial and organizational (high level) risks which are mostly connected to team, its performance and managing project.

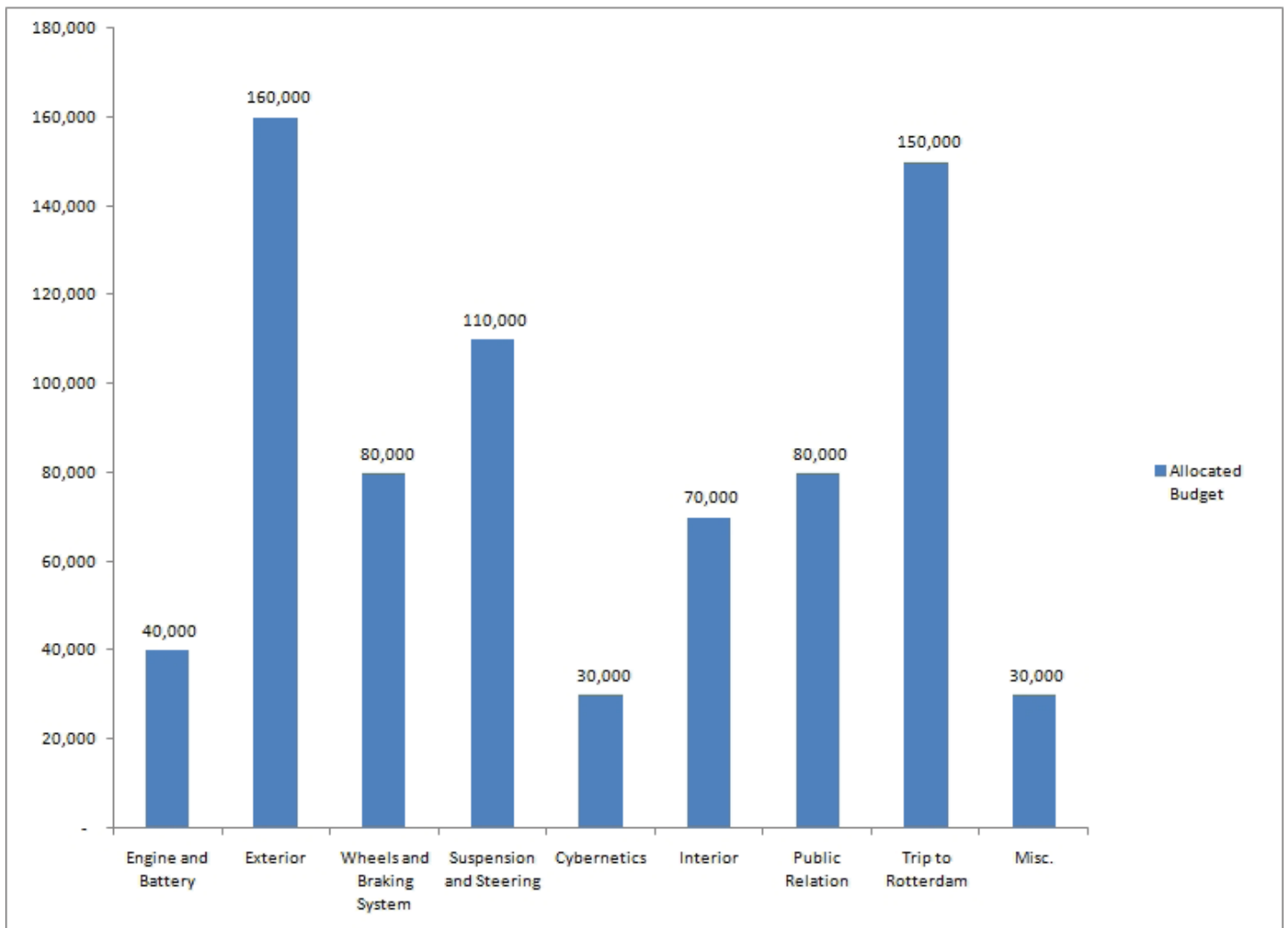


Figure 2.1.4: Detailed budget

3. Perform qualitative risk analysis: The purpose of following this process is organizing of identified risks in order to enhance execution of project by concentrating on high-priority risks. High-priority risks are those which have significant impact on time, cost and quality of project. For deciding how critical each risk is, two criteria are used: probability and impact. For assessing subjectively, a scale shall be defined for each parameter in order to have common understanding of rating system. Depending on project manager and project feature defined structure for scales varies. Often, "High, Medium, Low" or numeric "1-10" scale is used for measuring both probability and impact of risk, if occurred. Project manager needs to be aware that in qualitative assessment "risk is relative to the observer" (Kaplan & Garrick, 1981). Specified risk characteristics may differ from one team member to another as the knowledge and experience of the observer are important factors in organizing risks. Probability and impact matrix was used in order to accomplish qualitative risk analysis in Shell Eco-marathon 2012 project. Numeric "1-5" rating system was fixed for assessing two parameters of each risk. Numbers have following definition given in table 2.1.4.

This tool helps project team to know which risks need immediate response and which ones need to be reviewed later as they are not critical. Qualitative risk analysis has some advantages and disadvantages. Startienė and Remeikienė (2007) have indicated followings as its advantages:

- It is useful when enough experience is not available.
- It is flexible as scales can be altered easily because no complicated calculations exist behind them.
- It is less time consuming and cheaper compared to quantitative risk assessment

But this approach has following downsides as well:

- Less precise compared to quantitative approach because results are shown in subjective manner.
- Cost-benefit analysis cannot be done with outputs from this method

4. Perform quantitative risk analysis: For accomplishing this process, team tries to quantify

the likelihood of risk occurrence and its impact that mostly measured in terms of currency. According to Apostolakis (2004) this approach has following benefits:

- Delivering thorough comprehension of system failure manners by considering significant number of scenarios include different style of failures.
- It is unified method, so determining the requirements from various disciplines involved in project.
- By using this approach, the chance of taking intricate interactions between systems and operators into account will be increased.
- Unlike qualitative risk assessment approach, output of quantitative method can be used in cost-benefit analysis.

This technique has following limitations:

- Not modeling human errors in time of facing risk
- Not considering the culture of people who have the responsibility of handling the risk, as it is influential factor in how individuals will react when accidents happen
- Not taking design and production errors into account.

This approach wasn't used in Shell Eco-marathon 2012 project because it is time consuming and team members didn't have the experience and knowledge about following quantitative risk analysis.

5. Plan risk responses: Considering the outputs of identify risks process and all possible upcoming and expected events, team members developed mitigation actions individually (for responsible system) or in group (for interfaces of systems). Also, project manager build a list of responses for managerial and organizational (high level) risks.

#### 2.1.1.6 Risk Identification and Assessment Challenges

There is no guarantee for reaching expected outcome out of group sessions that are dedicated to risk identification and assessment. What makes it uncertain is the group effectiveness during meetings. This is a challenge for project manager to comprehend the status of team's effectiveness and make proper decision if it is low. This evaluation is very critical because in time of low efficiency, not only time is wasted but also the results are not reliable and the chance of facing



troubles during project advancement will be increased if risk management processes are based on untrustworthy judgments. Chapman (1998) has developed a model for evaluating group efficiency. According to model two factors can be assessed related to group sessions: "The Givens" and "Intervening Factors". In his paper each factor is detailed into few determinants but in this report only those that are connected to the project are discussed.

- Givens: this feature describes the status of the group, the tasks and the environment that are inputs for risk identification and assessment.
  - The group: Size of the group matters. Although increasing the number of the group for each session guarantees the involvement of various disciplines and knowledge but project manager should be aware that this might result in decreasing the individual contribution. Compatible members shall be present in meetings. Discordant members will decrease the effectiveness of group work. While productivity of sessions is the common goal for all participants, project manager shall have this awareness that members may try to include their personal objectives as well e.g. imposing own interest or trying to grab the lead. Therefore, an unbiased person who has enough knowledge to guide the meeting should be present.
  - The tasks: Team leader must be sure that team members take their responsibilities seriously and handling various tasks is important for them. Individuals show more commitment if they consider the task prominent. Lucidity of the tasks is important factor on group effectiveness as well. When the expected performance and outcome is less ambiguous for participants in a meeting who have same level of comprehension about what they have to do, effectiveness will be increased.

- The environment: It is important that participants in risk identification and assessment meeting feel that the location of session is proper. Quiet room that has enough facilities where people can find a comfortable seat gives good sense to team member and they can carry on the tasks in effective way. Members don't want to spend their time in assemblies in which the outcome of it is not communicated or put into effect. Therefore, team leader or director of meeting should provide an environment in that participants feel its significance for project e.g. to hold the meeting in structured or organized manner.
- Intervening Factors: The most important item in intervening factor is motivation. Risk identification and assessment sessions should be presented by team leader in way that team members wish to be part of them and approve the objective of meetings.

For Shell Eco-marathon 2012 project, risk identification was done by individuals and in group for ensuring, each team member benefits of own contribution and team work. Meetings weren't held for more than five members including system engineer as director. Director had the knowledge about technical group gathering to not let the members distract the flow of proceedings by their personal interest. All of team assemblies were carried on in presentation room in order to provide appropriate physical location. Before each meeting, participants were informed about agenda and topic, so they could make their opinions ready. Minute of each meeting was prepared of system engineer to communicate the result with all team members with purpose of showing the importance of assemblies to them. Not only project manager explained the significance of this step to team members, but also director of meetings, clarified why project needed it and what the goal was. Therefore, everyone had clear and common understanding of process and its objective.







Scale	Probability of Occurrence/Impact	Related Color
1	Very Low	
2	Low	
3	Medium	
4	High	
5	Very High	

Table 2.1.4: Definition of rating system

ls

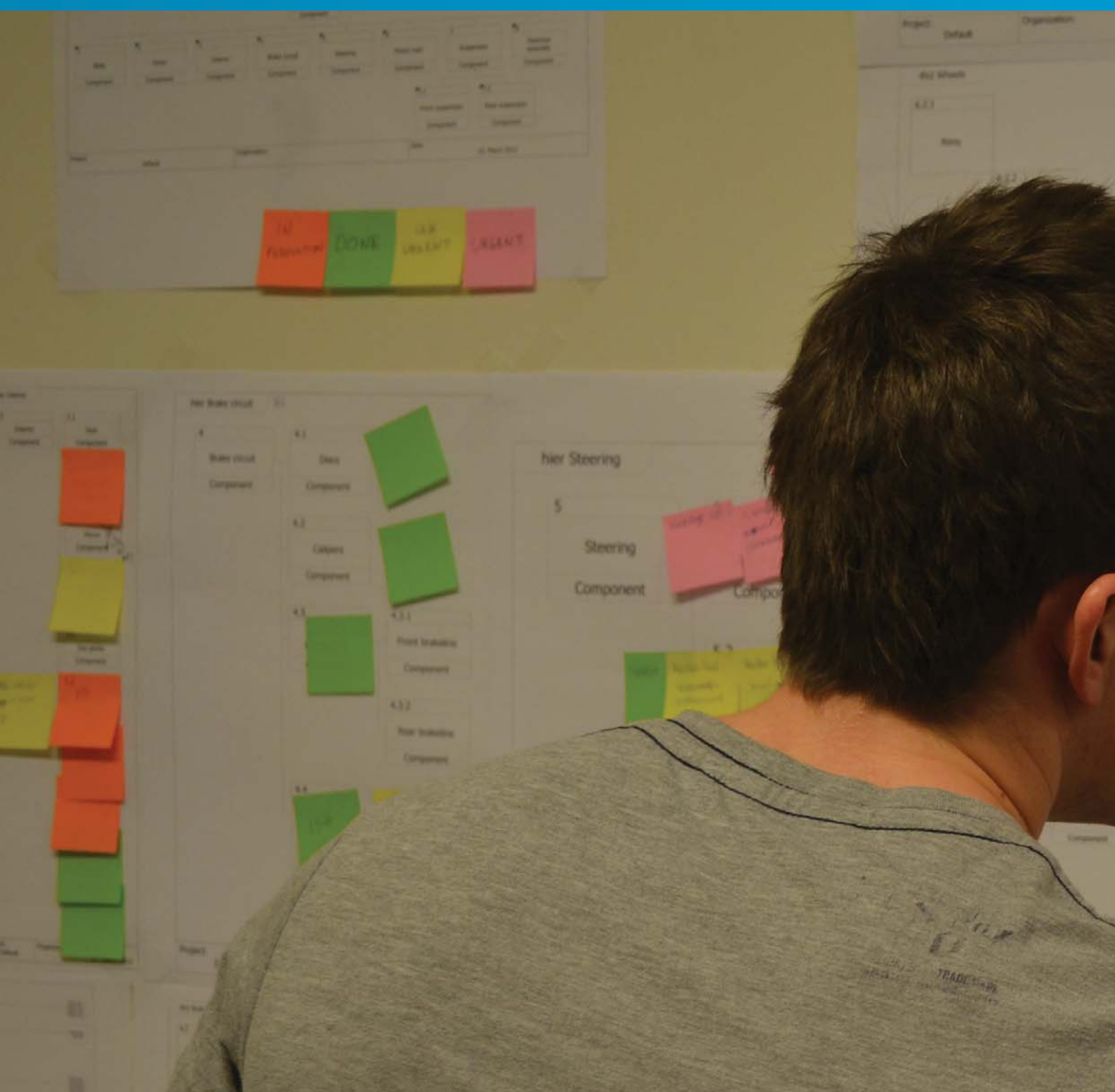
23

The background of the slide is a photograph of a wall covered with numerous colorful sticky notes in shades of green, blue, and orange. The notes are arranged in a somewhat organized manner, suggesting a brainstorming or planning session. A dark grey horizontal band is overlaid across the middle of the image, containing the text.

# **2.2**

# **SYSTEMS**

# **ENGINEERING**

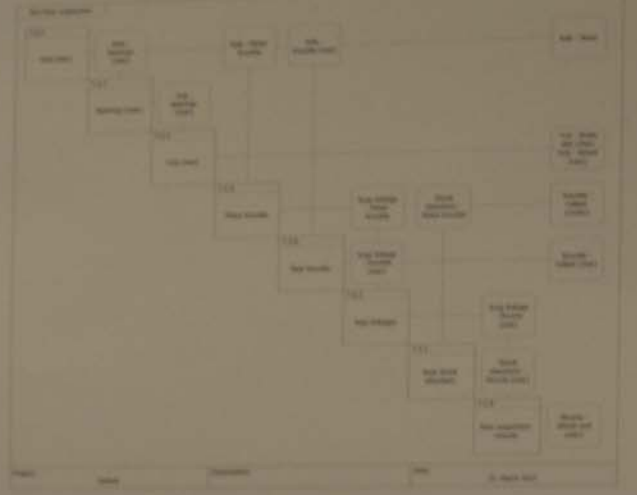
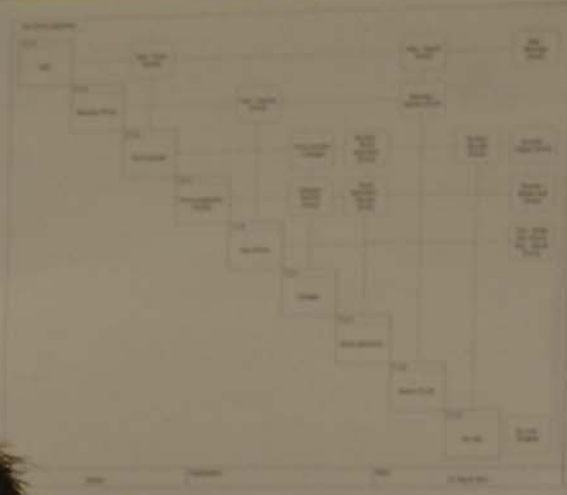


## 2.2 SYSTEMS ENGINEERING

The SEM 2012 team has integrated for the first time a systems engineering team. The Systems Engineering team consist of two system engineers. The SE effort lays on the knowledge management, Visual Workflow Management, risk analysis and management and in designing and performing a technology qualification.

### 2.2.1 KNOWLEDGE MANAGEMENT

One of the Systems Engineering tasks of 2012 was to secure a seamless transition from this year's team to the next, and to put in place a system for capturing and sharing knowledge for years to come. This is the topic for Oluf Tønning's master's thesis, and more details about this will be found there (Tønning, 2012). This section gives a summary of the contents of Tønning's thesis.



7.1 Front suspension Component

7.1.1 Upper control arm Component

7.1.2 Lower control arm Component

7.1.3 Steering knuckle Component

7.1.4 Hub (front) Component

7.1.5 Tie rod Component

7.1.6 Front knuckle Component

7.1.7 Front suspension mounts Component

7.1.8 Spacer (front) Component

7.1.9 Bearings (front) Component

Project: Default Organization: Date: 15 March 2012

7.2 Rear suspension Component

7.2.1 Upper control arm Component

7.2.2 Lower control arm Component

7.2.3 Rear knuckle Component

7.2.4 Hub (rear) Component

7.2.5 Rear knuckle Component

7.2.6 Rear knuckle Component

7.2.7 Rear Component

Project: Default Organization: Date: 15 March 2012

8.1 Electrical assembly Component

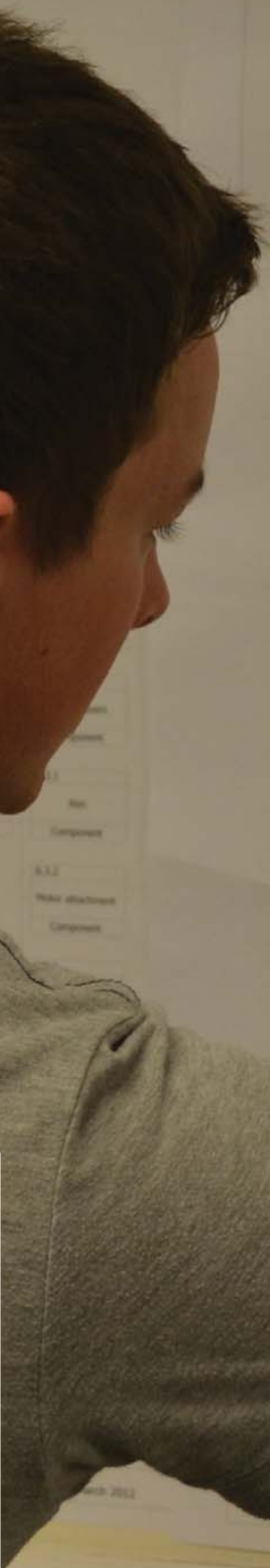
8.1.1 Lights Component

8.1.2 Horn Component

8.1.3 Wiper Component

8.4 Control systems Component

Project: Default Organization: Date: 15 March 2012



Theme	Ownership
Problem statement	Countermeasure selection
Problem analysis	
Goals	Verification method(s)
Alternative evaluation	Implementation and follow-up plan

Figure 2.2.1: The template uses a Plan-Do-Check-Act approach, meaning the problem is solved through analysis, testing, verification and then implemented

### 2.2.1.1 Capturing Knowledge with LEAN Techniques

A much-employed technique in Lean Thinking (a theory for efficient development and production from Toyota) is the Knowledge brief, better known as K-briefs. These are A3 sheets of paper containing short and visual explanations of a lesson learnt or a problem encountered and solved. The idea is to make the K-brief inviting to the reader, and to explain to the reader in short, summarized terms how to deal with a problem or about the decisions leading up to a certain design choice made in the development process. To best capture knowledge, the process needs to be standardized. Lean Thinking recommends having certain learning events at equal intervals during a development process. The most common is to have many milestones throughout the development process, and to have the learning events at these milestones. The teams will spend that day or period capturing knowledge from that interval. In particular interest are problems solved and decisions made.

Another way of standardizing the process is to have specific templates for the K-briefs. Templates reduce the time spent while making these K-briefs, as well as securing that nothing is left out that should have been included.

Figure 2.2.1 shows a template for a K-brief that addresses a problem solved.

The following three sides show a three-page

K-brief that Tønning (2012) has designed for capturing knowledge about sub-systems and components of the DNVFF2. This technical K-brief is meant as a deliverable at the end of the process, summarizing the entire development, production and utilization process.

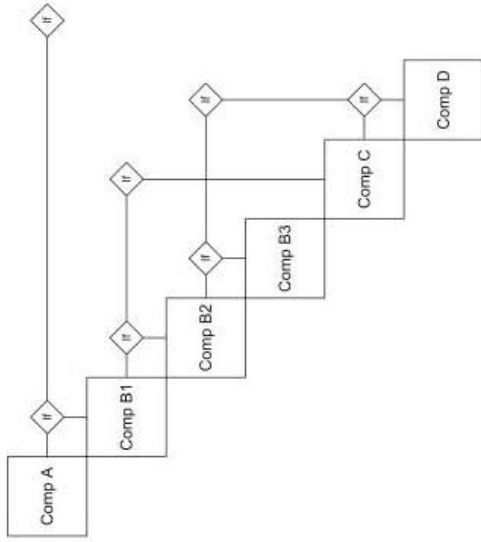
An example of a K-brief are available in Appendix G.

**Trade-off analysis/important decisions**

Why was this design chosen? What other designs were considered? Are any of the discarded design concepts worth another look?

What major decisions were made during the production of this subsystem?

**Interfaces**



**Interface details**

More detailed information about important interfaces. Maybe primarily external interfaces, what they are dimensioned for or what type of data they transfer.

Photo of subsystem

Component	Material	Dimensions [mm]	Design	Satisfaction [%]
1.1	Steel	10x15x25	NPD	100
1.2	Alu	1x3x6	R	80
1.2.1	Alu	12x89x78	P	75
1.2.2	Alu		NPD	75
1.2.3	CF		NPD	100
1.3	CF		P	100
1.4	Alu		R	0

NPD = new product design, R = reused part, P = purchased part

**Supplier data**

- Where purchased/manufactured
- Price
- Contacts
- Comments

Figure 2.2.2: The front page is dedicated to listing components, interface diagrams, describing major decisions and the manufacturing process. The components are categorized as 'New Product Development' (NPD) meaning designed by this year's team, 'Reused' (R) meaning an unaltered design or 'Purchased' (P) meaning bought from a manufacturer. Also, the components are rated for satisfaction stating how well the component behaved relative to its expected behaviour

Responsible/date

S.x Subsystem

<p><b>Analyses</b></p> <p><b>Background</b></p> <ul style="list-style-type: none"> <li>- Requirements</li> <li>- Software used</li> <li>- Assumptions</li> </ul> <p><b>Results</b></p> <p>Summary of results</p> <p><b>Conclusion</b></p>	<p>Photos/illustrations/charts with short explanations</p>
---	--

Figure 2.2.3: Page 2 is dedicated to the 3D-models, simulations and analyzes



S.x Subsystem

Responsible/date

**Identified risks**

Description	L	C	LxC	Mitigation
Failure	3	5	15	Just don't
Illness	1	3	3	Take vit-C

L = likelihood, C = consequence

This section presents risks the sub-system is facing, and tips on how to prevent them from happening or how to repair them if they do occur.

**Performance**

Summarize the verification process (testing history);

How was it tested? What tests did it fail and how was it fixed (quick solutions that may need attention in the future)? What was the root of the error?

Did the system function as intended during the race? How well did it work?

Did something go wrong? How was it fixed? Will it happen again? What was the root of the error?

This column should be reflected by the level of satisfaction stated on the first sheet!!!

**Proposed future work**

The way forward

Figure 2.2.4: Page 3 is dedicated to perceived risks, a description of problems and how they were solved, and proposed future work

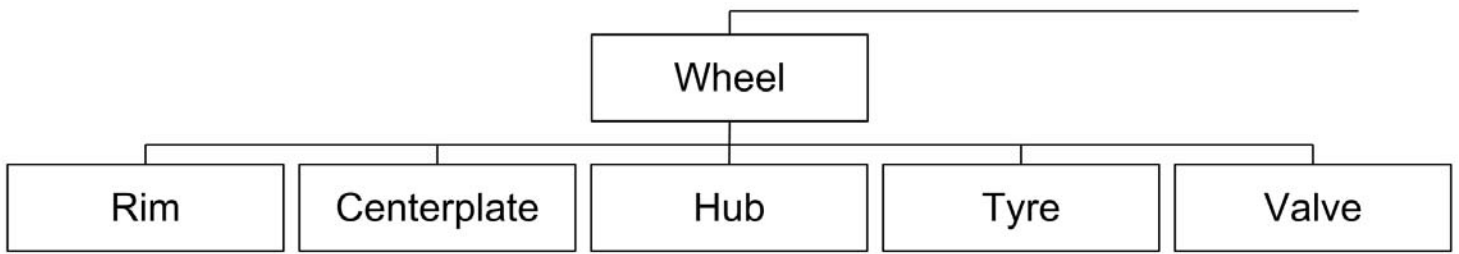


Figure 2.2.5: The sub-system “Wheel” broken down into its components

### 2.2.1.2 Storing and Sharing Knowledge with Model-Based Systems Engineering

Now that the team has decided on how, when and what to capture, the team needs to have a “where” to put it. Model-based Systems Engineering (MBSE) is a way of performing Systems Engineering through system modelling. A system model is a three-step description of a system, describing it by its requirements, functions and system architecture. The model uses hierarchies to illustrate how elements within model are related to each other, and to add detail to elements. Figure 2.2.5 shows how the element Wheel can be further described by breaking it into its minor elements.

Figure 2.2.6 shows how an N2 diagram may be utilized to show how the components of the Wheel are fixed together, or i.e. the interfaces between components.

Requirements, functions and components are strongly related to each other. A requirement says why a function or component is chosen. A function describes what a component or sub-system is intended to do, and components are

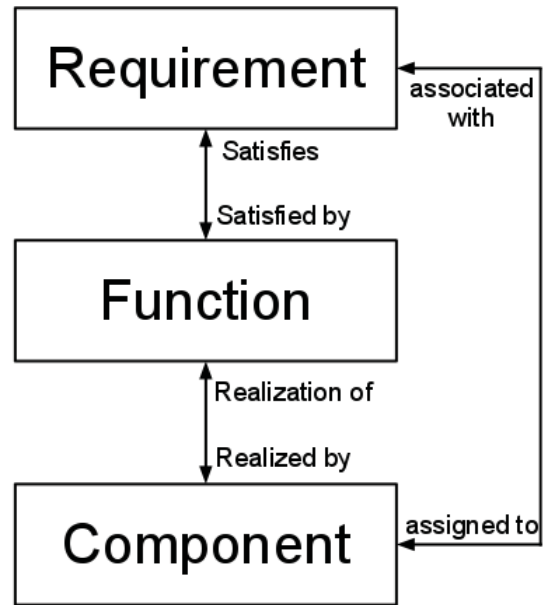


Figure 2.2.7: A requirement is satisfied by a function and assigned to a component. A function satisfies a requirement and is realized by a component. A component realizes a function and is associated with a requirement

N2 diagram depicting interfaces in sub-system Wheel

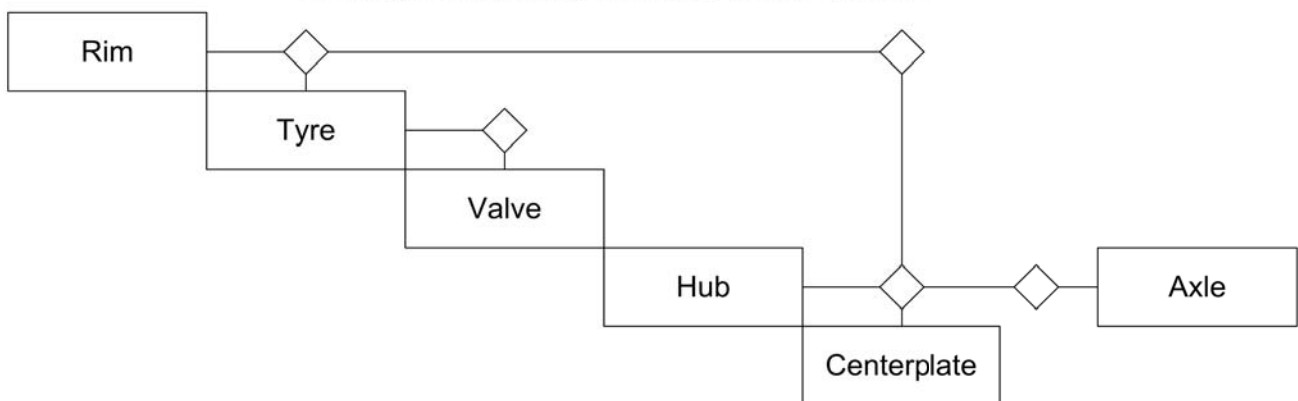


Figure 2.2.6: The elements that make up the wheel are positioned along the diagonal. Lines between the elements show interfaces between them (emphasized by diamonds). The Hub is the part that links the sub-system to the rest of the system

the actual realization of the concept idea. Figure 2.2.7 explains the relationships.

It is imperative that the system model show these relationships. When studying a single element in the model, the model must visualize the relationships this element has with the rest of the model.

The decision to use MBSE in knowledge management is based on MBSE's perceived benefit of increasing learning and easier training of new members of a team. This is achieved by so-called Model-based Documentation. This means linking documentation directly to the element in the model of which it describes. E.g. a K-brief about the production of the windshield could be linked directly to the element Windshield in the model. This way, the model acts as a repository for information. Anyone searching for information about a certain element may navigate through the model to the element-of-interest and retrieve a list of documents, CAD files or photos that directly describe the element. For PDF files, the hyperlinks may also link directly to specific pages within the document.

The system model is found in the root directory of the server space for the 2012 team. It opens in the web browser, and the user navigates through the model much like Wikipedia.

## 2.2.2 VISUAL WORKFLOW MANAGEMENT

The Systems Engineering team employed Visual Workflow Management (VWM) to monitor project progress, enhance communication between team members and spot problems before they occur. The tools used are Stand-up meetings with a tailored Visual Project Board, risk management, and two methods developed by the SE team themselves. Details about these tools may be found in Oluf Tønning's master's thesis. This report gives a summary of the tools and the process.

### 2.2.2.1 Stand-Up Meetings and Visual Project Board

Stand-up meetings are short team meetings where the team communicated to each other what they have done since last time, what will be done till next time and whether or not they are facing problems.

Tønning tailored a Visual Project Board (VPB) for using during the meetings. This is a whiteboard template, where every team member lists their tasks over the next fourteen days. Colour codes tell whether a task is on-schedule or slipping. Figure 2.2.8 shows the VPB for DNVFF2.

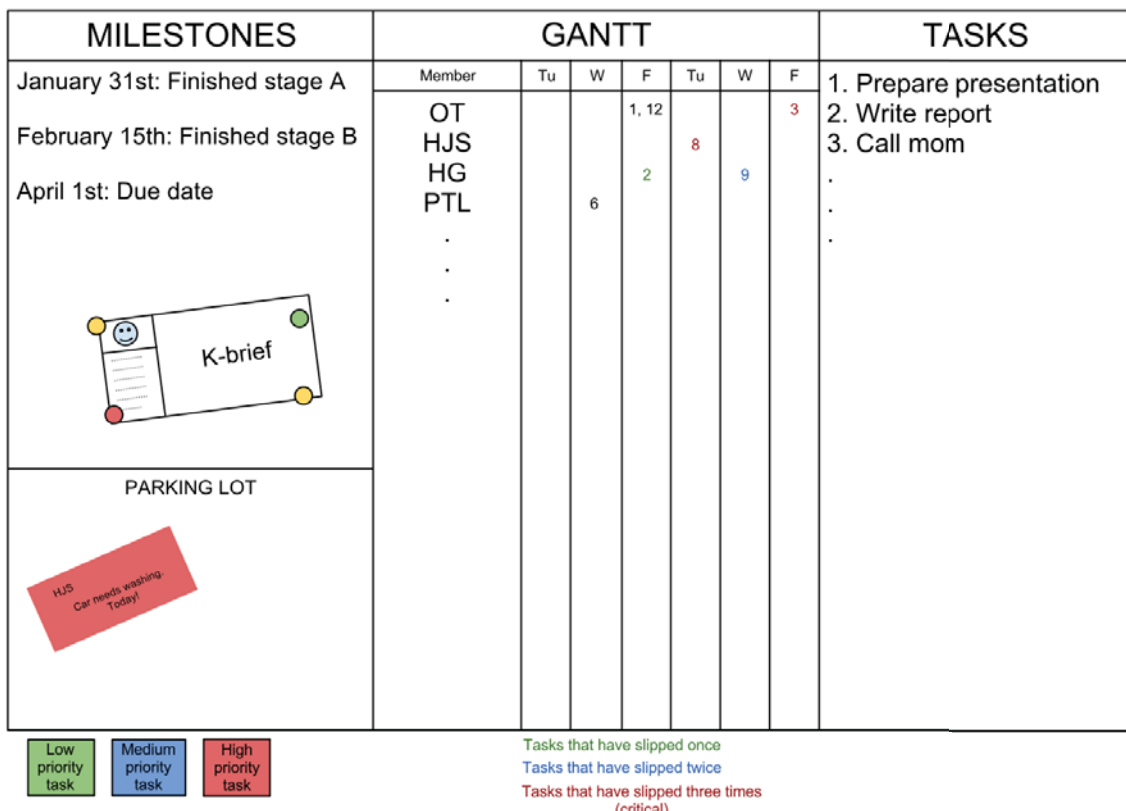


Figure 2.2.8: VPB for DNVFF2. Tasks are numbered on the right-hand side. The Gantt-diagram in the middle shows what day a certain task is due. Colors tell whether a task has slipped or not. The left-hand side is for information and exchanging messages

The SE team made these conclusions about Stand-up meetings and the VPB:

- Maximum number of active participants is 7 or 8
- 12 minutes is the maximum time limit.
- Location matters during production periods. The meetings must be held in or close to the workshop.
- Addressing the three questions (“what have I done since last time”, “what will I do till next time” and “what is preventing me from progressing”) makes the meetings shorter and more relevant to the listeners
- The meetings are best held in the morning, during production periods due to the accessibility of machines.
- Stand-up meetings are very important during the competition, due to the ever-changing environment that a competition is.
- Stand-up frequency
  - During production: three times a week is sufficient
  - During competition: At least twice a day
- VPBs are great tools for managing team work on a micro-level, and for communicating important messages between team members.

### 2.2.2.2 Visualizing Project Progress

The SE team used three tools for tracking and visualizing project progress. The argument for using three different methods was to gain alternative perspectives on the project. The three methods are:

- Average risk level; for early discovery of problems and mitigation
- Timeline; for overall system progress and communication
- Wall-Architecture; for system progress on a micro level and communication

### 2.2.2.3 Average Risk Level as a Tool for Tracking Progress

The system engineers made a huge effort in the risk analysis and management of the project. The first step in the risk management process was to identify the risk. To do so a “risk session” was organized. By arranging “risk sessions” the team identified and analyzed risks on a component level. Using a 1 to 5 scale, the team assessed the likelihood and impact of each risk.

The risks were stored in a Google spreadsheet that everyone had access to. The average risk of

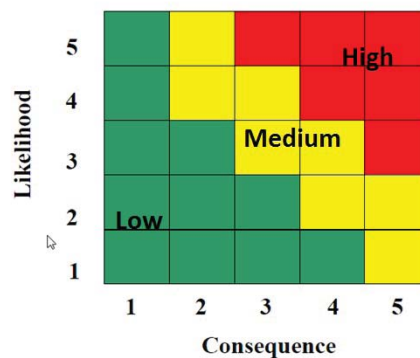


Figure 2.2.9: Risk cube display

the system was shown as a curve, updated on a weekly basis, as shown in figure 2.2.10.

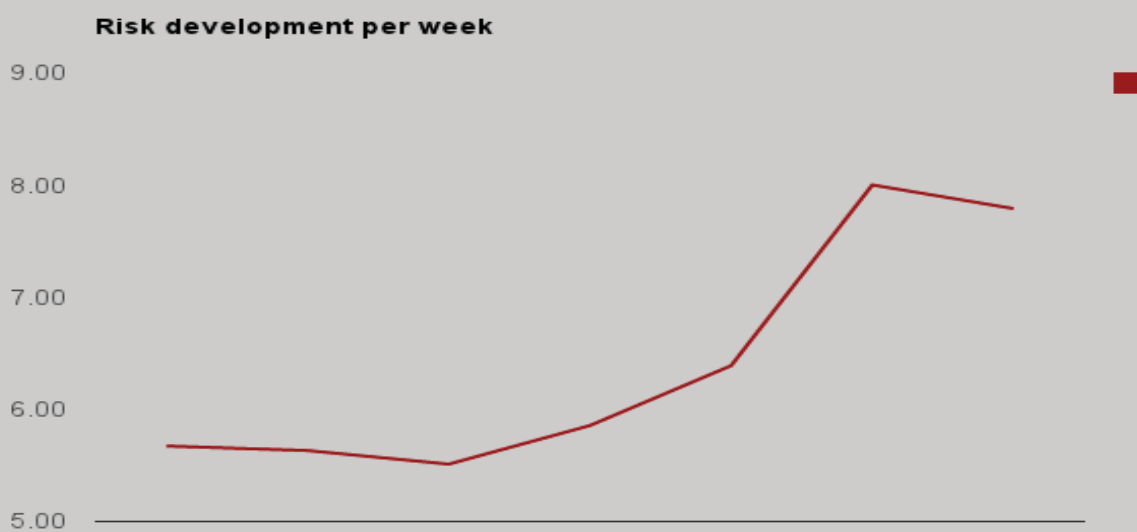


Figure 2.2.10: Curve showing how average risk level developed through the project

This way of visualizing project progress is a very powerful tool for identifying possible problems, and monitoring whether the team is good at solving problems as they are identified. In industry related projects the amount of risks that must be still in the project when the production phase is entered should be as low as possible.

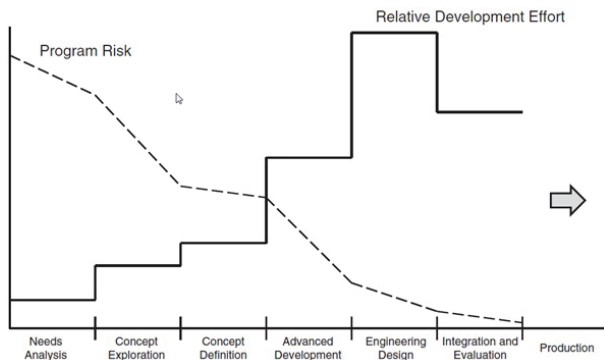


Figure 2.2.11: Variation of program risk and effort throughout system development (Kosiakoff et al, 2011)

However, for this project it did not do as well. Due to lack of expertise and time most of the risks were identified in the production phase. The team was not mature enough when it comes to working with risks, and there was not enough time get the experience needed or enough time to finish a proper analysis. More and more risks were identified, only adding to the risk level. The SE team decided to stop using this tool for visualizing project progress to avoid unnecessary stress in the working group. However, the team sees that this is a very useful tool if it is applied as

early as possible. Since the SEM 2012 team delivers their risk analysis to the next year’s team – an analysis based on experience and knowledge – the next year’s team may utilize this tool to its full potential.

### 2.2.2.4 The Timeline

For monitoring overall project progress the SE team developed a way of visualizing every sub-system’s progress using a timeline. This timeline was drawn on the big whiteboard in the office, next to where the team has its Monday meetings. The timeline was also meant as a place to show important happenings, and to induce a competitive attitude in the team.

The Timeline divides the project into one-week Takt periods. The responsible team member for a sub-system listed the major tasks for every week for the rest of the period of that sub-system. The sub-systems were indicated on the Timeline with pieces, like in a board game. The piece would move closer to the finish line (competition date) relative to the amount of tasks finished. E.g. a sub-system finishing two thirds of its tasks over three weeks will only move two weeks on the Timeline. The Timeline was updated on the Monday meetings.

Team members who were not native to the office, found the Timeline useful for gaining information on happenings and progress. Critique of the Timeline state it should have been employed earlier, with a stronger focus on work planning. Overall, the Timeline is a very useful tool that may gain much popularity within a team.

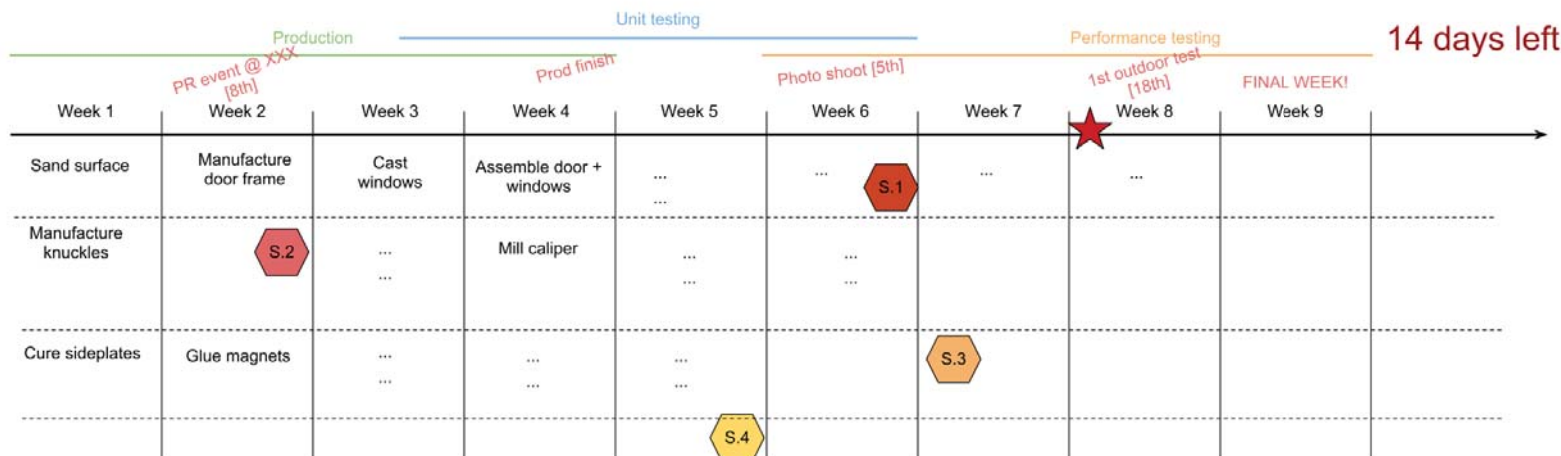


Figure 2.2.12: Template for the Timeline

### 2.2.2.5 Project Progress on a Micro-Level; The Wall-Architecture

To monitor progress on a micro-level, the SE team made use of the system architecture made for the system model (in the knowledge management). The system architecture shows detailed hierarchies of the entire system, down to a component level. By putting these diagrams on the wall in the workshop, the team members could show what components were in production (marked with orange sticky notes), delayed (marked with yellow sticky notes), critical (red), produced (green) and assembled (blue).

This visualization was developed to answer a need from one of the team members who wanted to know more of what was happening with the different sub-systems, in order to know where he could help when he had time available, e.g. while waiting for carbon-fibre to cure.

## 2.2.3 VERIFICATION, VALIDATION AND TESTING ACTIVITIES OF THE DNVFF2

One of the main focuses of Systems Engineering in the SEM project has been to design and perform a qualification strategy. The decision of making such a strategy was based on the SEM history where previous teams have had a lack of testing that made the car less reliable. Besides, the DNVFF2 is a complete new car and therefore testing all the components and its performance is of great importance.

The Verification, Validation and testing strategy was divided into four different and consequent

phases; Unit testing, Assembly test, Performance test and Race test.

More detail about the testing strategy can be found at I.Yuguero-Garmendia (2012).

### 2.2.3.1 Unit Testing

Unit testing takes place at the part or subsystem level the goal of this test phase is to verify that each part that a subsystem is composed of meets its requirements and specifications. Some of the parts of the subsystems were bought but most of them were made by team members. Verifying parts can be done by visual inspection, by measuring dimensions or by stress test to the parts.

The responsible of verifying the parts are the engineers that have designed that part.

### 2.2.3.2 Assembly Test

The assembly test phase was divided into two, the mechanical assembly test and the engine and the control system test. The main goal of this phase was to test all those Shell Requirements that are not related to performance and to check the interfaces.

The first testing day was done indoors with a smooth surface. The NTNUI let the team use Dragvoll's sport center. It was an excellent place to test the visibility of the car, to check Shell requirements and also to test the mechanical subsystems. The team thought that it would be a good idea to test the car for the first time on a smooth surface where the car was not going to be extremely demanded.

During the first day of testing some cones were set in zigzag. At the beginning the cones were quite far from each other, the steering was

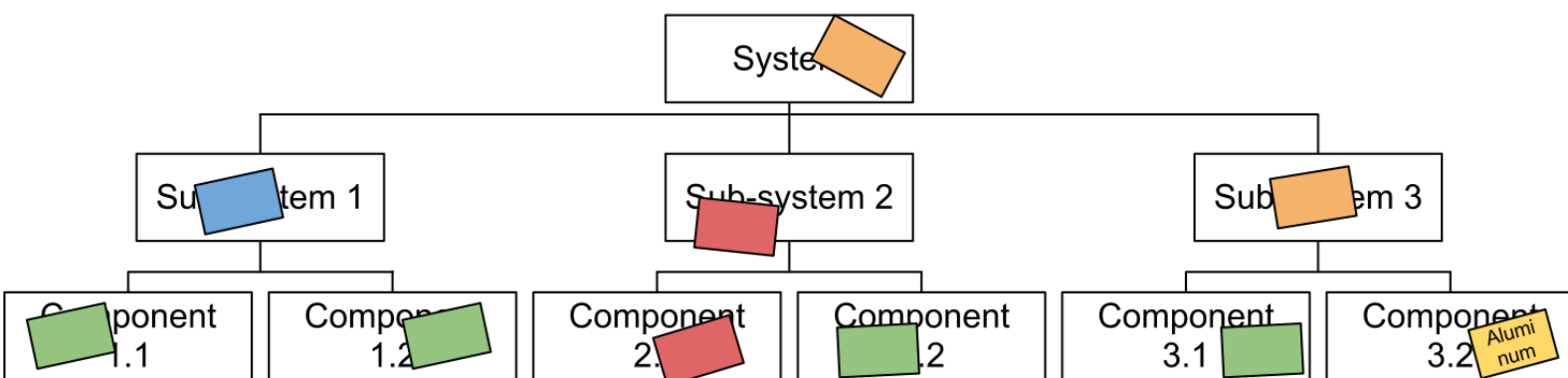


Figure 2.2.13: Template for the Wall-Architecture. Orange means "in production", red is "critical", yellow is "pending", green is "produced" and blue is "assembled"

performing well, then the distance between the cones was narrowed and at the 3rd trial one of the pulley mounting points that are used to support the Kevlar cable of the steering fell off. The surface where the pulley's mounting point was glued to the carbon fiber was not big enough. This problem was fixed by increasing the contact area between the pulley and the monocoque.

After the first test, when the car was in the workshop one of the rims experienced a small crack, the team thinks it was due to some problem during manufacturing at HPC. See chapter 3.6.

After testing and verifying the car at a smooth surface the next step was to use Dragvoll's parking lot to test the mechanical properties of the car under a more demanding surface. The engine was not on the car yet so the team members pushed the car to check rolling, braking and steering capabilities.

An example of the test procedures that were performed during the assembly test can be found in appendix H.

The other assembly test part refers to the engine and the control system. The assembly test of these two subsystems was held at SmartMotors. In order to test the propulsion with the control system a test bench that is located at SmartMotors was used. Not having an in house test bench made impossible to test as much as the team wanted as the sponsor was not always available.

The complete drive train was tested on test bench with different loadings at different speeds to measure efficiency for different operating points. The test bench was also used to study battery behavior for low battery voltage and over current. The DNVFF2 had two different types of batteries, one was provided by Altitec and the two others by Gylling.

The second battery pack from Gylling was ordered since the team thought that the one that was already delivered was not going to be able to provide enough energy to finish one attempt. This decision was made based on the tests made at SmartMotors. The issue with this decision is that it was based on the tests done to Altitec's battery, it was seen afterwards that it was not necessary to have ordered another battery from Gylling since the first one was able to supply more than enough energy. The cybernetic and electric engineers of the DNVFF2 had almost no time to test and that is the reason why the test were made for just one of the batteries, the one that was supposed to be the race battery.

The outcome of these tests was used to discover that under voltage protection was needed to prevent complete stop while racing, torque limitation to prevent under voltage and over current to prevent still stand while racing. Measurements were used to find the most energy efficient velocity/torque profile for the given track.



*SEM 2012 team preparing the visibility check*



### 2.2.3.3 Performance Test

Tests were performed in Dragvoll's parking lot, as it was impossible to get the airport or the army installations that last year's team used, the team also got the approval to test in Trondheim Havn but due to weather conditions and time problems it was not possible to test the car there.

Propulsion- and control systems were given most attention during this test, as most of the mechanical parts had already been tested. The rear suspension was tested in relation with the heavy motor as it was not designed to be used with this one. Starting parameters were tuned to the drivers weight. The starting parameters were tested with different starting slopes to check if the engine was able to supply enough torque. When the car was driving uphill, the motor had problems applying enough torque. Some motor

parameters and vectors were changed to solve this issue. The last adjustments had to be done in Rotterdam as the starting slope was not known.

The maximum speed could not be tested due to too little space. Ability to turn at high speed was tested for the car, with a satisfying result. Coasting made the turns even smoother as the engine was not supplying any torque.





*Left: SEM team at Dragvoll's parking lot  
Right: Performance test*

 DNV FUEL FIGHTER 2



DNV FUEL FIGHTER 2

# 2.3 PROMOTION



The whole project was depending on support from sponsors to survive, and to keep them interested, different kinds of promotion were done. Events, newspapers, TV and social media gave both the team and the sponsors important attention.

# DNV FUEL FIGHTER 2



# DNV FUEL FIGHTER 2



### *Graphical Profile*

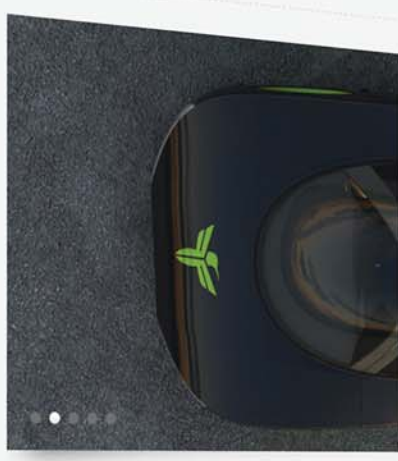
This years graphical profile was a simplified version of the previous years logo. The small collibri was still the main part, but with green colors and a simplified font.



THE ONLY NORWEGIAN

*Promotion Video*

Student TV was hired to make a promotion video for the team and the project. The result was a 2:29 minutes video that could be found on the webpage of the team.



## Blogg



av Silje, på mai 18, 2012 - | 1 kommentar

### Konkurransedag!

Let the game begin!! I dag har vi hatt vår første konkurransedag, og det har vært nervepirrende, skuffende, optimistisk og positiv på Tromsø (foreldrene til Håkon følger oss). Vi har [...]

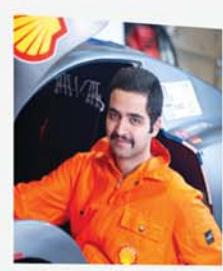
[Les mer](#) →



av Silje, på mai 17, 2012 - | Ingen kommentarer

The PM SEM 4 BILDE 2.jpg download has completed.

## Om Teamet



**Prosjektleder**

Fariborz Ali Heidarloou  
 Alder: 24  
 Hjemby: Tehran, Iran  
 Tlf: 451 19 914  
 E-post: aliheida@stud.ntnu.no  
 Utdannning: Bachelor i industriell ingeniørvitenskap, master i prosjektledelse



**PR og Media**

Silje Kristine Skog  
 Alder: 25  
 Hjemby: Trondheim  
 Tlf: 980 53 336  
 E-post: siljekri@sti  
 Utdannning:



**Systemingeniør**

Itxaso Yuguero Garmendia



**Motor**

Fredrik V. Endresen

### Om oss

DNV Fuel Fighter 2 er en studentgruppe fra NTNU som skal delta i den internasjonale konkurransen, Shell eco-marathon 17-19 mai i Rotterdam. Gjennom dette prosjektet ønsker vi å være en arena hvor studenter kan utfordre seg selv både faglig og sosialt, og gjøre studentene bedre rustet til å møte arbeidslivet.

### Hva gjør vi

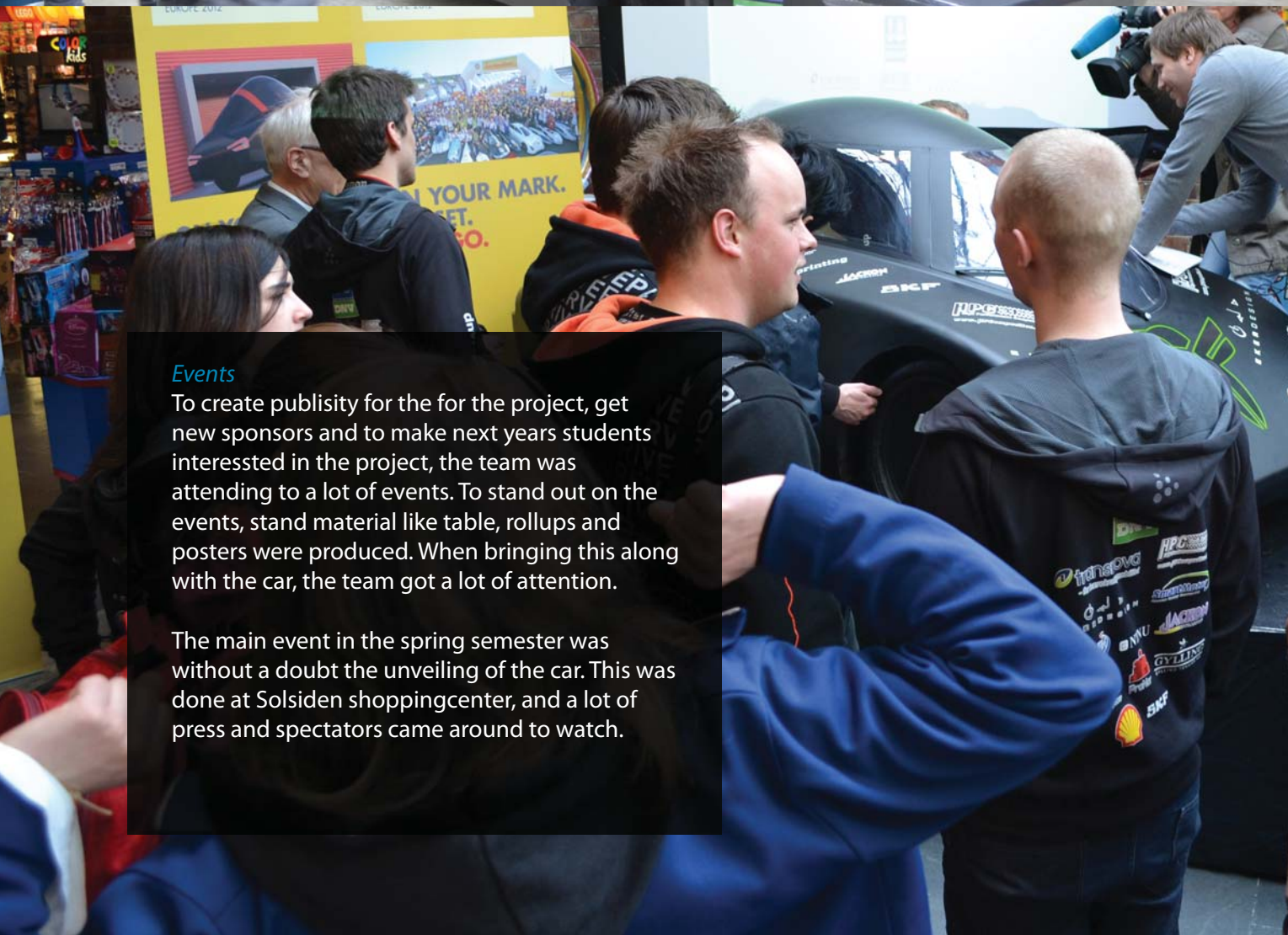
Målet med denne konkurransen er fremme løsninger for smartere Studenter fra ulike Universitet i Europa konstruerer motordrevne som skal kjøre så langt som mulig på mengde energi. Studentene designe og bygge en bil basert på tankegang og tekniske løsninger.



**Homepage**

When deciding what kind of webpage was wanted, the whole team agree that it was important that each member could edit it on their own. In this way one would get more updates, and therefore more visitors.

Wordpress was chosen as the Content Management System used on the page. This would allow all members in the team to have their own username and password, and blog posts could be added from anywhere at anytime. The system would also be easy to transfer to next years to, so that they could just continue filling it with posts.



**Events**

To create publicity for the for the project, get new sponsors and to make next years students interested in the project, the team was attending to a lot of events. To stand out on the events, stand material like table, rollups and posters were produced. When bringing this along with the car, the team got a lot of attention.

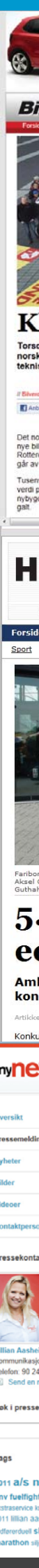
The main event in the spring semester was without a doubt the unveiling of the car. This was done at Solsiden shoppingcenter, and a lot of press and spectators came around to watch.



**NRK**  
Nyheter

### TV and Newspapers

To get as much media coverage as possible, the team hired a person to be responsible for PR and media. Even though the team got several TV interviews and a lot of newspaper articles, it was never close to the goal of 150 articles and 3 appearances on TV.





**Sommerpris på Polo Summer**  
fra 193.800,- - Spor 1500,-  
Les mer

**Norge.no**  
Abonnement Annonse- og medlemsinfo Om oss  
Billetter Bilnyheter Nybilpriser Bilutleie Bilutleie Bilutleie Bilutleie  
Bil // Genve 2012 // Larsengskalendar // Spor 1500 // Bilbilde // Bilspil // Bilutstillinger // Bilhistorie

**Start for Eco-maraton**  
Laget, på selveste 17. mai, starter årets utgave av Shell Eco-maraton. Det er laget går for ny verdensrekord. Men i dag råder usikkerheten i laget, siden de samme problemer truer med å sette en stopper for forsøket.

Publisert 19.05.2012 kl 16:06

**NYE PEUGEOT 208**  
OPPDAG EN NY SIDE AV PEUGEOT

**Hegnar Online**  
Sport

Hovedstørrelse: Dollar Euro Britiske Gall Spis Nibor 31 Dow 30 Nasdaq

Økonomi Aksjer Valuta Personlig økonomi IT-Kanalen Juss Liv

**5. plass til nordmenn i Eco-marathon**  
Ambisjonen var å ta ny verdensrekord, men årets konkurranse ble tøff for det norske laget.

av: Stein Ove Haugen (HegnarOnline - 20.5.12 08:58)

Arrangansen i årets Shell Eco-marathon var så... Del på: Facebook Twitter

**WSdesk** Search news Search companies Create ad

**A/S Norske Shell**

Feirer nasjonaldagen med testkjøring  
17.05.2012 15:11

Blant 3000 ungdommer og over 200 eksperimentelle kjøretøy i en stor hall i Rotterdam, er valgfritt et noe unvanlig innslag. Shell Eco-maraton er i full gang men det norske laget tar seg usansett tid til en liten nasjonaldagspause.

Valfer og medbrakt brunost blir raust delt ut fra de norske studentene, som har tatt et lite avbrekk fra bilen. Det er viktig for dem å få en liten smak av nasjonaldag, og omkranset av norske flagg er valfrelst i full gang. Franske og spanske studenter stiller seg litt undrende over tiltaket, mens svenske raskt skjønner hvorfor vaffelduften brer seg i hallen og stikker gjema innom for å være med på feiringen.

17. mai blir også dagen hvor bilen til studentene skal prøves på banen for første gang. Fra nå av følger løttere norske sleminer, er det i dag et mer avslappet

**NRK** Nyheter TV Radio Snarveier

NRK > Nyheter > Distrikt > NRK Trøndelag  
Trøndelag

**- Vi er veldig fornøyd**

Den lille svarte bilen kjørte 1581 km på det som tilsvarer en liter bensin. Laget fra Norge kom dermed på femte plass i Rotterdam landag.  
Foto: Lillian Aasheim/AV Norske Shell

**Det norske laget fra NTNU kom på femte plass i årets utgave av Shell Eco-maraton i Rotterdam.**

ELLA BERIT MATHEDEN  
ella.berit.matheden@nrk.no

Publisert 19.05.2012 16:04. Oppdatert 19.05.2012 17:00.

Del Tweet 40 5 Del/Tips Skriv ut

Målet var å kjøre lengst mulig på den energimengden som tilsvarer en liter bensin.

**Lenker**  
NTNU-studenter går for ny verdensrekord  
- Dette bør bilindustrien NTNU-til på andreplass i drivstoffkonkurranse

**E24 BIL**  
NYHETER BØRS JOBB MEDIA BIL KOMMENTARER

**Femteplass for norsk øko-bil**

Bilde 1/6: SPENSTIG DESIGN: I kanskje verdens mest miljøvennlige bilopp, Shell Eco-marathon, er målet å kjøre så langt som mulig på 1 liter med drivstoff. Det er årsaken til de ovnlige, strømlinjeformede bildesignene. Foto: Eivind Amundsen

**Med ambisjoner om verdensrekord, ble det femteplass for NTNU-studentene i årets mest miljøvennlige bilopp.**

**BIL** John Aare  
Publisert: 20.05.2012 14:13. Oppdatert: 20.05.2012 17:24

Selv om ambisjonen var å ta ny verdensrekord, var årets konkurranse i Shell Eco-marathon i Nederland så tøff at det norske NTNU-laget måtte se seg fornøyd

RSS: Abonner på siste nytt

**ua** Universitetsavis.no  
Forsiden | Student

**Avduket Fuel Fighter**

**Fredag dro rektor Torbjørn Digernes sløret av Fuel Fighter II. Allerede 17-19 mai står kjøretøyet på startstreken i Rotterdam for å delta i en konkurranse i Rotterdam hvor Europas mest miljøvennlige bil skal kåres.**

Tore Oksholm  
Mobil: 91897678

Publisert: 07.05.2012 kl. 12:48  
Endret: 07.05.2012 kl. 13:50

**Relatert**  
Fuel Fighter II

**Student**

"Shell EcoMarathon" har blitt arrangert i over 20 år. I fjor deltok 262 lag fra 20 land og 3100 fra NTNU i konkurransen. Dette er verdens største studentkonkurranse.

# Vil sette verdensrekord

**TRONDHEIDE:** Hans Gudvangen (24) fra Auro og 12 andre NTNU-studenter skal prøve å sette verdensrekord i stor internasjonal konkurranse.

**NRK** Nyheter TV Radio Snarveier

NRK > Nyheter > Distrikt > NRK Trøndelag  
Trøndelag

**NTNU-studenter går for ny verdensrekord**

Det norske laget er på plass i Rotterdam og håper at helga vil gi en ny norsk verdensrekord.  
Foto: Lillian Aasheim

**NTNU går for ny verdensrekord i årets utgave av Shell Eco-maraton i Rotterdam.**

JULIE HAUGEN EGGE  
julie.haugen.egge@nrk.no

Publisert 17.05.2012 16:01.

Del Tweet 5 0 Del/Tips Skriv ut

Torsdag, på selve nasjonaldagen, er det norske laget fra NTNU på plass i Rotterdam hvor de driver med testkjøring for årets konkurranse i Shell Eco-maraton starter.

- Det har vært en helt perfekt 17.mai. Bilen fungerer som den skal, og vi er veldig fornøyd, sier talsperson for gruppa, Silje Skogrand til NRK.no.

bygger bil:

# Snerten og energieffektiv

Studentene bak DNV Fuel Fighter 2 håper bilen kommer på førsteplass, og samtidig blir den fineste bilen av alle i konkurransen.

**DNV Fuel Fighter 2 suser snart avgårde gatelangs i Rotterdam. Men kan en energieffektiv bil også se kul ut? I dag viste designerne fram utseendet til bilen.**

Solveig Mikkelsen  
Mobil: 971.08.222

Publisert: 08.02.2012 kl. 14:41

- Dråpeformet, sier designerne Mats Herding Solberg og Eivind Sæter. En bil bør likne mest mulig på ei dråpe for å ha liten luftmotstand.



# 2.4 ROTTERDAM





## 2.4.1 SHELL ECO-MARATHON

The 2012 competition was held at the sport and concert venue Ahoy, south of Rotterdam. Shell claimed as many as 50,000 people visited the event during its four day duration. The track surrounds the venue, on parking lots and small roads. Shell has stated that the competition will be held in Rotterdam also in 2013. It is possible that Ahoy will be selected as venue again.

Every team had their own 5 m x 4 m paddock inside the main building. This area was also open to the public during daytime. The participants could spend the night here, but could not leave the area and return after 23.00.

The paddock quickly became cramped for Urban Concept cars, as they are bigger in size than prototype cars. Upon arrival, the paddock contained a locker, two chairs, a table and a power outlet. Bringing foldable chairs and a refrigerator for refreshments and food, is well worth it. The 2012 competition started on Monday May 14th. Teams registered and unpacked this day.

### 2.4.1.1 Track

For the first time in SEM history the competition was held on a street track. All the previous years that NTNU has participated the race has been on a race track. All the information concerning the road characteristics and quality was unknown for the SEM 2012 team. Next year's competition will also be held in Rotterdam. Therefore it might be important to share gained knowledge about the track.

Figure 2.4.1 shows the track but does not give any information about elevation. The official track length is 1630 m but the actual length, obtained by calculations, is 1602 m. A valid attempt will consist of driving 10 laps around the track in 39 minutes stopping once in each lap; this means that the average speed has to be 25 km/h. The track has some elevations that if not foreseen can cause invalid attempts or higher energy consumption. There is a defined place to stop the car but not a well defined stopping line in the track. Drivers can choose where to stop as long as it is within the stopping area defined by Shell. There was an elevated pedestrian crossing within the stopping area. If the car stops right before the elevation it will not be able to start again, due to high torque. The driver of the DNVFF2 was able to stop on top of the elevation in all runs.

The track was divided in four different sections, seen in figure 2.4.1. This was done in order to optimize the energy consumption (section 3.8).

One of the main changes that the DNVFF2 has implemented in contrast to the prior DNVFF has been the introduction of a fully damped suspension. The decision of introducing suspension was made when Shell announced that the race was going to be in a street track. The most of the other participants were competing with a stiff suspension. However, after examining the track and realizing that the road is quite bumpy the SEM 2012 team still believes it was a good decision to implement a new suspension.

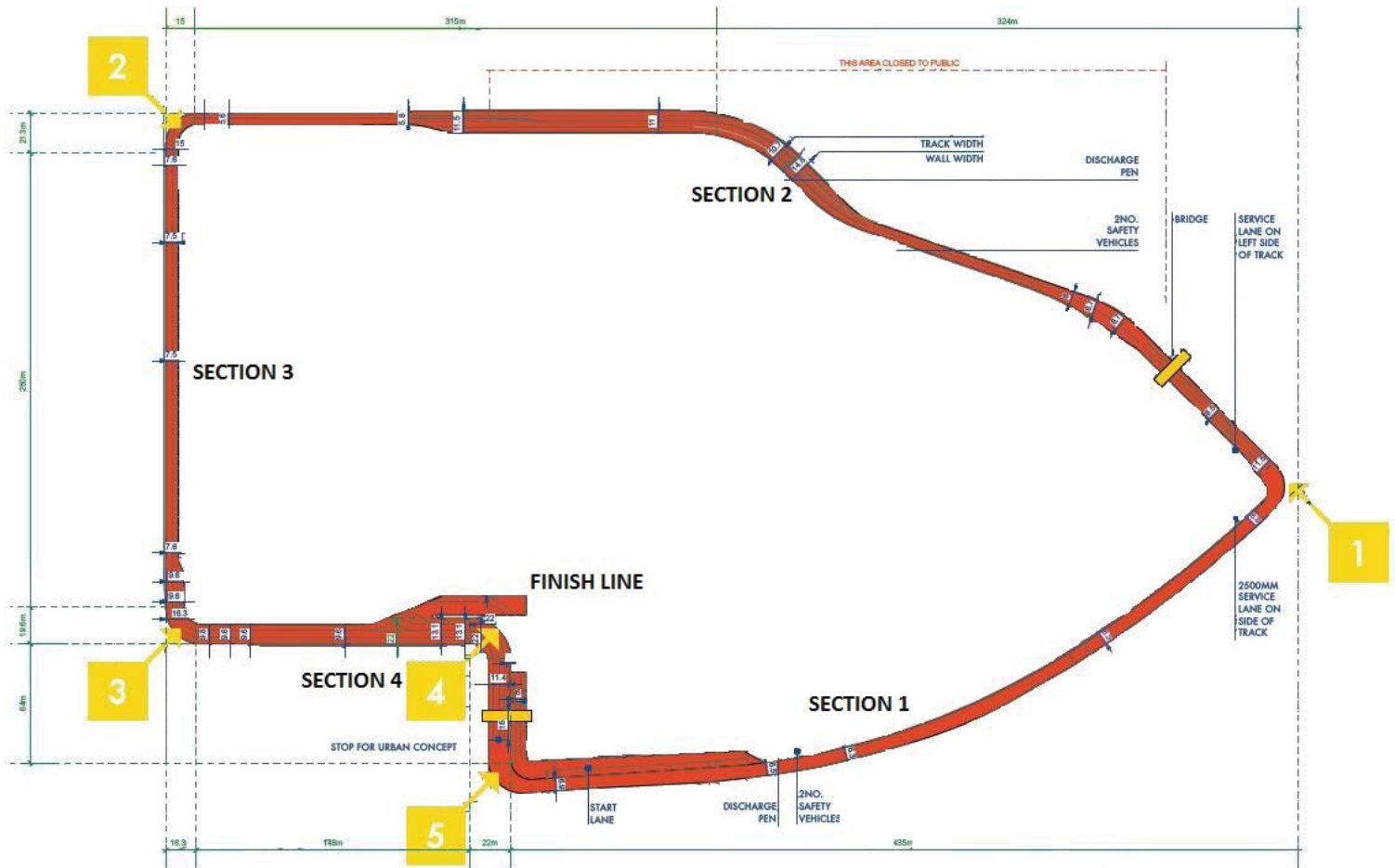
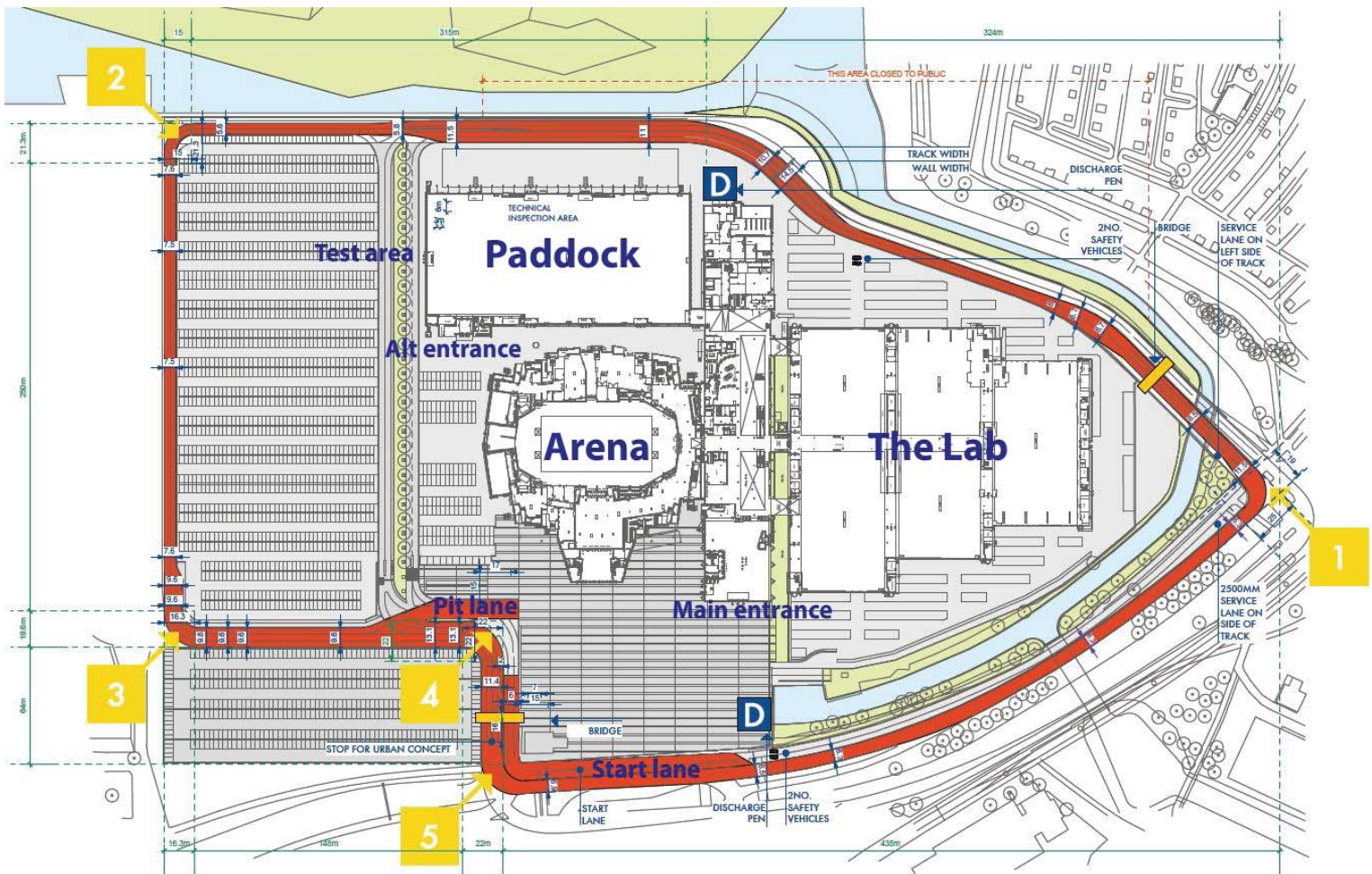


Figure: 2.4.1: Map of the Ahoy. The track is highlighted in red. The numbers indicate corners and driving direction



DNV FF2 being weighted

### 2.4.1.2 Technical Inspection

The team leader, both drivers and a fourth team member are allowed to the technical inspection. The SEM 2012 team decided that the cybernetics engineer would be the fourth team member, so he could answer the specific battery electric questions.

The technical inspection started Tuesday May 15th. It was important to be one of the first cars through technical inspection. This way more time could be spent fixing the car if it did not pass. The car entered the queue at 07.00. Seven cars were already in the queue and more kept on coming.

First the car and both drivers were weighed. Then the dimensions of the car were checked.

Shell Marshalls made sure the Shell logos and team stickers fulfilled the rules. Also the suitcase dimensions were measured.

The next step was to measure the brake effectiveness. This was done on a 20% slope. Visual inspection of the brake system was also performed.

The next step was the visibility check. It was obvious to the Marshalls that the front visibility was not a problem, so it was not checked. The driver was fully harnessed while the rear visibility was checked.

A Marshall walked behind the car with a stick. The driver had to say when he/she first saw the stick and when it was no longer possible to see.





After the visibility check, both drivers had to be able to vacate the car in less than 10 seconds.

The following tests were related to mechanical parts. Marshalls measured the tires' dimensions. They also made sure there were no sharp edges inside the car that might hurt the driver. The lights and the windshield wiper were also checked.

The last step in the technical inspection is the one that studies and verifies the propulsion system. In the SEM team the car is battery electric so the last test was to give information and to show the electrical system of the car. This part of the technical inspection was terribly hard for the team, luckily the Cybernetic Engineer was there

to answer the thousands of questions of the Marshall. The team was not lucky in this part because it was the first battery electric car in the inspection and it was used by the responsible of battery electric cars to brief the other marshalls about the information that they need to ask the teams.

The team did not pass the technical inspection at the first attempt. Questions related to the BMS of the auxiliary battery were not answered precisely enough. The Marshall was later brought to the paddock. After some research the team was able to answer the question satisfactorily and passed the technical inspection.







### 2.4.1.3 Testing

On Wednesday, May 16th, the track was open 3.5 hours for testing. During the first test the upper part of the door flew open.

The door was taped as a temporary fix so the testing could continue. The car reached its top speed of 36 km/h in section 1. High speed during cornering was not a problem.

In section 2 the car shut down. The same thing happened twice and also one time in the middle of section 1. Due to small elevations on the road the engine needed to supply a higher torque than expected. After the first shut down, the team was highly concerned that the battery might be damaged. The battery was checked and found to be in perfect condition. Then another attempt was done. Again the car shut down in section 2. During the last attempt this day another battery was used. This ruled out battery problems as the car shut down again.

Back in the paddock it was discovered that the BMS shut off the battery due to high current. There was also a problem with the coasting code, causing the battery BMS to shut down.

It was decided to test both batteries to see which one would provide the best chance of having a successful attempt. The code of the propulsion system was changed to reduce the maximum torque that the engine could supply. Coasting

would no longer set reference speed to zero. Pressing the coasting button triggered a deceleration function. The car was then consuming a small amount of energy. To coast without any energy consumption, the driver had to activate the brake pedal.

On May 17th, it was the last testing day and UC cars had 2,5 hours of testing. A test plan was developed to test both batteries and the new code for the Gylling battery. The plan was to start the testing with the Gylling battery to check if the problem with the BMS was solved. The car run for 3 laps with the Gylling battery and the result of the testing was successful.

Once the team had proved that the Gylling battery worked, the Altitec battery was checked. It was not able to supply the same energy as the Gylling battery. The acceleration was slower and the top speed was not reached. After the first stop, the car was not able to start again. The battery could not supply enough energy to start the car.

It was chosen to use the Gylling battery for the last test. The car drove 12 laps and the battery supplied sufficient energy.

More information about the batteries is provided in the K-brief in appendix G.

#### 2.4.1.4 Race

Friday 18th was the first race day for Urban Concept cars. 3,5 hours were set aside for racing. The first attempt was a safe run, where the motor parameters were set to safe values. This gave a valid attempt, and more risky parameters could be used.

Due to poor preparation routines the first attempt was not valid. The door came loose, and the driver was forced to end the attempt as she could not fix the door while driving.

The door was quickly fixed and properly secured, and the second attempt was started. This attempt was valid, and the team registered a result of 136 km/kWh.

It was decided to reduce the air gap in the motor to increase the efficiency.

Saturday the 19th was the second race day. Urban Concept cars had 4,5 hours available for racing. The first attempt was successful, earning a

result of 163 km/kWh. Winds were favourable and the vehicle did not have to overtake any cars.

The last attempt ended in failure. One of the steering cords snapped on the fourth lap. The cords were inspected before starting the attempt, and showed no signs of wear. From inspecting the vehicle and photos taken during the attempts, the team concluded the snapped cord was a result of multiple factors. Photos show that the outer front wheel does not touch the ground in some of the turns. From inspecting the vehicle, it was discovered that the grease on the draglink was saturated with dust from the track, causing the draglink to slide with high friction. These factors – along with the Z-rod (section 3.4) in the front suspension – may have contributed to undesired stresses on the steering cord.

The result from the third attempt became the final result for the team, giving the DNVFF2 a 5th place in the Urban Concept battery electric category. 22 teams entered, 20 teams passed the inspection and 15 achieved a valid result.



3

KERDESIGN  
ansnova  
for bærekraftig mobilitet





**TECHNICAL**

**TRANSIOND**  
- for bærekraftig mobilitet

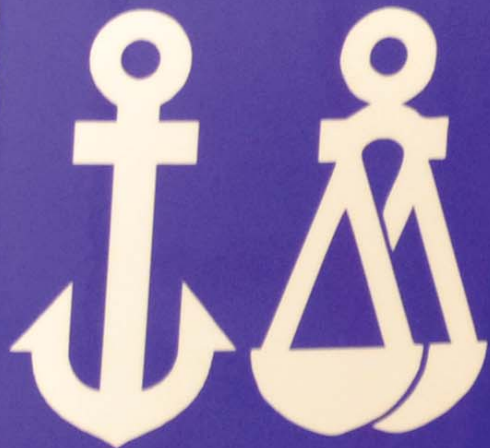
LEADERS  
DESIGN



**tra**  
- for bæ

# 3.1 EXTERIOR

**nsnova**  
*rekraftig mobilitet*





## 3.1.1 INTRODUCTION

The design of the body and production planning was completed in autumn 2011.

Final models were made and milling of the molds was executed at Eker Design. Actual layout and production was performed at High Performance Composites in Fredrikstad. A lot of work went into the final assembly of the body in the workshop at NTNU.

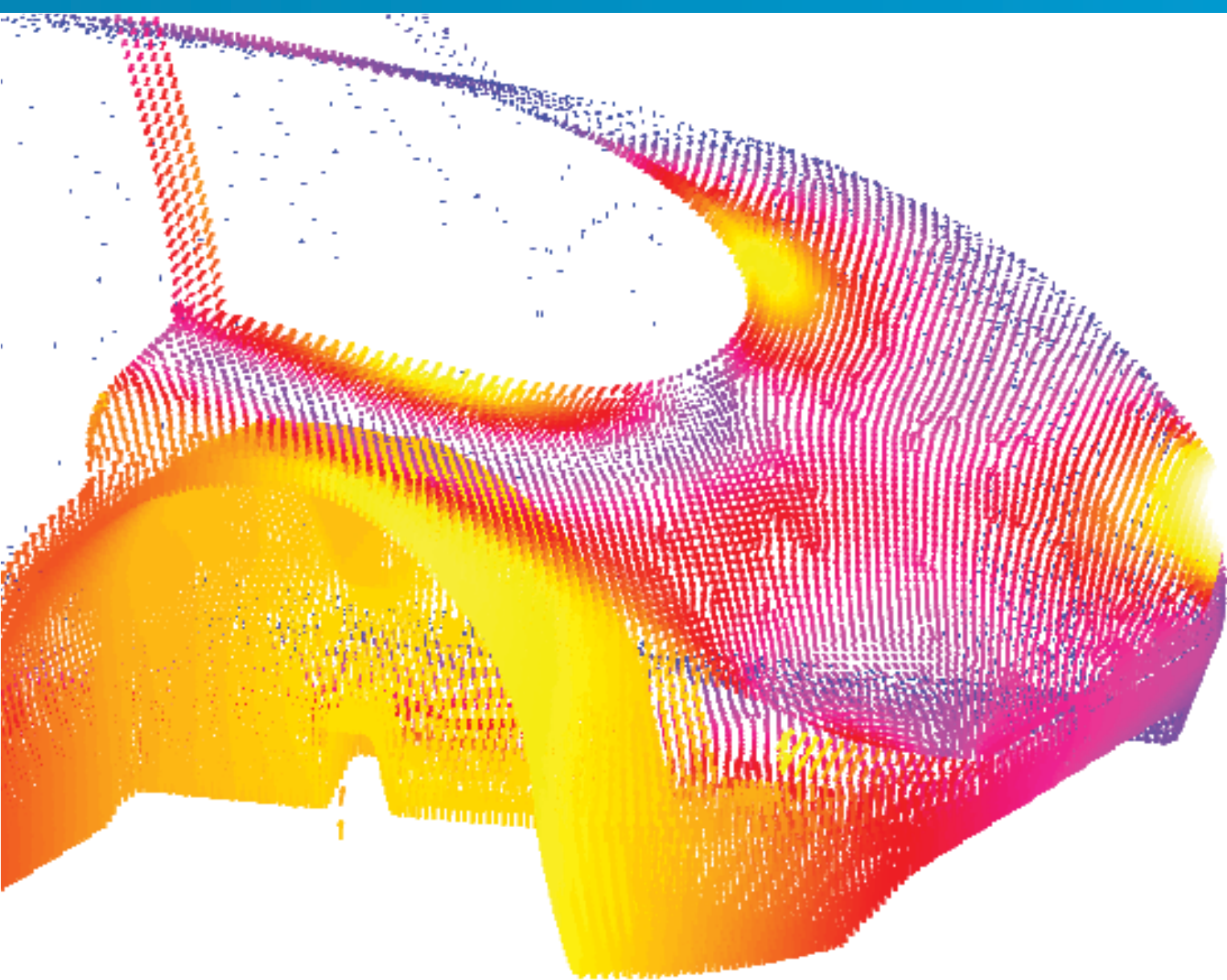
Detailed components, such as hinges, covers, towing hook and windshield wiper have been designed and produced. Windows for the monocoque had to be produced in-house, and special equipment was made for this purpose.

Exterior graphical design was defined and applied by Bilreklame to the surface of the car.

To verify the computational fluid dynamics results, the exterior has been tested in the wind tunnel at NTNU.







## 3.1.2 STRENGTH ANALYSIS

This work is a continuation of the work performed in the autumn 2011 (Endresen, et al., 2011). A more detailed load case and better boundary conditions have been developed. The load cases are reduced to the worst case, and applied in the most critical part of the vehicle. A layout configuration for the monocouque has been optimized and tested. The material data used in 2011 was changed due to change in production method.

### 3.1.2.1 Boundary conditions

To reduce the complexity of the problem, it was decided to reduce the number of load cases and only focus on the most critical load. The case that

would give the highest stress concentrations in the car is when the car is cornering and experience unevenness in the ground. The load values for this case are given by the calculations from 2011 (Endresen, et al., 2011):

Driver	70 kg
Cornering	510 N
Bump	780 N/960 N

These loads are applied in the left front wheel well. This is considered to be the weakest part of the vehicle, due to the door opening and little transverse support in the front. The suspension loads are located in the wheel and connected to

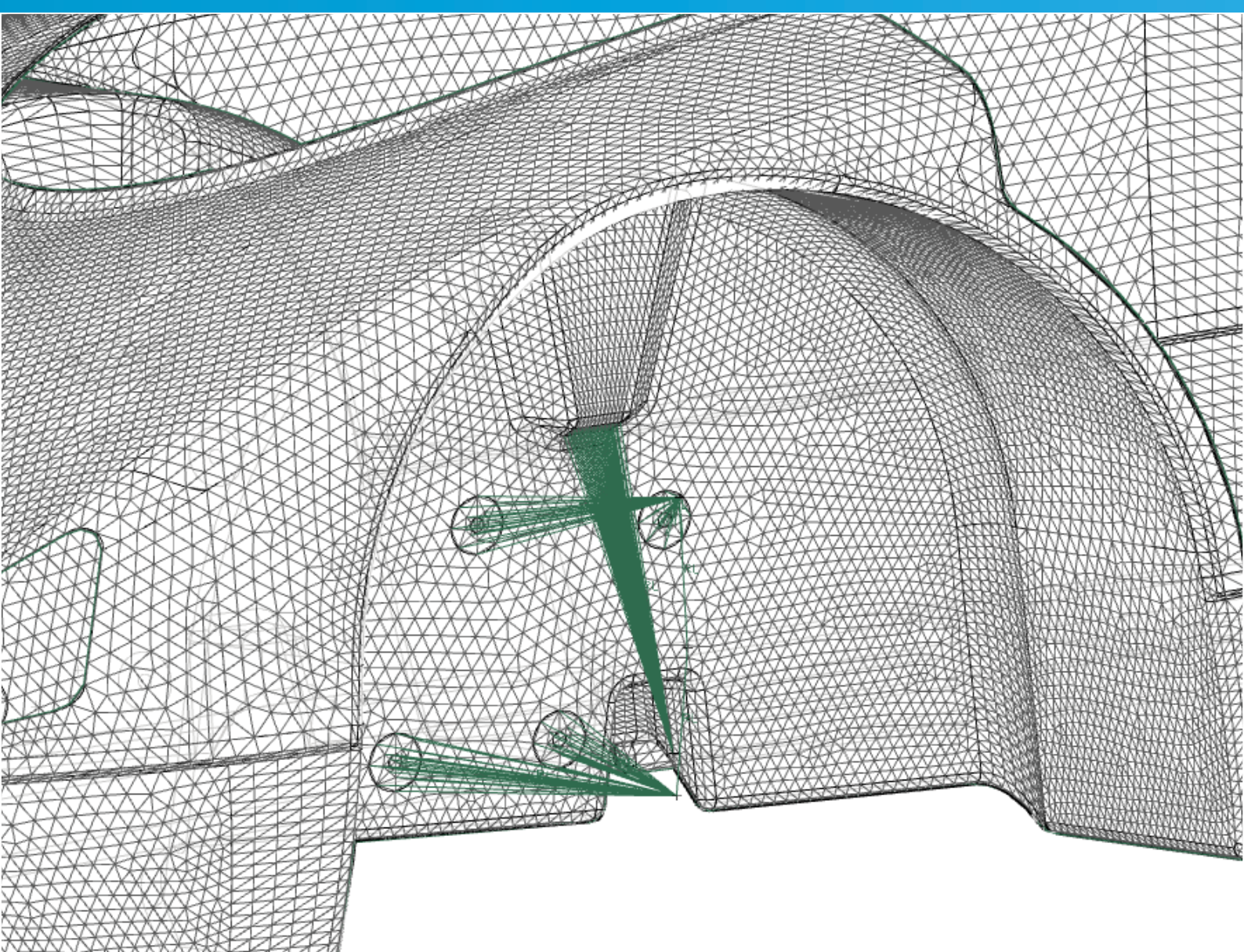


Figure 3.1.1: Suspension system modeled with RB2 elements, loads and moments are applied in the wheel center and transferred into the body through the stiff suspension system.

the body through RB2 elements.

When simulating the loads on the front left wheel, all other wheel wells are fixed. This is to remove the large reaction forces in these areas. The forces will generate a high moment in the other wheel wells, creating unrealistically high stress concentrations. The focus will only be on the front wheel well, therefore, the other wheel wells are of no interest. To remove any high stress concentrations in these areas, the wheel wells are sufficiently fixed.

To verify that the car is sufficient durable, the load case given by the SEM rules are also tested.

Driver	70 kg
Roll bar load	700 N
Towing hook load	2000 N

When applying this load case, the car is fixed in each hub with free rotating in longitudinal direction, which will represent real testing conditions.

### 3.1.2.2 Layup

The layup started with applying two layers of DB420 (Appendix B) on the entire body in a crisscross pattern. The floor of the car was reinforced with 10 mm thick Divinycell 80 core to add stiffness and to withstand the stresses from the driver. Two extra layers of DB420 on both sides of the core were added to give the sufficient strength to the underside of the body. The wheel wells were considered to be the most critical parts and needed the most reinforcements. A 6 mm Divinycell 80 core was placed on the side walls and total of 4 layers of DB420 were laid over the entire wheel wells. The roof was reinforced with 6 mm thick Divinycell 80 core. Figure 3.1.4 shows the overall layup for the car.

Displacement - Nodal, Magnitude  
Min : 0.000, Max : 10.968, mm

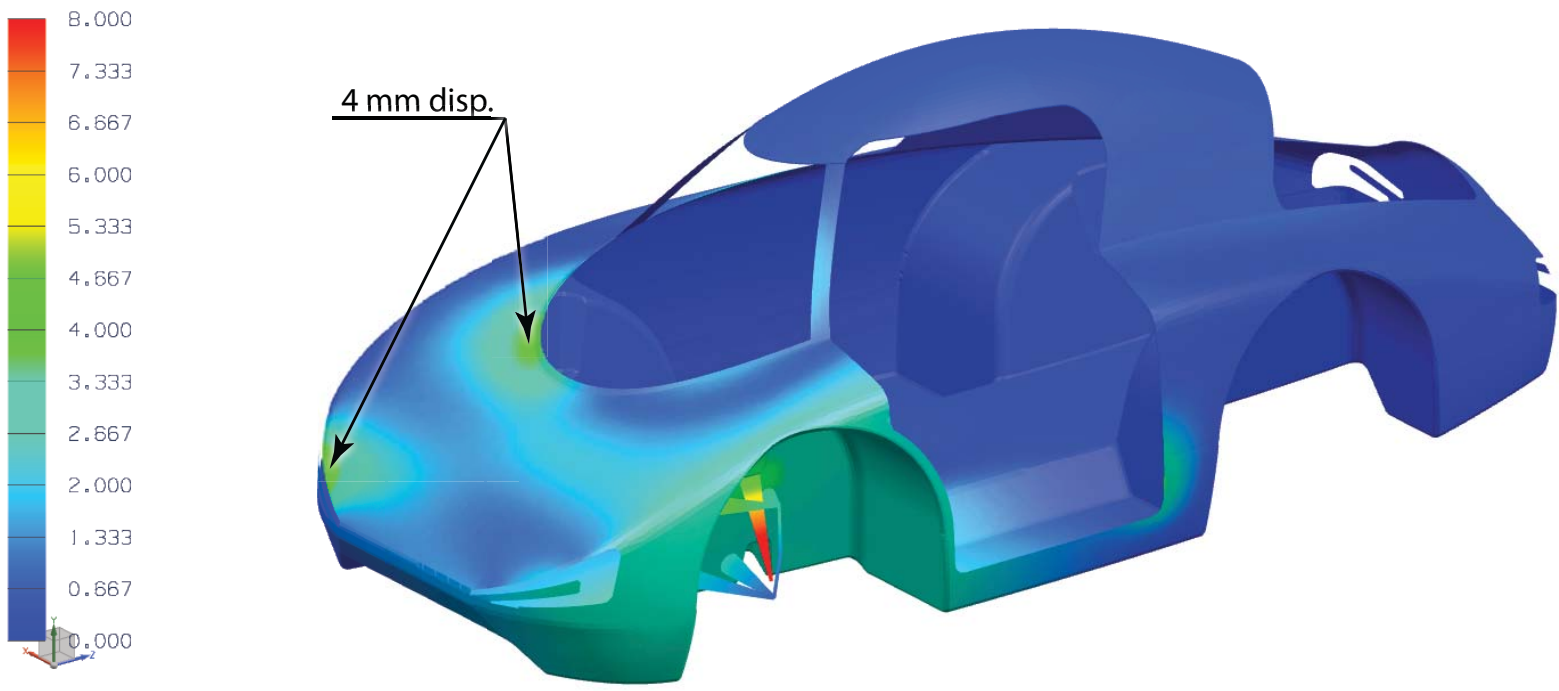


Figure 3.1.2: Displacement due to loads during race conditions

Displacement - Nodal, Magnitude  
Min : 0.00, Max : 26.92, mm

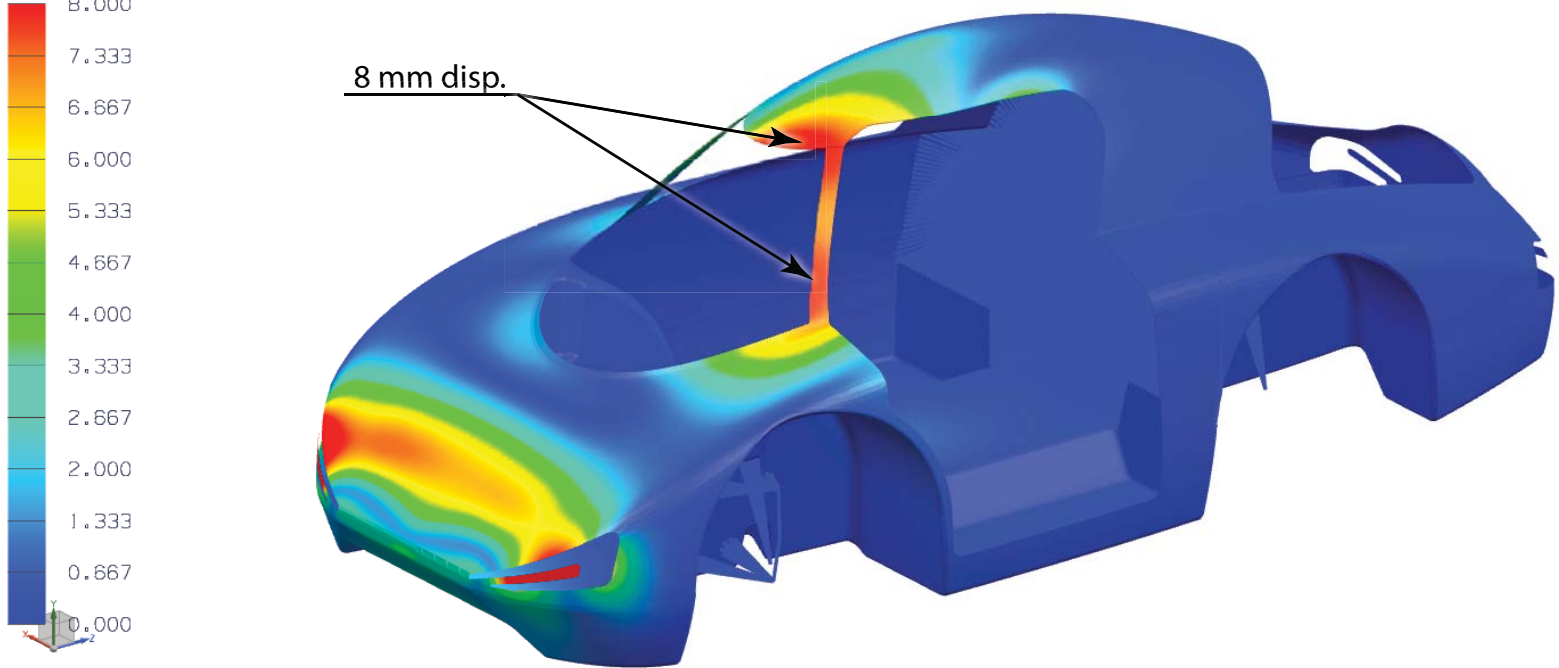


Figure 3.1.3: Displacement due to loads during testing

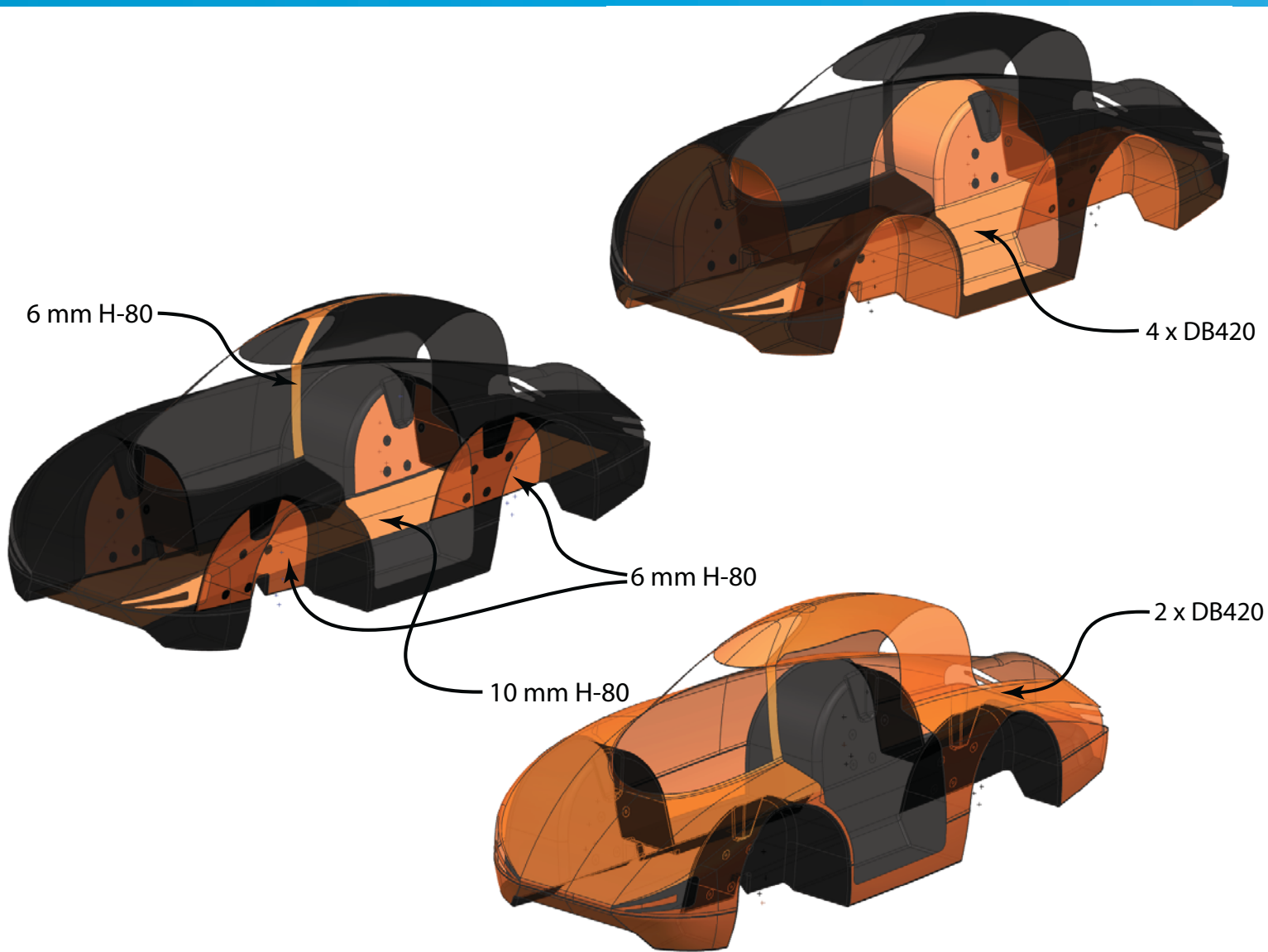


Figure 3.1.4: Layup for the car, placement of 4 layers (top), core reinforcement (middle) and 2 layers (bottom)

### 3.1.2.3 Results

When modeling with carbon fiber, the stresses usually are not the problem. The major challenge is to make the structure sufficiently stiff, so delamination, buckling and cracking are neglected.

The analysis of the loads from the race conditions shows a deflection in the whole wheel well and in the hood. Maximum displacement is located in the hood, flexing the hood 4 mm upwards. The consequence of this is considered to be small since further strength will be added when installing windows and a dashboard.

As predicted the highest stress concentrations is located around the fixing points for the suspension. The analysis shows rather small concentrations of stress, but a solution for distributing the forces to the wheel well wall must be established. This is to avoid ruining the sandwich structure by drilling holes through the core material. A

solution can be to make holes in the core material, filling up the holes with several patches of carbon fiber.

When applying the loads given by the rules, the displacement in the right a-arm is too high. A solution for improving this can be to further adding more core material, making the arm thicker. An even better solution is to widen the arm, making it symmetrical to the left side, and have the same laminate configuration. This is just a matter of adding more carbon fiber and a wider piece of core material during production. So no further optimization of this part is considered being necessary. The large deflections around the front lights due to the loads from the towing hook is not considered to be a problem, since the area around the placement of the towing hook is sufficient stiff. This case is also an extreme case, most likely never to occur.

### Stress concentrations

Ply Stress - Elemental, Von-Mises, Ply 1 Mid  
Min : 0.00, Max : 291.02, N/mm<sup>2</sup>(MPa)

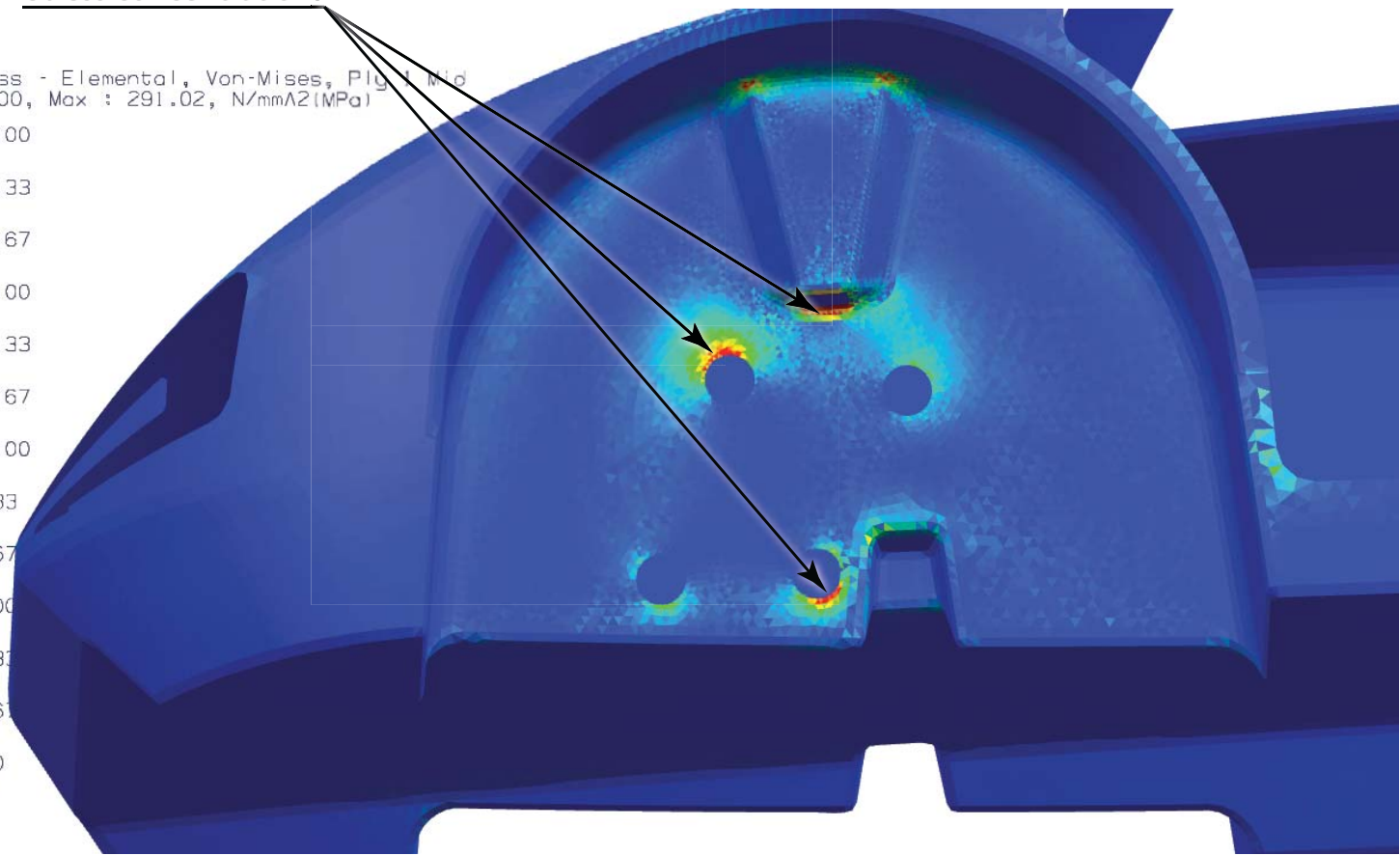
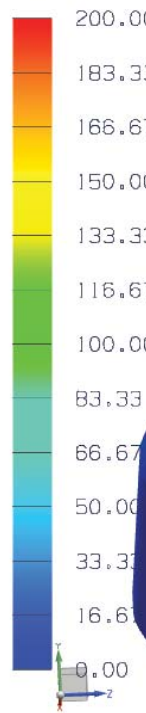


Figure 3.1.5: Stresses in the most highly stressed carbon fiber ply

#### **3.1.2.4 Conclusion**

The FEM analysis of the monocoque will make a basis for the production. This work also reveals critical areas and gives an indication on how the laminates will behave. The final configuration of how to implement the different laminates will be decided in cooperation with the experts in this field. The final configuration will also be highly influenced on the expert's expertise and production technique during production.

FUEL FIGHTER 2

 DNV FUEL FIGHTER 2



FUEL FIGHTER



FUEL FIGHTER



FOLLOW



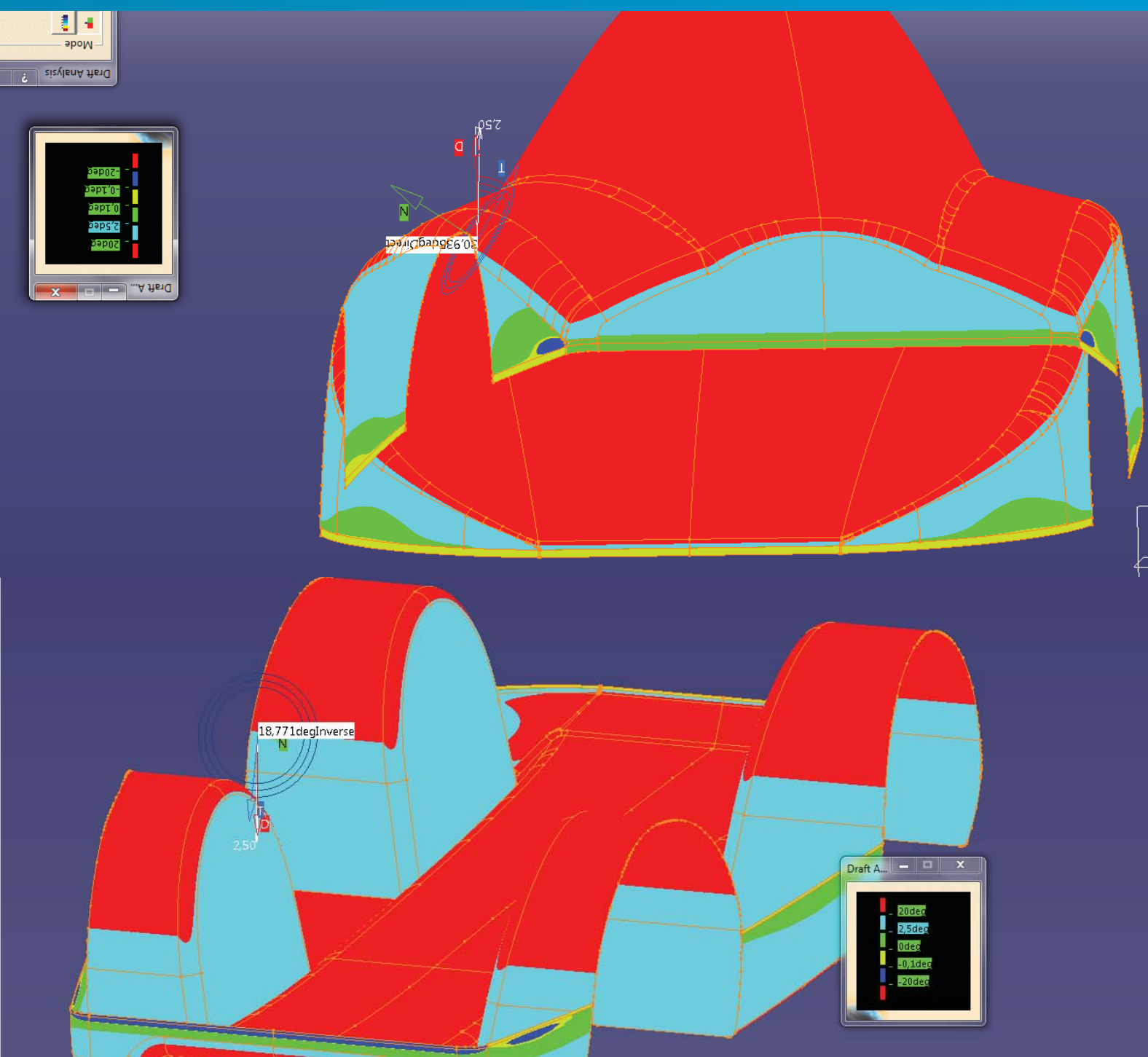


Figure 3.1.6: A draft angle analysis done in Catia to discover what needed to be improved before the production.

## 3.1.3 DESIGNING THE MOLDS

When the autumn semester was finished, a concept planned for production was made, but it was still not ready to be produced.

To make a 3D-model without any errors, it was decided to build it all the way from the bottom again, and then also include the results from the last strength and aerodynamic analysis as well as small changes in the shape based on feedback

from other designers. Since this model should be the base for later making the molds, it was important to keep split lines and draft angle in mind when drawing it.

When the process of making the molds started, the team got a lot of help from Eker Design. The contact in Eker Design, Ketil Humlekjær, gave a lot of feedback on how the mold would be made,



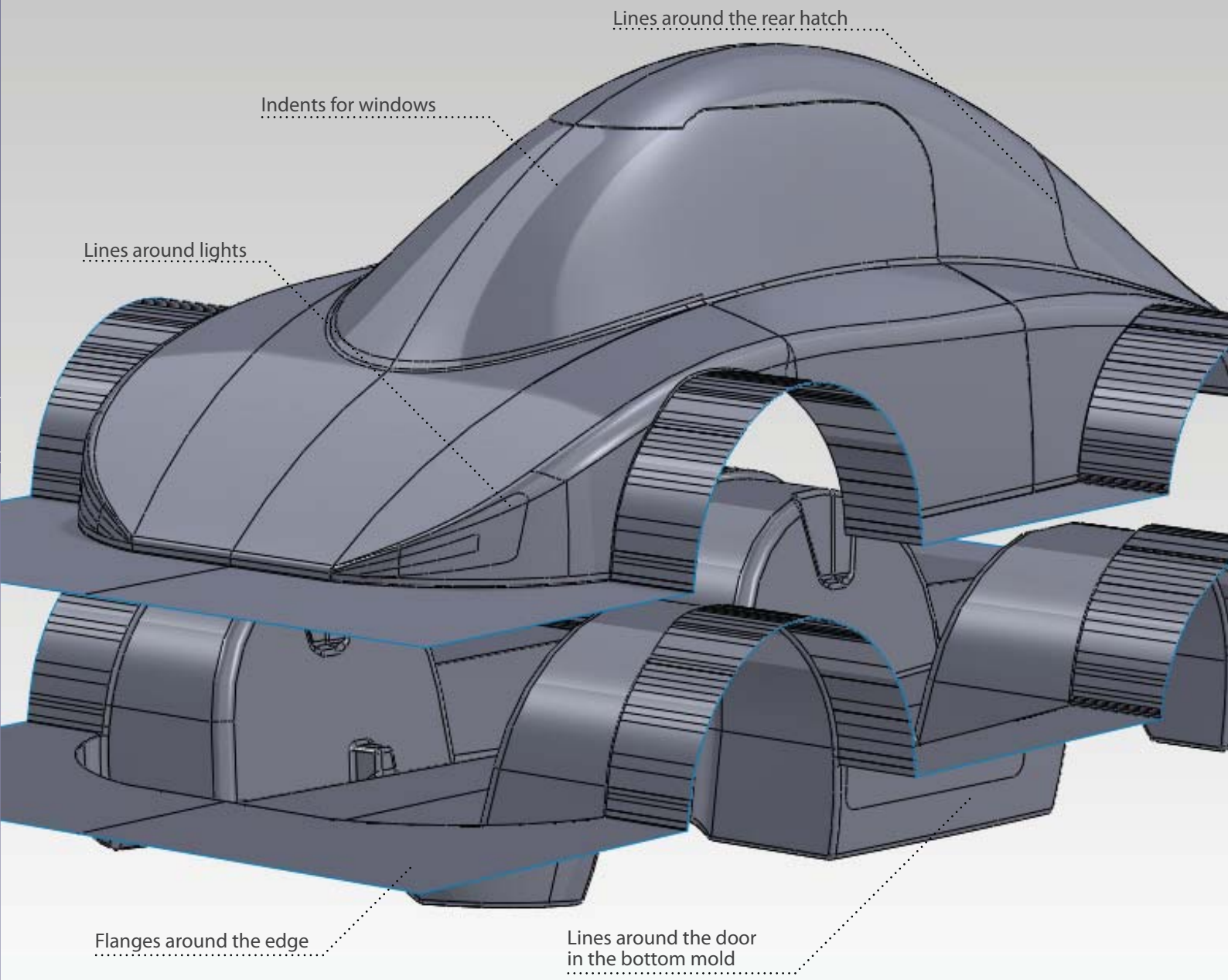
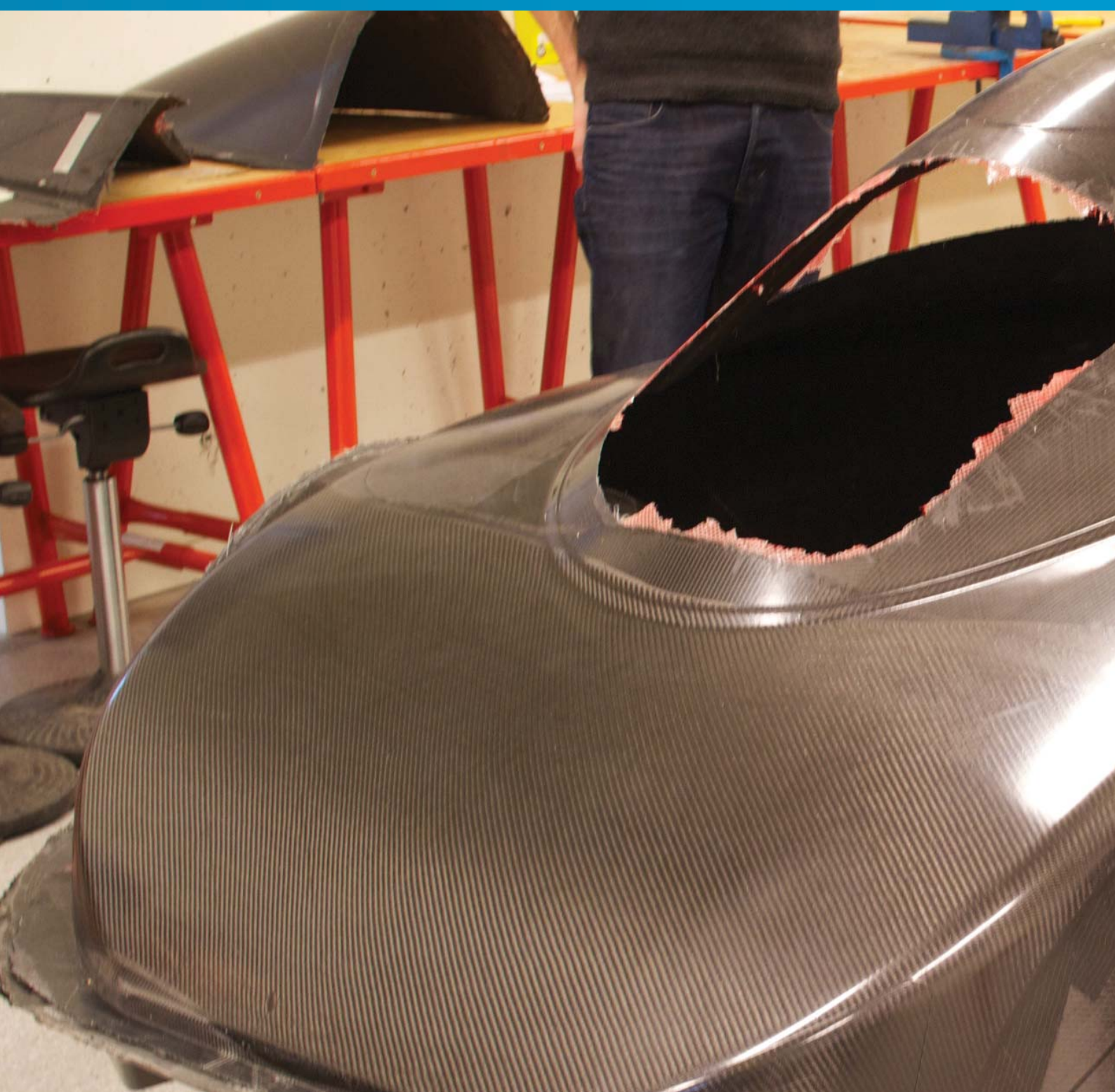


Figure 3.1.7: 3D model of molds

and what should be changed before production. Some of the draft angles needed to be improved (up to 7°), and the split line had to be moved. To find the split line, a split line analysis was done in Catia, and then added to the models. (Since SolidWorks do not have such functions)

To finalise the mold for production, horizontal flanges were added all around the edges to indicate where to make the cuts. Also small 1 mm thick lines were added around all cuts, like door, front and rear lights and rear hatch.

The final result was a .step-file that was sent to Eker Design, and the production could begin.



## 3.1.4 PRODUCTION

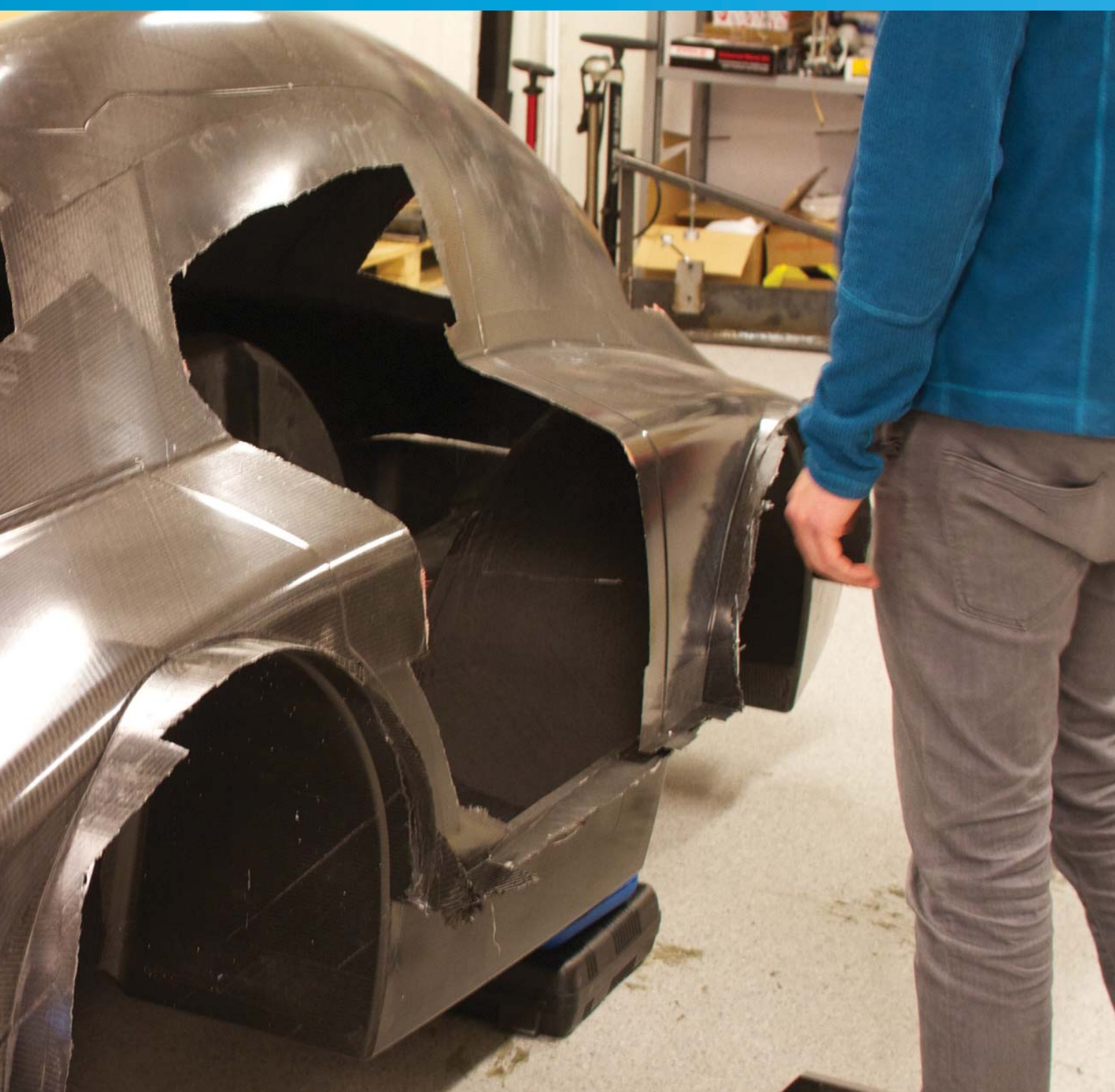
In autumn 2011 different production methods were considered. The method chosen was highly dependent on sponsors and expertise. At the end of the semester in 2011 all sponsors were in place and the production method of the monocoupe and molds was finally set.

For the production of the monocoupe it was chosen to use vacuum infusion in cooperation with Paal Fediuk at HPC in Fredrikstad. The molds

were decided to be made with seamless modeling paste. Jackopor would deliver the base molds and Svas Kjemi would deliver the epoxy paste. Further information about the production method and molds is given in the project report of 2011 (Endresen, et al., 2011).

### 3.1.4.1 Milling

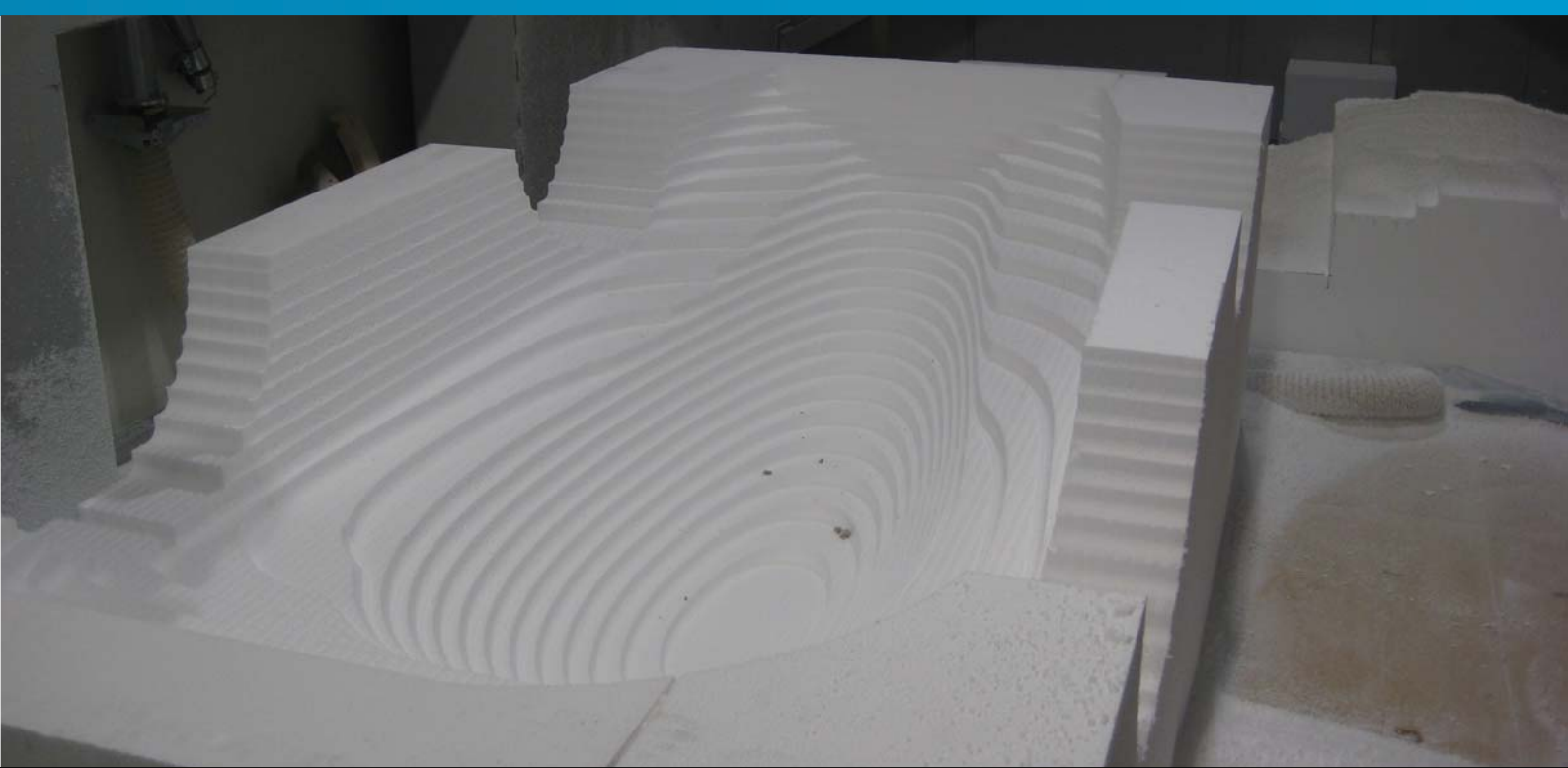
Before milling could start, the expanded polysty-



rene (EPS) (Jackopor 300), delivered by Jackson, had to be glued together to form the correct size. Since the mold was wider than the standard block size, two and two blocks had to be glued together. The blocks were glued together and glued to a piece of MDF plate. A plate of MDF was used on both molds to be able to fasten the molds to the milling machine. Screws were used to attach the plate to the floor in the milling machine. Epoxy glue was used to glue the EPS blocks and the MDF plate. The final result was two EPS blocks of 1555 x 3124 x 920 mm (top) and 1555 x 3124 x 560 mm (bottom).

The two blocks were first rough milled down with an offset of 10 mm to form the basis for a hard shell. Secondly, a finer milling was performed to even out the rough grooves from the first milling.

After the milling, all the milled off EPS had to be removed and the surface was cleaned to ensure a good bonding between the EPS and epoxy paste. A layer of epoxy paste (P25) was laid over the two parts in a thickness of 15 – 25 mm. The epoxy paste consists of two components mixed together forming a hard material. This material can be milled and shaped into the desired form.



*Rough milling of EPS blocks at Eker Design in Fredrikstad*



*Bottom mold after fine milling*

After curing of the paste, a new round of rough milling was performed followed by a round of fine milling, resulting in a 10 mm thick layer of epoxy paste. This round of fine milling cut down preparation work before the layup, ensuring a smoother surface.

Due to some calibration and cleaning of the mixing machine, there was a lot of P25 material going to waste. This resulted in a shortage of P25

material. The final part of the top mold had to be laid with P26, a material with higher density and viscosity. There were some concerns that the differences in material properties could create cracks during hardening, but the likelihood of these concerns was considered too small. Since there was not an option in postponing the mold production, the last part of the top was therefore laid with P26.



*Epoxy paste being applied by Markus Potthoff, a representative from Ebalta*



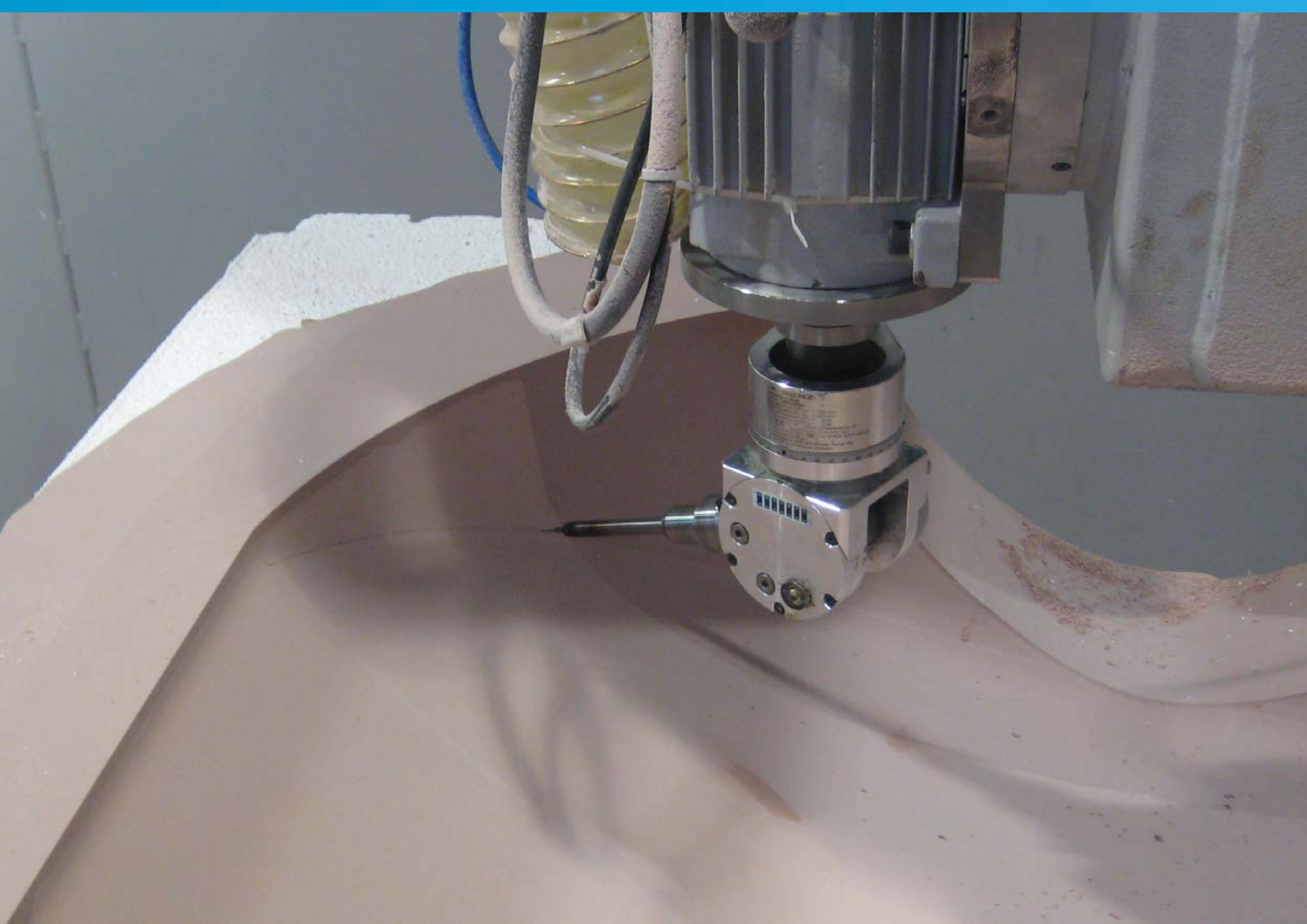
*Epoxy paste finished laid at the top part. The difference between P25 and P26 is clearly shown (P25 in light brown)*



*Milling of epoxy paste*

After the milling was finished at Eker Design, the molds were transported to HPC where the final preparations before layup was performed. Cavities and imperfections in the epoxy layer was filled and fixed and a final sanding smoothed out the surface. The molds were finalized with a coat

of polyurethane paint. This is an important step to fill all the pores and protect the molds. Some types of paint can react to the epoxy resin making the final product impossible to extract from the mold. It is therefore important to use the correct type of paint for this purpose.



*Tracing of lines for the lights was the final step for the milling machine*



*Finished prepared molds, treated with a layer of blue polyurethane paint at HPC*

### 3.1.4.2 Layup

Before the layup could start, the molds were treated with three layers of wax. The wax was applied and then wiped off, three times to ensure that every corner of the molds was treated. In some critical areas with complex geometry and steep corners the wax was applied four times. The wax will prevent the finished carbon fiber to stick to the mold, therefore it is important to be accurate when applying the wax.

The first step was to lay a line of vacuum sealer tape around the edge. It is important that there are no impurities in the tape edge or on the tape. The smallest fibers or particles can cause air leakage when the vacuum is applied. Therefore the layup process always starts with the vacuum sealer tape when the molds are clean and free of any carbon fiber and such.

Carbon fiber mats were cut and laid in the molds according to the plan made after the strength analysis. By using textile spray glue it was possible to firmly hold the mats in place. It is crucial not to use too much glue, since this can saturate the fibers, resulting in weakening the final product. The edges of the carbon fiber were always laid in corners and round edges with an overlay of 20 – 30 mm. Then the next mat was spliced to the first mat with an overlay of 20 – 30 mm on the other side of the edge, creating an over-

lap of 40 – 60 mm, see figure 3.1.8. By using this technique, the round edges, which can normally be an exposed area of stresses and strain, will be stiffer and more solid. These areas would achieve twice the amount of layers than the layer beside the splice. It is important not to position the splice on the same place, but always try to stack the overlay like shown in figure 3.1.8.



*Figure: 3.1.8: Overlay in a corner, two layer layup leads to four layers in the splice area.*

For extra reinforcements it was used different types of core material. The core material was cut out and placed in center between the carbon fiber layers. To ensure a nice finish on the core material inside the car and to ease the draping, the edges were rounded with sand paper.





*Waxing of molds*



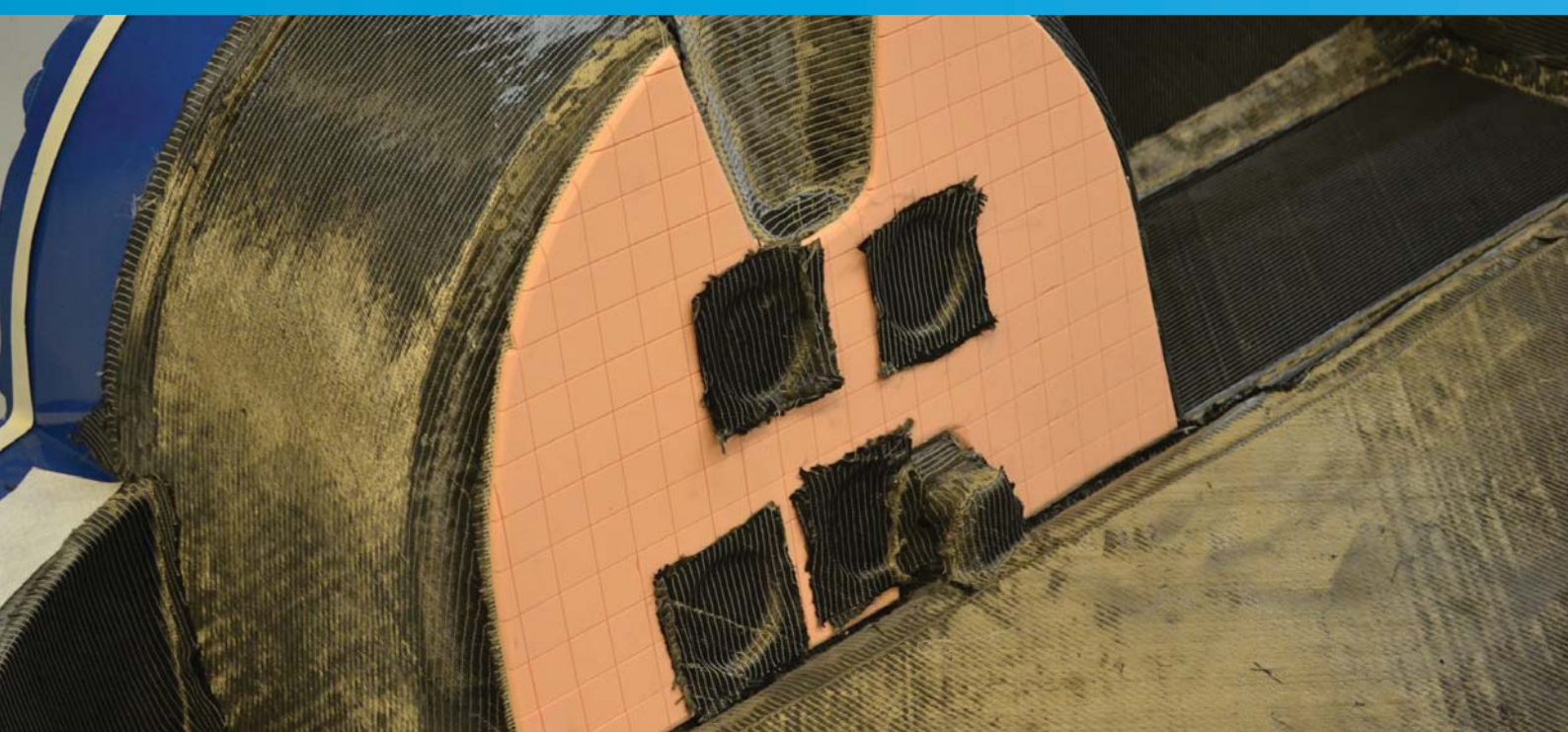
*Carbon fiber laid with an overlay of total 40 – 60 mm.*



*10 mm thick Divinycell core in floor and 3 mm thick Sorix core in the wheel well perimeter*

The mounting points for the suspension were reinforced with carbon fiber patches, creating a solid carbon fiber piece to mount the suspension in. This was done to prevent drilling holes in the core material, which will weaken and ruin the sandwich construction. A template was prepared

and used to mark out the suspension mounting points in core material. Then a round cut of 70 mm in diameter was made around the marks, creating circular holes in the core material. The size and number of layers of carbon fiber patches was decided on site.



Side wall reinforced with 6 mm Divinycell thick core and carbon fiber patches for the mounting points

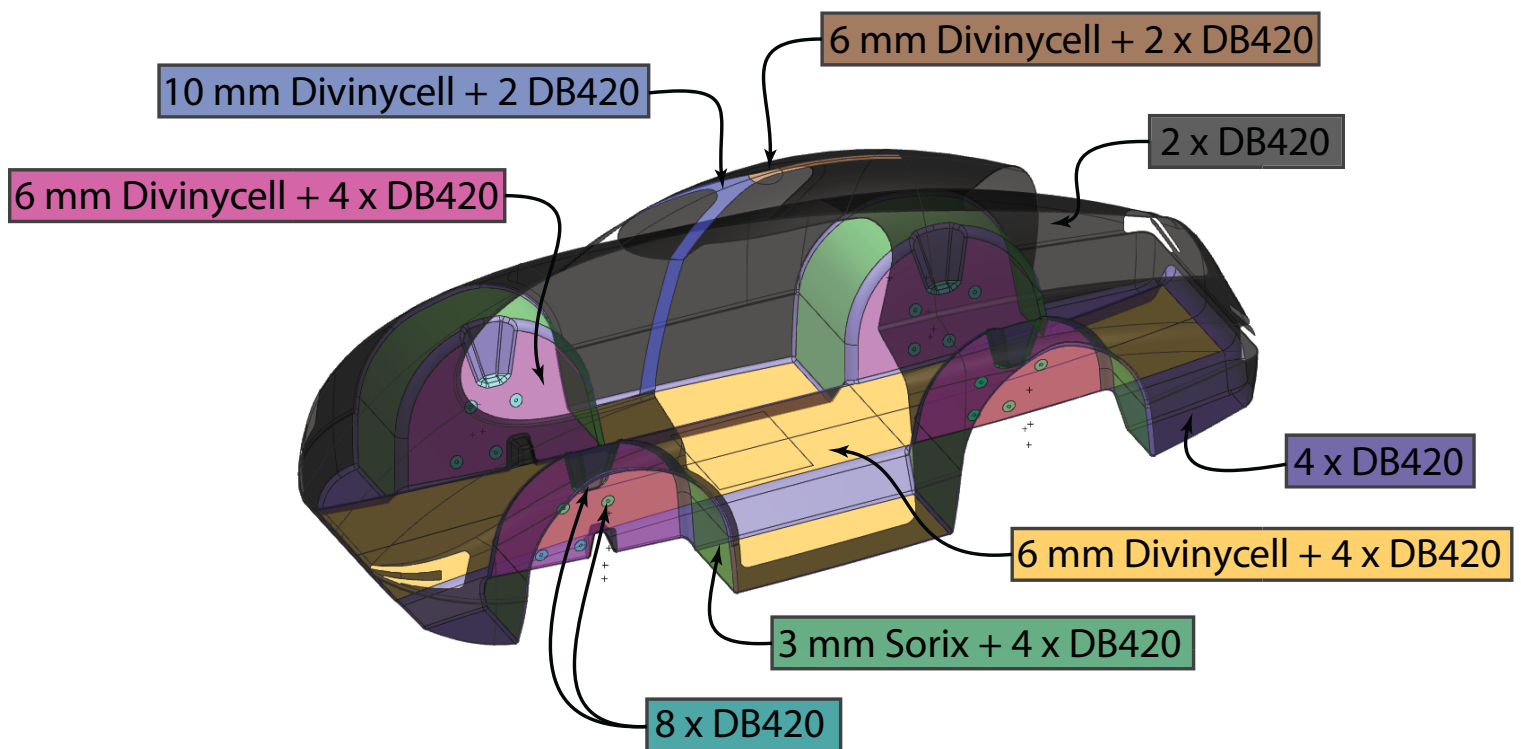


Figure 3.1.9: Overview of the final layup of the car

The carbon fiber mat used for layup was a  $\pm 45^\circ$ , the orientation on the car was not considered to be that important as long as the mats were laid in the most material efficient way. This resulted in crisscross pattern, ensuring strength in all directions, and minimum loss in material.

When all of the carbon fiber and core material was placed onto the mold, the molds were ready to be prepared for the resin infusion.



*Peel ply applied to the top part, held in place with textile spray glue*

First a layer of peel ply was placed over the carbon fiber. This is a layer that is easily removed after curing, preventing resin flow mesh, tubes and plastic bag from sticking to the finished product and ensuring a clean surface.

One layer of resin flow mesh goes on top of the peel ply. This is used to easier distribute the resin through the carbon fiber.

At the edges of the mold, the resin flow mesh was placed 80 mm from the edge. This is to slow down the resin at the edge, preventing the resin to exit before all the fibers are infused. By using multiple exit tubes and clamps, it is possible to further control the resin.

Finally the vacuum bag was placed over the molds. The bag must have sufficient size and slack to fit into every corner of the mold when vacuum is applied. The plastic bag is attached to the vacuum sealer tape around the edges. When attaching the plastic to the edge, waves are added along the edge, to create the sufficient slack that is needed. These are then sealed off

with the same sealer tape.

After placing tubes for resin inlet and outlet, vacuum was applied on the edges of the mold. Air leakages were discovered with the use of an air leak detector and sealed with tape. Then the resin was sucked from the center and out to the edges.

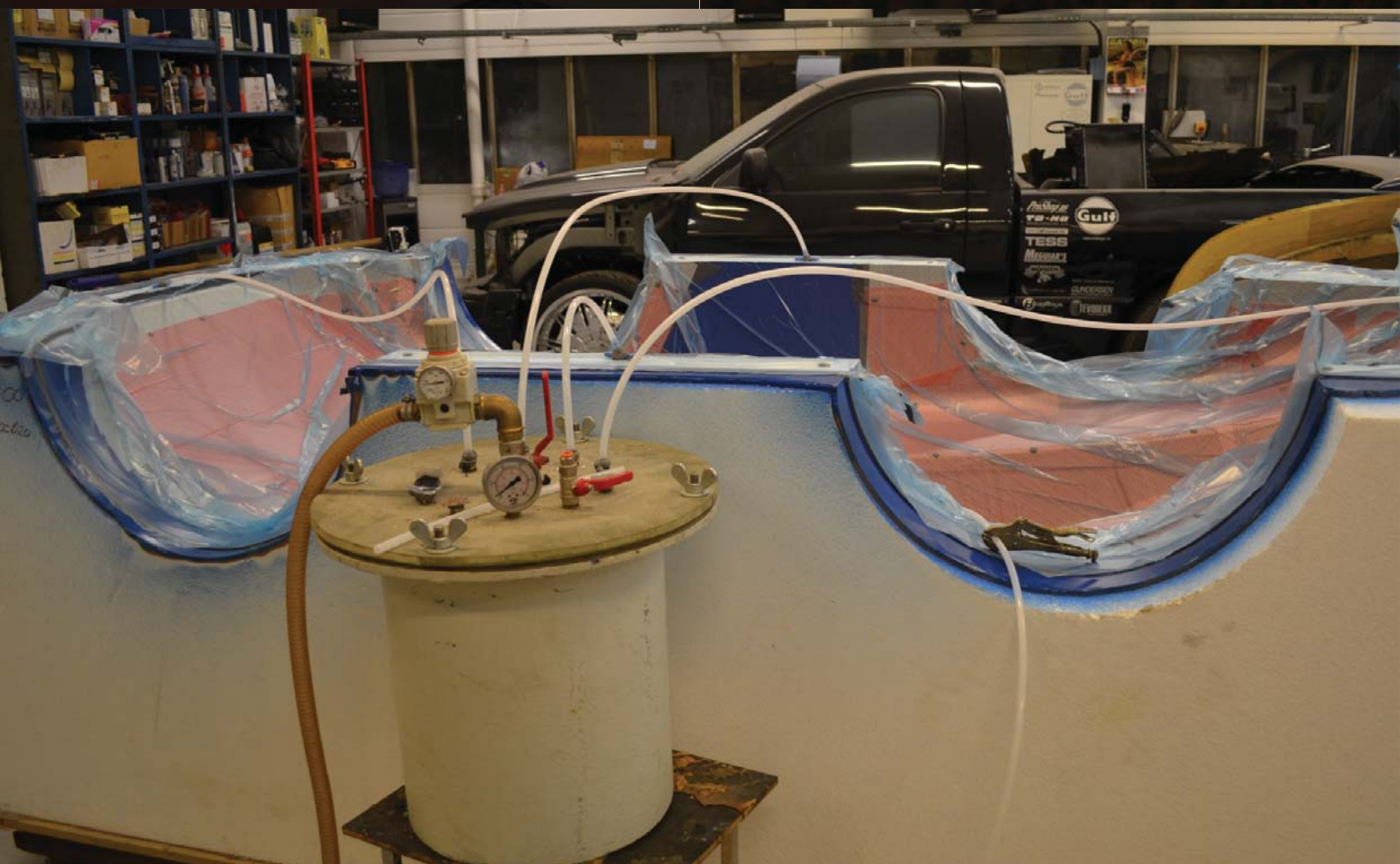
The infusion was stopped by clamping the inlet tube after the resin started to exit all the outlet tubes. Vacuum on the outlet tubes was still running after the infusion was completed to extract air trapped inside the fibers. The parts were set to cure in room temperature. Plastic bag, resin flow mesh and peel ply was removed after the curing process. The bottom and top part was removed from the mold with the use of wood wedges and brute force. Final stage was to post cure the parts at 80°C for 6 hours. Right after the first curing, the carbon fiber can be soft and pliable. To ease the process of releasing the carbon fiber from the mold, it can be a good idea to perform this task before final curing.



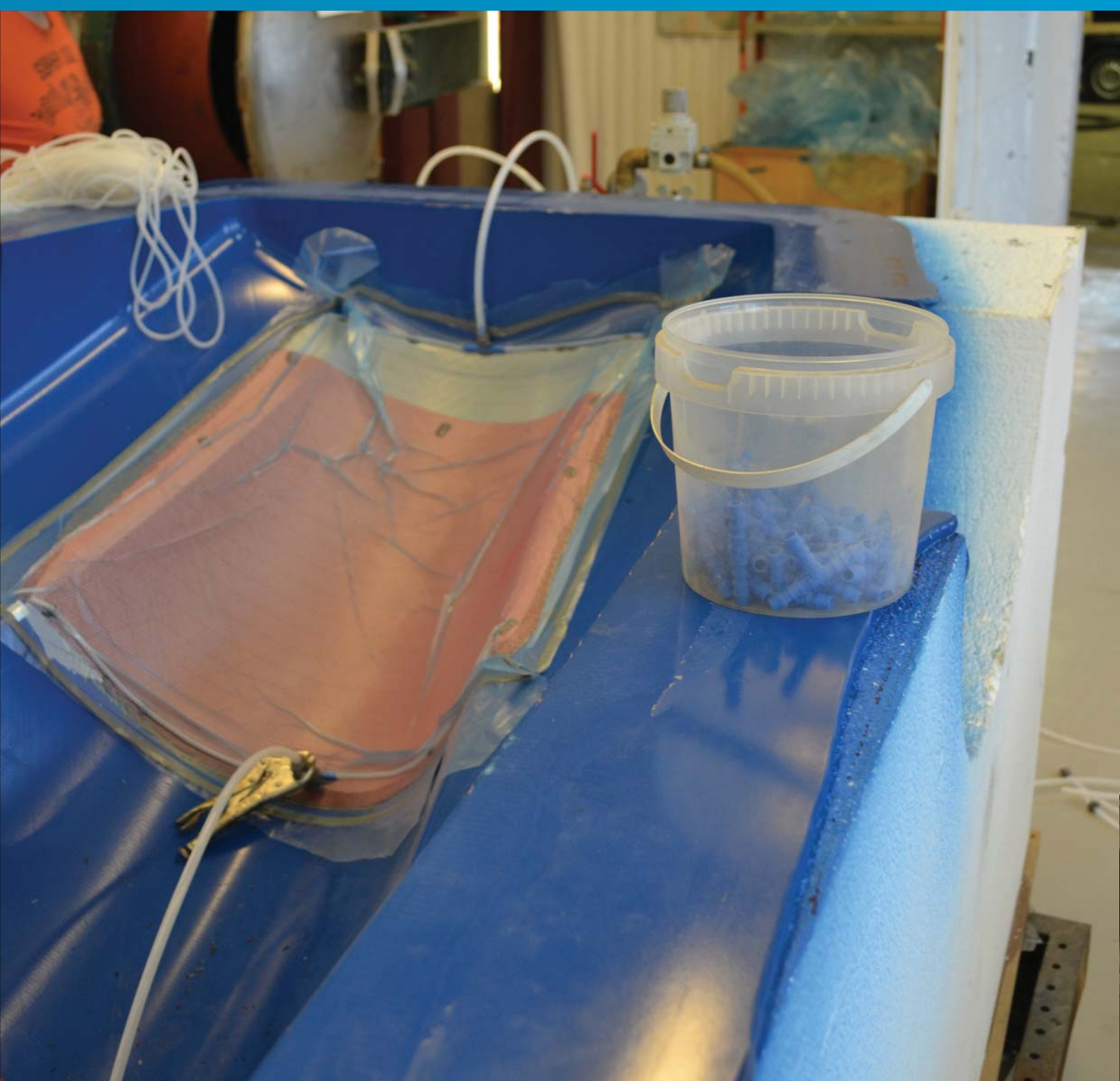
*Resin flow mesh, held in place with pieces of vacuum sealer tape*



*Resin flow mesh at the edges of the mold, the resin slows down considerable*



*Tubes for vacuum and resin. Resin trap is placed before the vacuum pump, preventing any resin entering the pump*



Layup of the back hatch

#### 3.1.4.3 Doors

The door and the back hatch is both produced with two layers of carbon fiber without reinforcements. It was decided in Fredrikstad that the door should be reinforced, back in Trondheim when the door was placed on the assembled car to ensure a perfect fit.

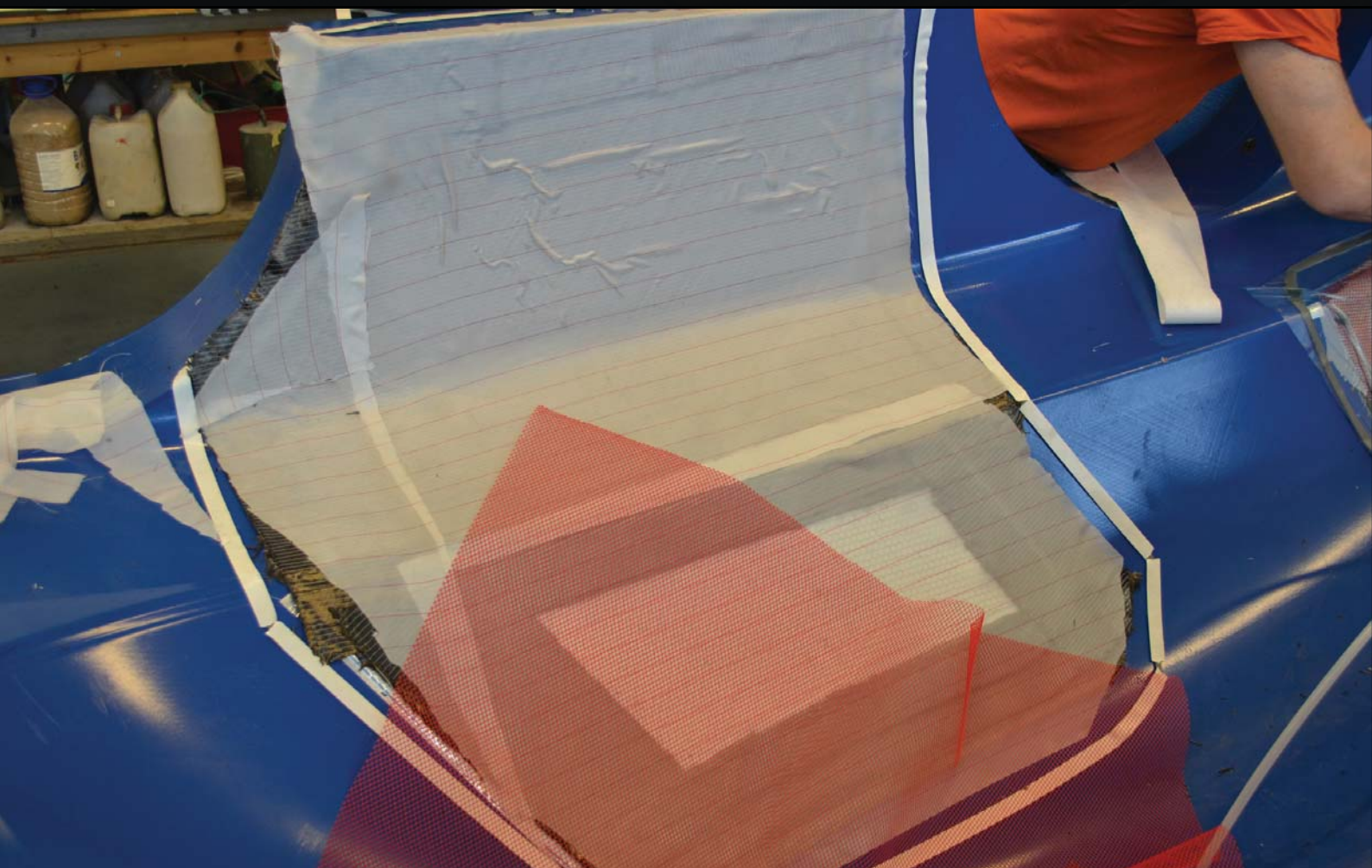
Production of the doors follow the exact same procedure as described for the monocoupe production.

#### 3.1.4.4 Firewall

The firewall consists of a sandwich structure with two layers of carbon fiber and a 6 mm Divinycell core between the layers. The wall was produced in a rectangular piece a bit bigger than the frontal area of the car with the use of vacuum infusion.



Indent made for the window with the use of 3 mm Sorix



Layup of the side door



*Water reservoir placed over the mold, creating pressure to the carbon fiber in the mold*

### 3.1.4.5 Wheel well covers

Since the bottom part of the monocoupe has integrated wheel wells it was not possible to use the bottom and top molds to produce the wheel well covers, as done in 2008. Therefore separate molds were produced at NTNU.

The milling machine at IPD is a 3-axis milling machine capable of milling maximum 70-100 mm deep. The molds were milled in two separate parts for every wheel well cover. On the sides an additional of 40-50 mm was milled to ensure sufficient size on the covers.

Front covers are design to be an integrated part of the car. To cut costs in production, it was decided to mill the molds in a cheaper material. Since these covers only needed to be produced once, and then be fixed on the car, the molds could be scrapped after production.

The molds were sanded down and filled with filler and then sanded down again. After final sanding the surface was painted and coated with release agent.

The production of the front covers was made in four parts. The two molds that made up the front covers on each side were not glued together, making it easier to fix it on the car on a later stage. Because of the porosity of the mold material, it was not possible to use vacuum to apply pressure during production. To apply pressure to the fibers, a new method was established. By creating a water reservoir over the mold, the pressure from the water is used to apply pressure to the wet carbon fiber. After filling up the reservoir with water, it is possible to remove wrinkles and air inside the fiber with the use of a roller. All parts of the front wheel well covers were made with one layer of carbon fiber.

For the rear wheel well covers, the two molds that made up one cover were glued together. Rear covers are produced with one layer of carbon fiber twill on the sides (exposed carbon fiber), one sheet of carbon fiber covering the whole part and strips of reinforcements on the edge to further stiffen the cover.

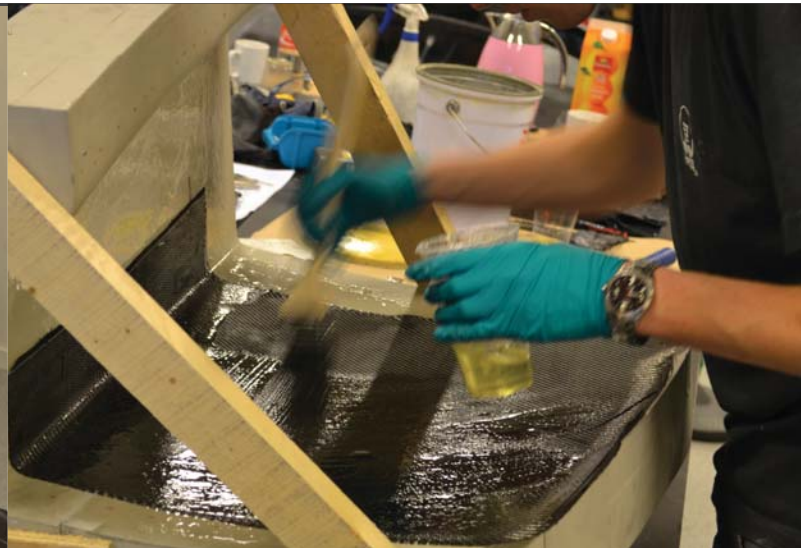
First the rear wheel covers were produced with wet layup and vacuum, but due to air leakage,



vacuum was not achieved. This resulted in air bubbles trapped inside the fibers and heavy covers, these were not approved. New covers were produced with the much simpler and successful water reservoir method.

Since none of the wheel well covers will contribute to the overall stiffness of the car, the parts are produced with a minimum use of carbon fiber to

reduce weight. For the front, the assembly technique will result in a total of two layers, making the front part more than capable to withstand the stress of normal use. Lifting or similar actions should never occur on the covers or in the wheel wells. Lifting should always be done onto the original monocoque structure on both sides of the wheel, by four or more persons.



*Rear wheel well covers*



*Water reservoir method used to produce rear wheel well covers*



## 3.1.4 ASSEMBLY

### 3.2.4.1 Monocoupe

After the doors, firewall, top and bottom part arrived in Trondheim, the assembly process began. First step was to fit the top and bottom part together. It was decided to use the flange from the production process to connect the two parts during assembly. The flange around the wheels on the top part was cut away and sanded down to make a perfect fit to the bottom part. The firewall was modeled according to the 3D shell model and milled at IPM. Final cuts in the firewall were done by hand.

First the firewall was glued to the bottom part

with Araldite to ensure the position of the firewall would remain in position during assembly. The final assembly of the three parts was done by laying strips of carbon fiber on the seams from the inside. Two layers of carbon fiber were laid between the top and bottom part, first one layer of 100 mm wide and second a layer of 150 mm wide carbon fiber. Between the shell and the firewall one strip of 100 mm carbon fiber was laid. Before the carbon fiber was laid, the area around the seams was roughened with 60 grit sandpaper, vacuumed and cleaned with acetone. The fiber strips was laid with normal wet lay-up, no pressure applied.



*Gluing of the firewall to the bottom part*



*Screw connection plates were made to hold the two parts together*



*Rough cutting of the monocoque. Thin red tape was used to strengthen the marks from the divider, making sure that the line would not disappear during cutting*

After curing and post curing at 80°C for 6 hours, the additional flange was cut away using a pneumatic cutting tool. Since the carbon fiber dust conducts electricity, the major part of the cutting was done outside with sufficient protective gear such as respirator, glasses, hearing protection and two pair of gloves. By using pneumatic tools, the dust would not be able to ruin the tools, and ventilation do not become that critical when working outside. Rough cutting the windows and doors was also performed outside.

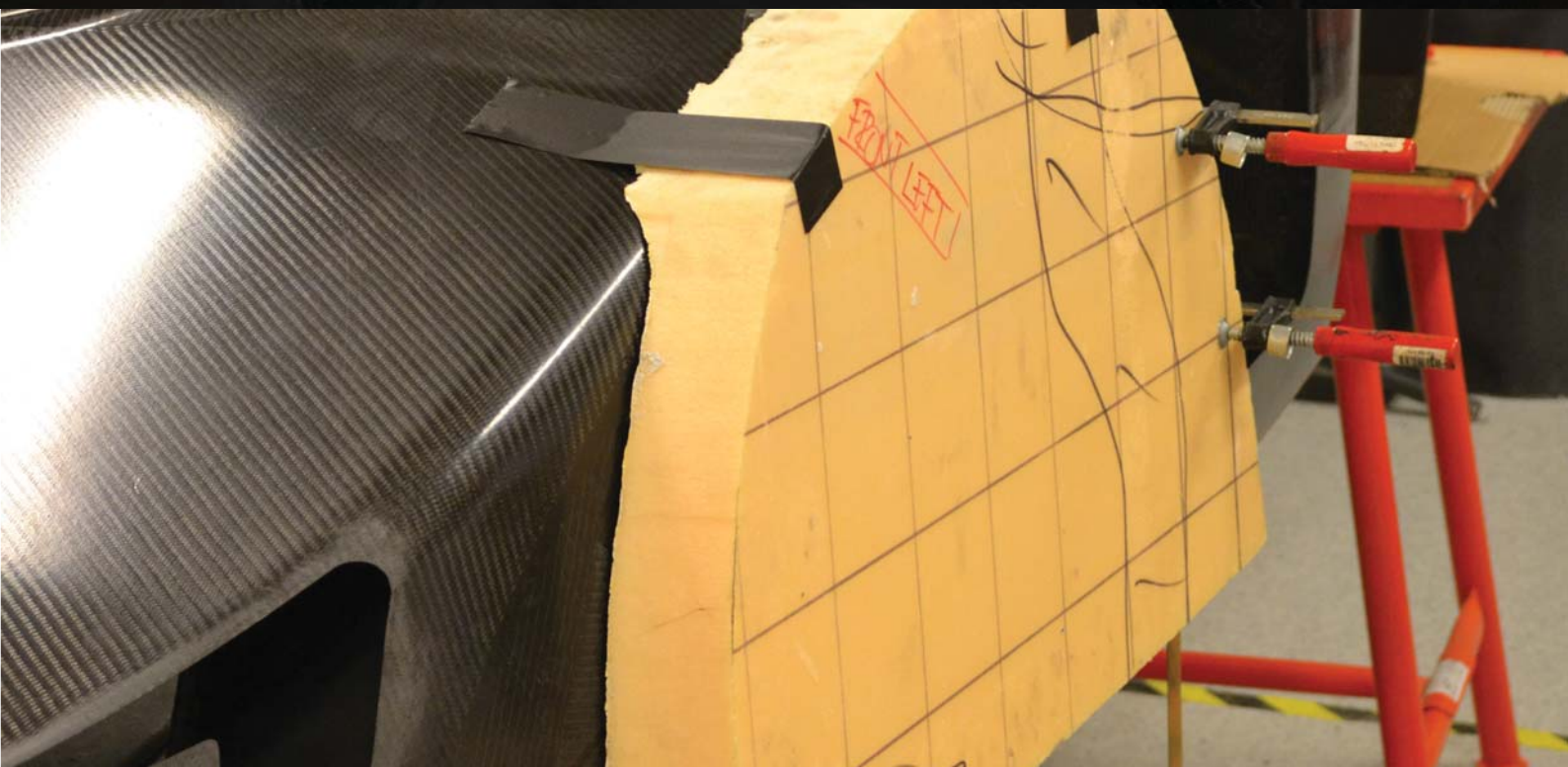
The outer side of the seams and all edges of the monocoque and doors were sanded by hand to ensure smooth and even edges. The edges and seams were sanded with the use of rough grit sand paper and files. A divider was used to mark the cutting line, 10 mm from the indent edge.

#### **3.1.4.2 Wheel well covers**

The front wheel well covers was cut around the edges and fastened to the monocoque with the same technique as for the firewall, with one carbon fiber strip of 100 mm. The task was



*Carbon fiber strips in the seams, holding the three parts together*



*Gluing of the side parts of the front wheel well covers*

performed in two operations. First the side part of the wheel well covers was fastened, the molds was used to hold the side part in the correct position throughout the fastening and curing process.

Secondly, the bottom part was fastened, using the same method with support from the bottom part molds.

In total, the front wheel well covers consist of two

layers of carbon fiber after fastening the covers to the monocoupe. This is more than adequate according to strength and stiffness for the covers.

The decision to postpone the final cutting of the covers was made to ensure that they would be as tight as possible around the tires. This proved to be difficult since the alignment of the front suspension is a challenging process and even harder without being able to mount the wheel. A template of the wheel was prepared and after a



*Both parts of the front wheel covers fastened to the monocoupe*

quick alignment of the suspension it was possible to make marks for the perimeter on the covers.

The final cut of the bottom part was done after the front suspension and steering was in place. Some modifications to these parts had to be executed during the whole process, mainly due to constantly fine adjustments on the front suspension. The final cut was performed in Rotterdam, the day before race day.

The rear wheel well covers were cut around the edges and fitted to the car. A rectangular slot was cut out for the wheel. As for the front wheel well

covers, the covers were constantly adjusted due to ongoing tweaking of the rear suspension. The final cuts for the rear covers were also performed in Rotterdam.

Fastening method of the rear wheel covers is described in section 3.1.7.4.

The constantly realignment of the suspension in front and rear lead to a bigger air gap around the wheels than what was desirable. But taken in to account the complex process of fine adjusting a suspension system and eliminating any risk of scrubbing, the end result is more than satisfying.



*Fine cutting of the wheel well covers, Dremel cutting tool and vacuum cleaner is used*



*Reinforcing the door with 50 mm wide Rohacell 31 core*

### 3.1.4.3 Doors

The edges of the door and back hatch were roughly cut along with the monocoque and sanded down by hand. Since the passenger door is only made out of two layers of carbon fiber, reinforcement was added in the door to stiffen the construction. The door was clamped on to the monocoque and the reinforcement was added when the door was in place. This would help to preserve a perfect fit to the monocoque. However, an error was made when the door was placed in the oven to post cure the reinforcement. This

resulted in softening the carbon fiber and the door losing its original shape. The hinge connecting the door to the monocoque is described in section 3.1.7.1.

It was decided not to reinforce the back hatch. The two layers gave the door some flex, making it easy to fit onto the monocoque. Carbon fiber brackets were used to mount the back hatch to the monocoque. Brackets for the back door is described in section 3.1.7.3





*Back hatch fitted to the monocoque*



*Rear wheel covers fitted to the monocoque*



*Finished car, foiling has commenced*

#### **3.1.4.4 Surface finish**

To create a smooth transition between top and bottom part and the front wheel well covers and body, the seams were filled with body filler. The filler was sanded down and new filler was applied to fill in the remaining gaps. This process was repeated until the seams were perfectly smooth.

The body filler was also applied to areas around the car where there were imperfections from body

production. After all the gaps, seams and imperfections were evened out with body filler, all the surfaces were sanded down. The car was sanded down 3 times; first with 120 grit paper, followed by 400 grit paper and finally 600 grit paper.

Just before foiling, the surface was cleaned several times with alcohol to remove any dirt and dust.



*Body filler applied around the front wheel well cover*



*Sanding of the whole car, a time consuming process*



## 3.1.5 WINDOWS

The aerodynamically design of the body includes double curved windows. Indents for windows were included in the negative base molds of the car body. Positive molds for all three windows could then be produced based on the base molds for the body. The SEM rules recommend windows made by polycarbonate, based on its impact abilities. It is important that the windows do not shatter into sharp shards if hit by a foreign

object. Because of the door the windshield needs to be divided into at least two smaller windows. Figure 3.2.10 shows the general shape and arrangement of these. The front window and side window could be combined into one, as the car only has one door. Ideally the shape and size of the front window should have been optimized towards production during the design of the body. Implementing single curved shape or lift-



ing the frontal part of the window would simplify the production process.

Several companies have been contacted regarding production of windows. The fact that the shape is double curved and the general size of the windows introduced some unforeseen complications. For production of these windows in polycarbonate, vacuum forming is the only possibility. Molds need to be produced, and the final result is highly dependent on the surface finish of these molds. The uncertainties regarding the optical properties of the final product lead to

negative response from most companies. Those who initially gave positive feedback were too busy within the time limits of the project. Decision was made to do the production in-house, with the equipment available at IPM and IPD. Size and shape of the window required a new vacuum table. The solution with three windows was chosen to reduce the size, cost and complexity of the production.

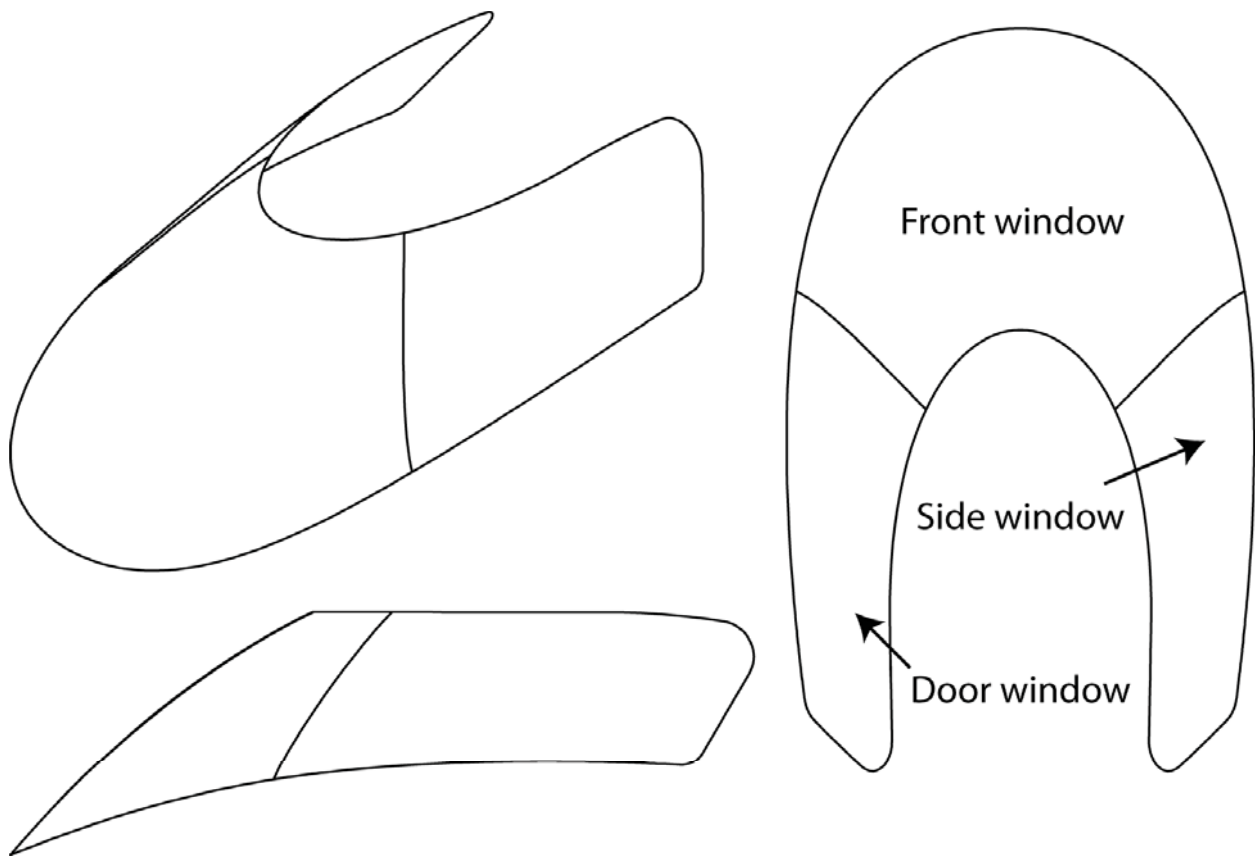


Figure 3.1.10: Arrangement of the windows

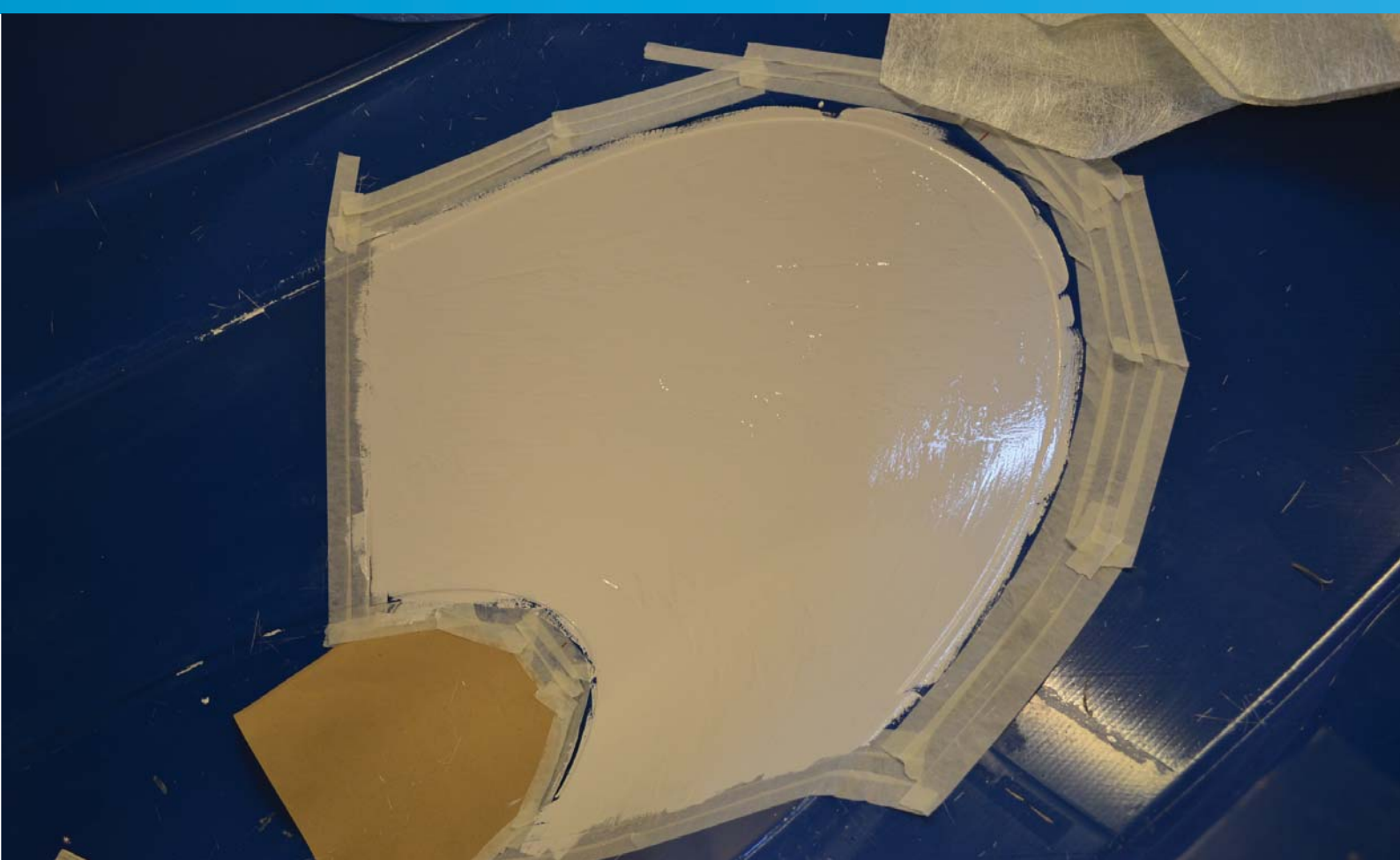
### 3.1.5.1 Molds

The molds from production of the car body are accurate and precise, it was desirable to reuse these in the production of the windows. The body mold was applied a release agent at the window surfaces. Then a thin layer of polyester based gel-coat was applied followed by several layers of fiberglass in polyester. The polyester was cured overnight and positive molds/plugs of the windows were retracted from the negative body mold. To secure overlap between the different molds the production was done in two stages. First the molds for the side windows were produced, then the front window.

Forming temperatures up to 220°C require strict control over the mold surface. Both texture and coating is important properties with direct impact on the final result. The surface roughness must decrease with increased forming temperature. The coating must withstand forming temperature while giving a smooth surface. To prevent waste of large plastic sheets, it is recommended to do small scale testing of the coating and surface roughness before production.

To improve the surface finish of the molds a lot

of sanding is usually required. Due to the smooth surface of the body mold, the window molds were quite good so start with. Fine grade sandpaper in the grit range from 120-600 was used to improve the surface of the molds. Several coatings were tested with varying results. Since the molds were produced with polyester, the mold itself cannot withstand high temperatures over time. Melting temperatures of polyester can be found down to 200 °C, and the polyester will lose its structural integrity even before that. Some coatings like heat resistant spray paint needs to harden at the working temperature. Local heating of the surface with a heat gun was tested on these types of coatings. The rapid heating caused small blisters and cracking of the surface. Coatings requiring heat hardening above the working temperature of polyester was therefore abandoned. For the side windows the gel coat used in the first step of production was sufficient regarding temperature resistance. Small deformations leading to low forming temperature made this possible. On the front window much higher temperatures is needed and epoxy was used as coating. The epoxy left some residue on the polycarbonate window which was removed with ROT WEISS Acrylic- & Plexiglas polish paste.



*Gel-coat applied to the front window mold, the layer will provide a high quality finish to the molds*



*After a quick hardening of the gel-coat, several layers of fibreglas infused with polyester was applied*



*Vacuum forming of the side window*

### 3.1.5.2 Vacuum Table

A vacuum table made out of plywood was manufactured for this project. Two plates of plywood were prepared in the same size. One plate was perforated with thousands of 5 mm holes. The other plate had air channels milled out to connect the holes when the plates were joined. Connection for the vacuum was included in the same plate. Silicone was added along the edge of the plates, and they were screwed together. Along with the vacuum table a frame to support the plastic is needed. IPD had an aluminum frame in storage, and to save money and time this frame was used. The size of the vacuum table was therefore given by this frame. Ideally the vacuum table should have been even bigger. This would lead to more waste of plastic, but could have made the forming process easier.

### 3.1.5.3 Production

The door and side window was produced with 1mm thick polycarbonate. As the front window is larger and subjected to external load from the windshield wiper, 1.5 mm thickness was chosen. Over time the polycarbonate absorbs humidity from its surroundings. If this humidity is not removed before heat forming, small bubbles will appear all over the formed plastic. This reduces the visibility through the polycarbonate windows, and must be avoided at all times. The producer of polycarbonate sheets used in SEM 2012 recommends drying the sheets at 125°C for about 1 hour (GE, 2012). When forming complex shapes which require high deformation and ac-

cordingly high temperatures, longer drying time and temperature should be considered.

Polycarbonate sheets were mounted in a solid aluminum frame that can withstand the temperatures and forces induced by the forming process. It is important to seal of all connections between the vacuum source and the plastic. Areas that require special attention is the connections between the solid frame, plastic and the vacuum table. During production an expanding sealer tape bought at biltema was used.

The frame with plastic was heated up to first drying and then forming temperature. When the polycarbonate was heated sufficiently it started to sag. The frame was removed from the heat source and pressed down over the mold located at the vacuum table. Vacuum between the table and plastic was created with two vacuum cleaners. After several attempts the suitable forming temperature was found, and the polycarbonate deformed perfectly around the mold. For the side window this temperature was about 180 °C. A considerable higher temperature was needed for the front window, due to larger deformations and increased thickness. The most successful attempt was done at about 220 °C.

Correct placement and fastening of the mold is important to achieve good results. Areas with low deformation should be placed close to the aluminum frame where the plastic is fastened. If possible areas with larger deformation should be



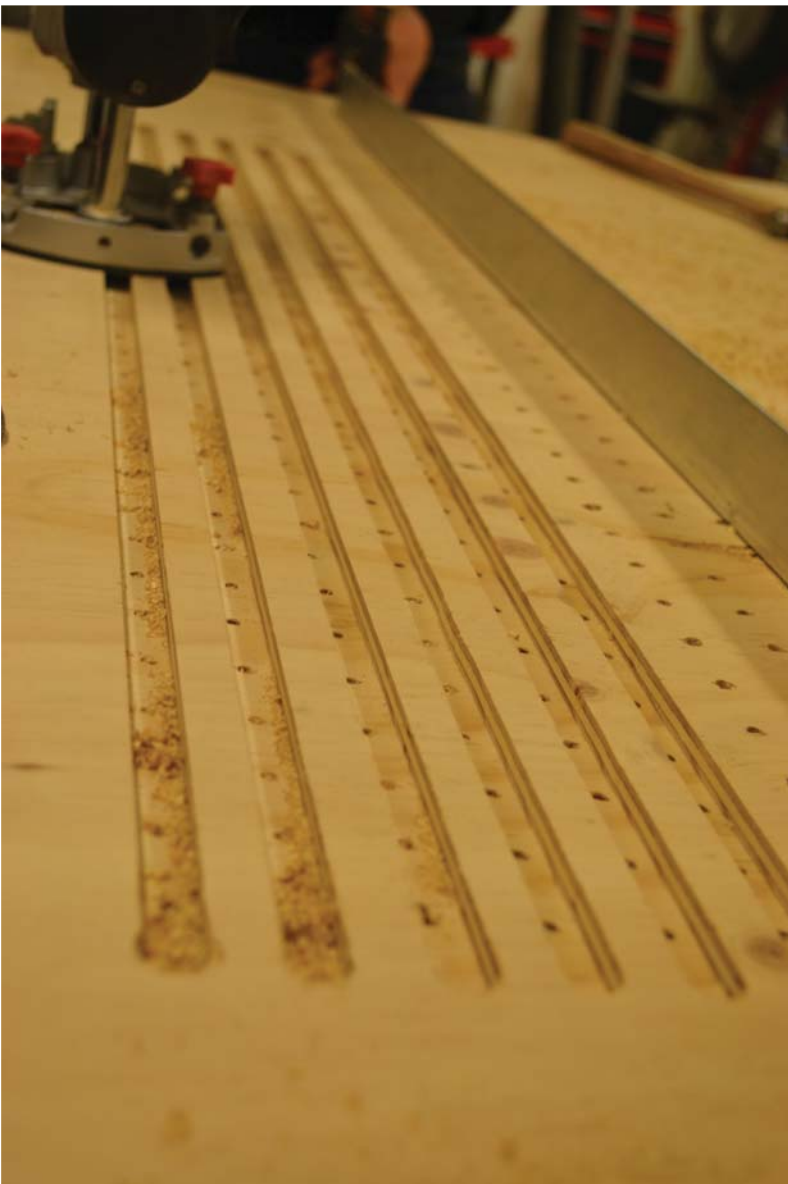
located close to the middle of the frame.

Production of windows in polycarbonate with double curves is a complex process. This is important to emphasize as many unsuccessful attempts were made. Sufficient time and resources must be planned for this part of the project. Since there is little experience and expertise to be found at the university, a professional company should be contacted early in the autumn semester. To further simplify the production process other plastics should be considered. Polycarbonate scratches quite easily, and mounting, cleaning and operation of the windshield wiper will over time leave marks on the windshield. Switching to acrylic plastics could solve some of the scratch problems. In addition forming without the need of vacuum might be a possibility. Molds made from a more suitable material should be considered. The ability to perform the entire

forming process above the forming temperature would most likely give great improvements on the result. Thickness of all windows can be reduced, either to 1mm for all windows or even less for the side and door window.

#### 3.1.5.4 Assembly

The windows were cut out from the plastic sheets, and fine adjusted to fit the body. First the front window was glued in place. Araldite 2031 was applied on the indented connection lip of the body and pliers were used to hold the window in place. The glue was cured overnight and the pliers removed. Next glue was applied on the body and the side window was put in place. Tape and wooden sticks was used to keep the windows in place, while applying pressure on the connection area. When the araldite had cured, Tec-7 was applied to create a smooth transition between the body and the windows.



*Milling of air channels in the vacuum table, connecting the holes drilled out in the ply wood*



*Windows assembled on the car*



*The lights of the former car was vacuum formed in plastic, and used three different LED-lights for high beam, low beam and indicator lights.*

## 3.1.6 LIGHTS

As a normal car, the Urban Concept cars in Shell Eco-Marathon needs to have the same lights that are required on the streets

### 3.1.6.1 Former Lights

The former lights were fulfilling the requirements by having a separate star-LED with lenses on each of the blinkers, high beams and low beams. In the back the car had a strip of red LEDs as break indicators. The front light glass' were made of PET, as well as the inside of the lights. Because of the heat from the star-LED some of the plas-

tic had melted, but everything did still work as it should. The front lights were attached to the body with velcro on the inside.

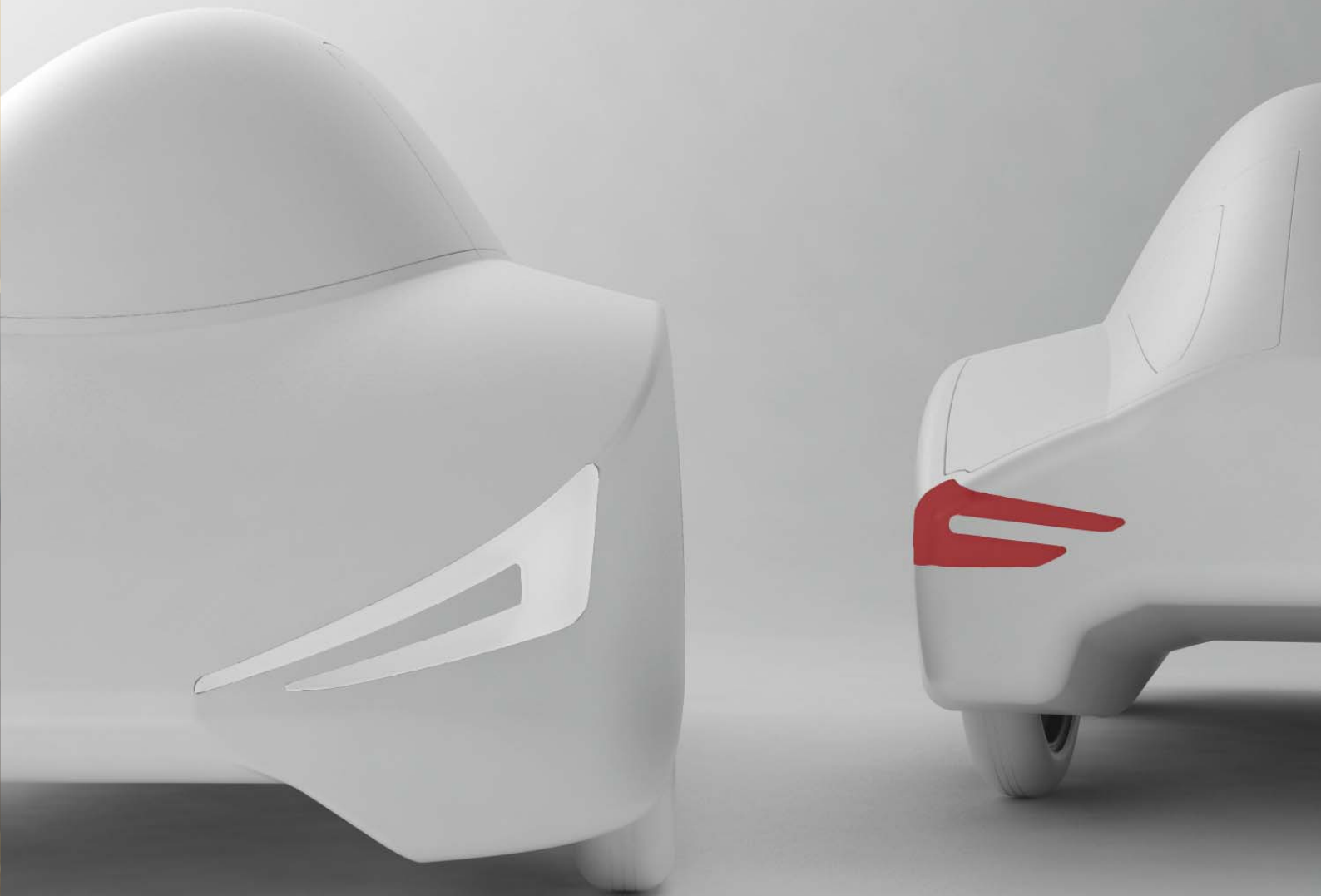


Figure 3.1.11: The holes for the lights needed to be planned before the production of the monocoque started, and therefore also before the inside of the lights were designed.

### 3.1.6.2 Interfaces

The only interfaces one would need to consider when designing the lights, were the monocoque and the control system. Holes for both front lights and rear lights needed to be planned before the production of the body started, to make the process of cutting the holes a lot easier.

The control system were depending on voltage of the lights, and therefore also the number of diodes. Because of these interfaces the light design needed to be finished early in the process.

### 3.1.6.3 List of Requirements

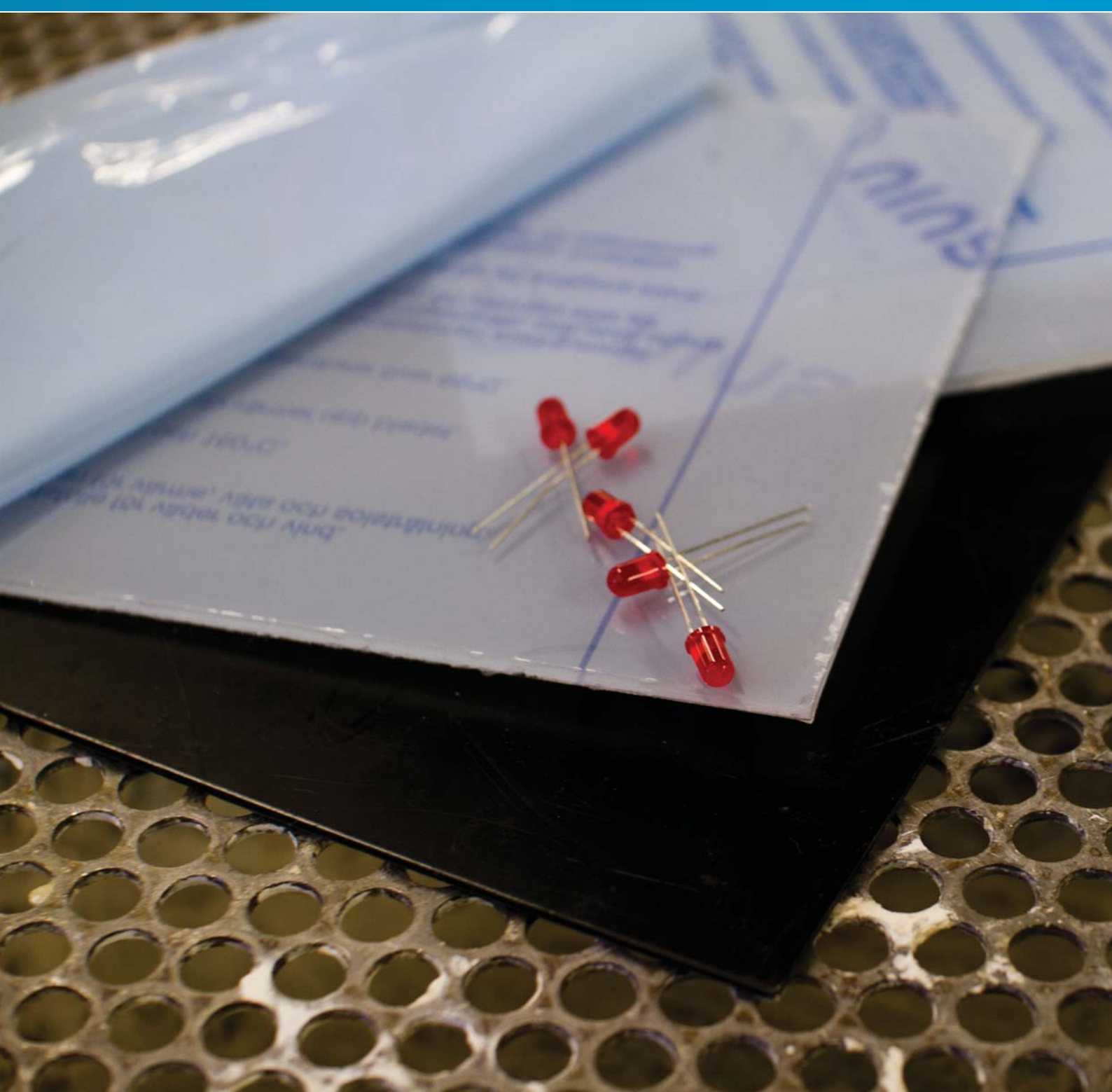
Both the rules and the team goals set requirements for the lights:

#### Rules

- Must have two front headlights
- Must have two front turn indicators
- Must have two rear turn indicators
- Must have red break lights in the rear
- Must have two red rear lights
- The center of each headlight unit must be located at an equal distance and at least 30 cm from the longitudinal axis of the vehicle.

#### Team goals

- Each light must not weigh more than 150 g.



#### 3.1.6.4 Materials and Technology

There were two obvious choices of material for the lights; either carbon fiber or vacuum formed plastic. Each of the choices would have advantages.

The carbon fiber would resist the heat from the LEDs much better, but would be the hardest one to produce. The plastic would on the other hand probably be both the lightest solution and the one that was easiest to produce. The heat problem could be solved by insulating the LEDs better.

The diodes selected were of two different types; Star LEDs for the high-beams and the blinker in the rear, and 5 mm LEDs in different colors for low beam, blinkers in the front and driving lights in the back. The 5mm LEDs would not emit any heat, while the Star LEDs should be isolated from the plastic.

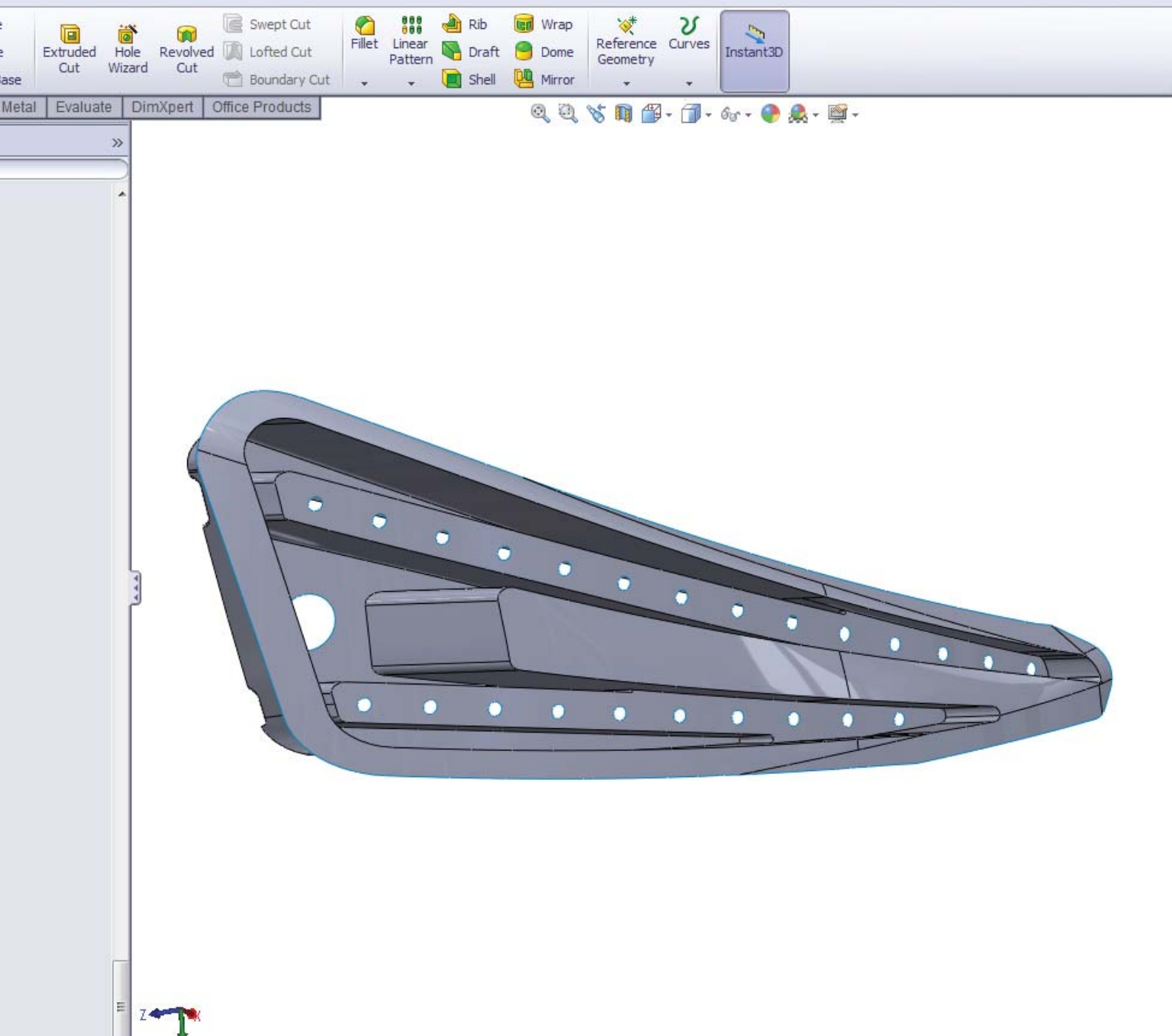


Figure 3.1.12: Different combinations of light placement were tested in SolidWorks.

### 3.1.6.5 Concept Development

Since the overall shape of the lights were developed last semester, the work that had to be done was to figure out how to finalize the design and make it possible to produce.

The initial sketching were done on printed CAD drawings of the front and rear of the car. In this way it was possible to generate a large amount of ideas in a short time, which was crucial since the design needed to be finished in a very short period of time.

The sketches and ideas could later be combined into CAD models in solid works, where it would be easier to plan and place LEDs. In the end all the best ideas were combined into one finished concept.

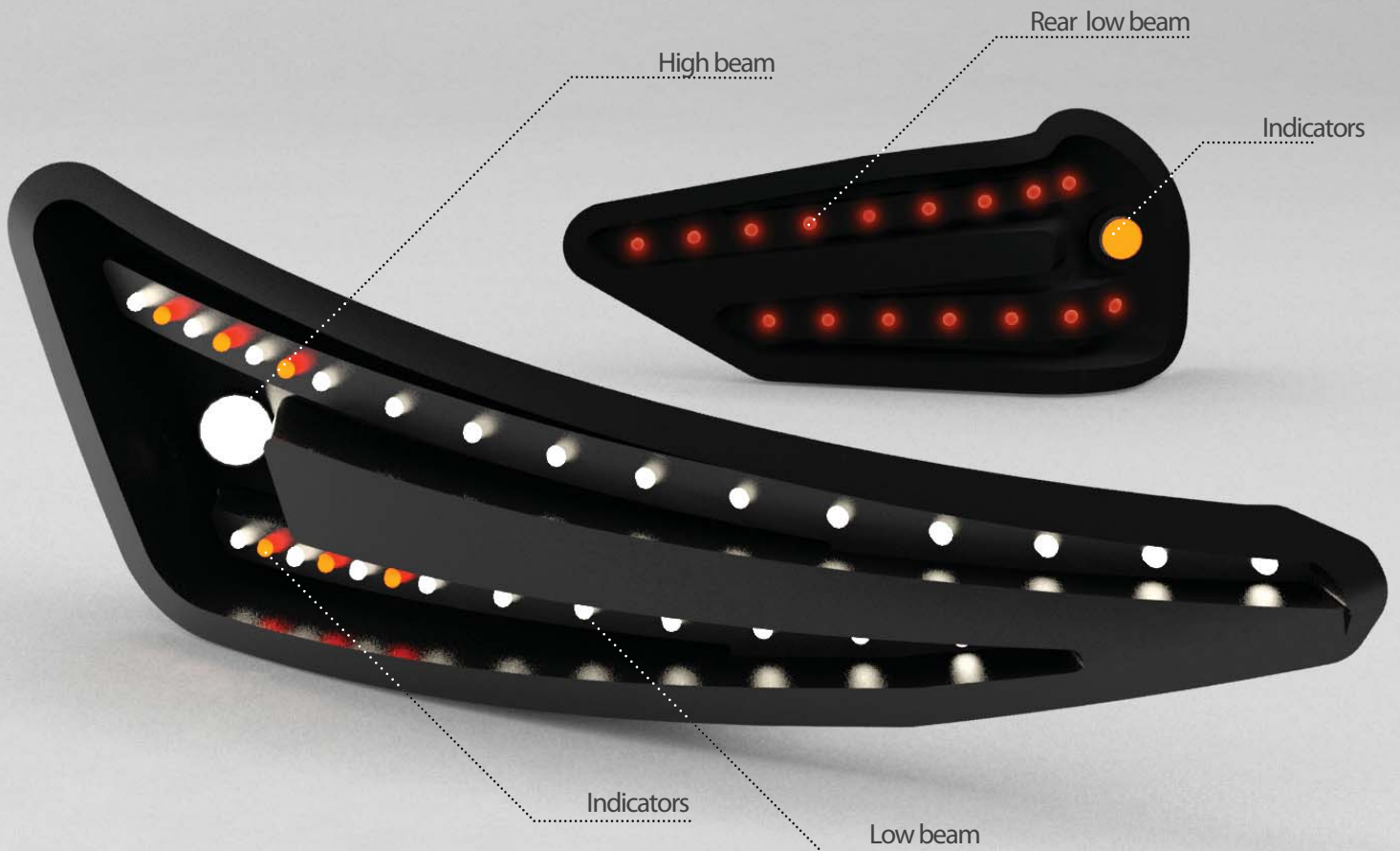


Figure 3.1.13: The final front light and rear light concepts.

### 3.1.6.6 Final Concept

The final concept basically looks like last semesters concepts, but have diodes as light sources instead of the laser lights. The front lights have strips of LEDs in top and in the bottom, and in between one can find the indicator lights, which also are 5 mm LEDs. For high beams, one Star LED is place on each side of the car, in the middle of the two low beam strips.

The rear lights are quit similiar to the head lights, it the way that they also got the strips of LEDs along the top and bottom, just that red lights are

used. The indicator lights are orange Star LEDs palced between the strips.

All the LEDs are mounted on a vacuum formed plastic part, made of spraypainted PET. The whole light is mounted on to the car with velcro.



8 different molds were made to vacuum form all the parts for the lights



The inside of the lights were vacuum formed in transparent PET, while the outside were made of poly carbonate.



The final front and rear lights mount in the finished car. The lights are attached to the car with velcro on the inside.

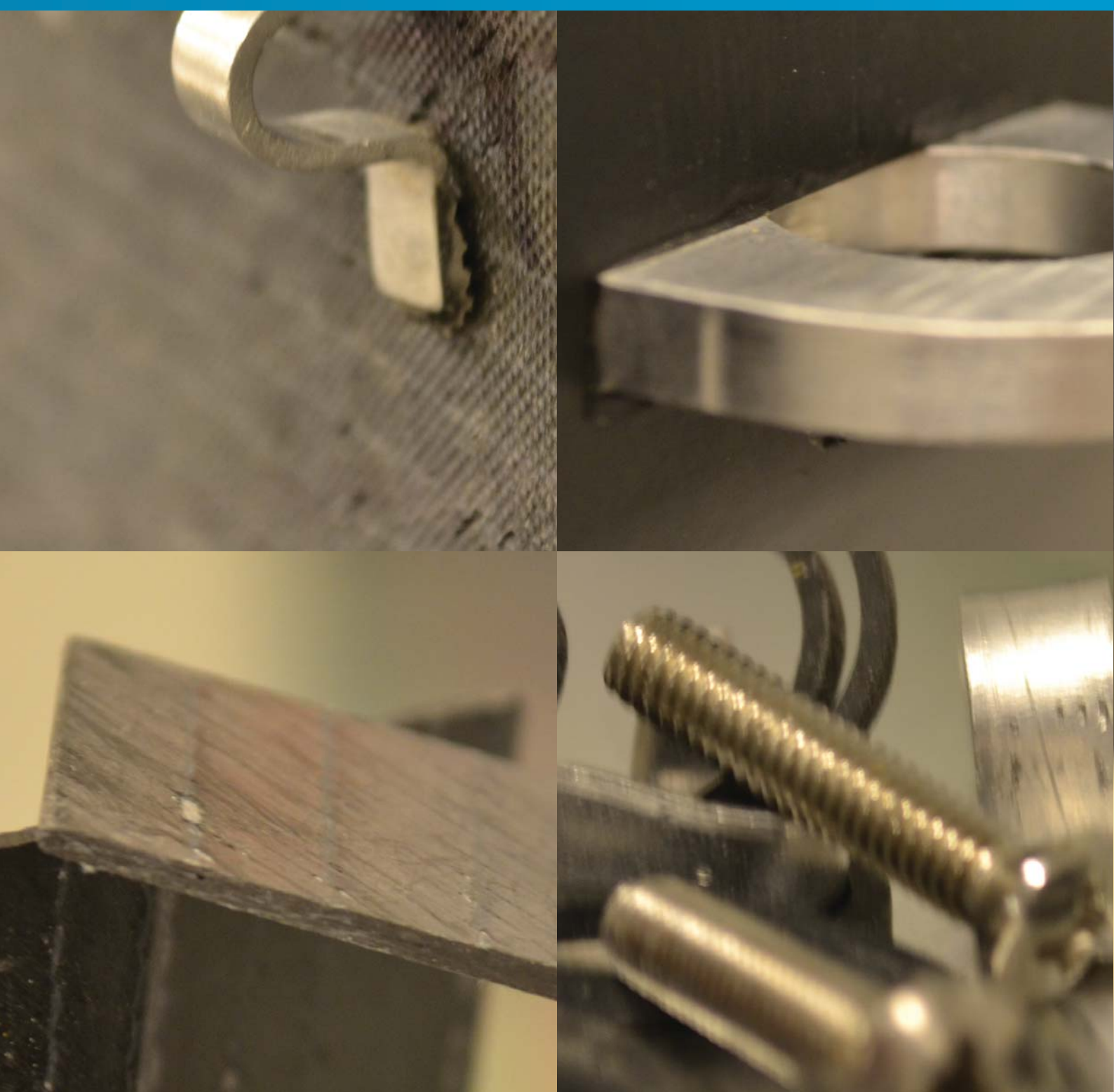


### 3.1.6.7 Production

Molds for both the glass and the inside of the lights were designed, and then milled on the CNC mill at IPD. The molds were then sanded down and painted, to get a perfect surface, since every single scratch would leave a mark in the glass.

When the molds were finished, the glass were vacuum formed with 1 mm poly carbonate, and the insides were formed in 1,5 mm PET. Holes for diodes were drilled and the whole thing painted in black.

To finalise the lights, the diodes were glued in and soldered together.



## 3.1.7 DETAILS

The design of DNVFF2 and SEM rules requires many small detail components. These have to be designed and produced along with other major parts. Saving weight in these small and relatively simple but numerous components will help to reduce the total weight of the car. SEM rules states that the urban concept cars should be able to drive in light rain. Sufficient ventilation and an effective windshield wiper are mandatory. Earlier years the detail components have not been given

proper attention. This has resulted in fast and simple solutions that in most cases lack the feeling of robustness. The sturdiness of the door has not been good enough. Specifications from the autumn semester (Endresen, et al., 2011) require proper design of all detail components. Robustness and a general feeling of quality has been the goal for the components mentioned in this chapter.





### 3.1.7.1 Door Details

Both door hinges and door handle are dependent on the placement of the door and in what direction it opens. Straight connection lines on planar surfaces should have been implemented in the design of the body. This would simplify both the design and production of the door details. The design of DNVFF2 does not include such design properties. Several different placements of the hinges shown in figure 3.1.10 were therefore thought of.

Another important factor is how many degrees

one have to open the door to reach the specified door opening by the SEM rules of 500x800mm. Simple CAD models of selected concepts are shown in figure xx. These were made to further investigate the different qualities of the solutions.

Gullwing doors shown in figure 3.1.15 are mounted in the roof of the car. This was initially the planned solution when designing the body. It looks good and gives the driver good access to the car. Reaching the required door opening is not a problem with this concept. Since the window is not stiff enough to carry any load, the

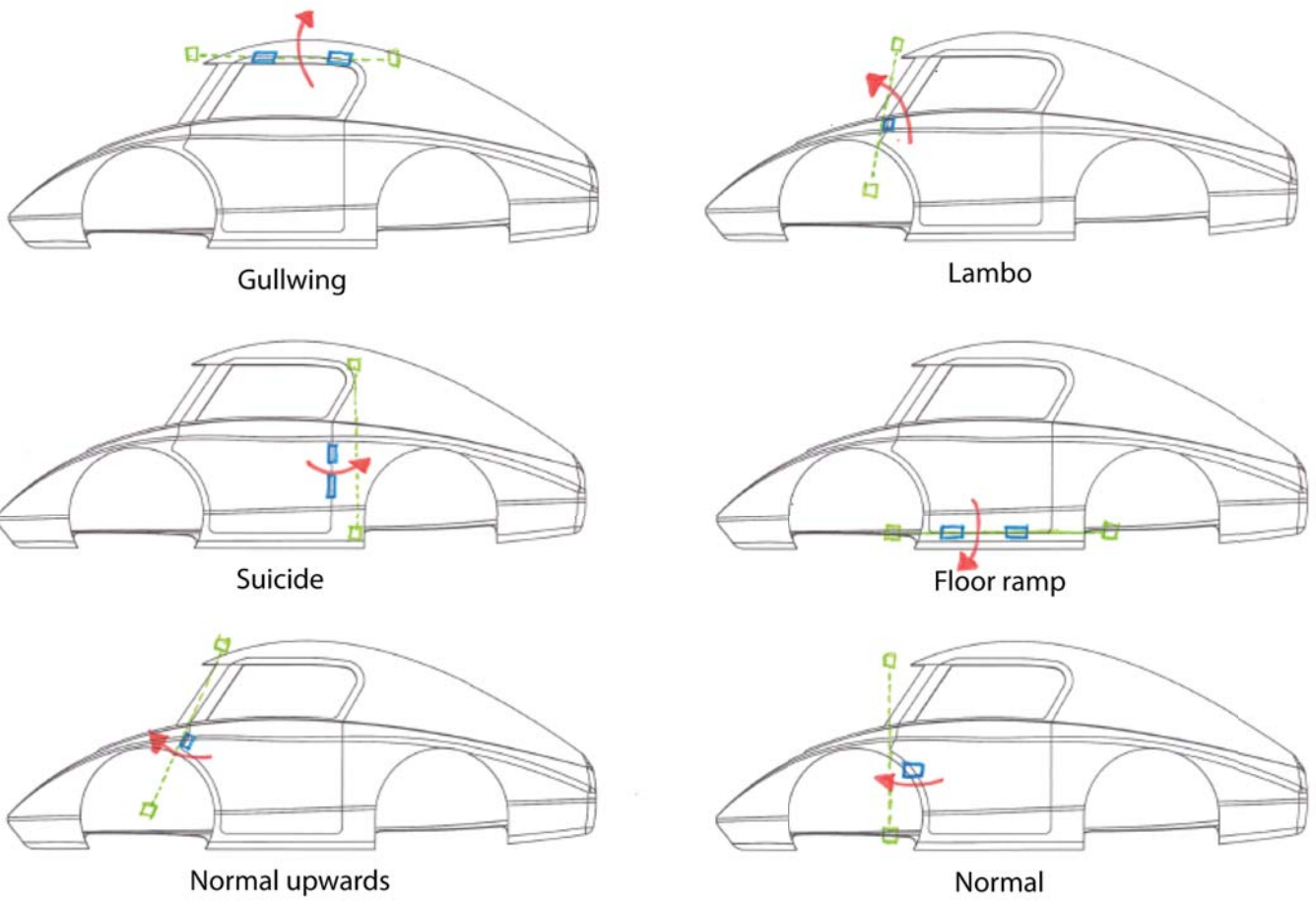


Figure 3.1.14: Different placements of the hinges

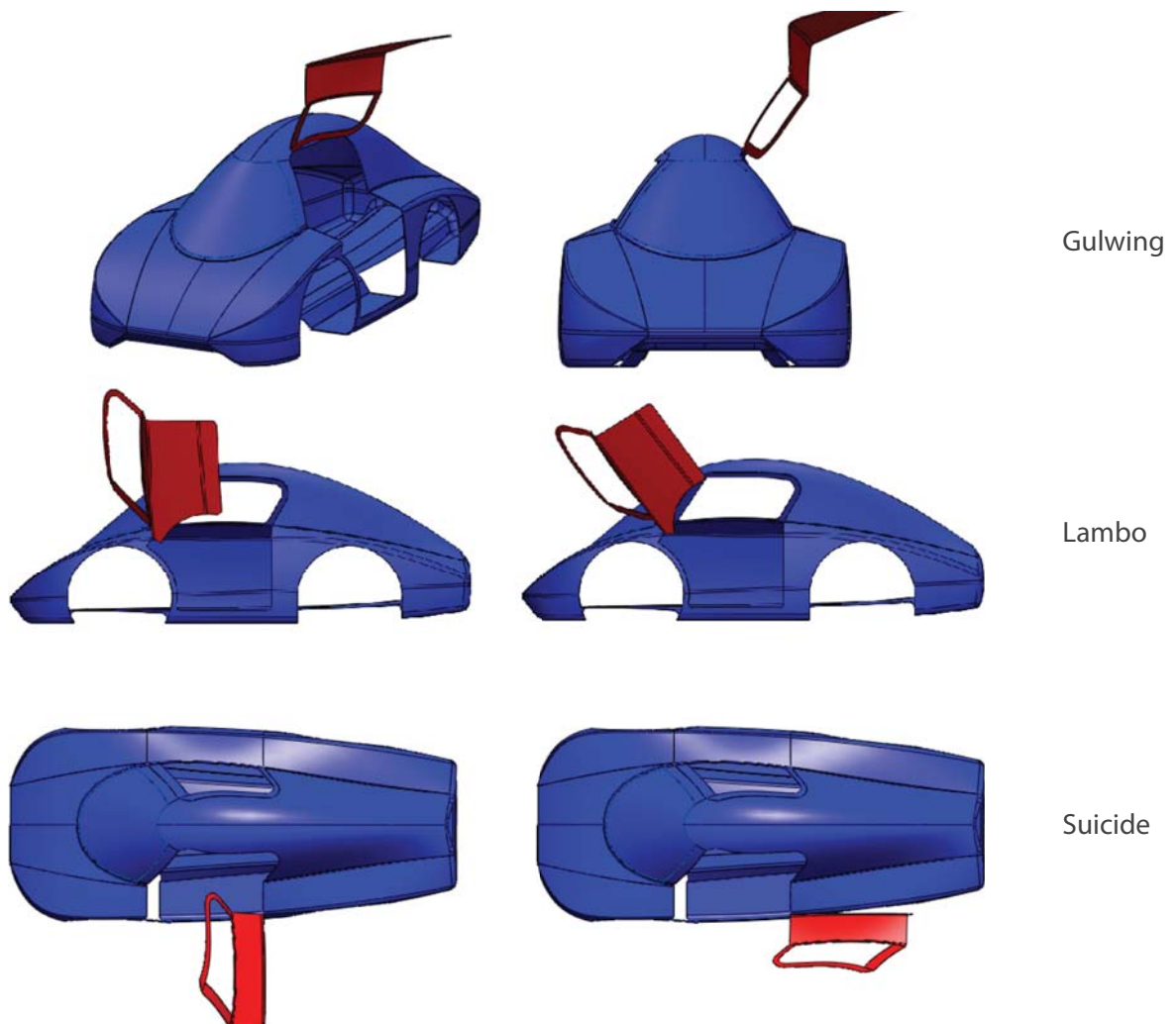


Figure 3.1.15: Different door opening solutions

frame around the window must be reinforced. A separate mold would have to be produced to manufacture the door. Connection line between the body and the door are quite curved in the roof, this increase the complexity of the solution. The door will not stay open by itself and a separate mechanism is needed for this purpose. The gullwing door was discarded for these reasons, but should be looked further into.

Lambo doors shown in figure 3.1.15 are mounted in the front part of the door. This concept takes advantage of the relatively straight connection line between door and body at this position. To reach the required door opening the door must be opened approximately 120 degrees. The front of the door would come in conflict with the windshield, and this solution was therefore discarded. It is not known whether the door would stay open by itself, or needs a separate mechanism like the gullwing door.

Suicide doors shown in figure 3.1.15 are mounted in the back part of the door. This solution takes advantage of the straight connection line between body and door. Door movement up to 180 degrees is needed to secure correct door

opening according to rules. This solution has the advantage of the door staying open in most positions by itself. The concept of suicide door was chosen as it would not require a separate mechanism to stay open or reinforcements of the door.

### Hinge

Earlier years NTNU SEM teams have used standard hinges from kitchen cabinets made in steel. The new requirement regarding stability and robustness, gave the need for a custom hinge. Designed to be as light and stable as possible, many concepts were considered. In figure 3.1.16 some of the iterations are seen.

A suicide door solution required the hinge to be opened 180 degrees. To reach the specification from 2011 (Endresen et al., 2011) and still maintain low weight, two small hinges was used. Each hinge weighs about 50 grams, and is produced in carbon fiber and aluminum. The final design takes advantage of two pivot points to secure 180 degree movement as shown in figure 3.1.18.

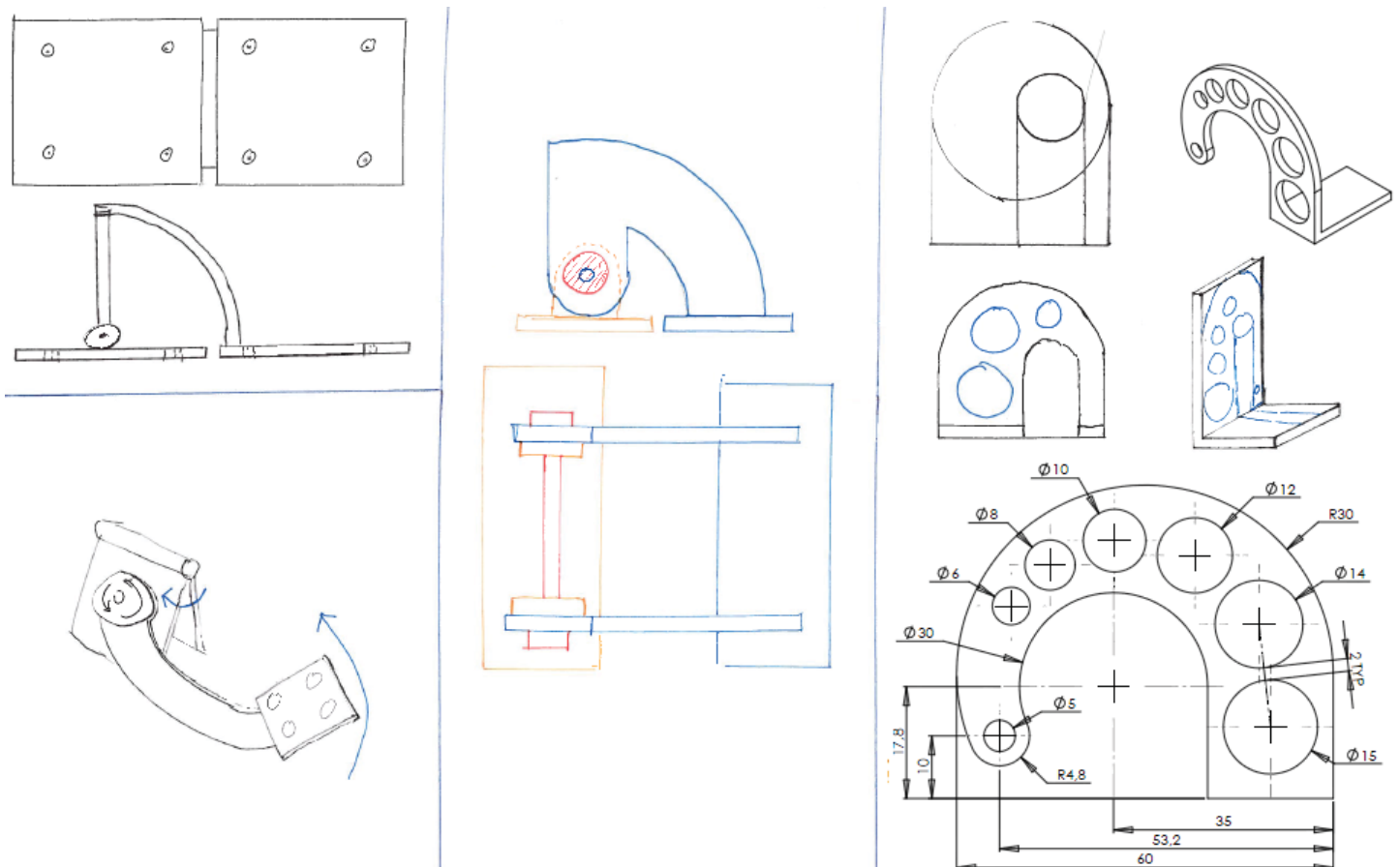


Figure 3.1.16: Idea generation of different hinge concepts



Final hinge design assembled. Two pivot points ensures 180 degrees opening. A combination of carbon fiber and aluminum results in a robust and light weight product

The arms of the hinge were milled out from a 2 mm thick plate made with prepreg carbon fiber. Araldite 3021 was used to glue the carbon fiber arms to the aluminum tube. To reduce wear it was important that all moving connections had metal to metal contact. The aluminum tubes are designed to completely separate the carbon fiber from moving components. This will ensure maximum stability over time.

Araldite was used to glue the hinge brackets on to the door and body. These surfaces are curved, and measures were taken to ensure correct alignment of the hinges. While gluing the upper and lower brackets were connected with rods. Wedges of araldite had been prepared to perfectly space out the brackets. Figure xx shows all the components in the hinge assembly including the araldite wedges.

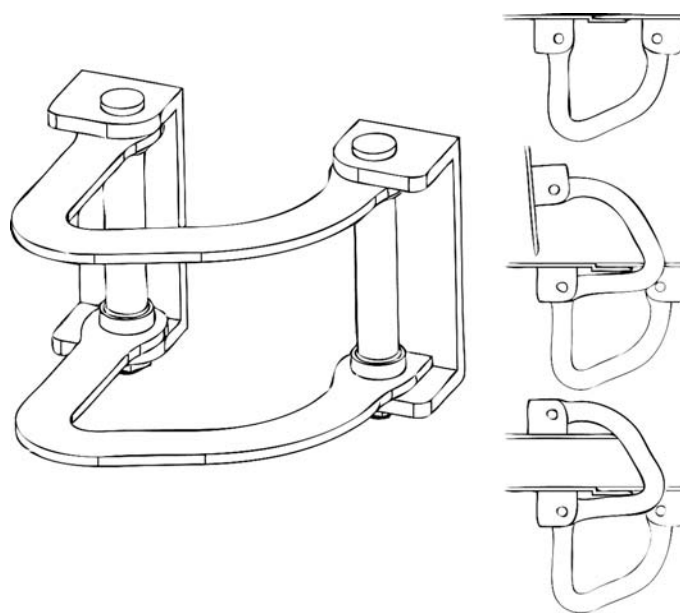


Figure 3.1.18: Principle drawing of the hinge showing the opening motion

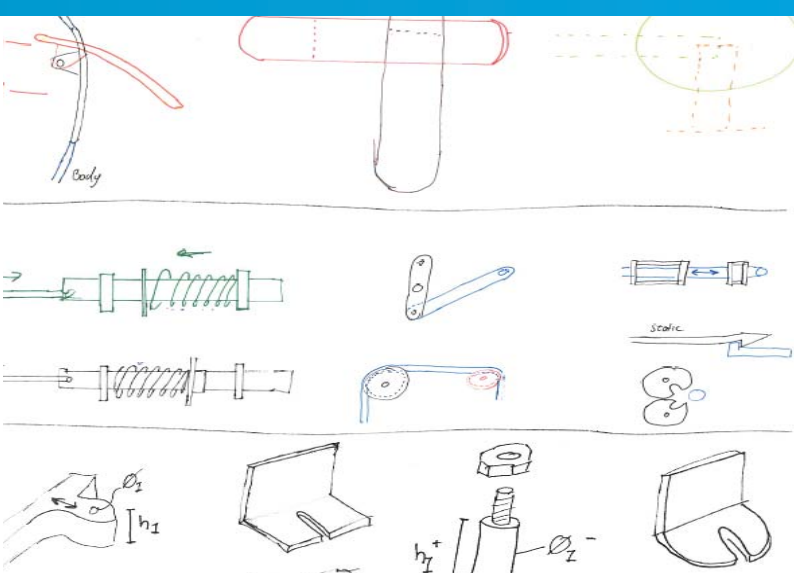
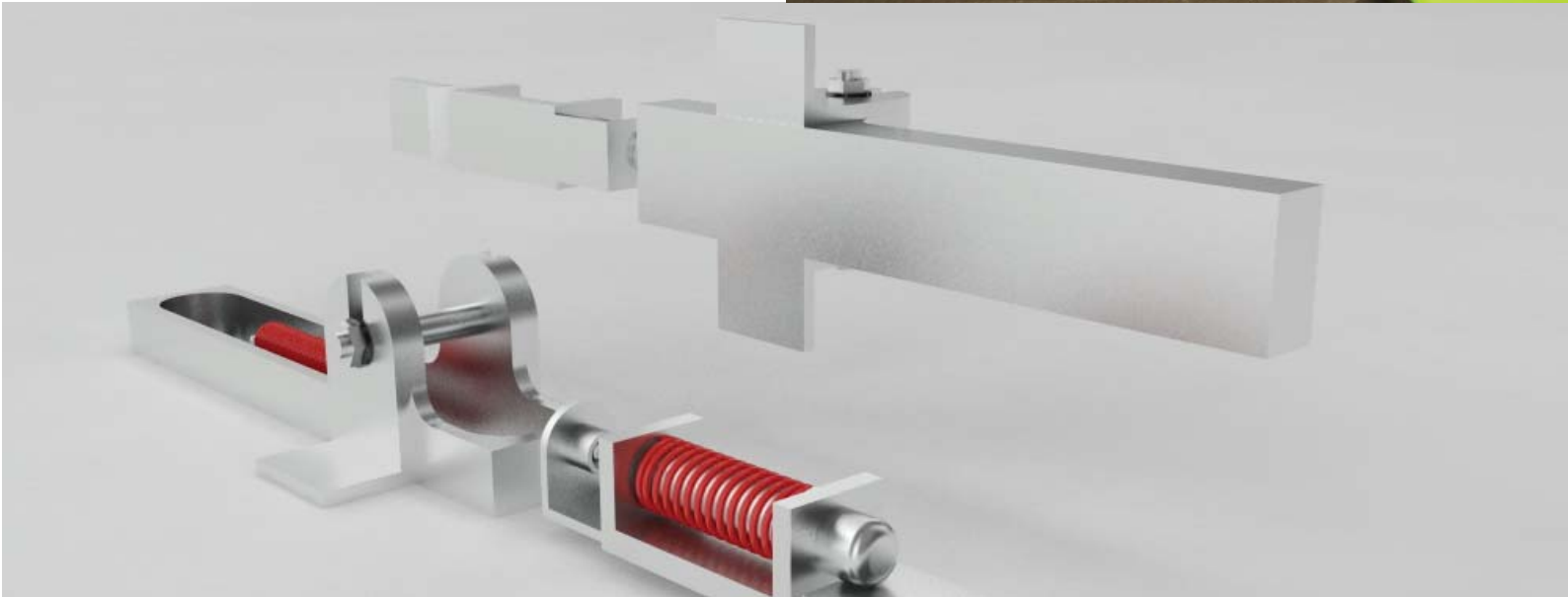


Figure 3.1.17: Idea generation of different door handle concepts



Spring loaded door handle made in aluminum safely secures the door in place. A flush finish ensures little interference with air flow.

### Door Handle

Along with robust details, it is important to keep the outer surface of the car as smooth as possible. The door handle must therefore be located inside the car, or kept flush with the body. In the design phase low weight, robustness and smooth transitions were the most important factors. To secure the door in closed position, a latch operated by the handle was introduced. Some varieties of the door handle and latch examined during the project are seen in figure 3.1.17.

Final design and its function are shown in figure xx. The front part of the handle is pushed in by the user, this reveals the back part now coming out from the car body. Further movement of the handle will engage the door latch releasing the door from the body. All components except standard fasteners and springs were machined in aluminum. The brackets were glued to the door

with Araldite.

Final design and its function are shown in figure 3.1.19. The front part of the handle is pushed in by the user, this reveals the back part now coming out from the car body. Further movement of the handle will engage the door latch releasing the door from the body. All components except standard fasteners and springs were machined in aluminum. The brackets were glued to the door with Araldite.

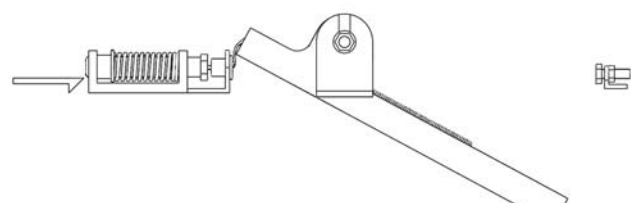


Figure 3.1.19: Door handle in the open position

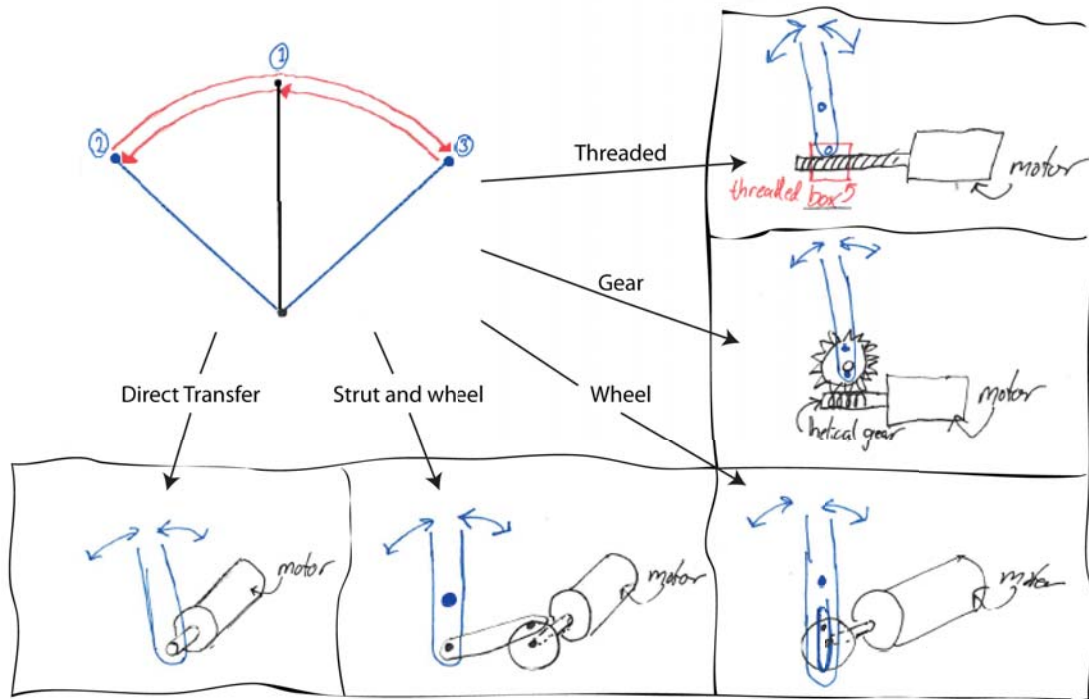


Figure 3.1.20: Idea generation of windshield wiper

### 3.1.7.2 Wiper

For the first time in SEM history, all cars in the urban concept class needs an effective windshield wiper. The type of wiper movement and placement had to be established. If the windshield is big or has a square or rectangular shape, the parallel wiper movement seen in figure xx might be the best choice. As DNVFF2's windshield is curved in all directions and far from rectangular in shape, the normal pendulum motion shown in figure xx is more suitable. The wiper motor and shaft can be placed all along the outer edge of the windshield, but needs some space on the inside of the body. The wiper was therefore mounted in center of the lower part of the windshield. The wiper arm and blade should be positioned vertically in the center while driving. Aerodynamically this will give the least interference with airflow over the body.

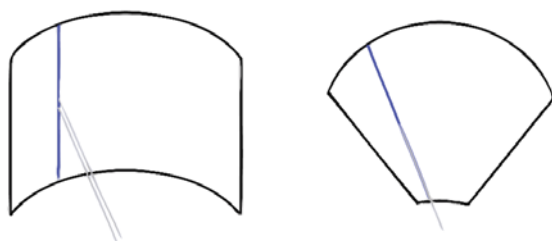


Figure 3.1.21: Different wiper motions

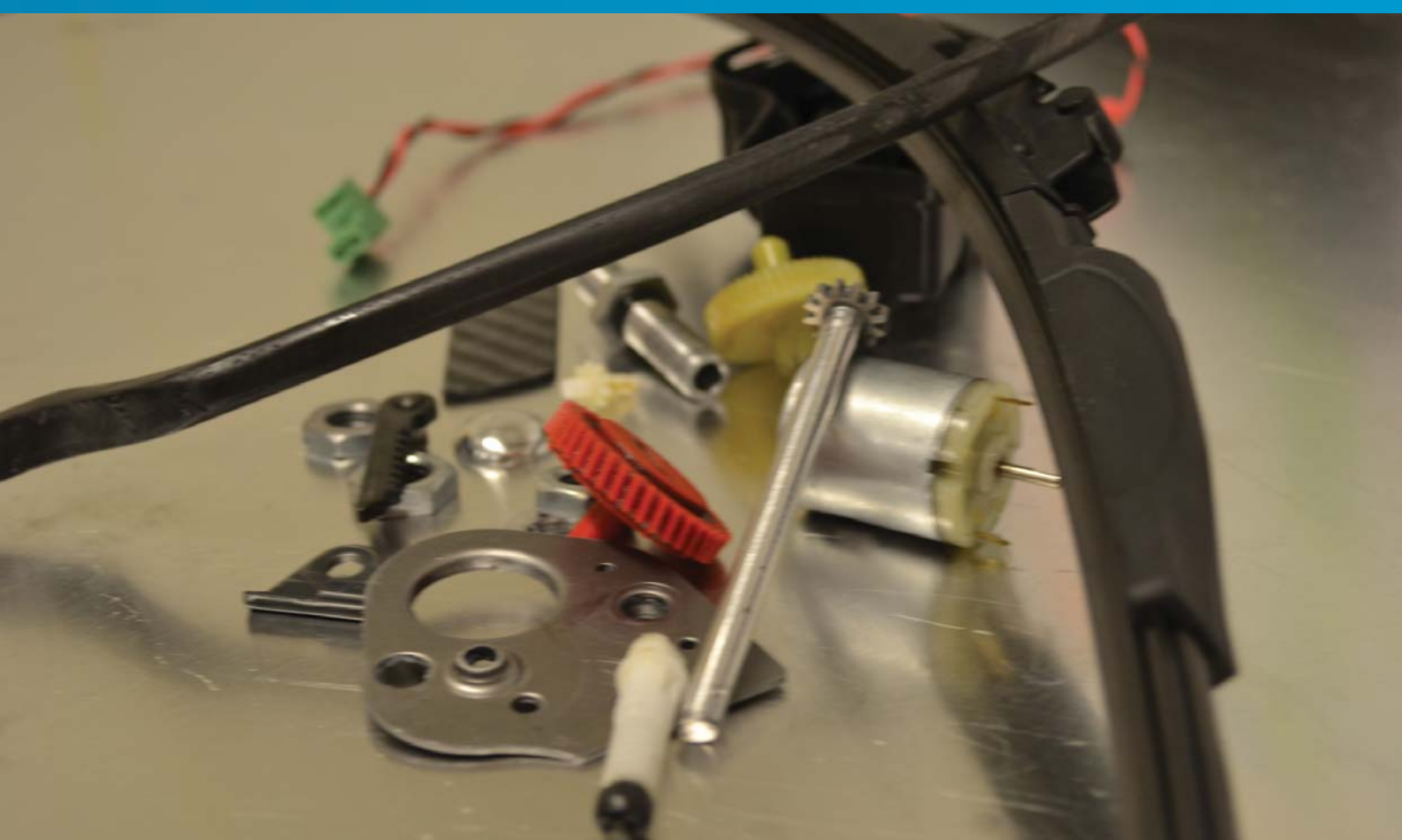
### Design

The idea of having only one component outside the car was introduced quite early in the design process of the wiper. Combined wiper arm and blade could reduce weight and impact on the airflow of the wiper. Because the windshield is double curved this type of wiper would have to be quite flexible. The stiffness needs to be perfect along the length of the wiper to secure contact between the blade and window at all times. A prototype of this concept was produced, but the performance of the wiper was not convincing. The uncertainties around the practical testing of SEM rule regarding the wiper in technical inspection made the team aim for a safer more standardized solution.

Figure 3.1.20 shows some early concepts developed for the wiper motor. Along with weight the simplicity regarding programming and control system was valued. The concepts called wheel and strut and wheel both have the advantage of mechanically providing the pendulum motion. To reduce weight it was important to examine the possibility to produce small parts. Gears to slow down and increase the torque of the electrical engine were required. With no possibility to effectively produce the components needed, buyable solutions was looked into. Conventional windshield wiper motors are usually over dimensioned and too heavy for this use. The focus was therefore turned towards headlight wipers. These motors turned out to be in the correct weight range, and a used headlight wiper motor from a Volvo 340 was bought.



*Final windshield wiper design with wiper motor, wiper blade and wiper arm.*



### *Production*

Most parts produced for the windshield wiper are machined in aluminum. The mounting bracket is made from prepreg carbon fiber with the same mold used to produce the horn bracket. This type of standardizing components saves a lot of time in both production and planning. By stripping down and replacing steel parts with lighter components, the weight of the motor was reduced by 40 percent.

To produce the first prototype of the wiper arm a mold was made from a steel plate. The plate was rolled to the desired curvature and supported by a plywood frame. By producing the arm in carbon fiber, the idea was to alter the stiffness throughout the length of the arm by the amount of layers. A 50mm wide sheet of carbon fiber with thickness ranging from 1-2 mm was produced with the water reservoir method. 10 mm wide strips were cut out from the sheet, were one of them had a 20mm in diameter mounting surface in the thickest end. The stiffness was tested on the mold for the front window. Several strips of different lengths were connected with tape to find the optimal thickness. As the window is double curved this appeared to be more difficult than first thought. The concept of combined wiper arm and blade was abandoned. A more conventional solution with a wiper arm connect-

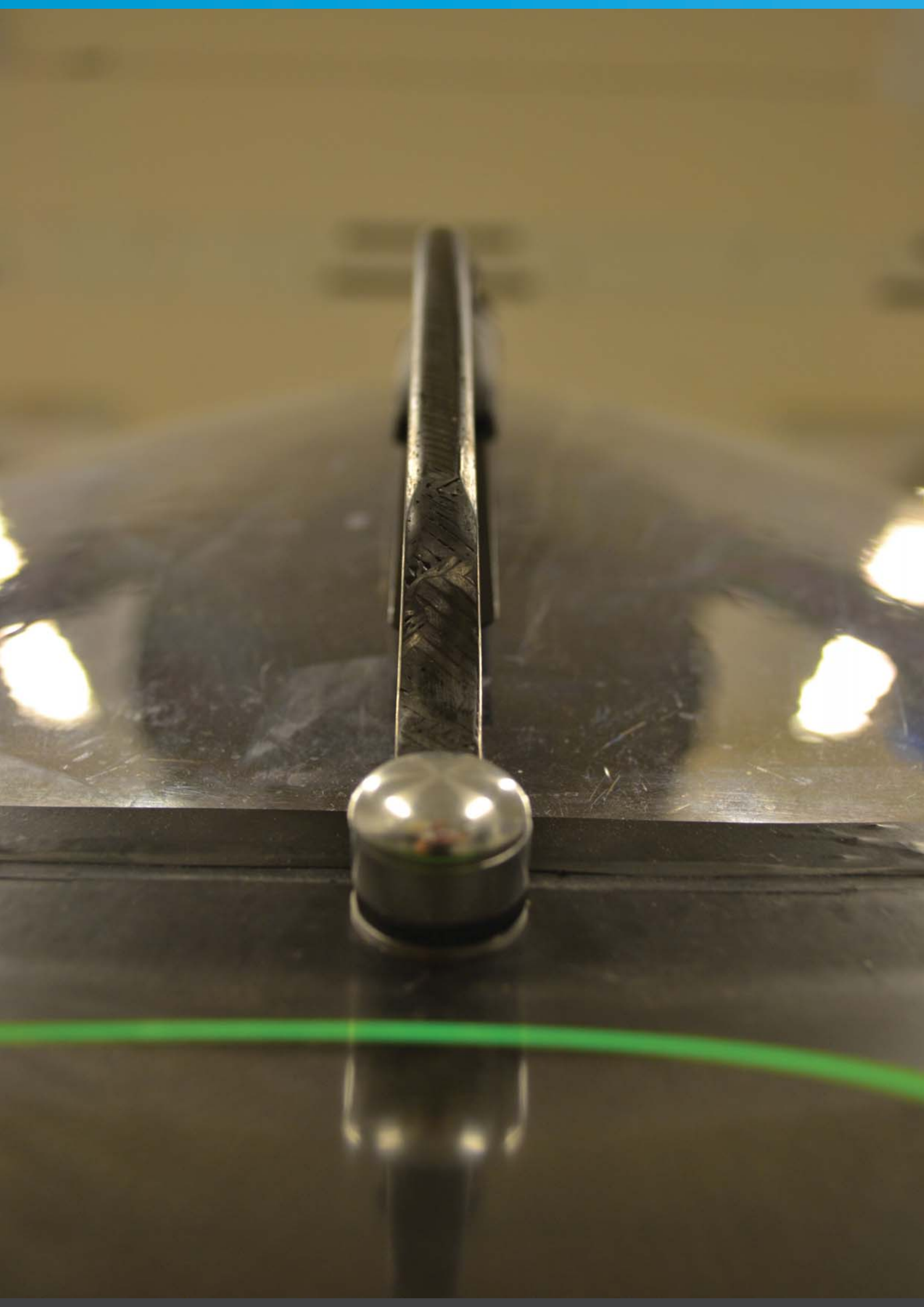
ed at the middle of the wiper blade was quickly designed.

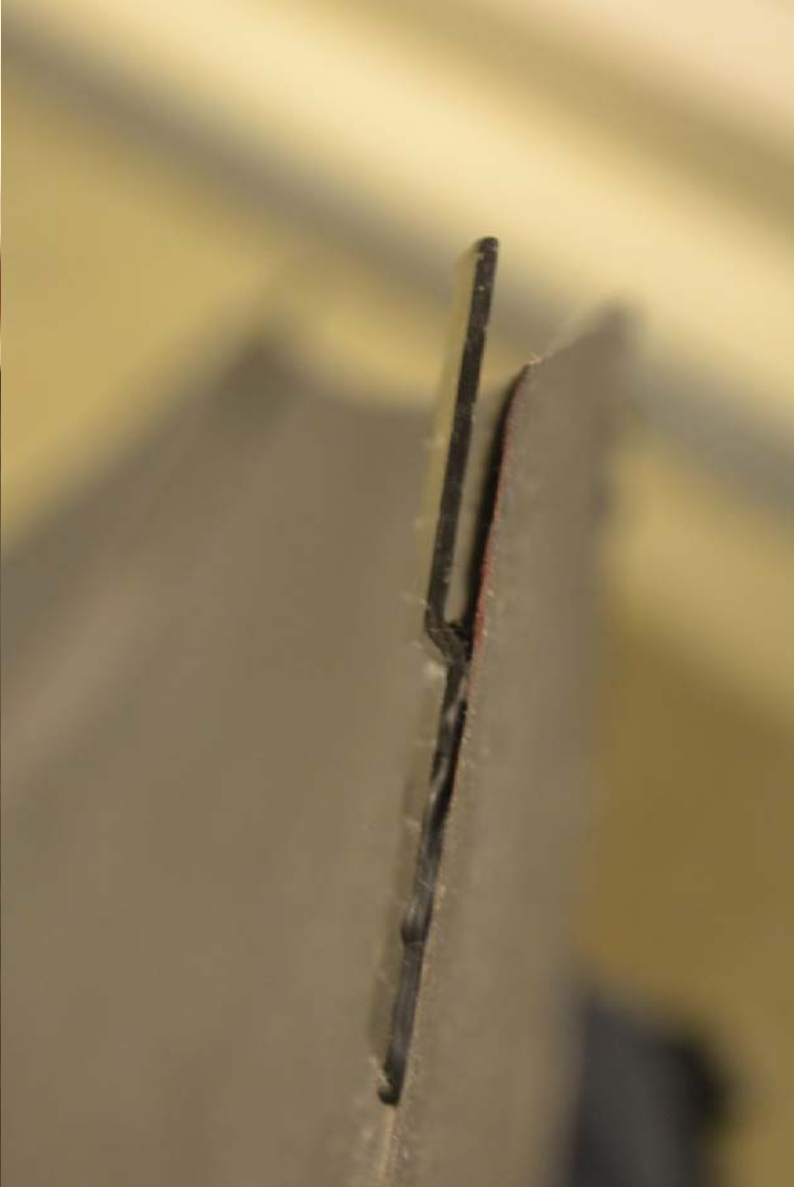
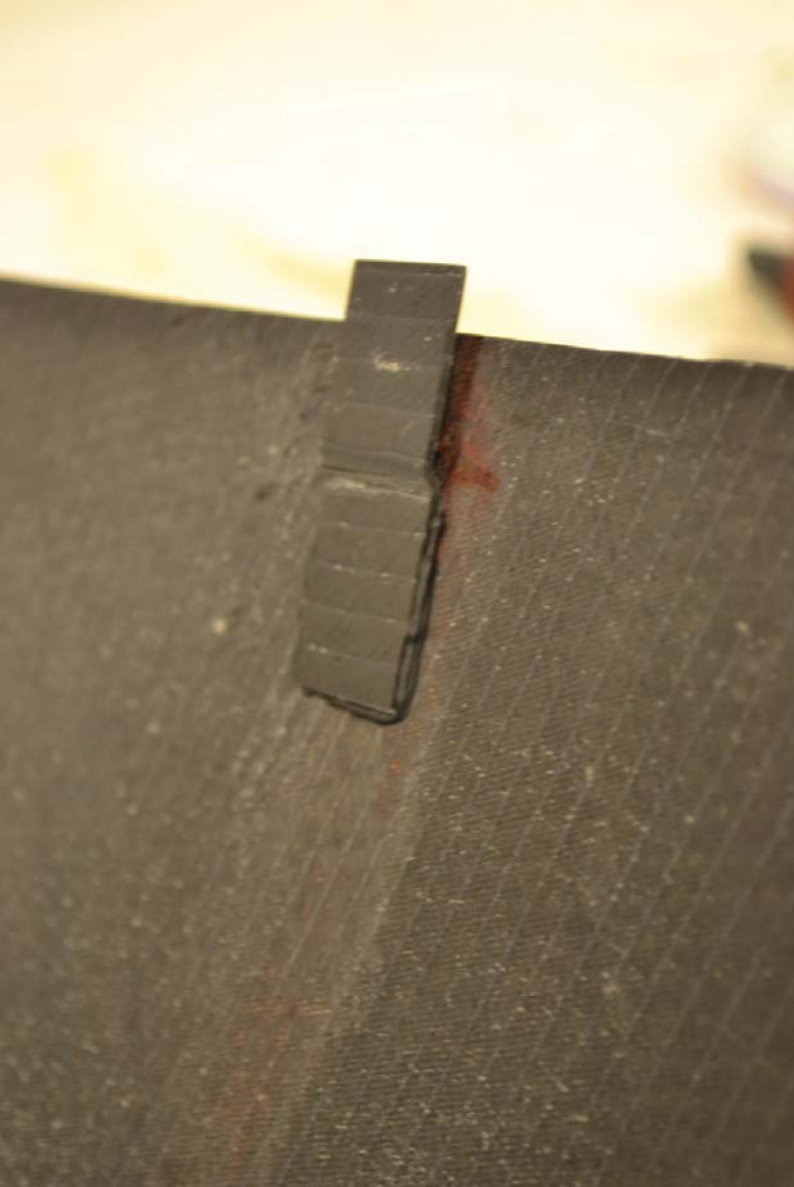
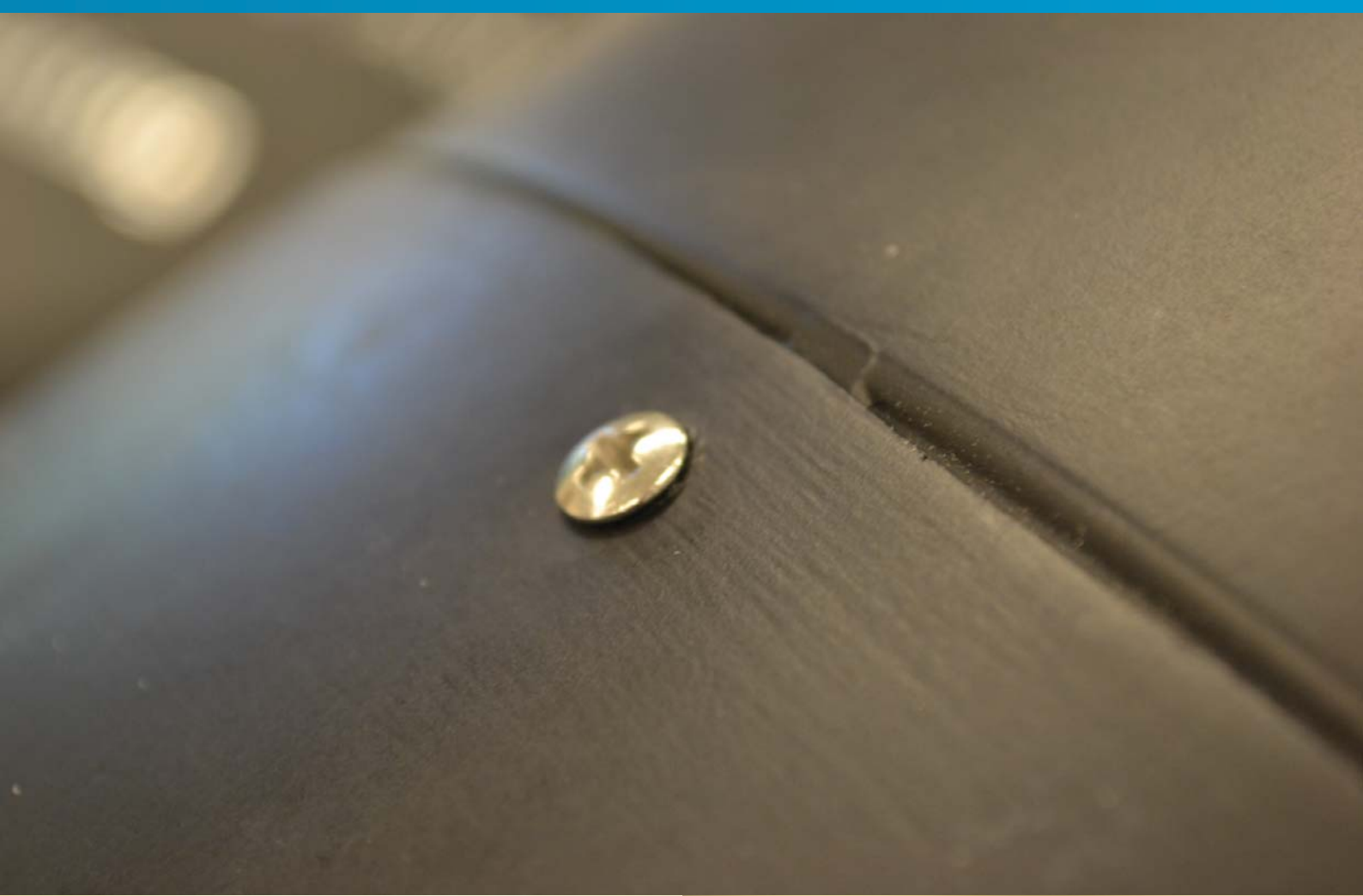
Strips of carbon fiber from the prototype were heated up to 110 °C. Each strip was pressed down on a mold giving them the desired s-shape in one end. The steel plate used in the prototype production was rolled once more to increase the curvature. Four strips of carbon fiber were glued together with Araldite, fixed to this new mold and reheated. After hardening of the araldite, the semi-finished wiper arm was grinded down to its final shape. It was important in this step to constantly check the stiffness of the arm, and not remove too much material. As a final touch the wiper arm was sanded down with fine grade sandpaper, and clear coat was applied.

### *Assembly*

When all the parts had been produced the bracket was glued to the car body with Araldite. After the glue had cured, the wiper motor was assembled and connected to the bracket. The altered wiper blade was fastened to the wiper arm, which was connected to the shaft of the wiper motor with two M3 set screws. It is worth mentioning that during the technical inspection of SEM 2012, the inspectors commented that this wiper was the most effective they had seen in the competition.







## BACK HATCH MOUNTING :

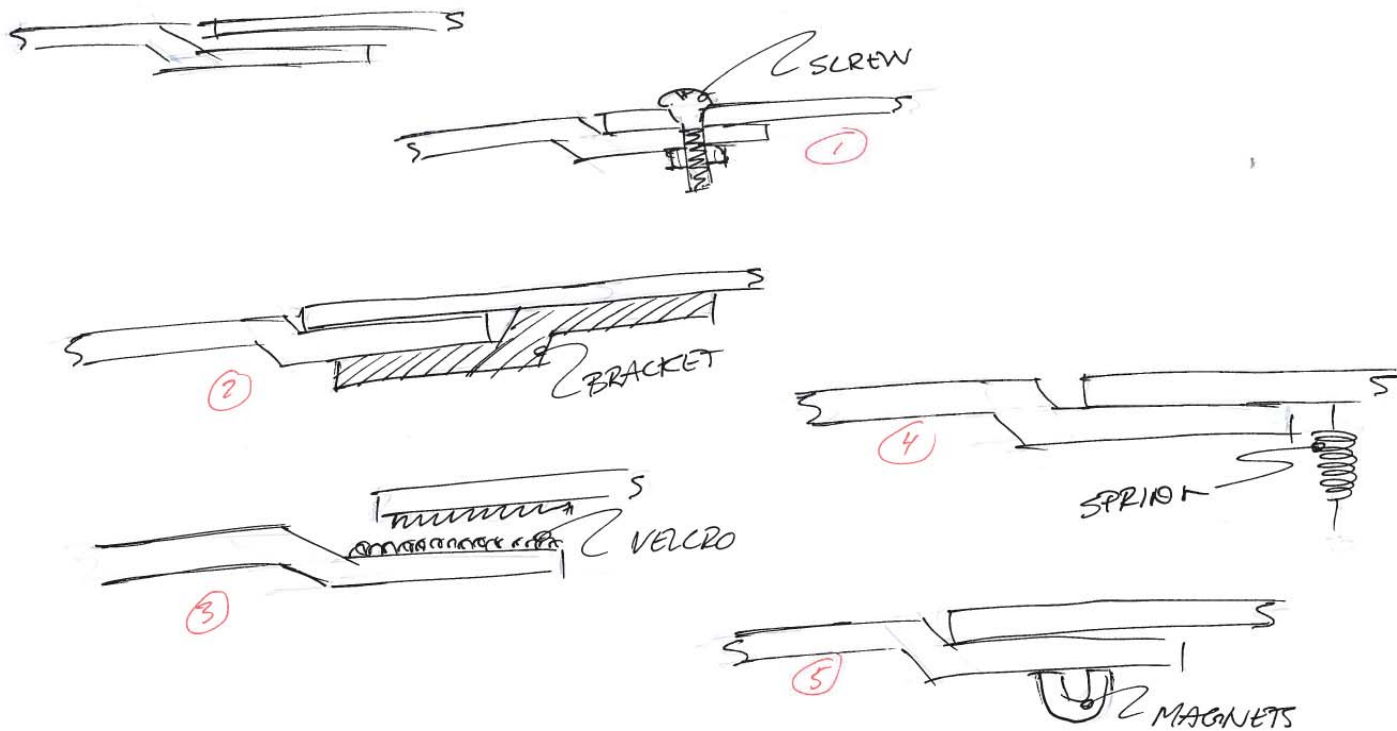


Figure 3.1.22: Idea generation for mounting the back hatch

### 3.1.7.3 Back Hatch Mounting

Attachment of the back hatch was considered to be easy and development of a mounting fixture was postponed until final assembly. Many different concepts were considered, but the desire to keep the surface clean and smooth gave a lot of restrictions. In figure 3.1.22 some of the early concepts are seen. A new SEM rule also stated that all covers and doors must be mechanically attached, so the old solution with Velcro and a tight fit was not adequate for the new car.

To maintain the smooth transitions and clean look of the exterior, an internal mounting was the best option. The bracket solution could use the flexing properties of the back hatch to keep it in place. It was decided to produce the brackets in carbon fiber. Two steel plates were milled down to form the molds. Four layers of carbon fiber were placed between the molds, clamped together and the carbon fiber was set to cure.

In addition to the bracket, a screw connection was placed on top of the cover. This was to prevent the cover from falling off during racing. A small aluminum disk was threaded and glued on the monocoque indent to make the back part of the screw connection.

The brackets performed very well in mounting the back hatch. The flexing of the door and the tight fit of the brackets made a perfect attachment. During racing, strips of foil were added around the seam of the door. This was to make the door waterproof and to improve aerodynamics.

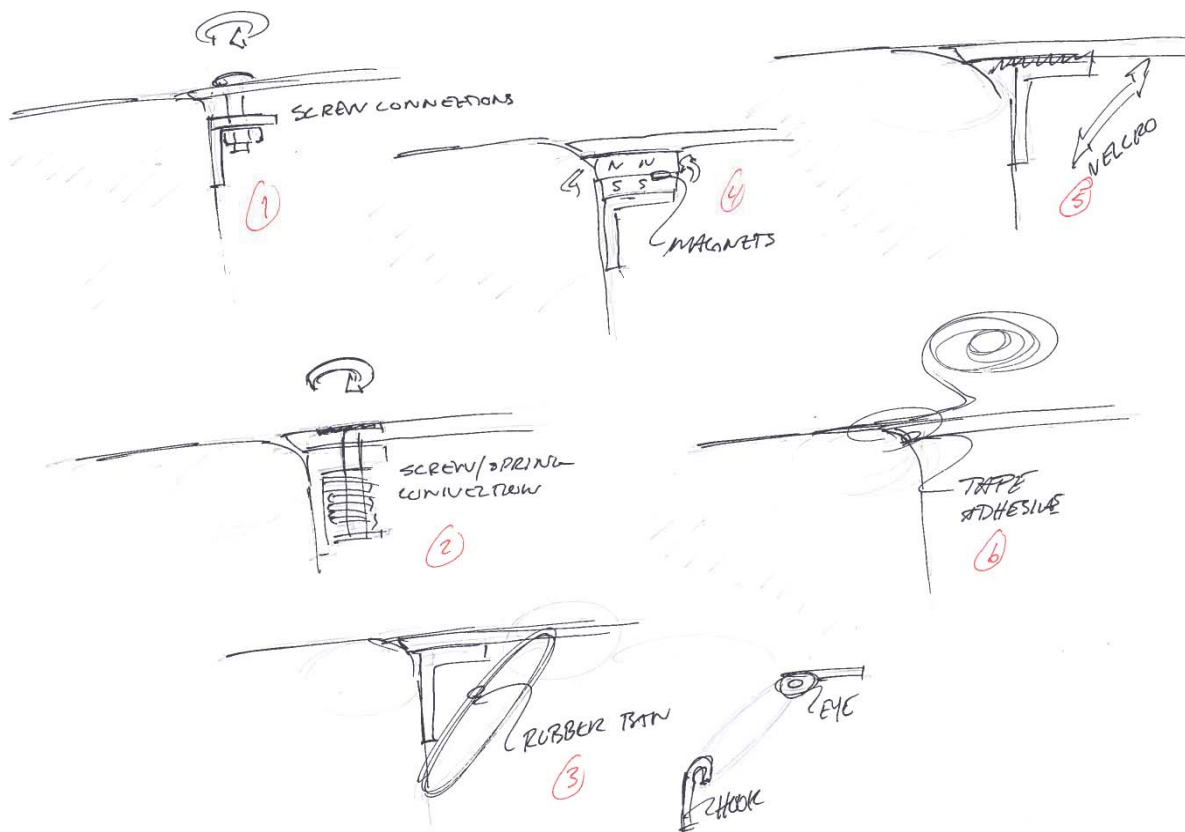


Figure 3.1.23: Idea generation for mounting the side covers

### 3.1.7.4 Side Cover Mounting

Attachments of the side covers were also postponed until final assembly. A solution to attach the covers was not established until a couple of weeks before departure, due to other more prioritized tasks. As for the back hatch, a smooth and clean look was the most important factors when designing the mounting fixtures. Different concepts were evaluated and a final concept was chosen. See figure 3.1.23 for the different concepts evaluated.

A solution with the use of rubber bands and screws was the solution chosen. Two screw connections were placed on the underside of the covers. Threaded aluminum disks were glued onto carbon fiber brackets and glued onto the side of the wheel well.

The side part of the side covers were attached with rubber bands. Aluminum fixings were produced and glued onto the side covers and wheel well. Carbon fiber brackets were also produced to stop the cover from sliding into the wheel well.

In addition to the two screws and three rubber bands per side cover, strips of green and black

mate foil were applied around the seam before racing. This further improved the transition and attachment between the monocoque and side covers.

The solution proved to be sufficient and no problems were experienced during testing and racing. Assembly and disassembly of the side covers can be a bit difficult. The screw connection is not easy to access, but sliding under the car when placed on the ground makes it easier. A new solution to improve assembly can be developed, but since the covers are just essential during race, this should not have a high priority.



*Top: Rubber band connecting the side cover and wheel well.  
Middle: Aluminum fixings on side cover and wheel well. Carbon fiber stopper used to secure the side cover.  
Bottom: Screw connections securing the cover in the tunnel, underneath the car.*

## TOWING HOOK

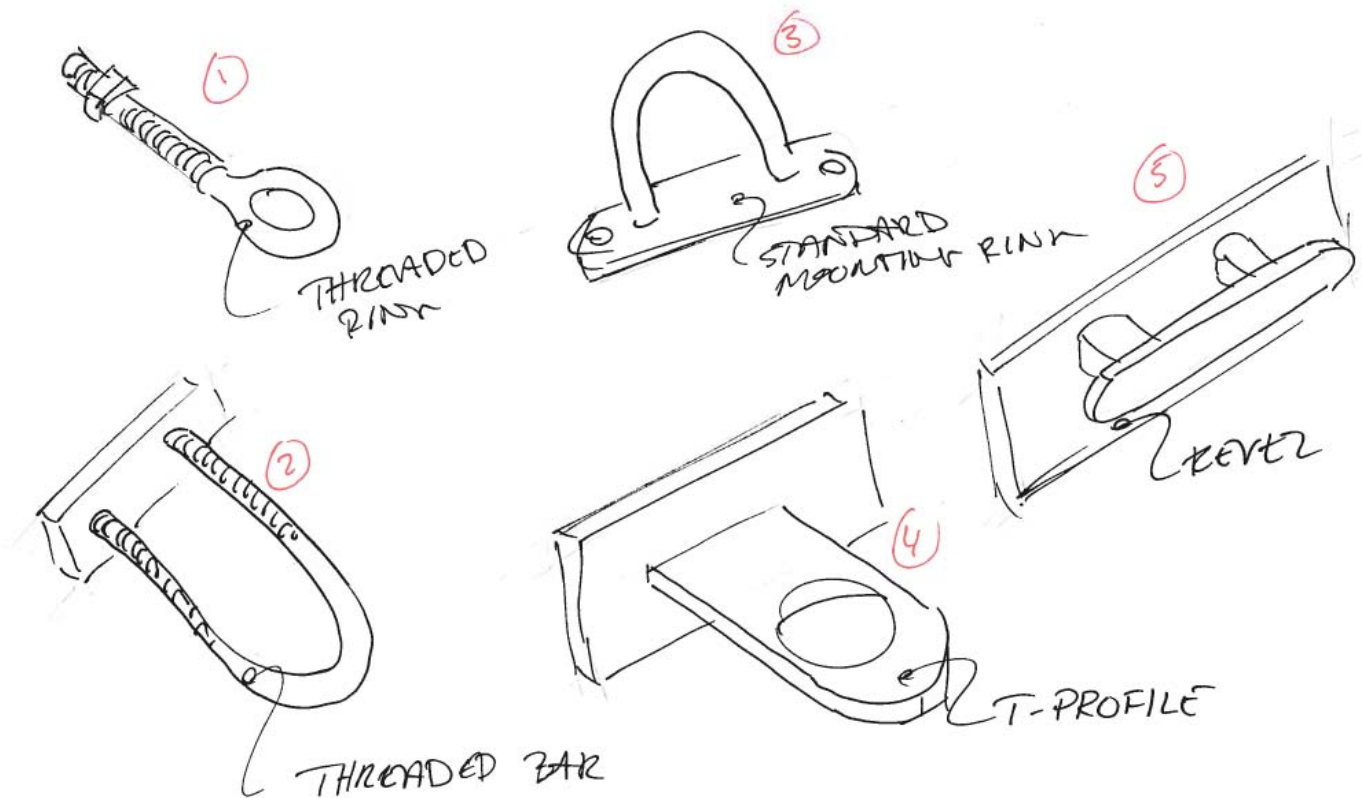


Figure 3.1.24: Idea generation for the towing hook

### 3.1.7.5 Towing Hook

A new towing hook was design and produced for the new car. The old towing hook for the DNVFF consisted of a steel threaded bar formed in a U-shape, attached to a steel plate glued inside the car. Reusing this solution was never considered. There was improvement potential concerning weight, looks, strength and aerodynamics.

To keep the weight down, the towing hook should be produced in aluminum. Because of the material properties of aluminum, welding was not an option. With a T-profile in aluminum the towing hook could be produced in one piece.

The towing hook was milled down to the correct dimensions and a rectangular slot was prepared in the monocoque. Araldite glue was used to fasten the hook to the monocoque.

The towing hook has never been tested in real conditions or but should withstand loads up to 2000 N. Final towing hook weighed 40 g, compared to the old towing hook of 120 g, is this a great improvement. The hook is placed in the split line, standing horizontally outwards. This is the placement where the hook has minimum influence on the airflow. The car should never be lifted in the towing hook, since the hook is designed to handle horizontal loads only.

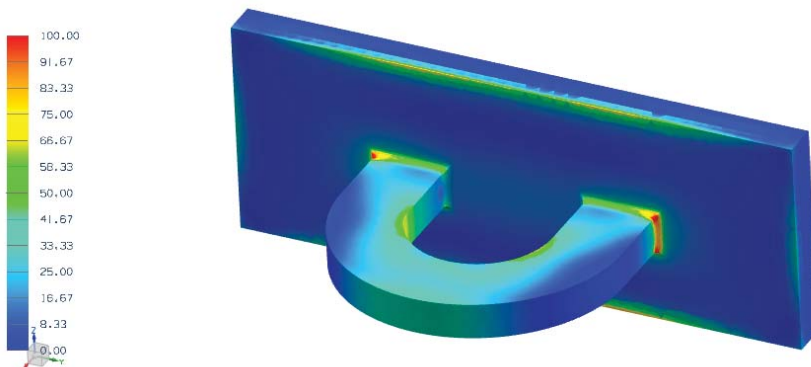
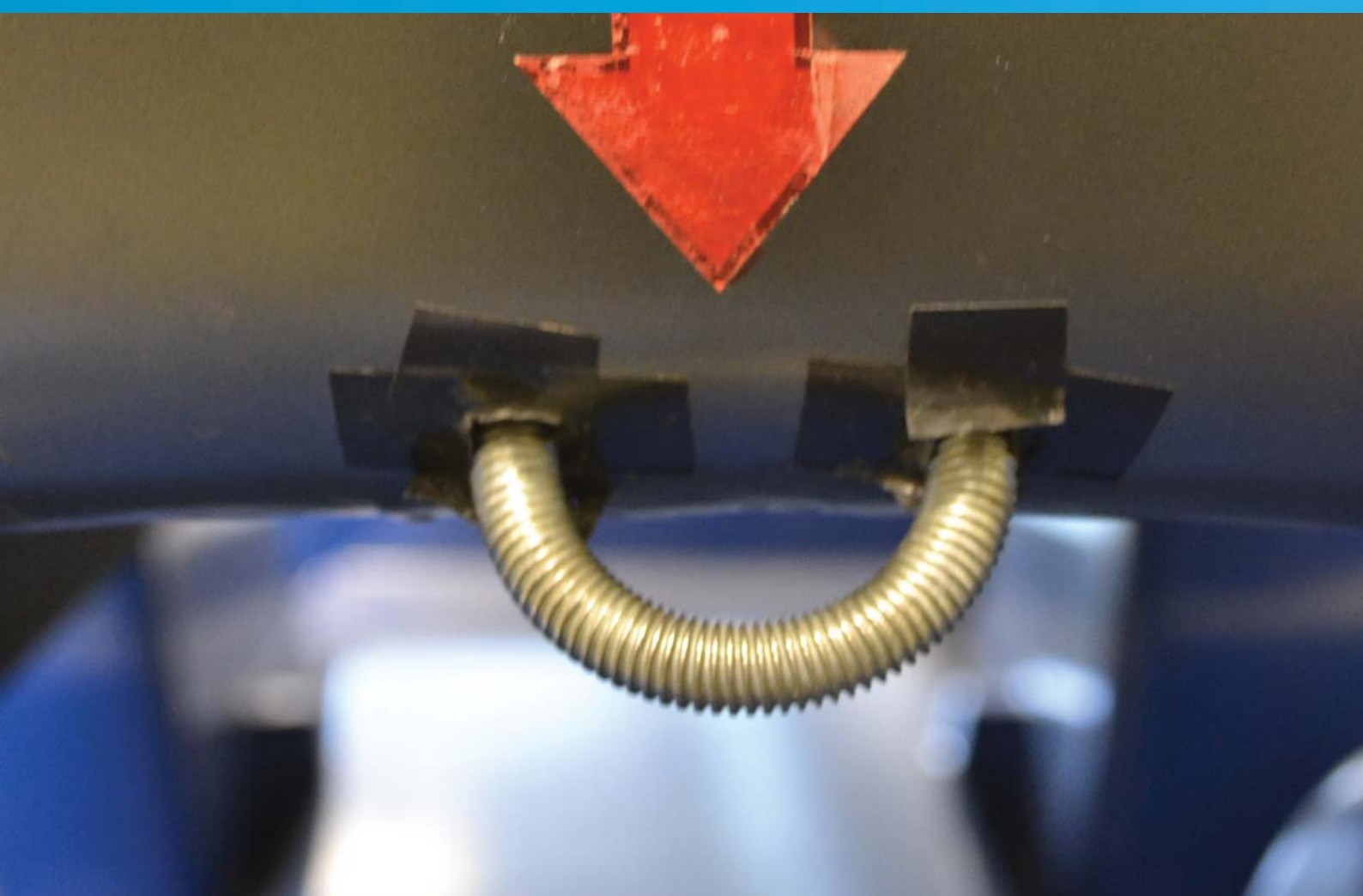


Figure 3.1.25: Strength analysis of the towing hook. The 2000 N load yield maximum stress of 110 MPa.



*Top: Towing hook of the DNVFF, threaded bar solution.  
Bottom: Final design of the towing hook installed to the DNVFF2. One aluminum part.*



*The former car had been painted several times, which have resulted in a rough surface*

## 3.1.8 FOIL

The surface of the car is important for the performance of the car. Just surface friction could have a large impact on the result, so the team was determined to put a lot of work into making it as perfect as possible.

### 3.1.8.1 Paint VS Foil

The former car have been painted every year, except the first year when it was foiled. Through

the years, four layers of paint have therefore been put on the car, which in the end have added a lot of weight. This problem would be avoided if foil had been used all the way, as well as the surface would have been smoother. Based on these arguments, the team decided to foil the new car.





### 3.1.8.2 Inspiration

The goal from the beginning of the design process had been to design and make a car that looked like a normal street car. Since our car was based on a monocoque structure, it did not have any split lines as the cars we are used to. To give the cars lines, and to make it more dynamic, we were depending on the features of the foil.

A large picture collection of cars that we liked, and that had interesting foiling features, helped us starting to get ideas on how to foil the car. Sport cars and concept cars often have the most

challenging and interesting foil, but in the end it was the eco cars and electrical vehicle that was the most inspiring. Since the car actually was a racing car, an idea formed to combine features from the racing cars with what one often can see on the electrical cars. Together these expressions could create exactly what was wanted.



*It was important to identify which areas that needed to be foiled and which areas could be left with the original carbon fiber finish.*



**Idea generation**  
*The ideation process of the foil had to be done really fast, the decision to print drawings of the car and sketch on these would be the fastest way to do the job. When a large number of drawings had been produced, selected ideas were tested in solidworks to see the result properly.*



#### *Final concept*

*The final concept was one of the simplest ideas that was generated. The main color of the car ended up as matt black, while details were done in bright green and glossy black. The Fuel Fighter logo should be cut out of the foil on the hood and the rear to show some of the carbon fiber structure. A glossy black bird should be placed on each side.*

*A normal car usually have four wheels, and so do this one. But it does not look like it, since the rear wheels are covered. To solve this problem we wanted to indicate the wheels with the foil. Green foil were therefore added around the wheels to give it the feel of a street car.*



*The foiling job was done by Trondheim Bilreklame*



### 3.1.8.2 Production and Mounting

The printing of the foil was done and sponsored by Printing in Oslo, while the mounting was sponsored by Trondheim Bilreklame. Illustrator files of the material was sent to Printing, and when the car was transported to Bilreklames garage. The foiling job was done in less than a day.

The foil is sticky and elastic, and to mount it on the car, it first needed to be cut into strategic parts. Later it could be "stretched" around the car, and somewhere heated to get the smooth

surface that was wanted. All edges and scratches were patched with foil, so that the final result was an almost perfect surface with minimal aerodynamic friction.





## 3.1.9 WIND TUNNEL TESTING

Wind tunnel testing was performed on the DNVFF2 in spring 2012. This was carried out by a group of students lead by one of the team members. Because of the size and work of this subject, the results are mainly used to verify the CFD from 2011 and a comparison of the old car. Some small changes to the exterior were also executed to see for some improvement areas.

This chapter will use the work carried out by Eike-

land and Lien(2010) as a basis.

### 3.1.9.1 Wind Tunnel

For wind tunnel testing in a closed tunnel, blockage is one of the main error sources (Eikeland and Lien, 2010). The car itself will block a certain part of the test tunnel, creating an acceleration of the air around the car. This acceleration will lead to an overestimated drag. A correction formula



can be used to correct the error. By using equation of continuity, a correction factor can be obtained.

$$V_{true}(S - A) = V_{indicated}S$$

Where V (true) is the actual speed around the car, V (indicated) is the air flow speed, S is the section area and A is the projected frontal area.

By solving for V (true) and inserting the drag coefficient

$$C_D = C_{D\ indicated}((S - A)/S)^2$$

obtains a formula for correcting the blockage of the wind tunnel.

In real conditions the car is moving relatively to the ground and the air is standing still. In the wind tunnel at NTNU, the floor is standing still, creating an error due to the boundary layer. There are several methods used to correct the boundary layer; moving belt, ground board and suction. The cheapest and easiest method is to use a ground board, where the car is lifted out



of the boundary layer. Moving the ground with the use of a belt is the most exact method, but can be a very complex process. Applying suction under the car to reduce boundary layer is easier and used in many wind tunnels.

### 3.1.9.2 Experimental Setup

Testing was carried out in the wind tunnel at NTNU. The car was placed on top of two metal supports placed on a scale. The scale consists of six electronic load cells, three for vertical loads and three for horizontal loads.

Before any testing can commence the equipment in the wind tunnel needs to be calibrated. There are two main measuring systems that needs to be calibrated; the load cells for measuring drag, lift and moments, and the pitot/monotube sensor for measuring the air speed in the tunnel. All sensors are routed through amplifiers and optional filters to get more accurate and visible readings. These amplifiers have to be tuned to get the signal within a desirable range, so that it always can be visually checked during the calibration process. A base reading has to be performed at the start of the calibration process, this is done with the test specimen securely in place and the wind tunnel fan turned off. The program used to read and sample values is a LabView

based program called Genlog. After the base reading is completed each individual load cell has to be calibrated. Three different weights (0.5 kg, 1 kg and 2 kg) are in turn placed on top of the load cell and a reading is made using Genlog. After all 27 readings have been made (the readings increase linearly) the calibration factors for the six load cells can be read from a excel sheet. Lastly the air speed sensor has to be calibrated. This is done by running the wind tunnel fan at certain revolutions per minute (rpm) and sampling the data using Genlog.

When calibrating the wind tunnel for the DNVFF2 there were some problems. The sensor signals displayed random interference on all channels, and a lot of time was spent on trying to identify and eliminate this. Different amplifier channels were tested, signal filters were used and even a power supply filter was employed, all to no avail. The team even searched the building for any equipment that might have been causing the interference, but could not find anything. In the end the only solution was to run very long sample periods, which meant the calibration process took a very long time to complete. To shorten the calibration time only the horizontal load cells measuring drag were calibrated and the rest of the calibration factors were taken from a previous



experiment. The two calibration factors acquired corresponded very well to those of the previous experiment and after consulting with students at department of Energy and Process Engineering the calibration factors were deemed OK.

For the actual test process another LabView based program called ForceLog was used. This program displays drag, lift and various moments in Newton directly, and also calculates various coefficients if the frontal area of the specimen has been specified. It also controls the load cell platform which can be rotated to test for side winds. Due to lack of time no side wind scenarios were tested.

The scope of the work was to test as many aspects about the car as possible, but most test scenarios were scrapped due to lack of time. In addition to testing the aerodynamic properties of the base setup of the car, it was planned to test the effects of several different aerodynamic tweaks. It was also desirable to see how or if the weight distribution of the car altered with the speed and how the body performed in side

winds. In the end only three cases were tested: Base, blocked tunnel and diffuser guide vanes. The car was also covered in small tufts made of wool to get a visualization of the flow around the car.

### 3.1.9.3 Results

Input data	
Air density	1.23 kg/m <sup>3</sup>
Projected frontal area	0.90 m <sup>2</sup>
Test section area	4.86 m <sup>2</sup>
Continuity correction	0.664

Table 3.1.1: Input data for calculations of lift and drag

All test scenarios were carried out with the same air speed of 33.7 km/h. The results from the wind tunnel testing are displayed in the table 3.2.2 (corrections made for drag and lift coefficients).

Test scenario	Lift [N]	Drag [N]	C <sub>l</sub> [-]	C <sub>d</sub> [-]
Base	3.88	9.03	0.08178	0.19029
Blocked tunnel	3.51	11.81	0.07397	0.24887
Diffuser guide vanes	2.18	8.59	0.04594	0.18102

Table 3.1.2: Results from wind tunnel testing





*The car during wind tunnel testing. Tufts located over the top remained still, tufts flapping at the sides due to flow separation after the open front wheels.*

#### 3.1.9.4 Conclusion

Wind tunnel testing verified the results from the CFD analysis performed in autumn 2012. The CFD analysis gave a drag force of 6.33 N when travelling at 30 km/h. Compared to the results from the wind tunnel testing, which gave a drag of 9.03 N with air speed of 33.7 km/h. Measured in same speed, the result from the testing would give a drag of 8 N.

An increase of 20 % in drag from the CFD to the wind tunnel results is as expected. The details on the real car are much more complex than for the simplified 3D model. All seams, unevenness and misalignments of doors and covers will all lead to an increase in drag. These are all factors that were not considered in the CFD analysis.

The large variance in lift is mainly due to lifting the car higher in the wind tunnel to eliminate the moving road problem. An increase in ground clearance will increase the lift. The lift is also influenced by the fact that the ground is stationary, moving more air over the car, creating lift.

The results from the wind tunnel testing show that the car has a very low drag coefficient. There was observed very little flow separation over the car. The flow was completely attached over the

top of the body, and the only signs of turbulent flow were behind the front wheel wells (as expected). This flow separation can be reduced by developing efficient front wheel covers.

Covering the tunnel geometry proved to have a negative effect. The drag increased and lift decreased. But due to the wind tunnel testing configuration, the decrease in lift can be proven to increase down force in real conditions.

Diffusor guide vanes proved to have a positive contribution to the drag. But more thorough analysis of the effect and placement must be executed before these changes can be implemented.

It is also important to note that the aerodynamics counts for only about 50 – 60 % of the total resistance in the car when travelling at 30 km/h. With the recent changes in the competition over the years with more stops and turns, 30 km/h is the maximum speed used only for small parts of the track. Therefore, large aerodynamic changes which will increase total weight can be proven to be negative for the fuel efficiency.





# 3.2 INTERIOR





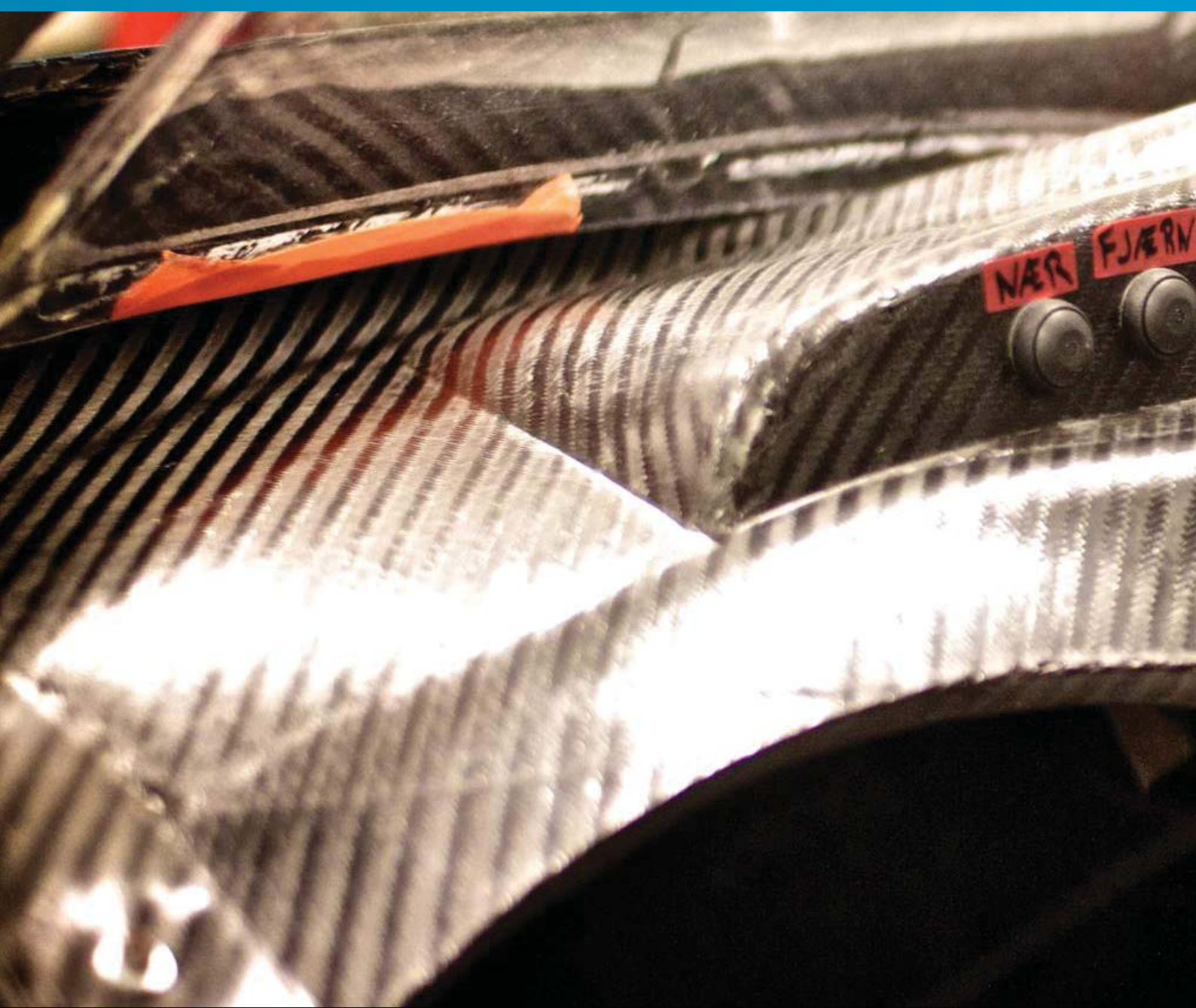
## 3.2.1 INTRODUCTION

All the way from the start of the project, performance had been the main focus. Aerodynamics and weight had always been prioritized before looks and userfriendliness, and all resources had been put into finishing the body in time. The designing of the interior was therefore postponed until the beginning march, and had to be

done over a short period of time with few design iterations. To develop parts that could affect the performance of the driver, like steering wheel and seat, was then put in focus. Ergonomics and weight was now the most important factors, while styling was not prioritized.



*The monocoque was already designed and in production when the design of the interior started*



*The dashboard in the DNVFF was made of pre-preg carbon fiber, and was attached to the car with two screws to each wheel well*

## 3.2.2 DASHBOARD

To have a dashboard is not a requirement from the Eco-marathon rules, but it would help covering all the mechanical and electrical parts in the front of the car, as well as being a mounting surface for buttons that did not fit on the steering wheel.

### 3.2.2.1 Last Cars Dashboard

The dashboard in the former car was made of pre-impregnated carbon fiber with a foam core. It was attached to the wheel wells on each side of the cockpit, and did in addition to being a dashboard, work as a cross beam to make the

car stiffer. The top surface was effectively hiding most of the components in the front of the car, and making the overall impression a lot tidier. Most of the buttons used by the driver during the race were mounted on the dashboard instead of the steering wheel. This would make the driver change the grip everytime a new command needed to be initiated. Sometimes this would probably affect the drivers performance.

The dashboard was attached to the wheel wells with screws, and could therefore be taken out anytime if reparations or adjustments needed to





be done. This could be useful both when working on the dashboard, and when working on the mechanics and electronics in the front.

### 3.2.2.2 Interfaces

When designing the dashboard, the interfaces to four different sub-systems needed to be considered.

#### *Steering Wheel*

The dashboard needs to be able to support the steering wheel and keep it stable all the time while driving. In addition to the steering rod, the cables from the steering wheel needs to go through the dashboard, either through the rod or in another way.

#### *Control System*

All cable from the steering wheel and from the buttons on the dashboard needs to be organised and led to the control system.

#### *Monocoque*

The dashboard needs to be attached to the monocoque in some way. Preferably to a rigid part, like the wheel wells to support the steering wheel in a best possible way, but it could also be attached to the floor or the shell.

#### *Steering*

Must be a bridge between the steering wheel and the steering system.

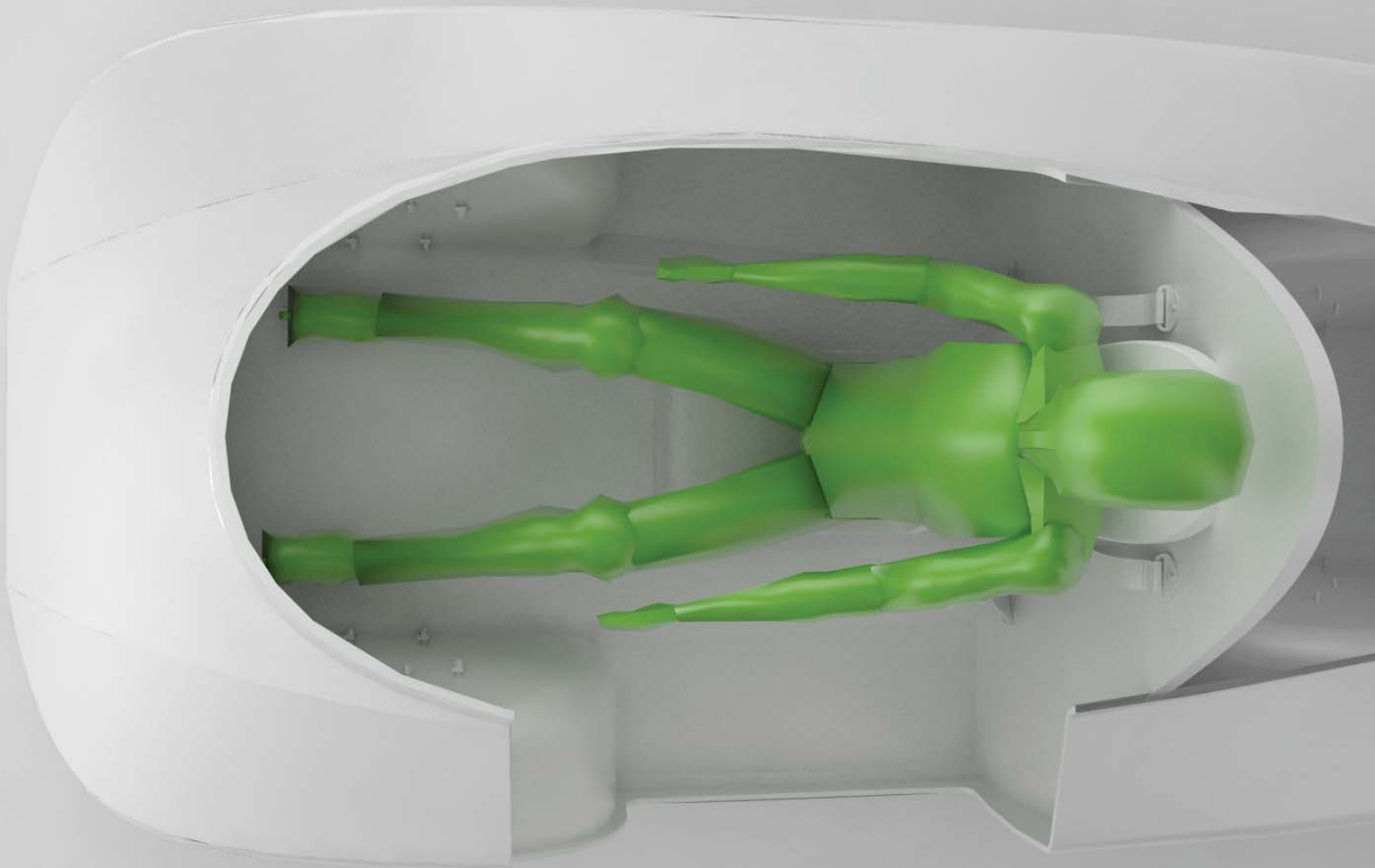


*Figure 3.2.1: Before the design of the interior could start, one needed to establish a layout of the cockpit, and in that way set an outline for the size of each component*

### **3.2.2.3 Ergonomics**

In a car like this, the performance of the driver could count up to 50% of the result, so the ergonomics in the cockpit environment is really important.

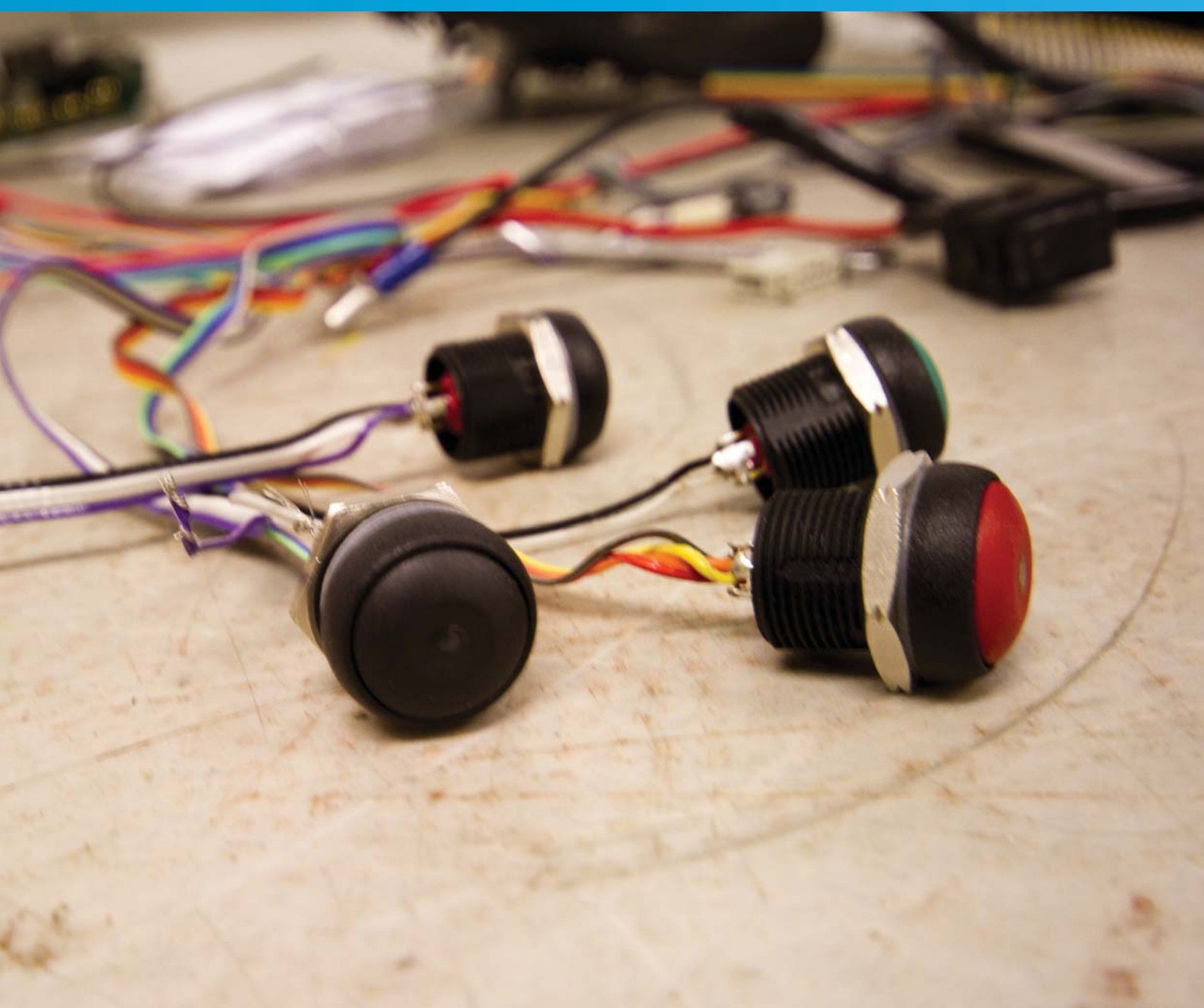
Even though the driver should always focus on the road and never look down, she should be able to see all necessary buttons at any time. They should never be covered by the steering wheel, mirrors, hands or other disturbing elements. At the same time, buttons that are used when racing, should be within reach without moving out of a comfortable driving position.

The car should be ready to drive in all kinds of

weather. When it is sunny it is important that all displays are either angled in a way that do not make uncomfortable reflections, or that they are shielded from the sun.

The dashboard should support a correct height and distance for the steering wheel, and at the same time not block the view for the driver. All of this should be customized for the selected driver, but possible to use for most people.

Buttons that are used before and after the race, and during testing should be placed on the dashboard. The rest should be placed on the steering wheel to optimize the drivers performance.



*To give the driver proper feedback when pressing the different buttons, it was important to be selective when choosing buttons. Important factors were lights and tactile feedback*

#### **3.2.2.4 Analysis of Functions**

A lot of factors have an impact on the placement of the buttons. The diameter of the steering rod limited the amount of wires that could go through it. And of course the space on the steering wheel itself would be a limiting factor.

The most logic way to divide the functions would be to place the least used buttons on the dashboard, and the most used on the steering wheel. The result was two different categories:

##### *Used before race*

- Emergency shut-down.
- Start/stop.
- Wind shield wiper.
- LED-display.

- LED-control.
- Blinker indicators.

##### *Used during race*

- 6 engine control buttons.
- Horn.
- Low-beam.
- High-beam.
- Indicator (left/right).

### 3.2.2.5 List of Requirements

The list of requirements can be divided into four different categories based on whether they are demanded by rules, users, team goals or other sub-systems.

#### Rules

- The vehicle interior must not contain any objects that might injure the driver in case of a collision.
- The driver must have access to a direct arc of visibility ahead.
- A fully harnessed driver must be able to vacate the car at any time without assistance in less than 10 seconds.
- The emergency shutdown system must be operable from the driver position.
- The door opening must have a minimum dimension of 500x800 mm.

#### Other Sub-Systems

- Must have a 30 mm wide hole to mount the steering column in.
- Must be stiff enough to keep the steering stable.
- Must include one start/stop button which

should be reachable from the outside.

- Must include two indicator lights (left/right)
- Must include one emergency shut off button
- Must include one LED-display with a separate control button.
- Must include one wind shield wiper button.

#### Users

- All buttons should be visible and reachable from a comfortable driver position.
- Must not limit the range of view.
- Should be able to see all buttons at all time.
- Displays should be angled towards the driver.
- Should have a mounting point for the steering wheel

#### Team Goals

- Should be made of carbon fiber, and have a maximum weight of 2 kg.
- Should cover mechanical and electrical parts in the front part of the car.
- Should have a simple shape that fits with the rest of the car without drawing too much attention.
- Must be possible to produce at NTNU by the team.

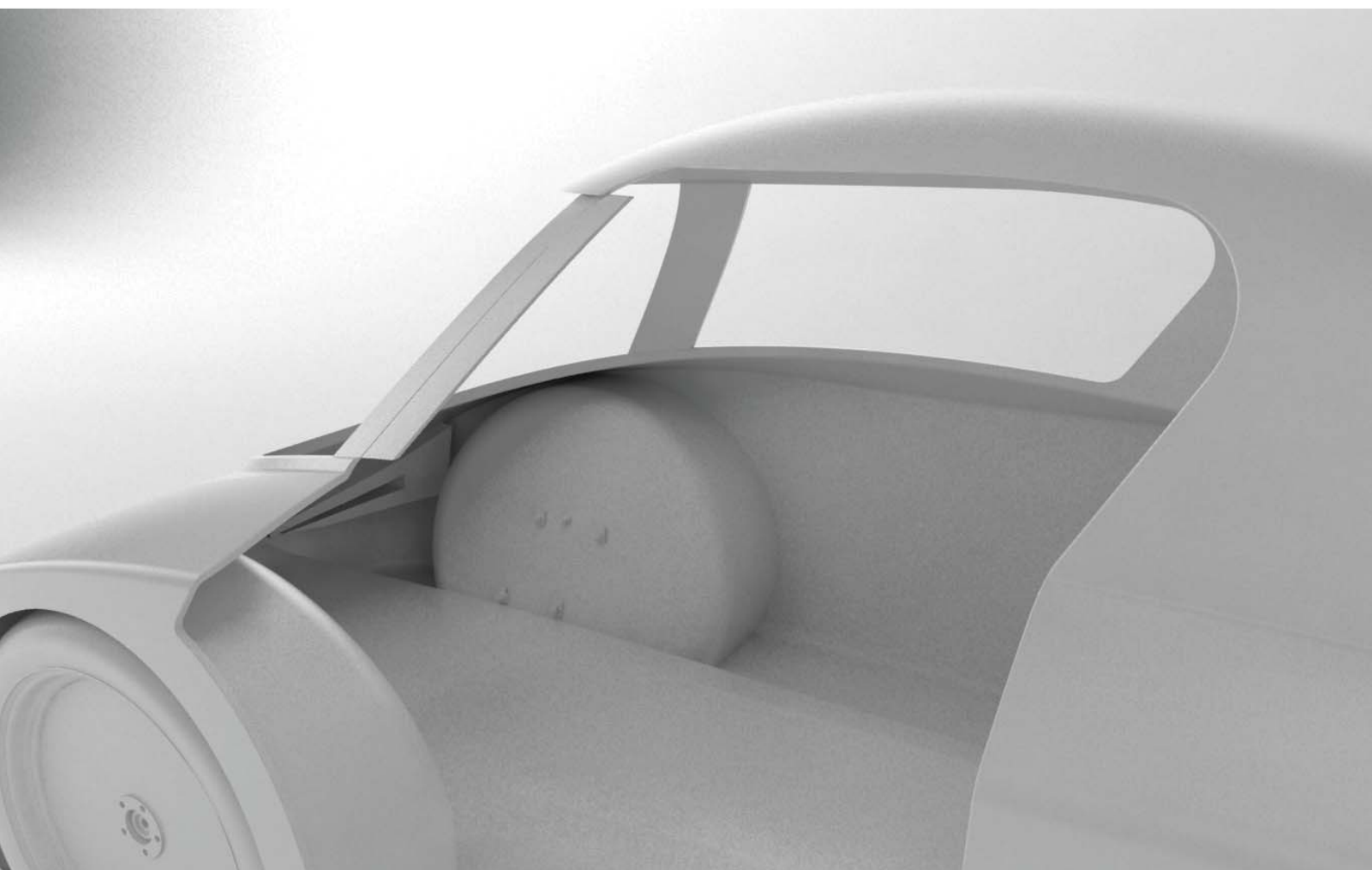
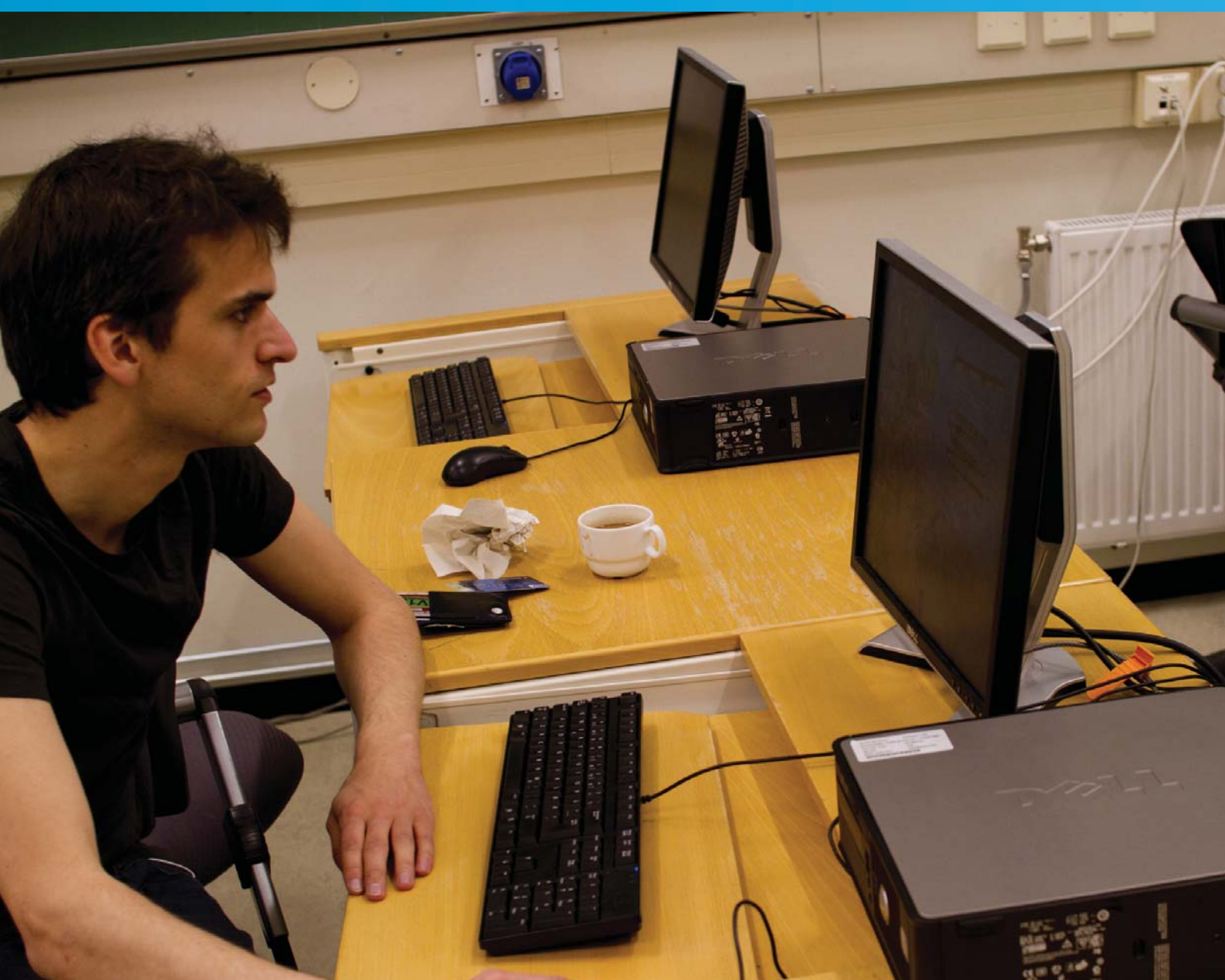


Figure 3.2.2: An 3D-model with the outlines for the dashboard were given to group working with idea generation



*The students working on the dashboard were using UGS NX for the surface modelling, while the rest of the interior was designed in SolidWorks*

### **3.2.2.6 Cooperation With Other Students**

The design process around the dashboard were done in cooperation with fourth year students at Institute of production and materials. As a part of the course PuMA 8, where one of the goals was to learn surface modelling in NX.

The design process were a iterative process where the team gave the students an outline of what was wanted in the form of 3d-models, basic dimensions and rules. In a few weeks the students produced initial sketches and came up with a lot of ideas. In the start the goal was not to limit the students to much, and in this way come up with as many new ideas as possible.

Along the design process, short meetings were held so the team could give feedback on the

ideas. In this way one could make sure that the process moved in the direction that was wanted, and that the finished product would fit into the car.

The final delivery from the PuMa students was several early concepts that could be used as a baseline to develop the finished dashboard. Because of a short time limit, the last part of the design process was done by the designers on the team. The product was taken from early concept phase into a finished concept and production in a short time, to make sure that no other sub-systems would be delayed due to the late production of the dashboard.

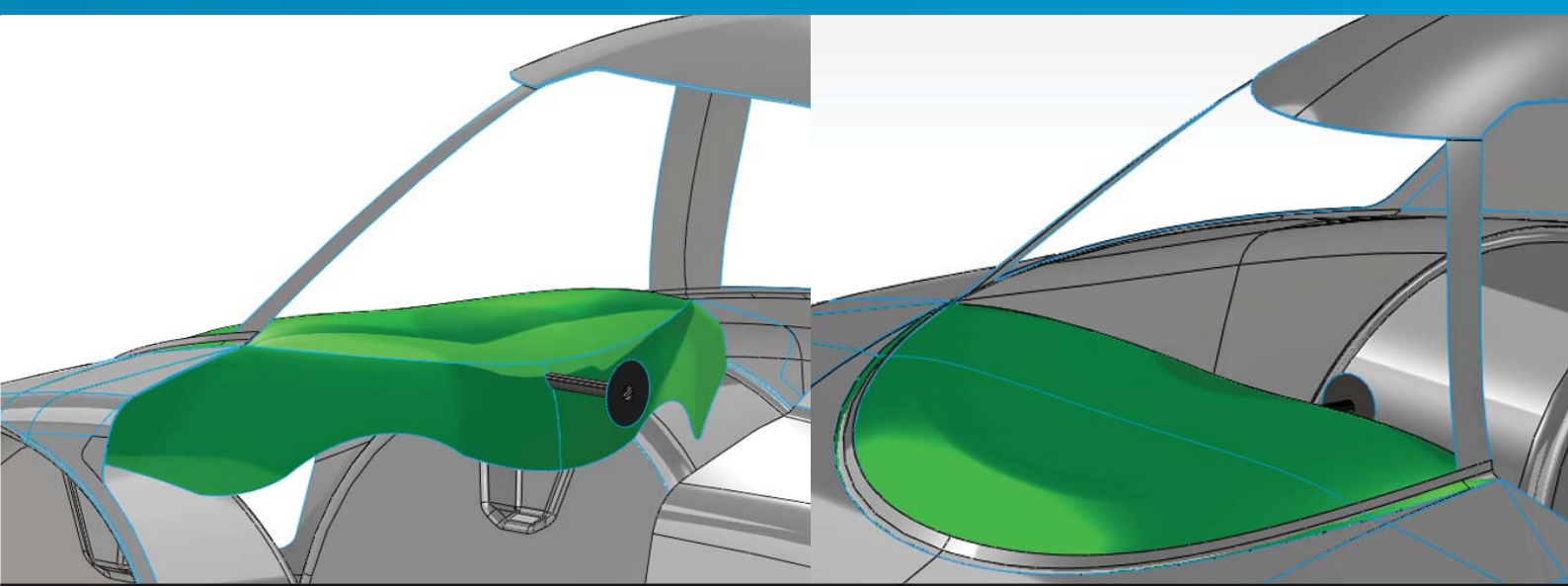


Figure 3.2.3: Concept 1 had a removable top cover to provide easy access.

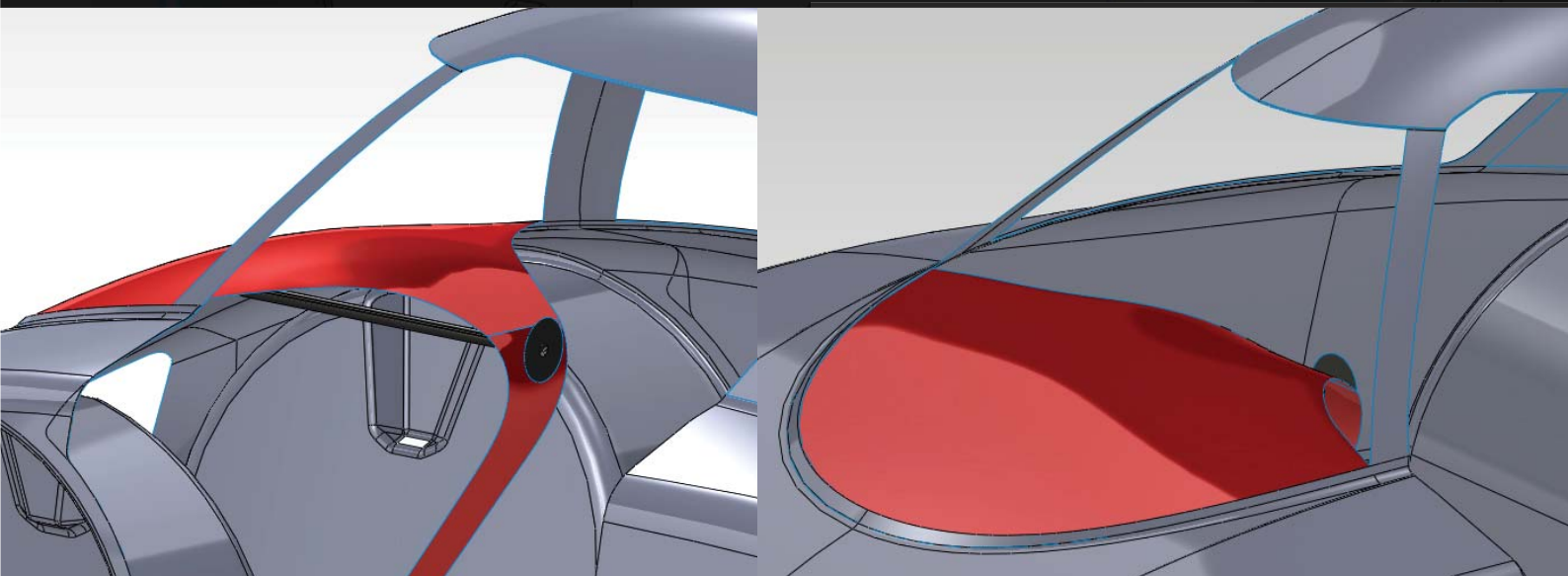


Figure 3.2.4: Concept 2 consisted of a light construction attached to both the monocoque shell and the floor. It had no removable parts.

### 3.2.2.7 Concept Development

When the PuMa students finished their work, there were two definite favourite concepts. The two concepts were quite different and hard to combine. One of them needed to be chosen to continue the further work.

#### Concept 1

The first concept was not that different from the one in the DNVFF. It was resting on the wheel wells, and therefore also making the whole car stiffer. The front beam was curved and closest to the driver in the middle. It could support the steering wheel in a best possible way. The curves on the bottom should provide more than enough free space for the feet, and to access or evacuate the car in less than 10 seconds should not be a problem. On the top of the dashboard an

easily removable top cover should be attached. The purpose of this cover would be to hide the mechanical parts and wires beneath it.

#### Concept 2

Concept 2 was not attach to the wheel wells, but in the top shell and in the floor. The beam in the middle of the car could be used to place buttons on. It could be a problem when the driver should evacuate the car. Before this concept could be chosen, a lot of testing would have to be done on the placement of this beam.

The second concept would support the steering wheel in a really good way, but did not hide the electronic components in the same good way as the first concept. On the other hand it would give the whole car a really light expression.



*The final design of the dashboard, containing two different parts; the top cover and the front beam.*

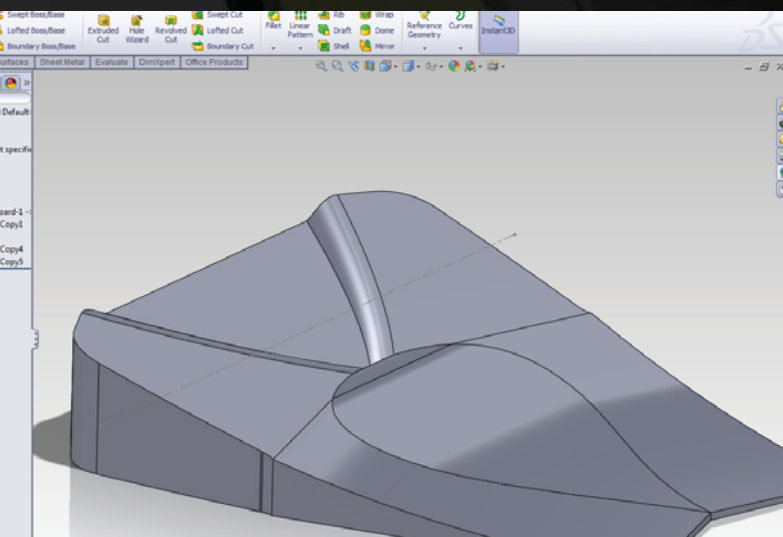


*Figure 3.2.5: 3D-model of front beam mold ready for milling. The mold is milled in two parts and then glued together later.*



*Finished mold ready for production of the front beam.*

### 3.2.2.8 Final Concept

After a short meeting the team decided to make a dashboard similar to the first concept, but with simplified curves. This way the concept would have few double curved surfaces and be easier to produce in carbon fiber.

The reason why the first concept was chosen, was mostly because it would provide much free space for the feet and simple access. The team could not risk that the driver would not be able to evacuate the car quick enough, and therefore not pass the technical inspection. Compared to

the the second concept it would also give better mounting access because of the removable cover on the top. This would make the job for the mechanics and the cybernetics a lot easier. The production would also be a lot easier.

The dashboard was produced in two separate parts, the front beam and the top cover. The molds were milled out of eba-board and sanded down. The carbon fiber was then layed. Three layers of carbon fiber was used in each part. The front beam was reinforced with a Rohacell core. The end result was glued in place inside the car and then foiled with matt black foil.



### 3.2.2.9 Placement of Buttons and Display

The buttons were used for several purposes. The only common demand was that they should be accessible from the drivers driving position. It was therefore important to think thoroughly through where they should be placed.

#### *Emergency shutoff*

Should be placed close to the door so it was accessible both from the inside and the outside.

#### *LED-screen*

Could be hard to read in sunlight and should therefore be shielded from the sun. It should never be covered by the steering wheel, neither the hand while operating the control button. The control button should be placed right beside the display. Summing up these arguments, the best place for the LED-screen would be out to the right, shielded from the sun by the monocoque.

#### *Start/Stop*

Should also be accessible from the outside, and should therefore be placed far to the right.

#### *Windshield wiper*

This is the least important button, since the wiper probably never is going to be used. It should be possible to reach it from the outside, just for adjustment purposes, and it should therefore be placed on the left side of the dashboard.

#### *Indicator lights*

Can be placed wherever it is most convenient, as long as they are in sight of the driver. Since no buttons would be placed on the right side of the steering wheel, this would be a perfect placement for these lights.





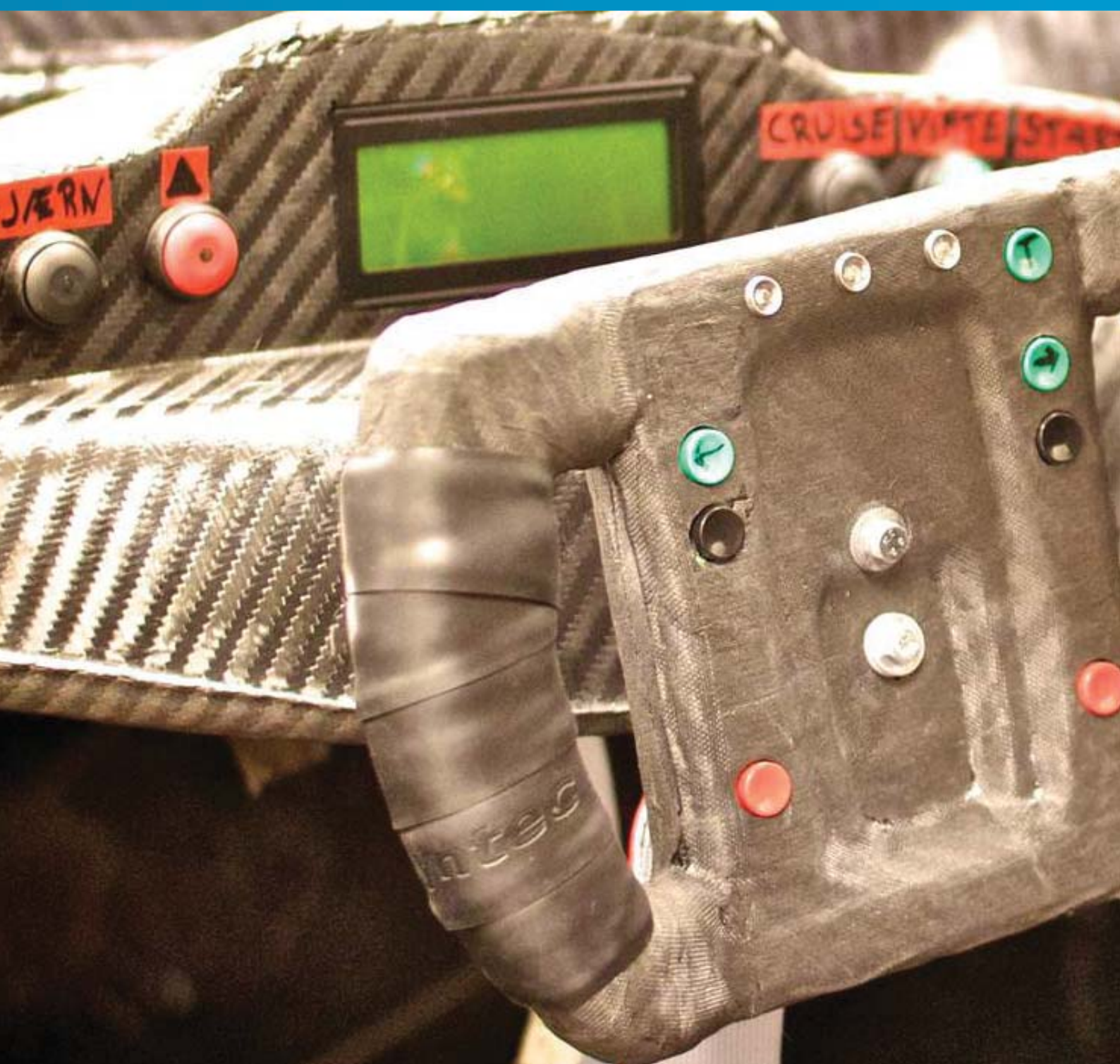
*The front beam of the dashboard was glued on to the wheel wells. The reinforcement with a foam core made it stiff enough to support the steering wheel.*



*The finished dashboard with holes for emergency shut-off button, start/stop button, windshield wiper button and steering rod.*



*Both the front beam and the top cover was foiled with matt black foil for a better finish. The main sponsor logo was also placed on the top cover.*



*The former steering wheel in the DNVFF was made of carbon fiber wrapped around around a foam core. This, in addition to the use of really lightweight buttons gave the steering wheel a low weight.*

## 3.2.3 STEERING WHEEL

Since the outcome of the competition was also depending on the skills of the driver, the design of the steering wheel could affect the result. Through the design process the main focus was on ergonomics to increase the performance of the driver.

### 3.2.3.1 Last Cars Steering Wheel

The steering wheel in the former car have been changed a few times, and the last version was a simple steering wheel of carbon fiber. It was made by cutting out a foam core in the desired shape, and then wrapping carbon fiber around it. The result was a steering wheel with a rough



finish. Most of the buttons were placed on the dashboard, while the few that were placed on the steering wheel were small buttons with little response when pressing them. The buttons were placed far to the middle, and were therefore not accessible without changing the grip.

Because of the way it was constructed, the steering wheel had no cover for the wires in the back. This could be an advantage when mounting it, but did not look very nice.

### 3.2.3.2 Necessary Functions

As discussed in the dashboard chapter, the steering wheel should contain all the buttons that are used during the race, so that the driver never has to let go of the grip. The needed buttons would be:

- 6 engine control buttons.
- Horn.
- Indicators (left/right).
- High beam.
- Low beam



### 3.2.3.3 Production Methods

When choosing production method for the steering wheel there were especially two important aspects; weight and production time. In the end three different production methods were considered.

#### *Carbon Fiber*

This is a strong and light material. Pre-impregnated fibers or wet layup can be used. Carbon fiber can be laid in a negative or a positive mold. The surface in contact with the mold will get the smoothest surface.

#### *Vacuum Formed Plastic*

This is a fast production method. Plastics that can be used are poly carbonate, ABS or PET. One will need a positive mold to vacuum form the plastic.

#### *Aluminum*

This is the heaviest option compared to the others. The product can be made of sheets, or milled from a solid block.



### 3.2.3.4 Inspiration

The collecting of inspiration could be divided into three parts. Shapes of existing steering wheels were studied, just to get an idea of how a normal steering wheel looks.

Testing similar products was the largest source of inspiration. Walking through computer stores trying out different joystick- and steering wheel solutions inspired to a lot of new ideas. Especially the ergonomics in the product were inspiring, since they at most times are well designed.

To differentiate the ideas and to be inspired to do something new, it was decided to collect inspiration on different steering solutions. Solutions like formula 1, student formula, airplanes, and other eco-marathon cars were of course obvious to include in this collection. In addition solutions like helicopters, trains, normal cars, scooters, boats, bikes and gaming consoles were included.



### 3.2.3.5 List of Requirements

As in the process of designing the dashboard the requirements can be divided into four different categories; Rules, users, team goals and other sub-systems.

#### Rules

- Must be possible to use the steering wheel with gloves.
- Must not prevent the driver from getting out of the vehicle.
- Steering must be achieved by using a steering wheel or section of a wheel.

#### Users

- Should be customized to fit the selected driver, but possible to use for everyone else.

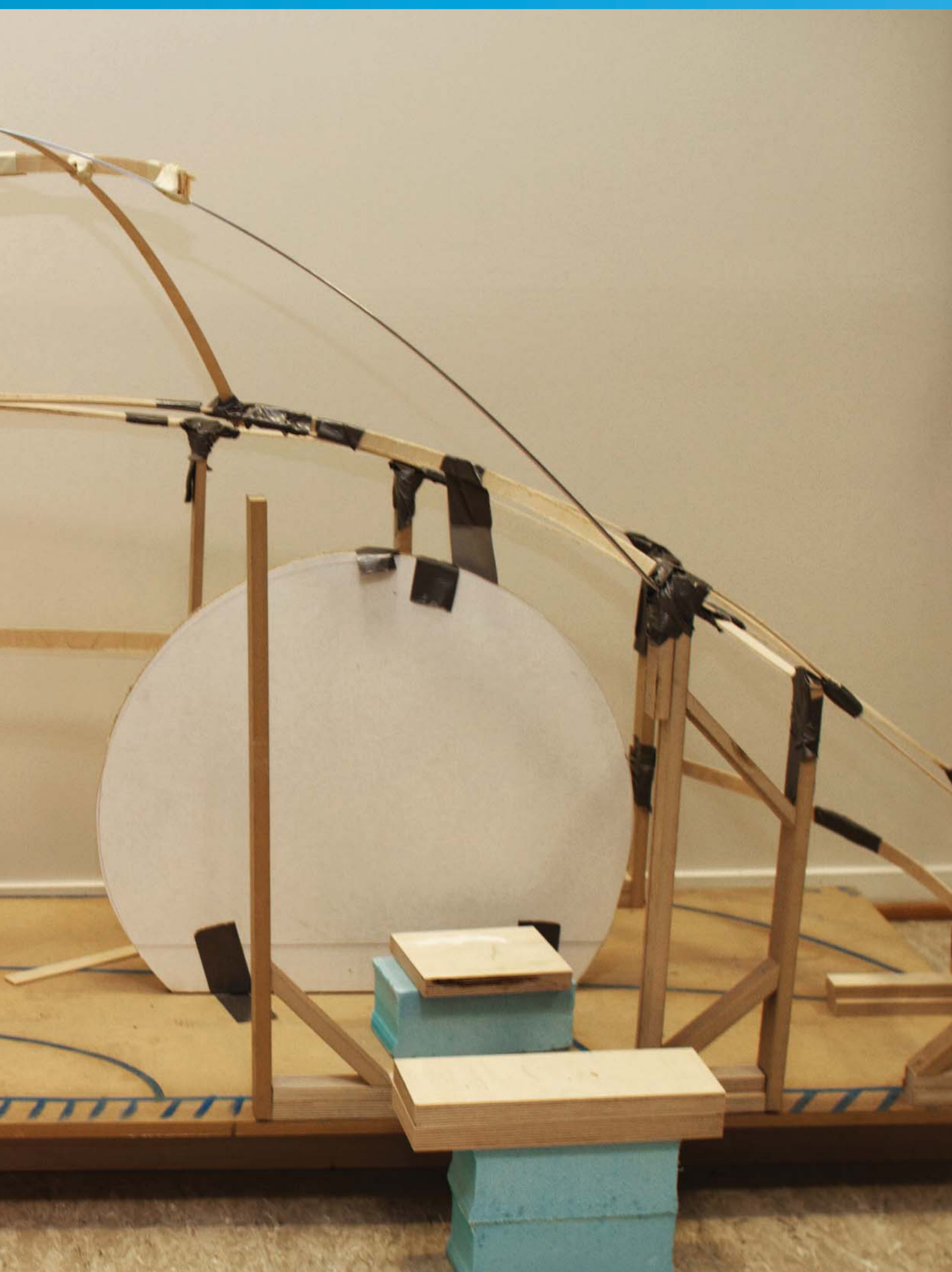
- Should include all buttons in one grip.
- Buttons must give clear feedback when pressed.
- All on/off buttons should have light indication.

#### Team Goals

- Should have a nice finish.

#### Other Sub-Systems

- Must contain 6 engine control buttons.
- Must contain two buttons to control the front lights (high beam and low beam)
- Must contain at least one button to control the horn.
- Must contain two turn indicator buttons
- Must contain one warning flasher button.



*Since the monocoque was not ready for testing when the interior design started, it was built a mockup to do ergonomic testing and set an outline for the design*

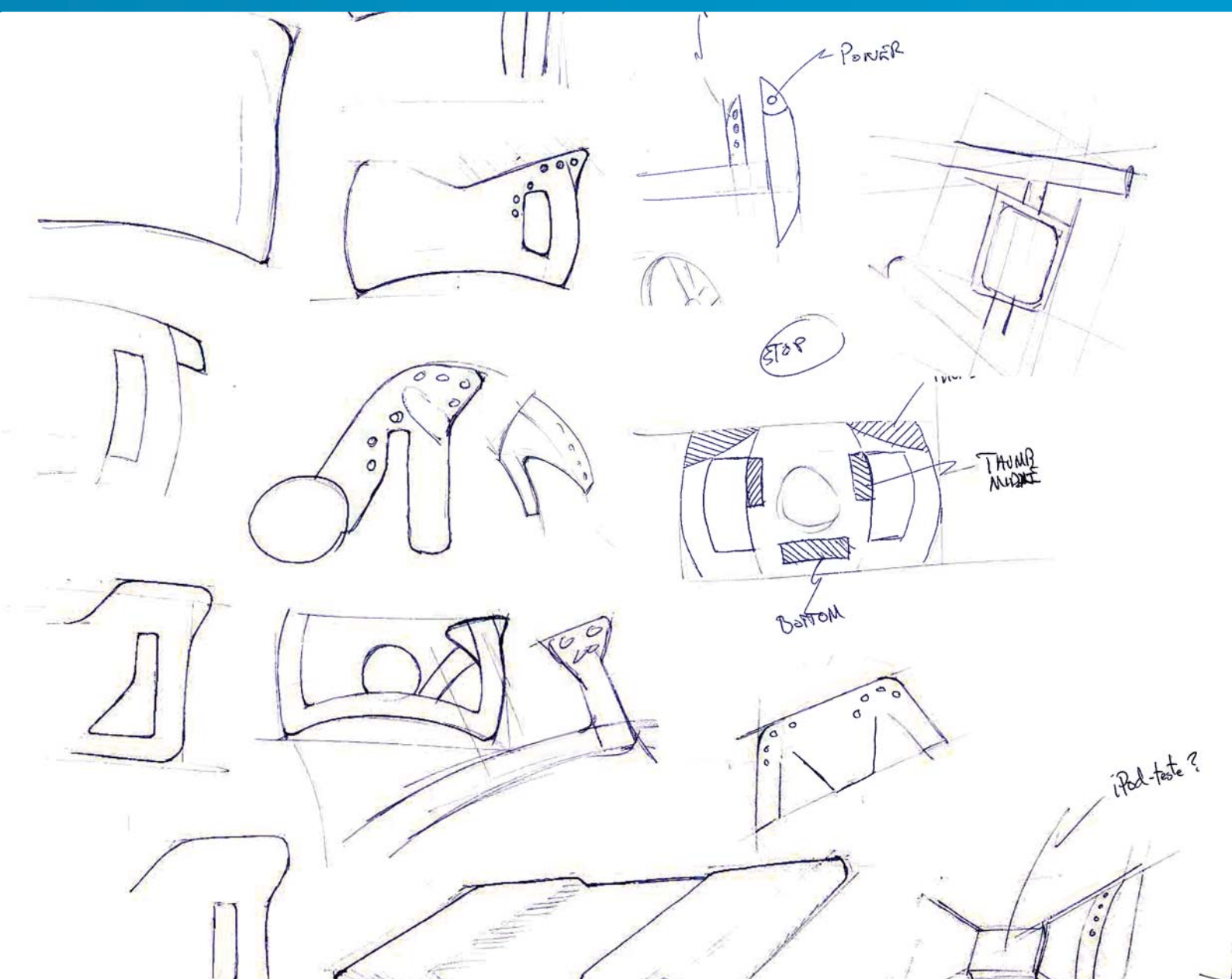


Figure 3.2.6: Sketching was done to explore ideas, but most of the ideation process was done with physical models and 3D-models.

### 3.2.3.6 Idea Generation

To be able to finish the ideation process as fast as possible, rapid iterations between fast freehand sketches and physical models were done. The freehand sketches were used to explore ideas, while the physical models were used for testing them. Most time was spent on the models, since the quality of a steering wheel is highly dependent on the ergonomic properties. This way, a lot of feasible ideas could be generated over a short period of time, and put together into final concepts.

### 3.2.3.7 Ergonomic Testing

When the design process for both the steering wheel and the seat started, there was no finished car to test them on. Without the possibility to physically test the ideas and basic ergonomic

dimensions, it was hard to relate to the ideas. It was therefore decided to build a full scale mock-up of the car.

The mock-up had the same dimensions as the real car, but only the left half was built. It was now easy to get instant feedback from a person testing different concepts.

To do the testing of the ideas, foam models were produced. These models were tested on the driver or other persons with the same size. The goal was to build a steering wheel that fit the driver perfectly, and could be used by most other persons.







Figure 3.2.7: Concept 1

### 3.2.3.8 Three Different Concepts

All the ideas from the ideation process were grouped into three different concepts, all made with different production methods.

#### Concept 1

The first concept can be produced by cutting out a foam core in two parts, and put a tube for wires through it. Carbon fiber can be wrapped around it, and holes for easy access cut out.

The basic idea is that all buttons can be accessed without changing grip; all the control buttons

with the thumb, and the rest with the index finger. On each side of the steering wheel removable lids will be placed to make the mounting and wiring simpler. All the wires are pulled from the buttons, through the tube and the steering rod, and out behind the dashboard.

Because of the production method, this would be a really lightweight product, with quite rough finish. The production is simple, but a bit more time consuming than the other concept.

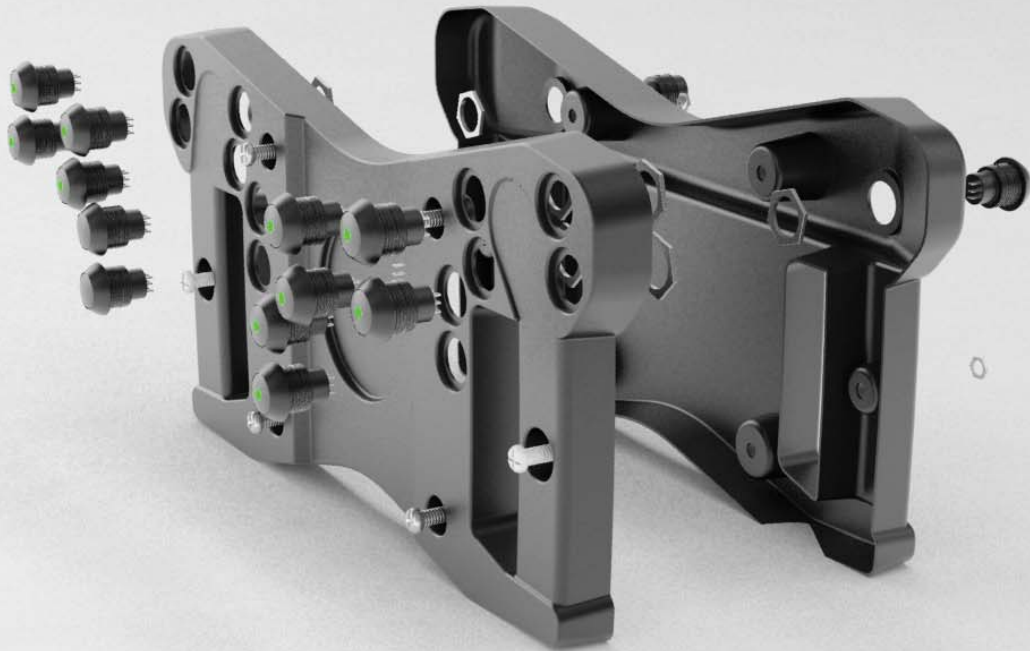


Figure 3.2.8: Concept 2

### Concept 2

The second concept is vacuum forming either PET or poly carbonate in two separate parts. Six screws are used to screw it together to form a steering wheel. All the wires are hidden inside to give it a clean and organised look. The fact that it is made out of two parts makes both mounting and possible adjustments a lot easier, since it can be taken apart.

Vacuum forming is a fast production method, since it is only the milling of molds that takes time. A big advantage is that spare parts can be

made in just a few minutes.

Like concept number one, this concept also got all the most important buttons accessible within the same grip. All the engine control functions are placed in a circle around the thumb. The other buttons are also accessible by the thumb, except the indicator lights, which are placed on the back of the steering wheel.

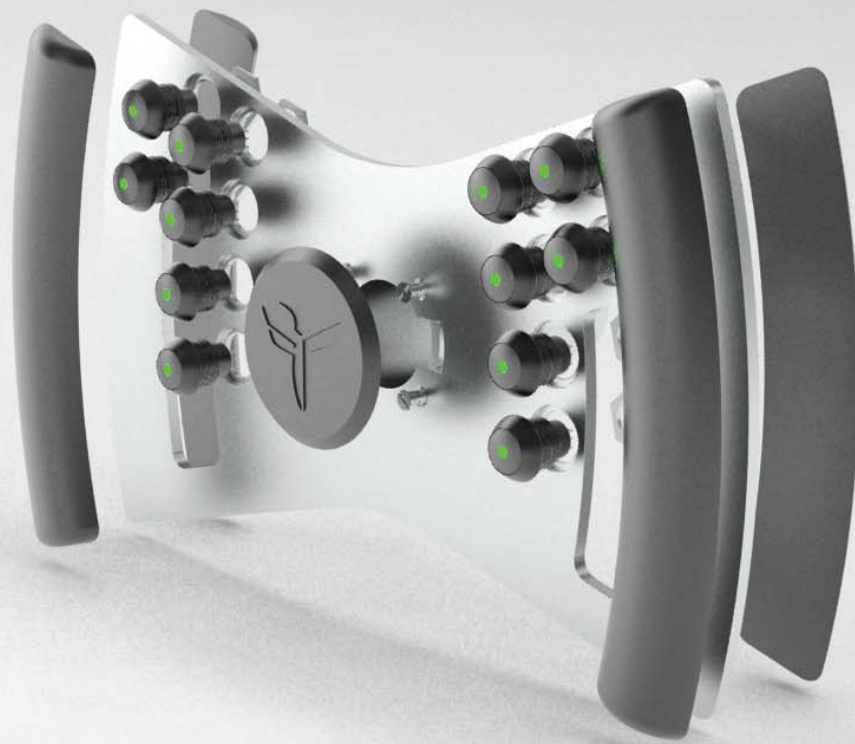


Figure 3.2.9: Concept 3

### Concept 3

The third concept is the simplest of the three and also the easiest to produce. The main part is milled out of an aluminum plate, while the grip is milled out of rubber. All the buttons are screwed on to the plate, and soldered on the back. The wires are not hidden in the same way as the other concepts, but are still pulled through the steering rod to make the driver environment more organized.

Since the concept is made out of only one plate, there is no possibility to mount buttons on the back of the grip. It is hard to place all the buttons within the range of the thumb.

The surface finish of this concept would be better than the other concepts. All parts are milled out, and the details could be done really well. The production time of this concept would by far be the shortest one. On the other hand it would be the heaviest alternative.

	CONCEPT 1	CONCEPT 2	CONCEPT 3
PRODUCTION TIME (5)	3	5	4
FINISH (2)	3	4	5
ERGONOMICS (5)	3	5	3
WEIGHT (4)	4	4	2
PRICE (1)	4	4	3
EASY MOUNTING (3)	3	5	5
	65	93	71



Figure 3.2.10: Criteria matrix

### Choosing concept

Since the decision of which concept to choose was depending on so many different factors, it was decided to create a criteria matrix to make the process easier. The different criterias were rated from one to five, where five was the most important.

Good performance in the competition was the main goal, and the one thing that could really affect that was the ergonomics. This together with

weight and production time was therefore rated as the most important criterias. The over all finish and easy mounting was of still important, while the price would have almost no impact on the choice.

When rating, number two ended up as a clear winner.

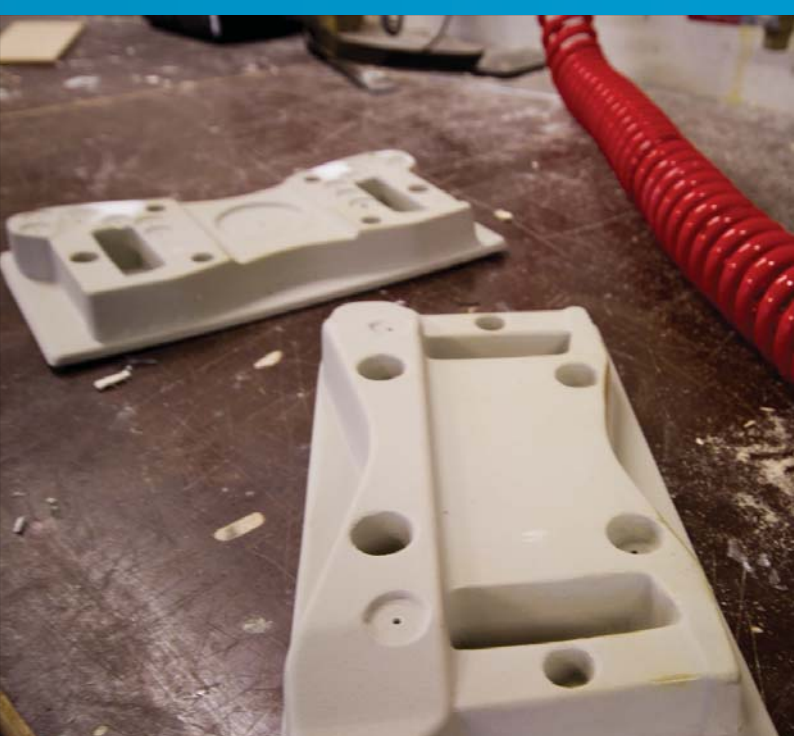
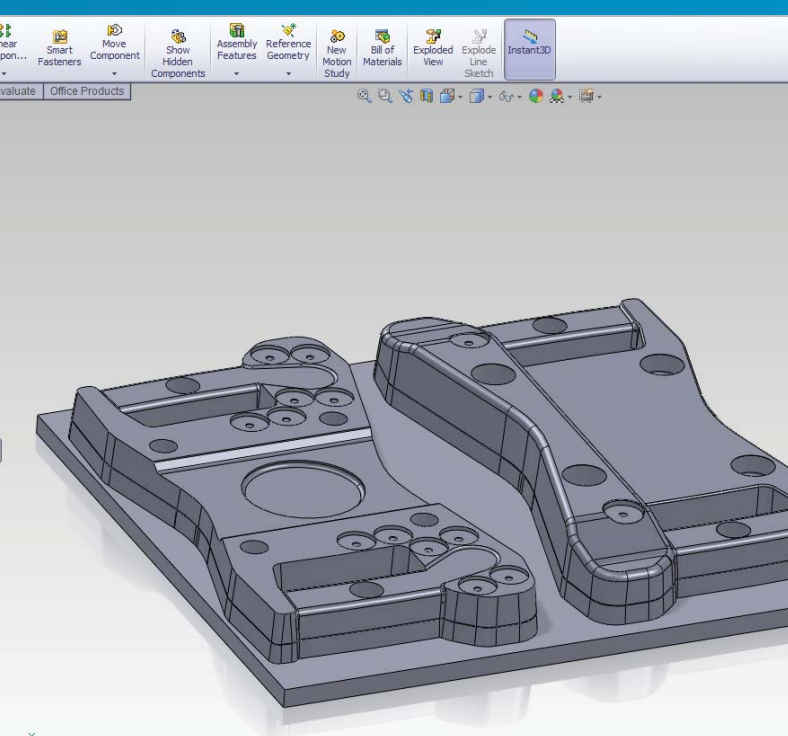
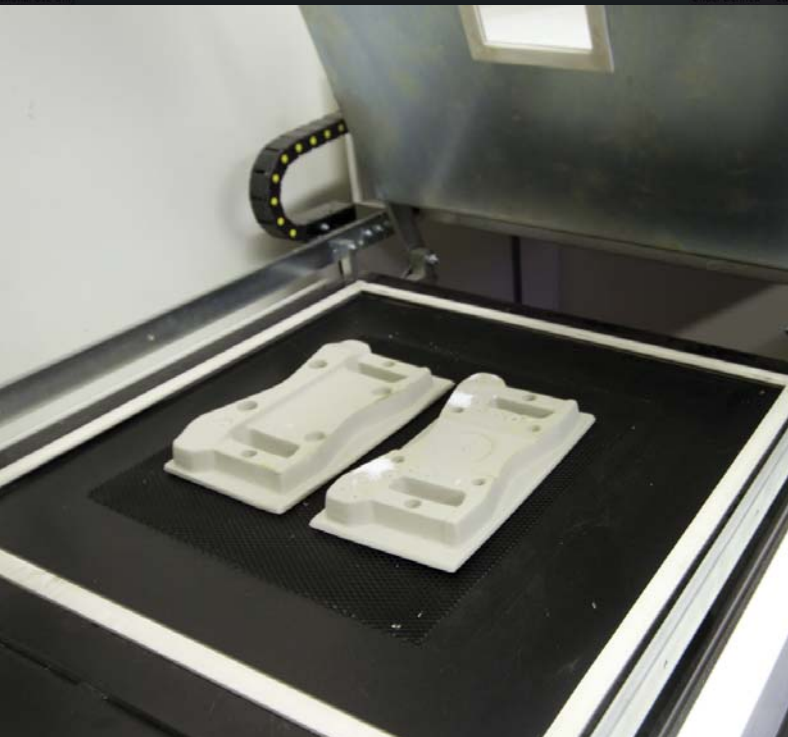
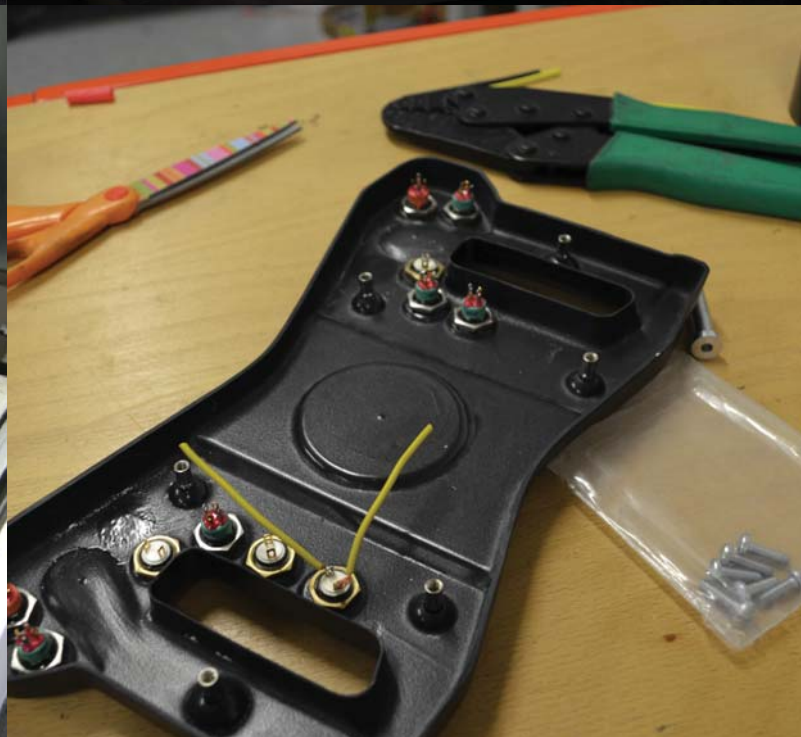


Figure 3.2.11: The molds for the vacuum forming was first designed in SolidWorks and then milled out in a CNC milling machine



The steering wheel was vacuum formed in two parts



Holes for the buttons were drilled in the plastic

### 3.2.3.9 Production

Drawings for production of the molds had to be made. Two molds were modelled in solidworks, with a 2 mm offset of the original shape. 5 degrees of draft angle as well as small indents were also added.

The milling of the molds and the vacuum forming was done in the workshop at IPD. The mate-

rial used was 2 mm black PET, with a slightly structured surface.

When the vacuum forming was finished, the holes and indents were drilled out. Then the buttons could be mounted and details like logos could be added. Finally all the buttons were wired and the steering wheel was mounted on the steering rod.



*All the wires from buttons on the steering went through the steering rod which was placed in the middle of the steering wheel*



*The finished steering wheel mounted to the dashboard*



*The seat from the DNVFF placed inside the cockpit of the DNVFF2*

## 3.2.4 SEAT

To be able to performance the best, the driver needs to have a comfortable driving position. The seat is one of the most important factors in providing this.

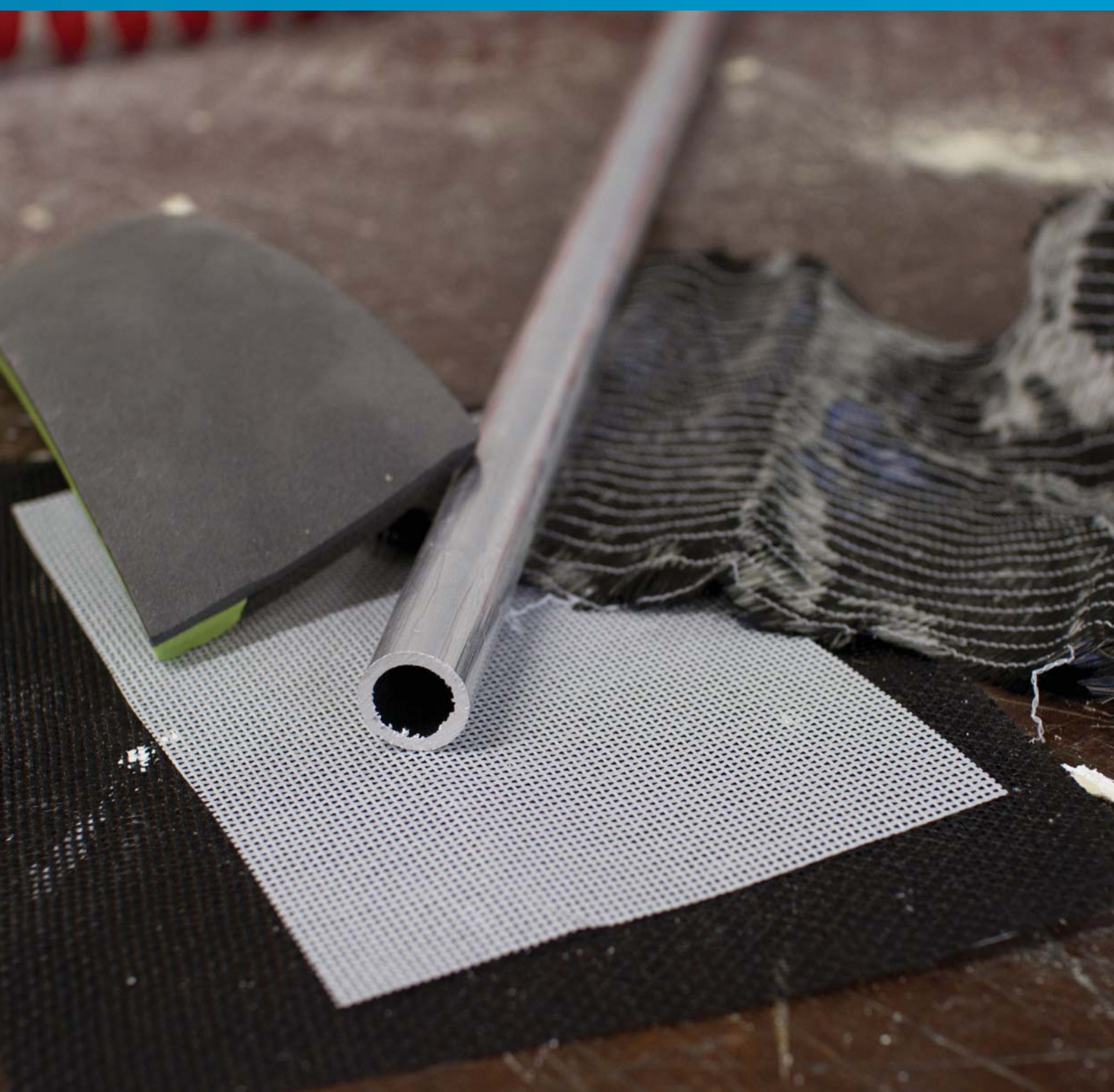
### 3.2.4.1 Former Seats

When looking back at former project reports, it seems the seat have never been prioritized. It has always been one of the last parts to be made, and

the finish and ergonomics have generally been poor because of an extreme weight focus. Three different seats have been made for the DNVFF over the years. Two of them have had the possibility for adjustments, while one of them was customized to fit only the selected driver. All the seats were made of carbon fiber to make them as light as possible.







### 3.2.4.3 Possible Materials

#### *Carbon Fiber*

As in most of the other parts, carbon fiber can be used to produce the seat. Without too many layers of fiber, the material can be quite flexible, and therefore perfect to make a comfortable seat.

#### *Fabric*

A lot of lightweight chairs are made out of mesh or lattice which are buckled up between several mounting points. This is probably the lightest solution.

#### *Foam*

Different kinds of foam could be used to make the seat more comfortable. It could also be the main part of the seat. The recommended foam for this application weighs 45 g/l, which is really light compared to the other materials.

#### *Aluminum*

Pipes and frames of aluminum could be an alternative to the carbon fiber. It can be easier to work with, but heavier.

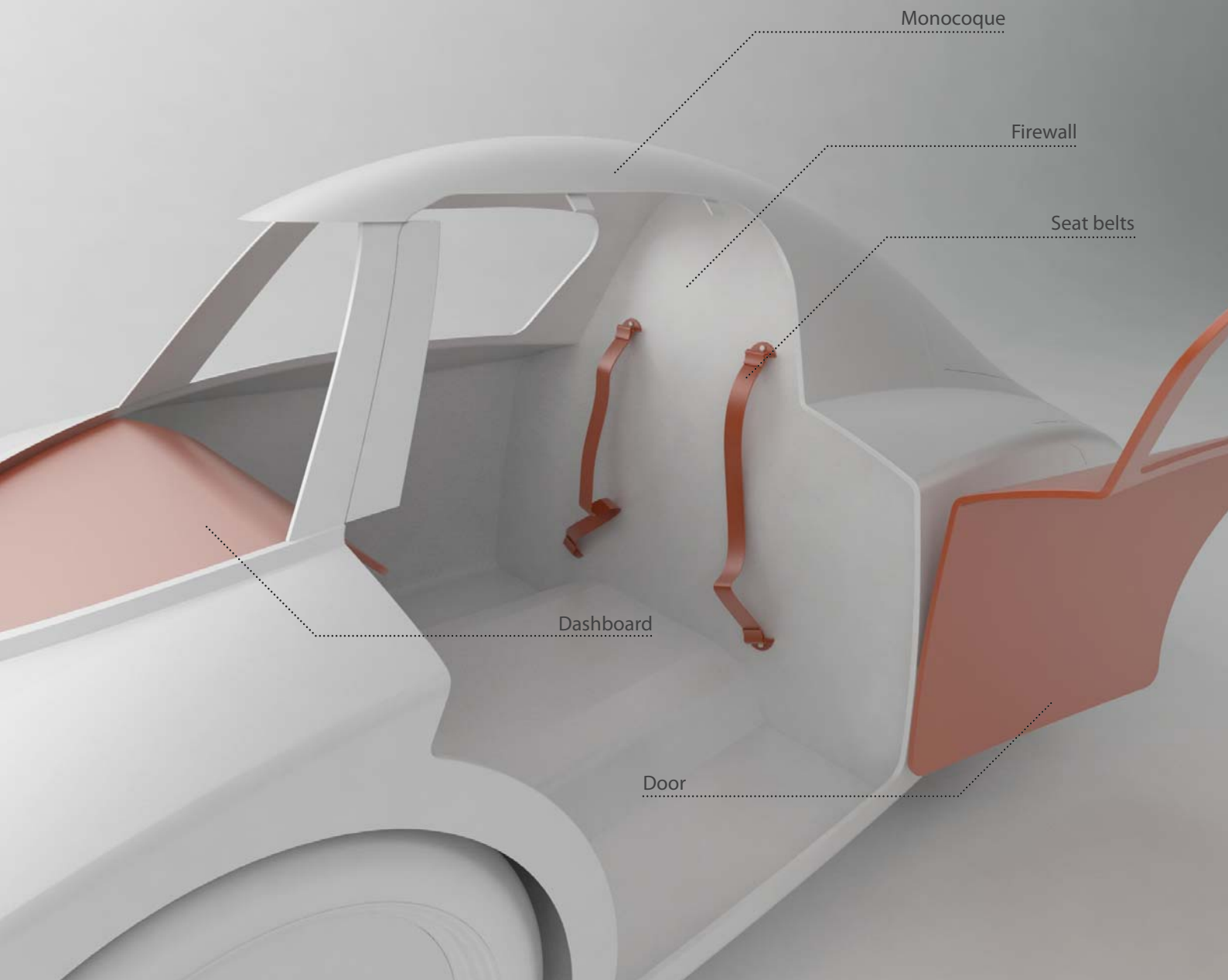


Figure 3.2.12: Seat Interfaces

### 3.2.4.4 Interfaces

#### *Monocoque/Firewall*

The monocoque and the firewall are surrounding the interior, and the seat must be attached to one of these.

#### *Dashboard/Steering wheel*

The seat has to be placed in a way that makes it possible for the driver to reach both the dashboard and the steering wheel, while still having a comfortable driving position. Some of the buttons on the dashboard are rarely used in a driving situation and does not have to be within

a comfortable range.

#### *Door*

According to the rules the driver must be able to evacuate the vehicle in less than 10 seconds. This means that the seat must not prevent the driver from opening the door and getting out in time.

#### *Seat belt*

A 5 point seat belt must be mounted, and it has to fit around the driver sitting in the seat.

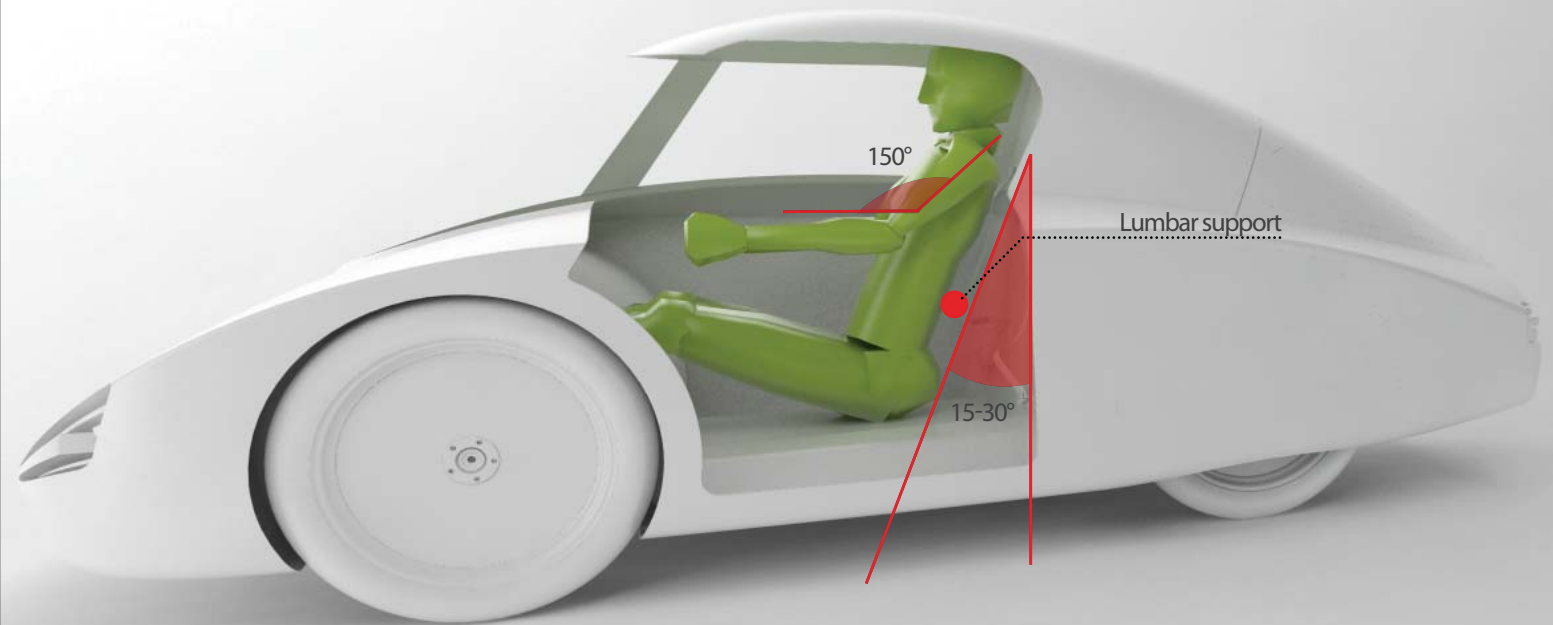


Figure 3.2.13: Basic Ergonomics

### 3.2.4.5 Basic Ergonomics

The car was already designed and put into production when the design of the seat started. The seat had to be designed to make the driver comfortable while driving the car.

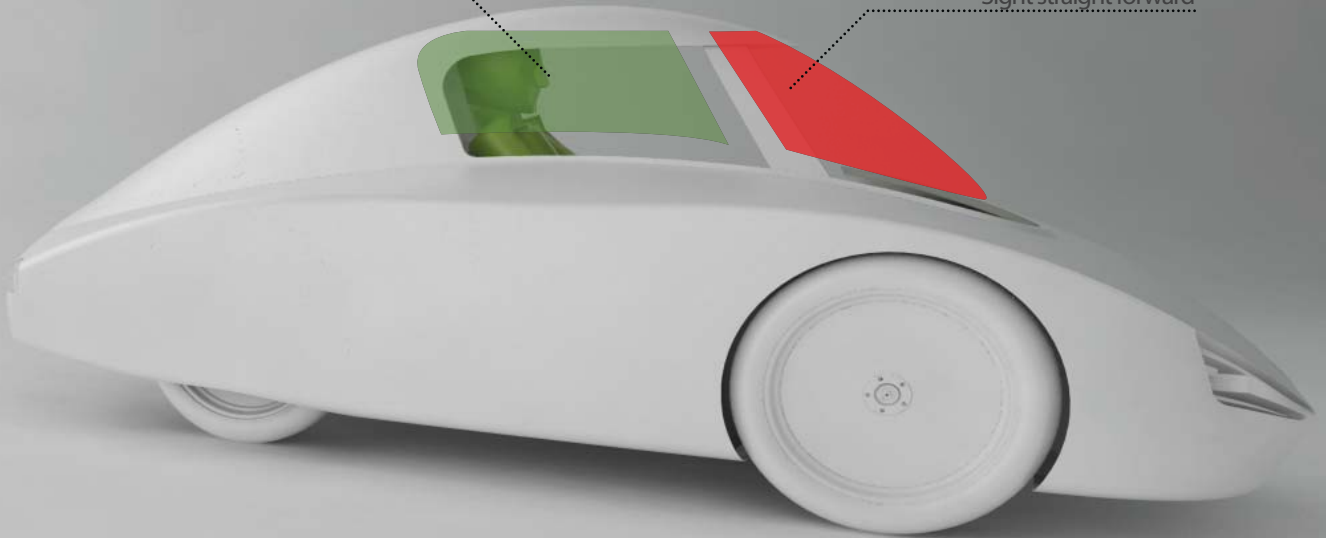
A normal car seat is usually designed to fit the range of people between 5 percentile women and 95 percentile men. It was already known that the driver was 50 percentile woman. Parameters like the distance from driver to steering wheel, perfect arm angle, back angle and where to place the lumbar support could be set to exact values instead of a range. It has to be remembered that the seat should also be usable for other persons.

The parameters were set by doing a lot of testing, first in the car mock-up, and later in the finished car. A test person, either the driver or a girl at about the same size were used. In addition recommended dimensions and angles were found in the Human Scale collection.

When driving a car in Shell Eco-marathon, it is hard to determine wanted driver position. Most times the decisions were based on the drivers wishes. It was always important to keep a good balance between a close steering wheel, and one further away which would be more comfortable.

Must be able to see 90° to the side

Sight straight forward



### 3.2.4.6 List of Requirements

The requirements for the seat were mostly set by the driver to make the cockpit environment both comfortable and user friendly. On the other hand the most important requirements were set by the rules.

#### Rules

- Must not prevent the driver from evacuating the vehicle in less than 10 seconds.

#### Other Sub-Systems

- Should be possible to remove from the car in a fast and simple way.

#### Users

- Should be customized to fit a 50 percentile woman.
- Must be possible to adjust to fit users outside the main user group.
- A 50 percentile women should have a 15-20° angle in the back and a 25-35° underarm angle when sitting in the car.
- A 50 percentile women must have lumbar support and support along the spine.
- Must be possible to buckle up the seat belt when sitting in the car.

#### Team Goals

- Should have a nice finish.
- Should weigh less than 500 g.



Figure 3.2.14: A lot of explorative sketching was done to generate as many ideas as possible

### 3.2.4.7 Idea Generation

The ideation process started with exploring sketches to get to know the product. In addition a lot of physical mock-ups were built and put into the car mock-up to test limitations, and decide on basic dimensions.

When both sketches were drawn and physical mock-ups were built, the result were put together into more detailed ideas. The later

stages of the ideation consisted of more rapid iterations between sketching, physical models and 3D-models. This generated a lot of different ideas, while at the same time validating them and speeding up the process.

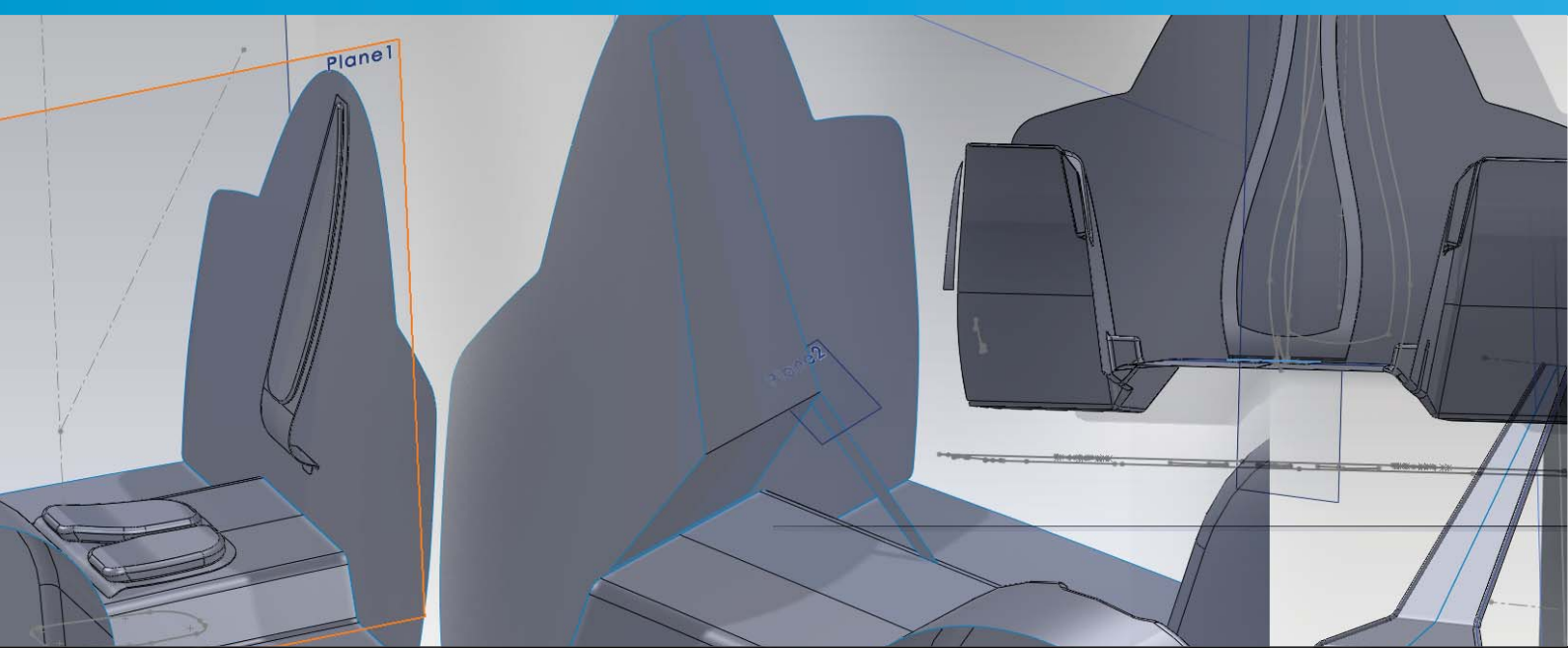


Figure 3.2.15: 3D-modelling was used to test different ideas and to decide on different dimensions in a fast way



A full scale mock-up was used for testing before the monocoque could be used for this purpose



Fast mock-ups of different concepts were built during the process to validate the different ideas

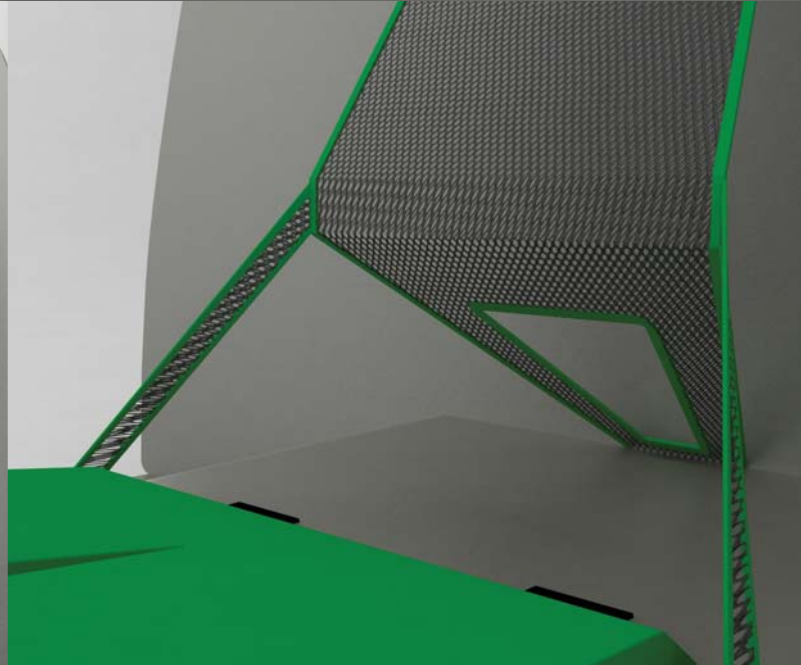
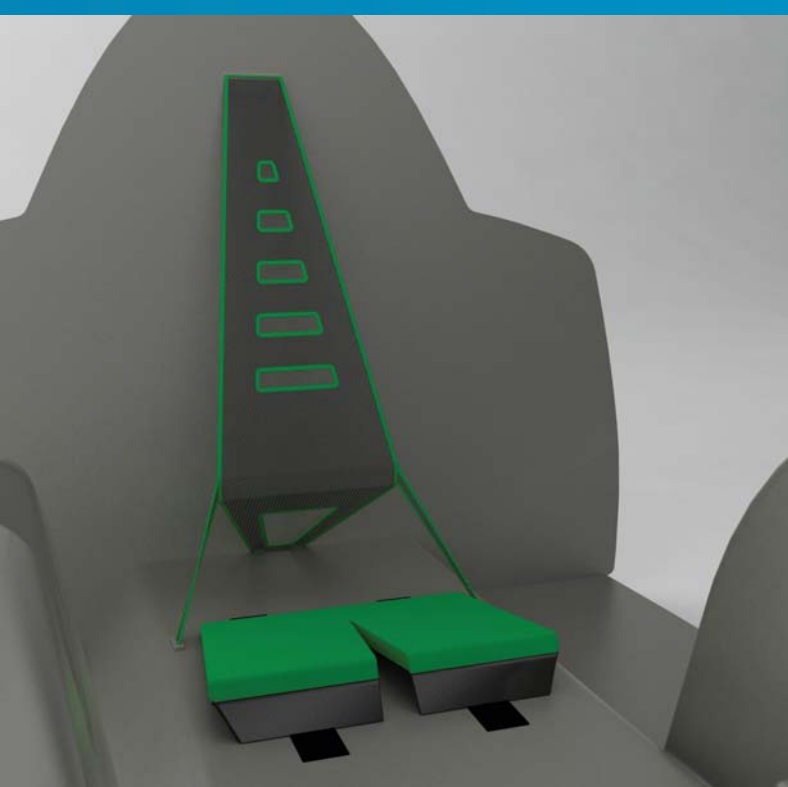


Figure 3.2.16: Idea 1

### 3.2.4.8 Three Ideas

The ideation process resulted in a lot of sketches, and to get an overview of these, they were organized into three different idea groups. Because of the lack of time, these were not finished concepts but rather more developed ideas.

#### Idea 1

The first idea group was based on all the ideas around use of stretched mesh. A sheet of lightweight mesh was stretched between four fastening points in the monocoque. Two of them were straps attached in strategic places to give lumbar

support when tightened. This idea would probably be the lightest solution, but it would not be adjustable as it was planned at this stage. If the idea had been developed further, adjustable fastening points could have been added, and therefore made it more flexible.

A tilted pillow was placed on the floor, attached with velcro to make it possible to move it back and forth. The bottom of the pillow would be made of carbon fiber.





Figure 3.2.17: Idea 2

### Idea 2

The second idea group would be the most adjustable one. The back support is attached to the monocoque in two points, both with velcro so that it can be moved. It is made of a carbon fiber frame with a stretched mesh in the middle to both save weight and make it more comfortable for the driver. The shape is curved to give some lumbar support.

The back support is attached to the pillow which is another adjustable part. It is attached to the floor with velcro and can therefore be moved

back and forth. It has three joints which makes it possible to adjust the sitting angle, and comfortable for most persons. The adjustable pillow consist of carbon fiber plates in the bottom to stiffen the construction.

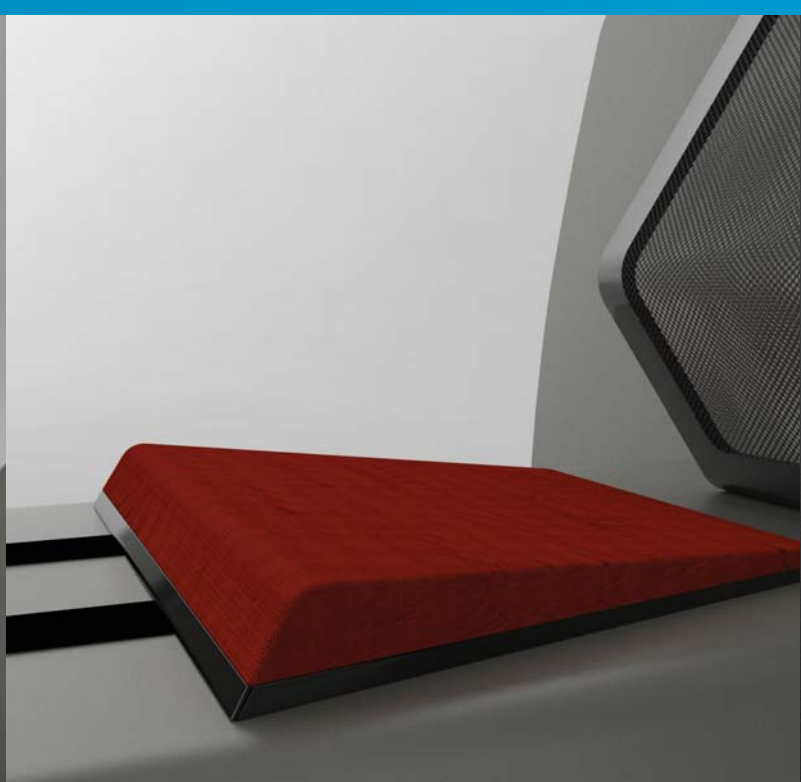


Figure 3.2.18: Idea 3

### Idea 3

This is the simplest solution, and is therefore also the least adjustable. The pillow is the only part that can be moved. This was to keep the design as simple as possible, and have few loose parts.

The back support is similar to concept 2. It is made as a carbon fiber frame with mesh stretched between, and is mounted to the monocoque with screws at the top and the bottom.

When made, this seat should be optimized for the driver. It could be a problems when larger

persons want to try the car, and it could also be a problem when evacuating. On the other hand, a fixed seat is a safe solution, and few things can go wrong during the race.

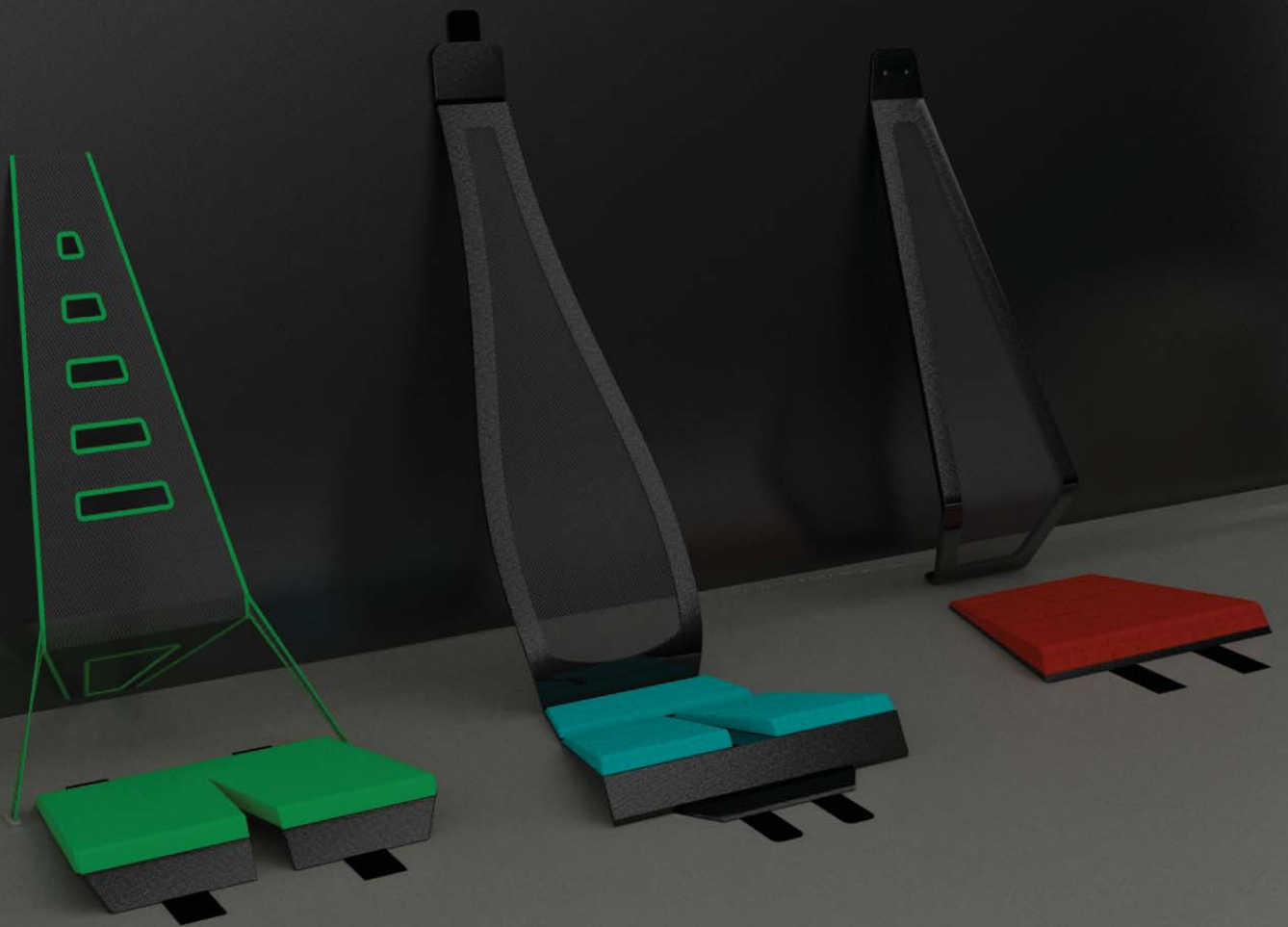


Figure 3.2.19: All the different seat ideas, where idea number 2 was selected for further development.

#### 3.2.4.9 Selecting Ideas

It was hard to choose the final concept. Discussing with team members and other designers, it was early agreed that idea number 3 would probably create problems during the technical inspection. Both idea 1 and 2 were very interesting. Idea 1 was really lightweight, while idea 2 had all the adjustment possibilities.

It was agreed that if idea number 1 should be used, it had to be further developed to include adjustment possibilities. Because of the lack of time, this was not a possibility, and idea 2 was the

most logical choice. It was light, had adjustments and would be easy to produce. This also needed to be developed further, but this was not considered being a time consuming job.



Figure 3.2.20: Details of the final concept , cushions added

#### 3.2.4.10 Detailing of the Final Concept

To make a final concept the basic ideas from idea 2 were taken further. A lot of changes were made.

The back support got a totally new and more exciting shape. Stretched mesh was replaced by thin pillows along the spine supports and across the lumbar support.

To make the concept even more adjustable, a width adjustment was added. This was done because of the discoveries made during the final mockup testing of the concept. Unfortunately

there was no time left in the end to produce this mechanism.

The angle adjustments in the pillow were removed. It was found unnecessary during testing, and it would add extra weight to the car. The final pillow was milled out of lightweight foam, and attached to the floor with velcro.



*The mold was milled out of Ebaboard with a CNC-milling machine*



#### **3.2.4.11 Production**

The molds for the back support were modelled in SolidWorks as negative molds. This way the part would get a smooth surface without too much sanding. When the 3D-model was finished, the molds were milled out in ebaboard and sanded down. The carbon fiber layup was done as a wet layup with a core of rohacell. To give the driver a more comfortable position, the layup was made to give a small flex in the back.

The finished carbon fiber parts were cut out, sanded down and painted with transparent

glossy paint. Small strips of lightweight foam were glued on along the spine and on the lumbar support. The back support and the pillow were attached to the car with velcro.

On each side and in the front middle of the seat, a 5-point seat belt was attached. The belt was the smallest found, originally meant for junior racing. It was modified with some lighter parts, and adjusted for SEM rules and use. The weight was reduced from 2.5 kg to 1.5 kg.



*The mirrors of the DNVFF were larger than required by the SEM rules*

## 3.2.5 REAR VIEW MIRRORS

According to SEM rules, the car must have two rear view mirrors. Since this was one of the less important features affecting the performance of the car, the design process was relatively short.

### 3.2.5.1 Mirrors on DNVFF

Same mirrors have been used on DNVFF since 2009. The mirror surface is several times larger than what is required by the rules, and could

with benefit be reduced. The mirrors are placed inside the cockpit to reduce the aerodynamic drag.



### 3.2.5.2 Inspiration

A lot of work is often put into design and production of beautiful rear-view mirrors by the car producers. It is therefore no problem to find a lot of good inspiration on this area. On the other hand very few car producers are focusing on weight and aerodynamics when designing the mirror. Especially indoor mirrors are a rare thing to find.

evo  
MAGAZINE

cars.net



Figure 3.2.21: Detailed model of the interior without mirrors

### 3.2.5.3 List of Requirements

Since the rear-view mirrors have few interfaces with other sub-systems, the list of requirements is based on the rules, and on requirements from the users.

#### Rules

- The vehicle must be equipped with a rear-view mirror on each side, with a minimum surface area of 25 cm<sup>2</sup>.

#### Users

- The mirrors should be adjustable in a way that makes it possible for the selected driver to get the perfect view.
- The quality of the the mirror glass should be good enough to spot competitors driving behind the car.
- The mirrors should not block the drivers view.
- If placed on the outside, they should be easy to clean.



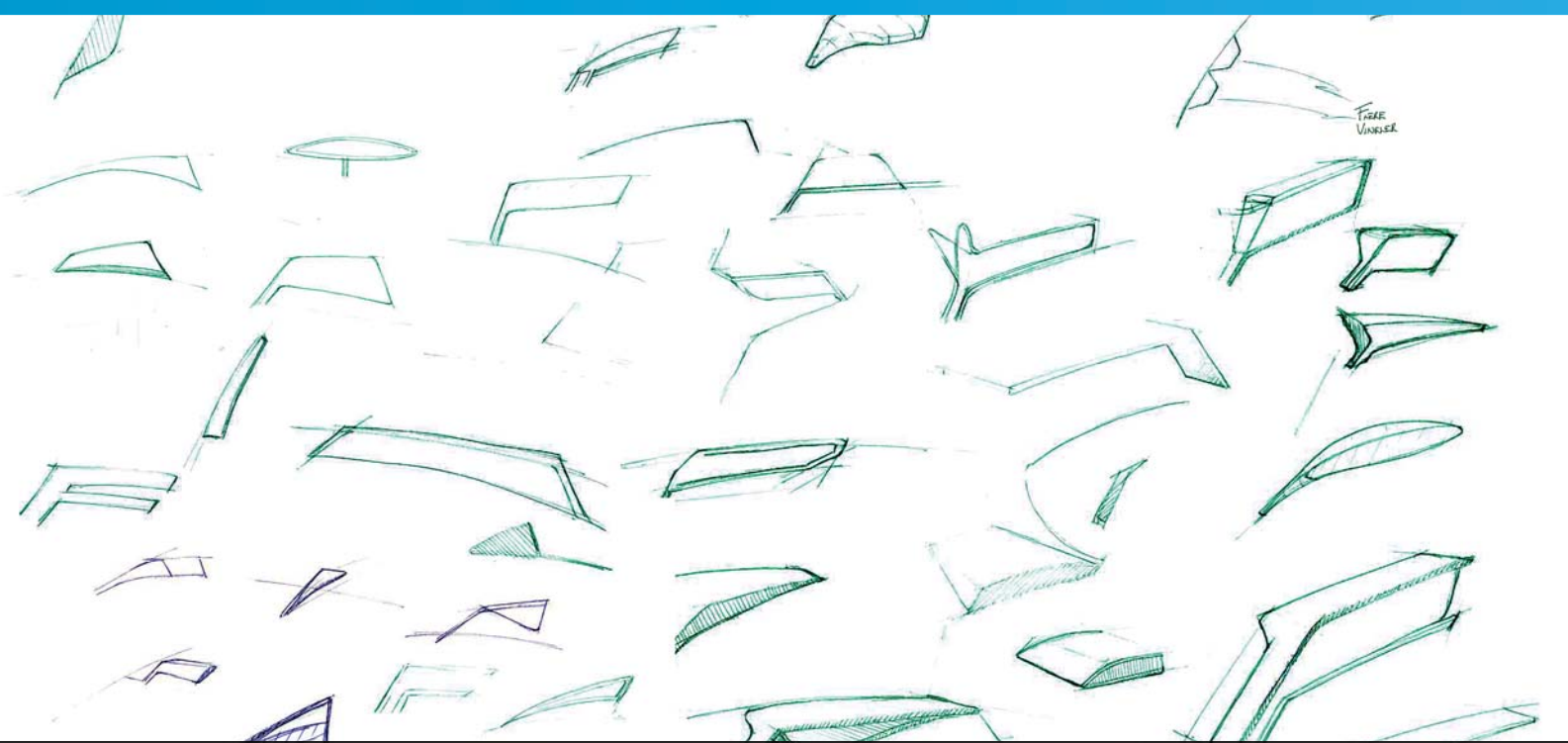
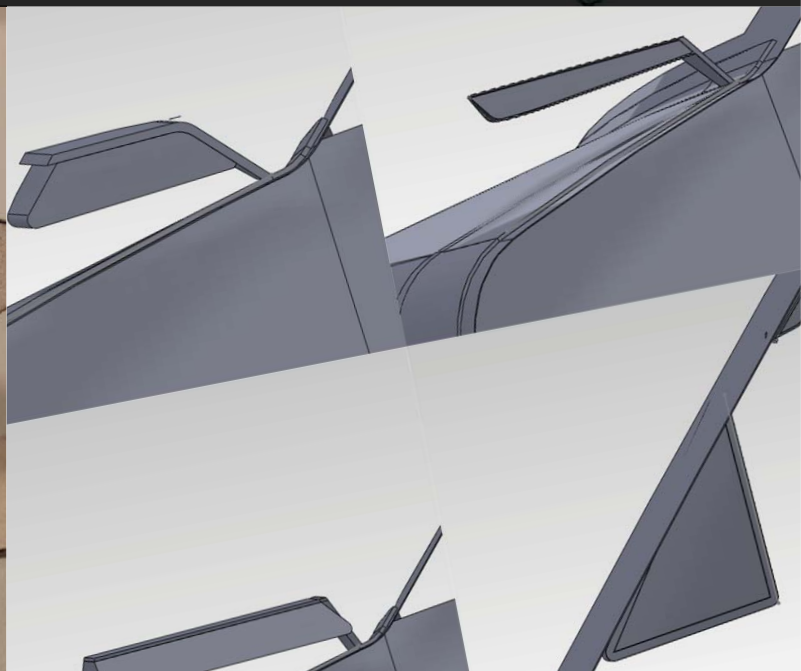
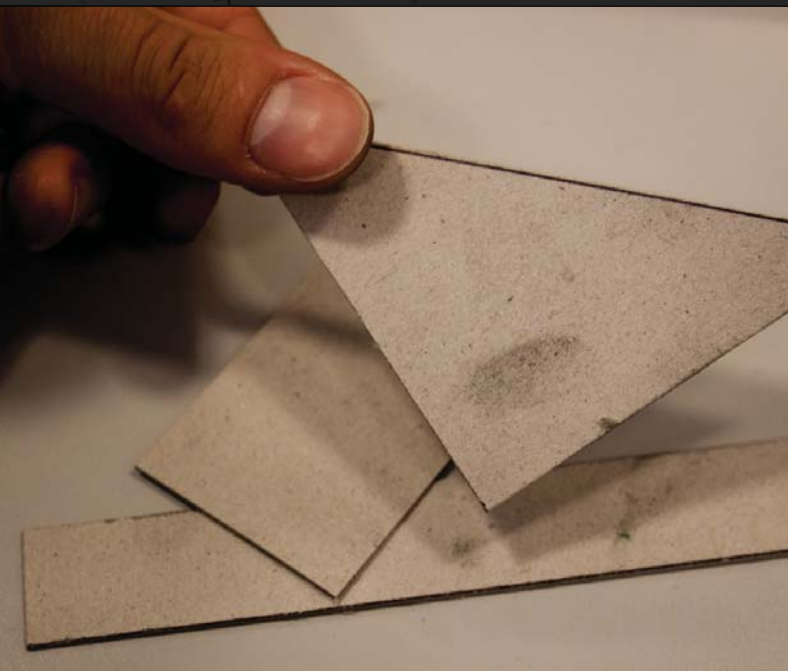


Figure 3.2.22: Explorative sketching was done to generate ideas



To get an idea of how big the mirrors should be, different cardboard models were made with the required area. By using these models together with the sketches it was possible to make 3D-models of the ideas

### 3.2.5.4 Idea Generation

Quick drawn freehand sketches was the main tool in the ideation process of the mirrors, but also physical models were used to get an impression of the actual size. When experimenting with physical mockups we realised that 25 cm<sup>2</sup> was really small, and did therefore make different samples of this size in different shapes. This was really handy through the rest of the process.

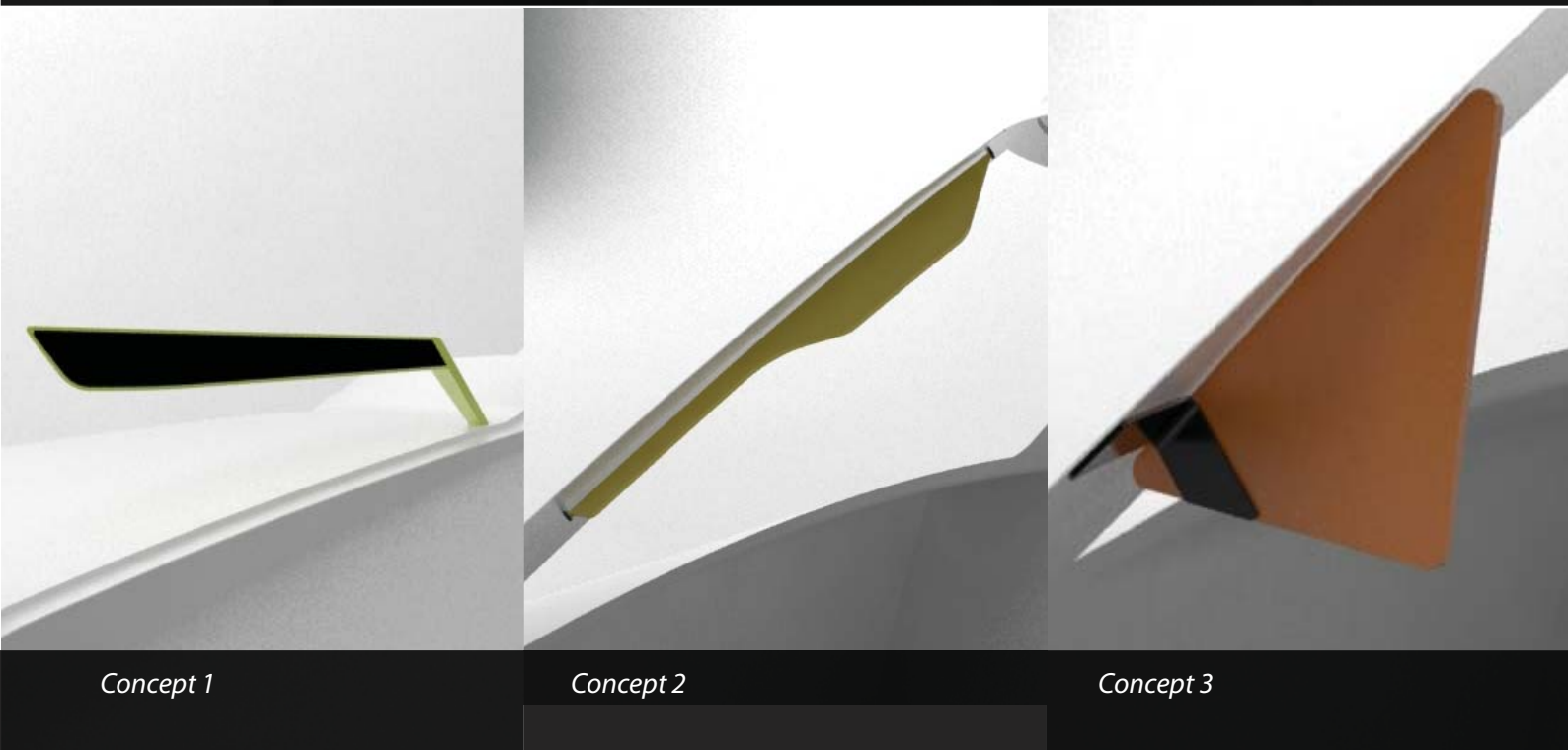
The resulting ideas can basically be divided into

two different categories; interior and exterior mirrors. The exterior mirrors were the biggest challenge. They had to be aerodynamic, really small and have nice details.

Most interior sketches were of mirrors hidden behind the a-beam, which was the only place where they did not block the drivers view. The interior was easier to draw, since the main focus there should be to hide them, not give them nice details, and a beautiful shape.



Figure 3.2.23: The three different concepts seen from the drivers view. Closeup of the different concepts are shown below



### 3.2.5.5 Different Concepts

The result from the ideation process was developed into three different concepts. All of them were really small (25-30 cm<sup>2</sup>). One was exterior, while two were interior.

#### Concept 1

The only exterior concept, and it has a flat shape which gives it a light and floating look. The shape is made as aerodynamic as possible, but will always induce some drag. Since the mirrors are

small, they can be hard to use when mounted on the outside of the car.

#### Concept 2

Was the first interior concept. It had a long shape so it could be placed on the a-beam. With joints in each end it could be adjusted to fit the driver. When testing the mirrors later in the process it was discovered that it could be hard to spot cars, because it was too narrow.

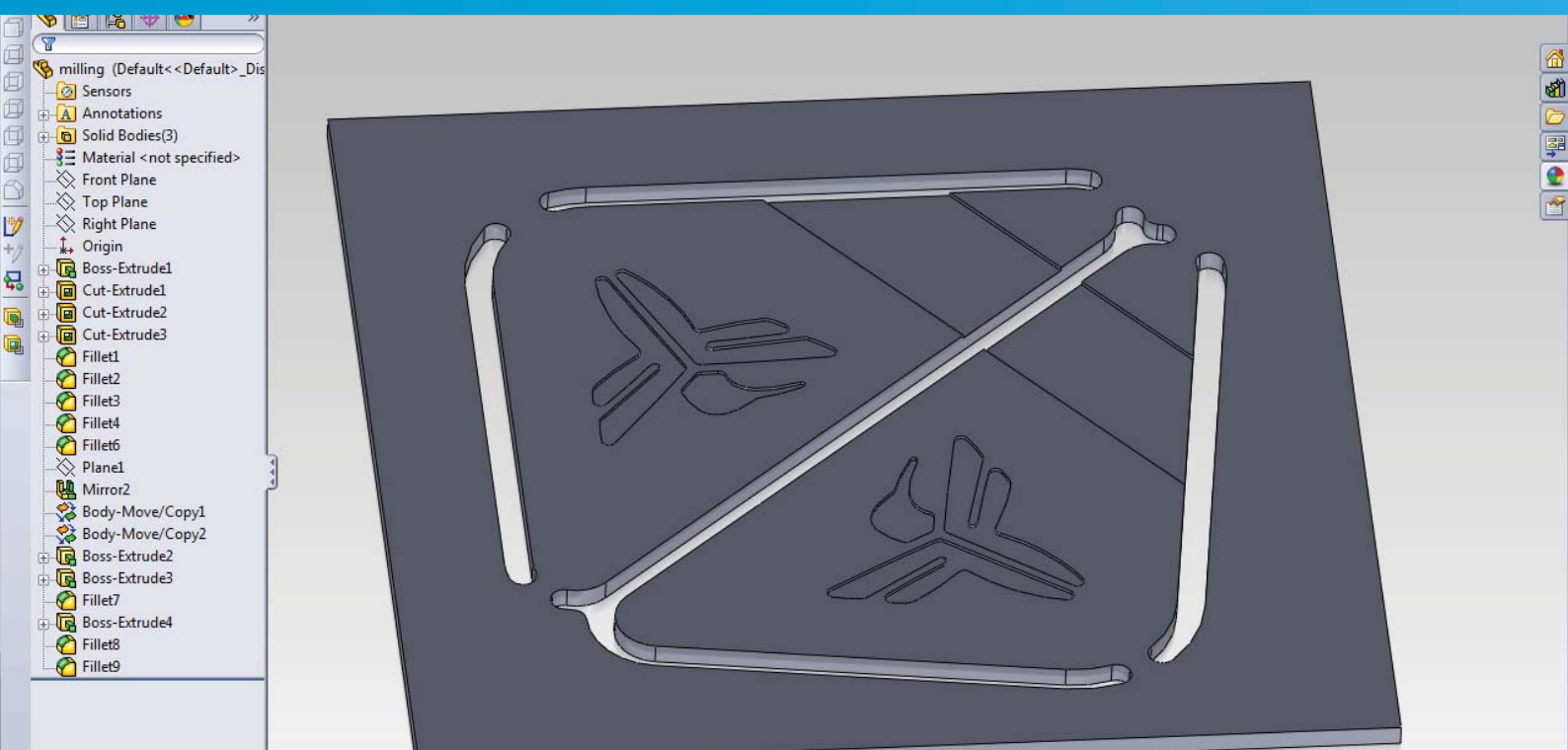


*Figure 3.2.24: The main part for the mirrors designed in SolidWorks. The model was planned in a way that made it easy to mill*



*The finished mirrors seen both before and after being mounted in the car*

### Concept 3

An interior mirror with a triangular shape. It can also be placed on the a-beam. The mirror is attached with a sheet of brass, this way it can be bent and adjusted many times without braking.

### 3.2.5.6 Production and Finished Product

Concept 3 was the chosen concept. It would create the best view and not interfere with the aerodynamics. The fact that the adjustment mechanism would be so easy to produce, did

also count in a positive way.

The mirror base was milled out of acrylic, and the glass and brass were glued on. It was mounted in the car while the driver was sitting in the driving position.

The finished product is an anonymous mirror, that is almost invisible from the outside. It has a satisfying view range to the back, and does not block the front view.

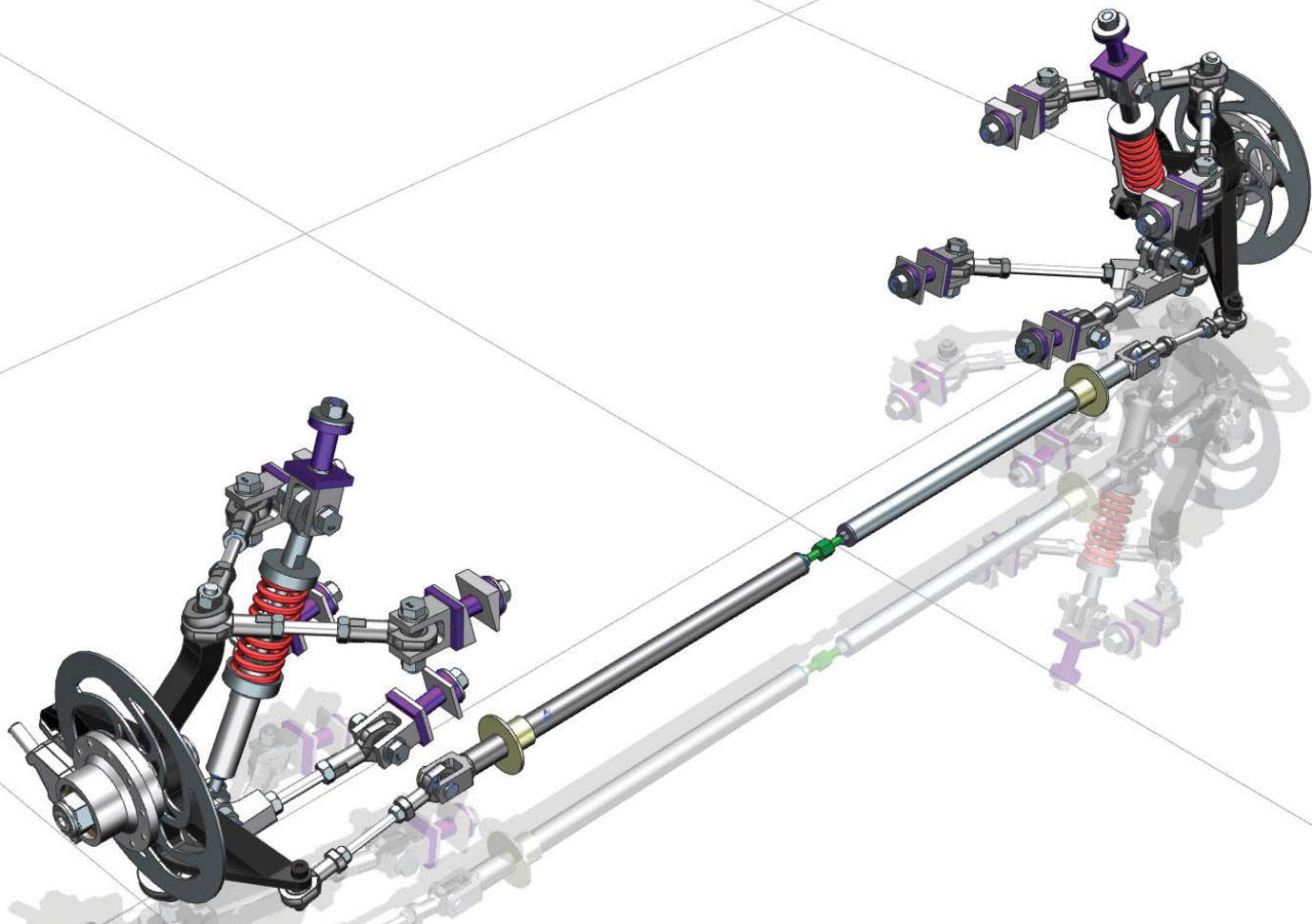


DNV





# 3.3 SUSPENSION



# 3.3 SUSPENSION

## 3.3.1 FRONT SUSPENSION

It was important to keep all wheels in contact with the ground at all times for the sake of safety and fuel efficiency.

The aerodynamics, size and weight of the car has been prevalent during the design phase and overruled some of the design freedoms of the suspension. For instance, the diffuser underneath DNVFF2 is crucial for eliminating aerodynamic lift (Endresen, et al., 2011) and its geometry affects where the lowest mounting points for the suspension linkages can be placed. This means that an optimal roll center, placed as low as possible, cannot be achieved as the linkages will slant upwards into the body, especially for the rear suspension where the diffuser slants up and away from the ground as it meets the car's tail.

Figure 2.3.2 shows the parts that the steering knuckle must have in order to provide proper steering and spring action. Swivel joints allow the knuckle to rotate about its vertical axis to steer

the attached wheel. The placement of these relative to each other are absolutely crucial to obtain the desired motion.

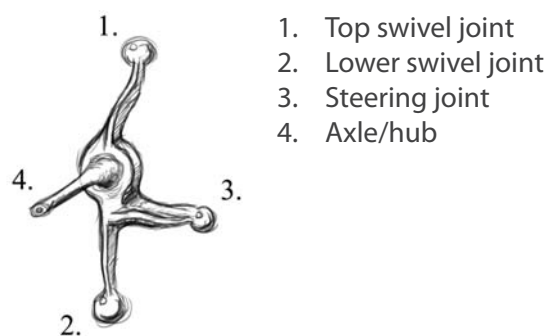


Figure 3.3.1: Typical steering knuckle concept

### Change in camber angle

When the car drives through a curve, the lateral acceleration will transfer weight to the outer wheels. With the ground as reference frame, the car will tilt to the side, and depending on the suspension kinematics, the wheels will alter camber angle. Since the camber angle both affects energy efficiency and lateral thrust force, the camber angle relative to the ground should

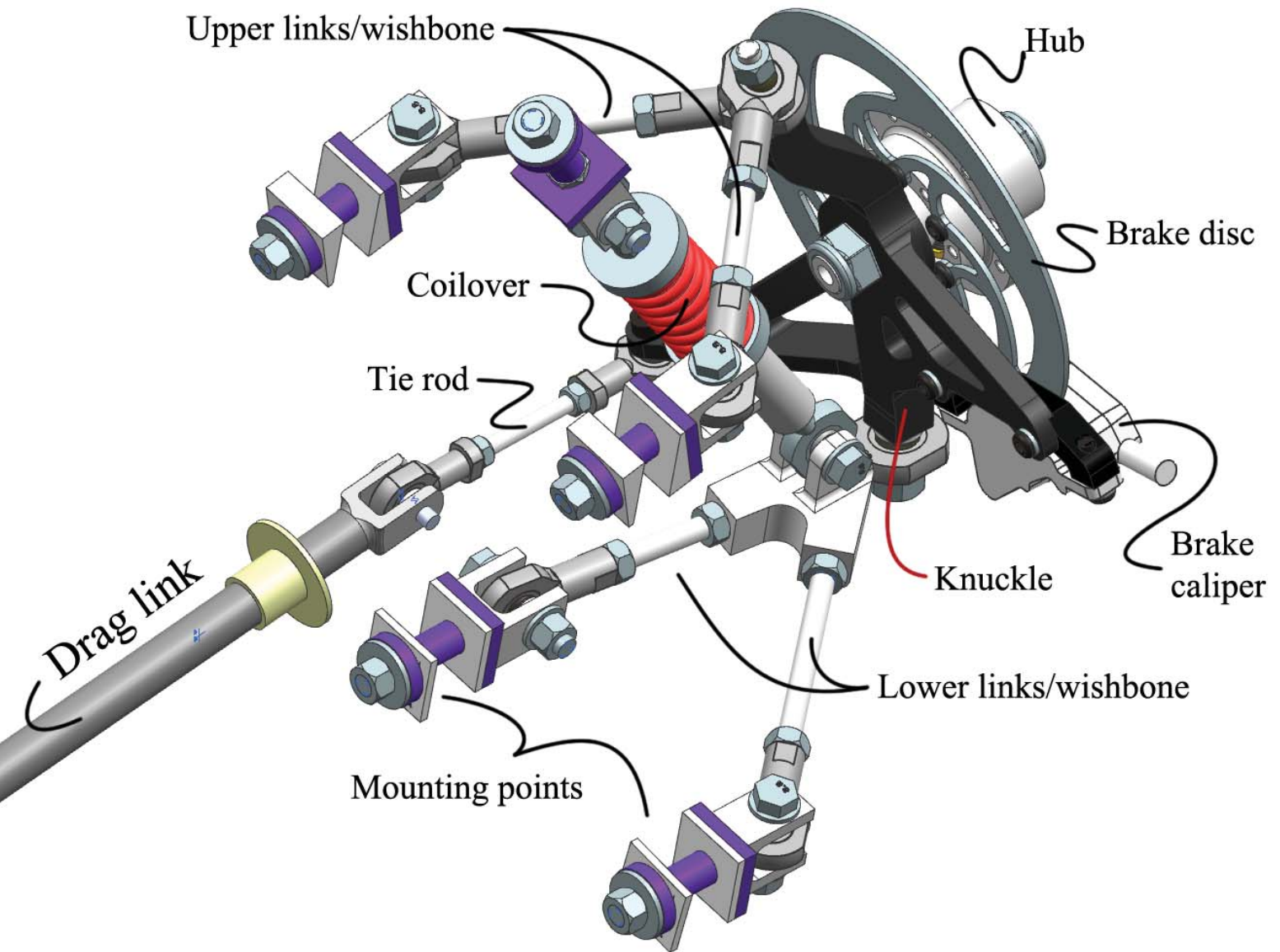


Figure 3.3.2: Double wishbone system, parts annotated

remain fairly constant, or rather it should at least not become positive.

With a positive camber angle less lateral force than required may be developed, with the possibility of slipping. The cornering stability is reduced because the contact point is moved towards the center of gravity.

A negative camber angle would rather increase the stability, but could also lead to over steer.

With the car as reference frame, the negative camber change can lead to unwanted effects regarding suspension.

The chosen solution was to optimize the camber angle change for minimizing the ground-to-camber-angle during cornering action. With an axle width of 100 cm, and a maximum delta change of  $\pm 2$  cm, the car's roll angle and the corresponding

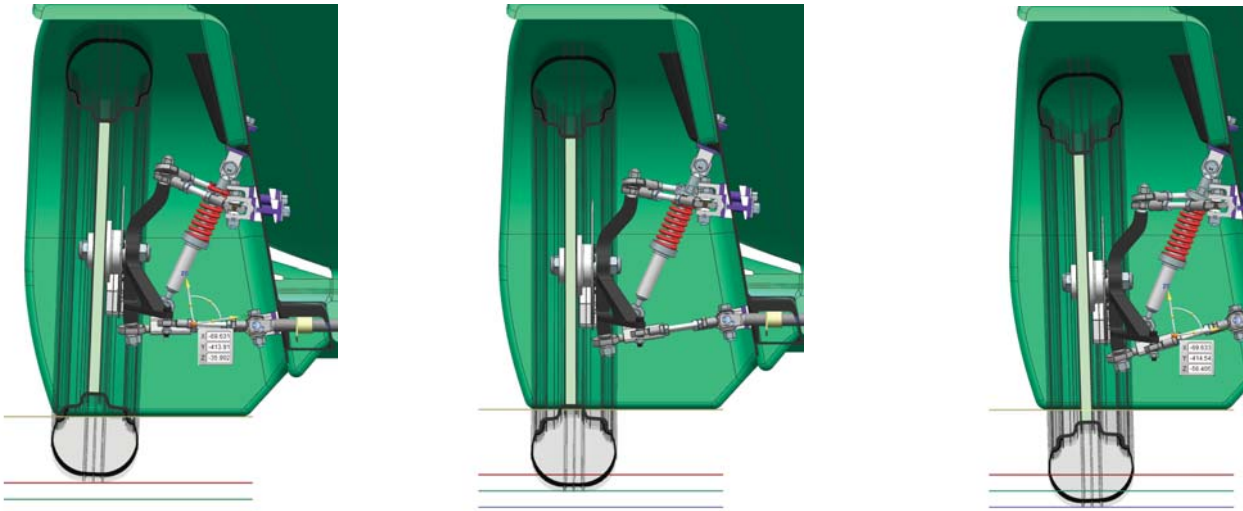


Figure 3.3.3: Camber angle change during spring action

camber angle compensation can be calculated as follows:

$$\Delta\theta_{\text{camber, front}} = \arctan \frac{20\text{mm}}{500\text{mm}} = 2.29^\circ$$

The CAD assembly with its constraints was used to modify the link geometry until the desired camber angle change was achieved. A model with three sheets spaced 2 cm apart was made to show the different wheel positions during spring action when placed correctly beneath the shell model of the car. From left to right in figure 3.3.3: Lowest (wheel hanging), ride height, highest (compressed by bump or hard braking or cornering).

#### Wishbone Angles

Seen from above, the links form triangles that, coupled with the rod ends and clevis mount points as hinges, define the vertical swinging motion of the knuckles, and otherwise completely lock the knuckles from moving sideways or forward or backwards. The angle subtended by the links in the horizontal plane determines the force absorbed during braking and cornering. The angles can be optimized for reducing stress during braking or cornering. The middle ground is 90°. However, to avoid the links interfering with the wheels turning about the steer axis, and because the car will corner harder and more frequently than braking, this angle was reduced to 80°.

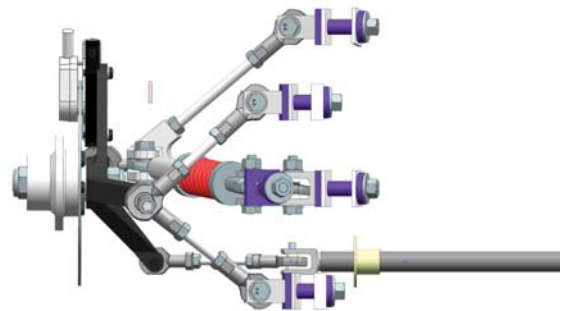


Figure 3.3.4: Top view front view of front left suspension links

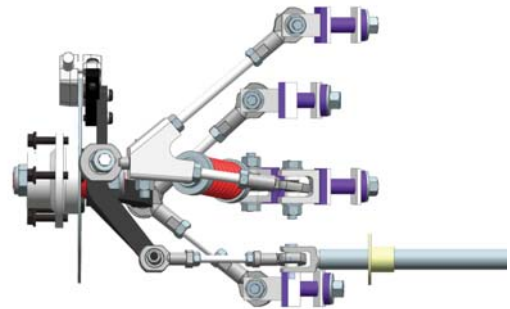


Figure 3.3.5: Viewed from beneath, front right suspensions

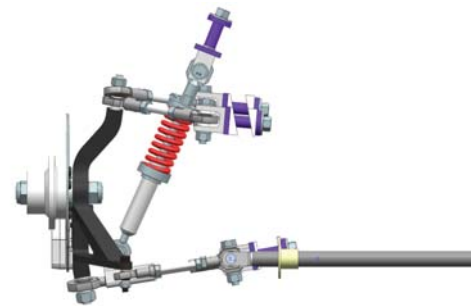


Figure 3.3.6: Rear view of front left suspension links



For the lower links, the rear link had to be rotated and moved forwards to give space for the tie rods. Since energy efficiency and safety are so important, the no bump steer-requirement required that the tie rods be moved down into the plane of the lower links. The angle of the lower, rear link was thus reduced to  $8^\circ$  from the lateral axis of the car.

### Calculation of Link Forces

The principal forces acting on the wheels that the suspension must support are derived and readily explained in the Project Report autumn 2011 (Endresen, et al., 2011).

The  $P_1$  and  $P_2$  forces will be used to determine the forces acting through the primary linkages, and  $P_4$  the force acting through the coilovers on the front suspension. To find these forces, the system(s) can be modeled as rigid bodies with loads and fixed constraints where the bodies are connected to other linkages or mounting points on the body.

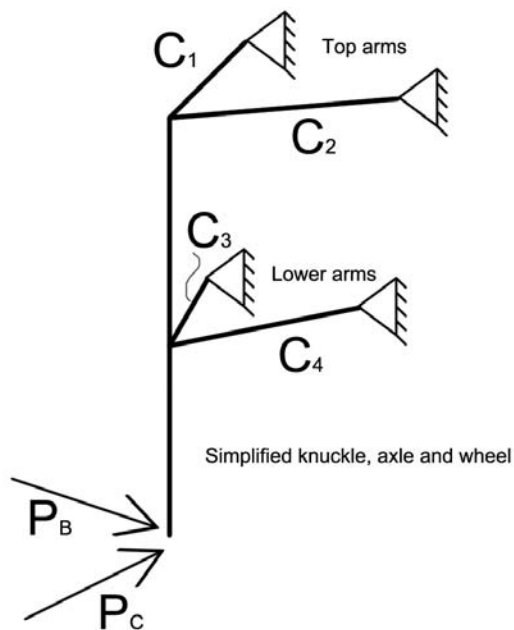


Figure 3.3.7: Rigid body model of front suspension, where  $P_B$  and  $P_C$  are the braking and cornering forces, and  $C_{1,2,3,4}$  are the support forces acting through the wishbone links

The calculations are simplified by splitting the mechanical joints into three separate problems:

1. The steering knuckle experience longitudinal braking force or lateral cornering force
2. The top linkage triangles
3. The lower linkage triangles

This greatly simplifies the derivation of the constraint equations to be solved as a set of matrix equations. The steering knuckle can be modeled as a beam supported on two points where  $T_B$  is the torque generated from the braking force  $P_B = P_2$ ,  $R_W$  is the wheel radius and  $L$  is the height of the knuckle:

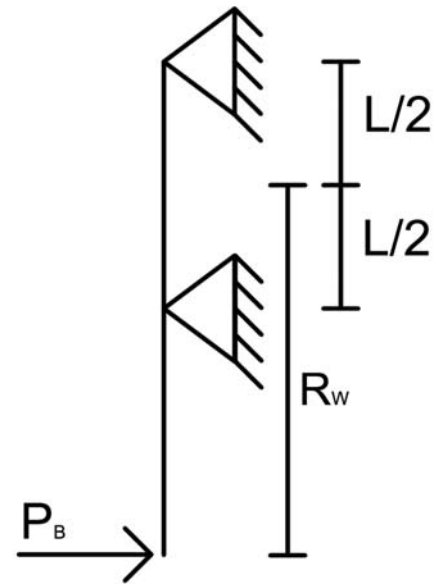


Figure 3.3.8: Force and constraints on the knuckle

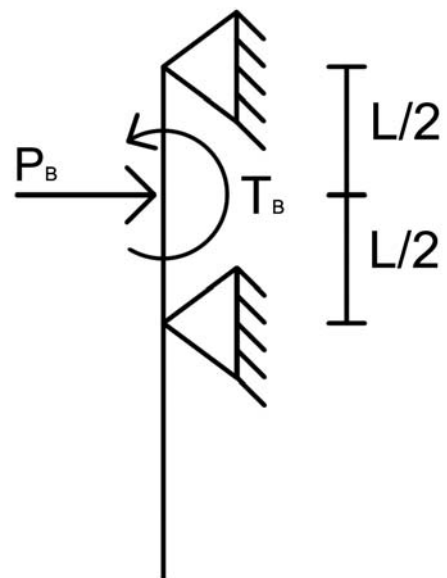


Figure 3.3.9: Simplified force and torque on knuckle

To further simplify the system, the reaction forces can be annotated so that the two unknowns for the knuckle are clearly shown in figure 3.3.10.

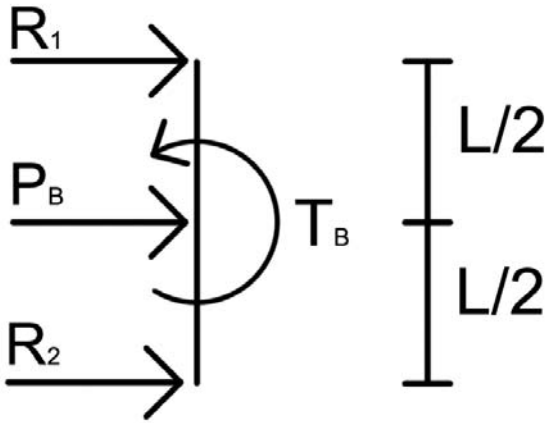


Figure 3.3.10: Steering knuckle modeled as a beam with load and reaction forces

This setup can also be reused when the effects of the cornering force are calculated. The system is then expressed as the following linear equations:

$$\begin{aligned} \Sigma F_x = 0 &\Rightarrow R_1 + R_2 + P_B = 0 &&\Rightarrow R_1 + R_2 = -P_B \\ \Sigma M = 0 &\Rightarrow -R_1 \frac{1}{2}L + R_2 \frac{1}{2}L + T_B = 0 &&\Rightarrow -R_1 \frac{1}{2}L + R_2 \frac{1}{2}L = -T_B \\ &&&\Rightarrow -\frac{1}{2}L (R_1 + R_2) = -T_B \end{aligned}$$

In matrix form this gives:

$$\begin{bmatrix} 1 & 1 \\ -\frac{L}{2} & \frac{L}{2} \end{bmatrix} \begin{bmatrix} R_{B,1} \\ R_{B,2} \end{bmatrix} = \begin{bmatrix} -P_B \\ -T_B \end{bmatrix}$$

Thus, given that  $P_B = P_2 = 550 \text{ N}$ ,  $R_w = 279 \text{ mm}$  and  $L/2 = 100 \text{ mm} = 0.1 \text{ m}$ :

$$T_o = P_o R_w = 550 \text{ N} \times 279 \text{ mm} = 154 \text{ Nm}$$

$$\begin{bmatrix} 1 & 1 \\ -0.1 & 0.1 \end{bmatrix} \begin{bmatrix} R_{B,1} \\ R_{B,2} \end{bmatrix} = \begin{bmatrix} -550 \\ -154 \end{bmatrix} \text{ N}$$

$$\Rightarrow \begin{bmatrix} R_{B,1} \\ R_{B,2} \end{bmatrix} = \begin{bmatrix} 1 & 1 \\ -0.1 & 0.1 \end{bmatrix}^{-1} \begin{bmatrix} -550 \\ -154 \end{bmatrix} = \begin{bmatrix} 0.5 & -5 \\ 0.5 & 5 \end{bmatrix}^{-1} \begin{bmatrix} -550 \\ -154 \end{bmatrix} = \begin{bmatrix} 495 \\ -1045 \end{bmatrix} \text{ N}$$

The top arms must thus exert a backwards force of 495 N and the lower arms a forwards force of 1060 N. To decompose these reaction forces into the arising axial forces in the top and lower links, the following model and equations are derived:

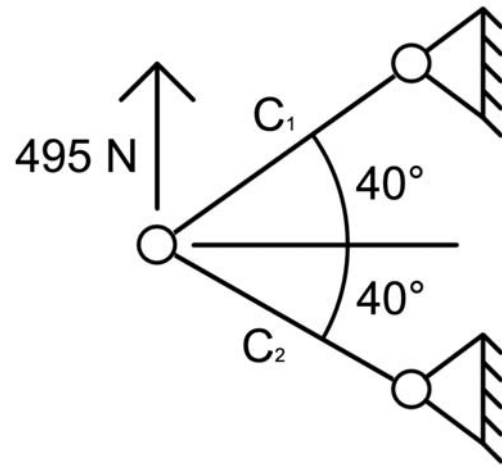


Figure 3.3.11: Constraint model for top arms during braking

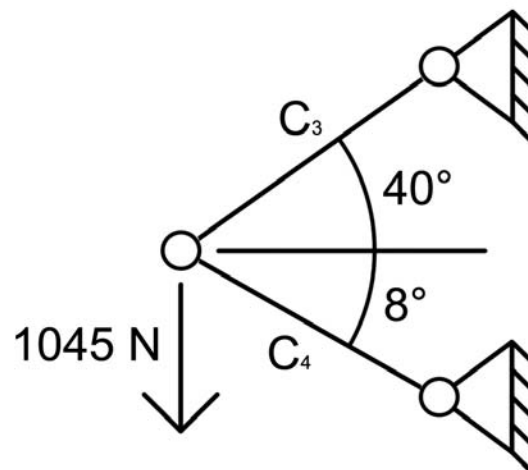


Figure 3.3.12: Constraint model for lower arms during braking

Solving for the support forces in the beams can be done with the following equation:

$$\begin{bmatrix} \cos \theta_1 & \cos \theta_2 \\ \sin \theta_1 & -\sin \theta_2 \end{bmatrix} \begin{bmatrix} C_u \\ C_v \end{bmatrix} = \begin{bmatrix} P_x \\ P_y \end{bmatrix}$$

Where P is the force acting on the swivel joint,  $C_u$  and  $C_v$  are the axial support forces in the beams, and  $\theta_1$  and  $\theta_2$  are the angles from the horizontal plane. Applied to the top arms this becomes:

$$\begin{bmatrix} \cos 40^\circ & \cos 40^\circ \\ \sin 40^\circ & -\sin 40^\circ \end{bmatrix} \begin{bmatrix} C_1 \\ C_2 \end{bmatrix} = \begin{bmatrix} 0 \\ -500 \end{bmatrix} \text{N}$$

$$\Rightarrow \begin{bmatrix} C_1 \\ C_2 \end{bmatrix} = \begin{bmatrix} \cos 40^\circ & \cos 40^\circ \\ \sin 40^\circ & -\sin 40^\circ \end{bmatrix}^{-1} \begin{bmatrix} 0 \\ -500 \end{bmatrix} = \begin{bmatrix} -389 \\ 389 \end{bmatrix} \text{N}$$

And applied to the lower arms this becomes:

$$\begin{bmatrix} \cos 40^\circ & \cos 8^\circ \\ \sin 40^\circ & -\sin 8^\circ \end{bmatrix} \begin{bmatrix} C_3 \\ C_4 \end{bmatrix} = \begin{bmatrix} 0 \\ 1045 \end{bmatrix} \text{N}$$

$$\Rightarrow \begin{bmatrix} C_3 \\ C_4 \end{bmatrix} = \begin{bmatrix} \cos 40^\circ & \cos 8^\circ \\ \sin 40^\circ & -\sin 8^\circ \end{bmatrix}^{-1} \begin{bmatrix} 0 \\ 1045 \end{bmatrix} = \begin{bmatrix} 1392 \\ -1077 \end{bmatrix} \text{N}$$

Here, a positive value means that the element undergoes tensile load, and negative values compressive loads.

For the cornering force, we observe that we can scale the result for the steering knuckle and avoid solving the same equations again:

$$P_1 = 510 \text{N} = P_2 \frac{P_1}{P_2} = P_2 \times \lambda$$

$$\lambda = \frac{P_1}{P_2} = \frac{510}{550} = 0.9273$$

The reaction forces on the steering knuckle become:

$$\begin{bmatrix} R_{C,1} \\ R_{C,2} \end{bmatrix} = \lambda \begin{bmatrix} R_{B,1} \\ R_{B,2} \end{bmatrix} = 0.9273 \times \begin{bmatrix} 495 \\ -1045 \end{bmatrix} = \begin{bmatrix} 459 \\ -969 \end{bmatrix} \text{N}$$

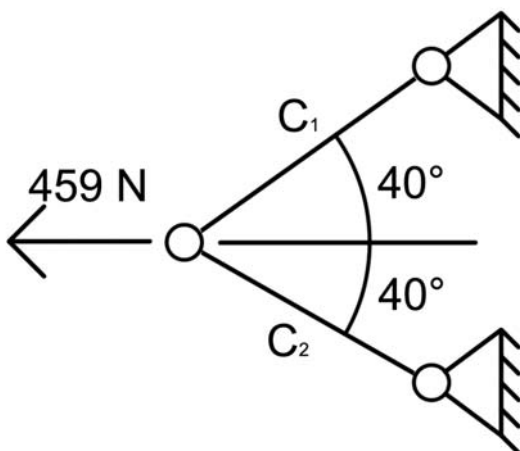


Figure 3.3.13: Constraint model for top arms during cornering

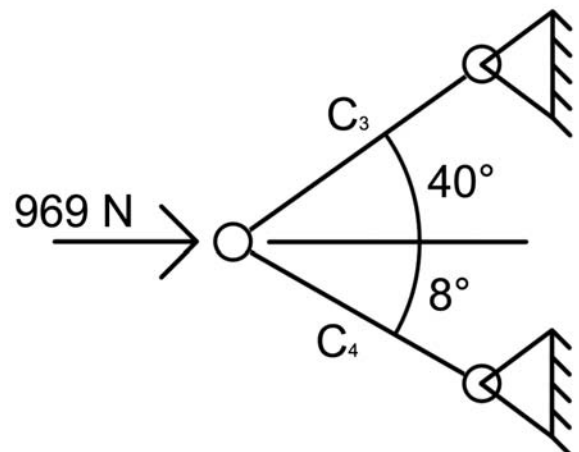


Figure 3.3.14: Constraint model for lower arms during cornering

$$\begin{bmatrix} \cos 40^\circ & \cos 40^\circ \\ \sin 40^\circ & -\sin 40^\circ \end{bmatrix} \begin{bmatrix} C_1 \\ C_2 \end{bmatrix} = \begin{bmatrix} 495 \\ 0 \end{bmatrix} \text{N}$$

$$\Rightarrow \begin{bmatrix} C_1 \\ C_2 \end{bmatrix} = \begin{bmatrix} \cos 40^\circ & \cos 40^\circ \\ \sin 40^\circ & -\sin 40^\circ \end{bmatrix}^{-1} \begin{bmatrix} 495 \\ 0 \end{bmatrix} = \begin{bmatrix} 323 \\ 323 \end{bmatrix} \text{N}$$

$$\begin{bmatrix} \cos 40^\circ & \cos 8^\circ \\ \sin 40^\circ & -\sin 8^\circ \end{bmatrix} \begin{bmatrix} C_3 \\ C_4 \end{bmatrix} = \begin{bmatrix} -969 \\ 0 \end{bmatrix} \text{N}$$

$$\Rightarrow \begin{bmatrix} C_3 \\ C_4 \end{bmatrix} = \begin{bmatrix} \cos 40^\circ & \cos 8^\circ \\ \sin 40^\circ & -\sin 8^\circ \end{bmatrix}^{-1} \begin{bmatrix} -969 \\ 0 \end{bmatrix} = \begin{bmatrix} -181 \\ -838 \end{bmatrix} \text{N}$$

For cornering in the opposite direction, the forces are inverted.

From these calculations we observe that the greatest axial loads in the links occur during braking, and the force of greatest magnitude (1392 N equals 1.4 kN) will be used as dimensioning criteria (with a safety factor) as it simplifies CAD modeling and manufacturing by reusing parts as much as possible.

### Calculation of Coilover Forces

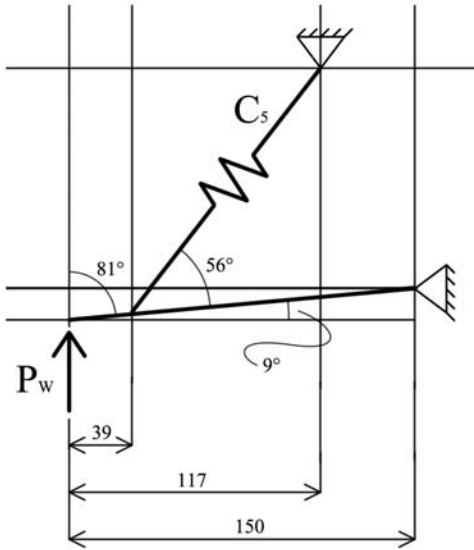


Figure 3.3.15: Diagram of weight force and link geometry view from behind the car, where  $P_w$  is the weight on the wheel and  $C_s$  is the coilover's reaction force

Since  $\cos 9^\circ$  equals 1 the calculation for the relation between the force  $P_w$  and  $C_s$  becomes:

$$C_s \sin \phi = -LP_w \sin \theta$$

$$C_s = -\frac{LP_w \sin \theta}{l \sin \phi} = -\frac{L \sin \theta}{l \sin \phi} P_w = -\frac{150 \sin 56^\circ}{(150 - 39) \sin 81^\circ} P_w = -\frac{150 \sin 56^\circ}{111 \sin 81^\circ} P_w = -1.13 P_w$$

And with:

$$P_w = \frac{1}{4} W = \frac{1}{4} \times 140 \text{ kg} \times 9.81 \text{ ms}^{-2} = 343 \text{ N}$$

$$C_s = -1.13 P_w = -1.13 \times 343 \text{ N} = -388 \text{ N}$$

The negative sign indicates that the coilover undergoes a compressive load, or if its unit vector points up to the right in figure 3.3.15, it exerts a reaction force down to the left. As the wheel bounces up and down, the angles change and the multiplying factor will change too, however this value is useful for the coilover calculations.

### Calculation of Tie-Rod Forces

One of the load scenarios, which happened during the competition in 2011, is that the entire weight of the car lands on one of the front wheels during a less fortunate lift. The car is assumed to have a roll angle of  $45^\circ$  if this event should reoccur. To calculate the force experienced by the responsible tie rod, the following criteria are set:

1. Car roll angle is  $45^\circ$ . The weight force is then multiplied by  $\sin 45^\circ = 1/2^{1/2}$
2. The caster angle is approximately  $8^\circ$
3. The tie rod length is 72 mm

Since the ground-tire force is higher (about 71% of the car's weight, 971 N, compared to the cornering force of 510 N in section 3.3.1.4) than the cornering force, this will be the determining scenario for the tie rods.

The force on the tie rod occurs from the transfer of the force on the ground acting through the king pin axis to produce torque. The "Caster-length" is:

$$L_{\text{caster}} = R_W \tan \theta_{\text{caster}} = 279 \text{ mm} \tan 8^\circ = 39.2 \text{ mm}$$

The tie rod force follows from the torque:

$$140 \text{ kg} \times 9.81 \text{ ms}^{-2} \times \sin 45^\circ \times 39 \text{ mm} / 72 \text{ mm} = 526 \text{ N} \approx 0.53 \text{ kN}$$

As the wheel turns about the steering axis, the tie rod force will increase.

### Anti - Dive

The dive effect of the weight transfer towards the front when braking can be countered by exploiting the generated torque from the brakes to generate torque on the body that tries to lift the front up from the dive (Gillespie, 1992). Experimentation with the top arm plane angle revealed that it affected the caster angle during spring action, which again influenced the steering-angle of the wheel, which again could adversely affect handling and fuel efficiency. The caster angle changes as a result of the top swivel joint moving forward or backwards, so that the tie rods change angle in the horizontal plane. Therefore, the anti-dive was reduced so that the caster change was negligible, while still trying to maintain some degree of anti-dive effect.

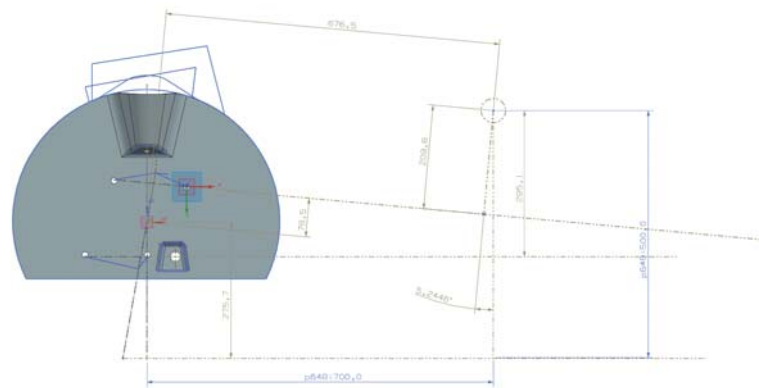


Figure 3.3.16: Sketch setup in NX to obtain measurements for anti-dive calculations

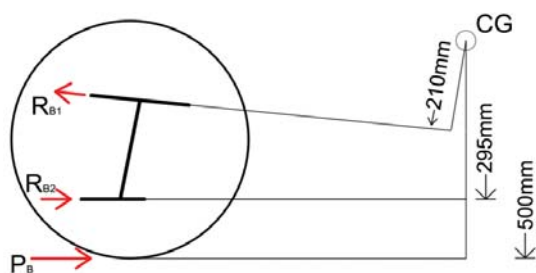


Figure 3.3.17: Force diagram of dive/anti-dive contributing forces

The knuckle reaction forces arising from braking, calculated in the previous section, can be used to estimate the resulting dive effect. The center of gravity of the car is assumed to be fairly low, namely 50 cm above the ground. Disregarding the anti-dive effect completely, the dive-torque from the front wheels braking is:

$$P_B \times 500 \text{ mm} = 550 \text{ N} \times 500 \text{ mm} = 272 \text{ N m}$$

By splitting up into torques arising from the lower and upper arms, this becomes:

$$T_{\text{dive}} = R_{B,2} \times 295 \text{ mm} = 1045 \text{ N} \times 295 \text{ mm} = 308 \text{ N m}$$

$$T_{\text{anti-dive}} = R_{B,1} \times 210 \text{ mm} = 495 \text{ N} \times 210 \text{ mm} = 104 \text{ N m}$$

$$T_{\text{tot}} = (308 - 104) \text{ N m} = 204 \text{ N m}$$

From this it can be concluded that the non-horizontal plane of the top arms significantly reduce the dive effect; but no more than a quarter. Although the anti-dive angle had to be reduced to avoid "bump steer", some effect positively remains, and the design choice is verifiable. Unfortunately, it will not be possible to measure the effect of the anti-dive geometry once the test driving starts, as the mounting points cannot be moved.



Figure 3.3.18: Front and back view of the hub

### 3.3.1.1 Hubs

The hubs were made for easy installation of bearings, held in place by retaining rings.

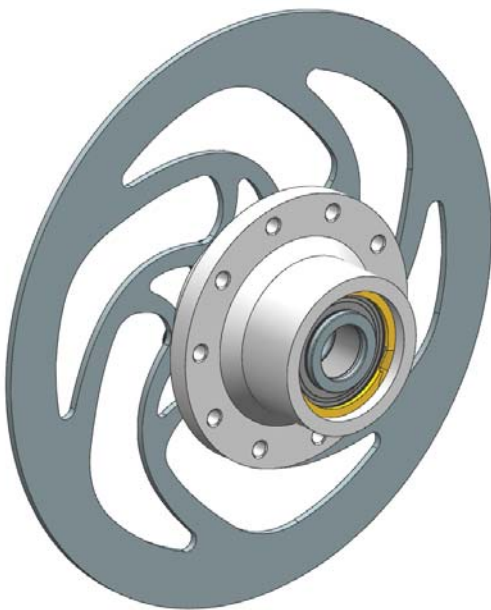


Figure 3.3.19: View of hub assembly

The hub design sports a double set of lug bolt holes and brake disc holes. These extra sets of holes can be used as spares in case the threads should fail from wear or other accidents. The five lug bolts concept was chosen over the previous center nut solution as it allows faster machining of the hubs, and no slow machining of large center nuts.

On recommendation from SKF, the internal hole tolerance was set to JS7 to allow a slight interference fit with the ball bearings to allow easy insertion and replacement.

FEM simulations were only done for braking and cornering, since the car's weight is transferred directly from the rims, through the hub, to the bearings.

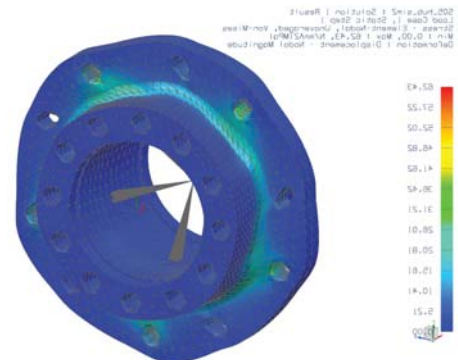


Figure 3.3.20: FEM analysis of hub during braking

The simulation of the braking situation shows that the stress concentrations stay below the fatigue limit of Alumec 89, which is about 100 MPa.

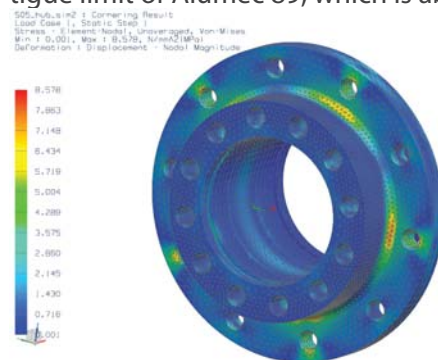


Figure 3.4.21: FEM analysis of hub during cornering

During cornering, the hubs undergo much lower stresses.

Three hubs were produced by NOMEK AS for about 6 700 NOK, including the material, Alumec 89.



Hubs and coilover parts received from Nomek

### 3.3.1.2 Axles

If the axles deform during operation they might interfere with the brakes. Sufficient stiffness is therefore required.

Since only the outer circumference of the cross section of a round bar significantly contributes to the stiffness, the axles could be made hollow to reduce weight without significantly reducing stiffness.

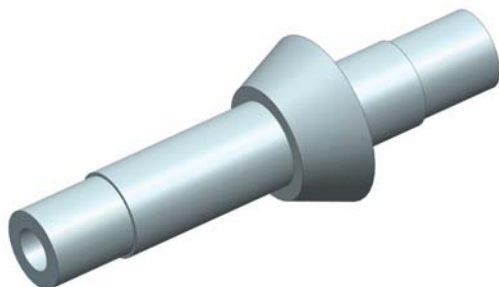


Figure 3.3.22: CAD model of axle

The axles are improved from the previous ones by using a large, conic flange to transfer the bending moment from the car's weight and braking to the knuckles.

505\_cax1a\_61 | Corning Result  
Load Case | Static Step |  
Stress | Element Model: Unaveraged, von-Mises  
Min: 0.00, Max: 145.97, N/mm<sup>2</sup>(MPa)  
Deformation | Displacement: Node Magnitude

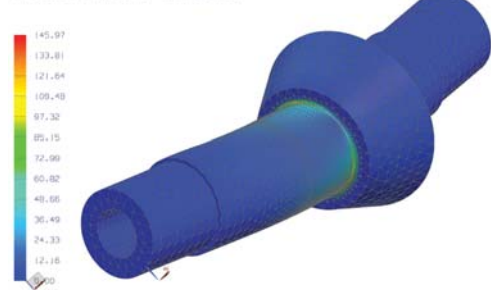


Figure 3.3.23: FEM analysis of axle during braking

The axle design was analyzed under the hardest braking scenario. Even though the maximum stress concentration climbs above the fatigue limit of aluminum, the ball bearings and spacers will help transfer loads to the face of the conic section, so the real stress concentrations are expected to be much lower. The deformation was so low (less than 0.1°) so the brake discs will not be affected.

The axles were produced from a round bar of Alumec 89.

### 3.3.1.3 Steering Knuckles

The use of carbon fiber was recommended by HPC, and would allow low weight. Carbon fiber composite parts are often shell-shaped and differ from the more massive solids usually made in metal, due to the anisotropic properties of composites. However, the steering knuckles will still require a rather massive piece.

One of the strong arguments for massive carbon fiber was that less material would go to waste in the production. If the knuckles were to be made in aluminum, they could either be sintered (additive) or machined from a solid block; both of which are expensive, and the latter leaves a lot of expensive waste material. Casting aluminum would raise the cost even higher because of the molds required. The carbon fiber would rather be cast on a rough mould, and then later be machined into the final shape (figure 3.3.32). As seen in table 3.3.1 this is where the carbon fiber solution gains advantage over metal.

#### Ackerman Steering

Ackerman steering is necessary to accommodate the smaller turning radius that the inner wheel experience. The behavior has been closely checked in the CAD models. Although the formulas for calculating the angle of the toes can be easily derived, experiments showed that this does not necessarily lead to a satisfactory solu-

tion.

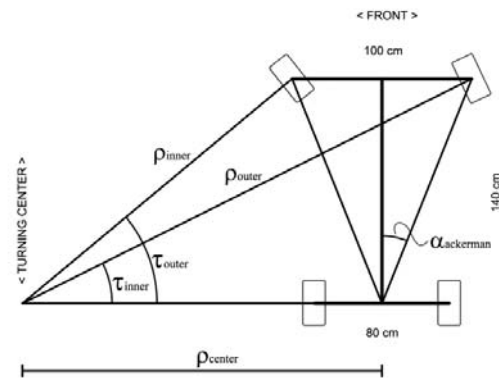


Figure 3.3.24: Ackerman steering based on sketch in the PD-journal, wheels and angles annotated.  $\alpha$  is the typical toe-angle when driving straight ahead.

This mode of analysis has two goals:

1. Ensure satisfactory ackerman steering.
2. Ensure a turning radius of 6 m (as required by Shell Eco-marathon) or less .

The exact requirements for the steering angles was not well documented in the literature studied. The Ackerman steering geometry is only optimal at low speeds when the tires develop little to no lateral forces. At higher speeds the behavior changes, the turning center moves forward (Gillespie, 1992).

According to IMechE, (1993) full ackerman is not

Criteria	Weight	Aluminum		Massive carbon fiber	
		Score	Weighted score	Score	Weighted score
Low weight	5	4	20	5	25
Adjustability	4	1	4	1	4
Manufacturability	3	4	12	4	12
Reliability	4	5	20	4	16
Low cost	4	2	8	3	12
Maintainability	3	4	12	3	9
Weighted sum			76		76

Table 3.3.1: Trade-off matrix for steering knuckle material selection



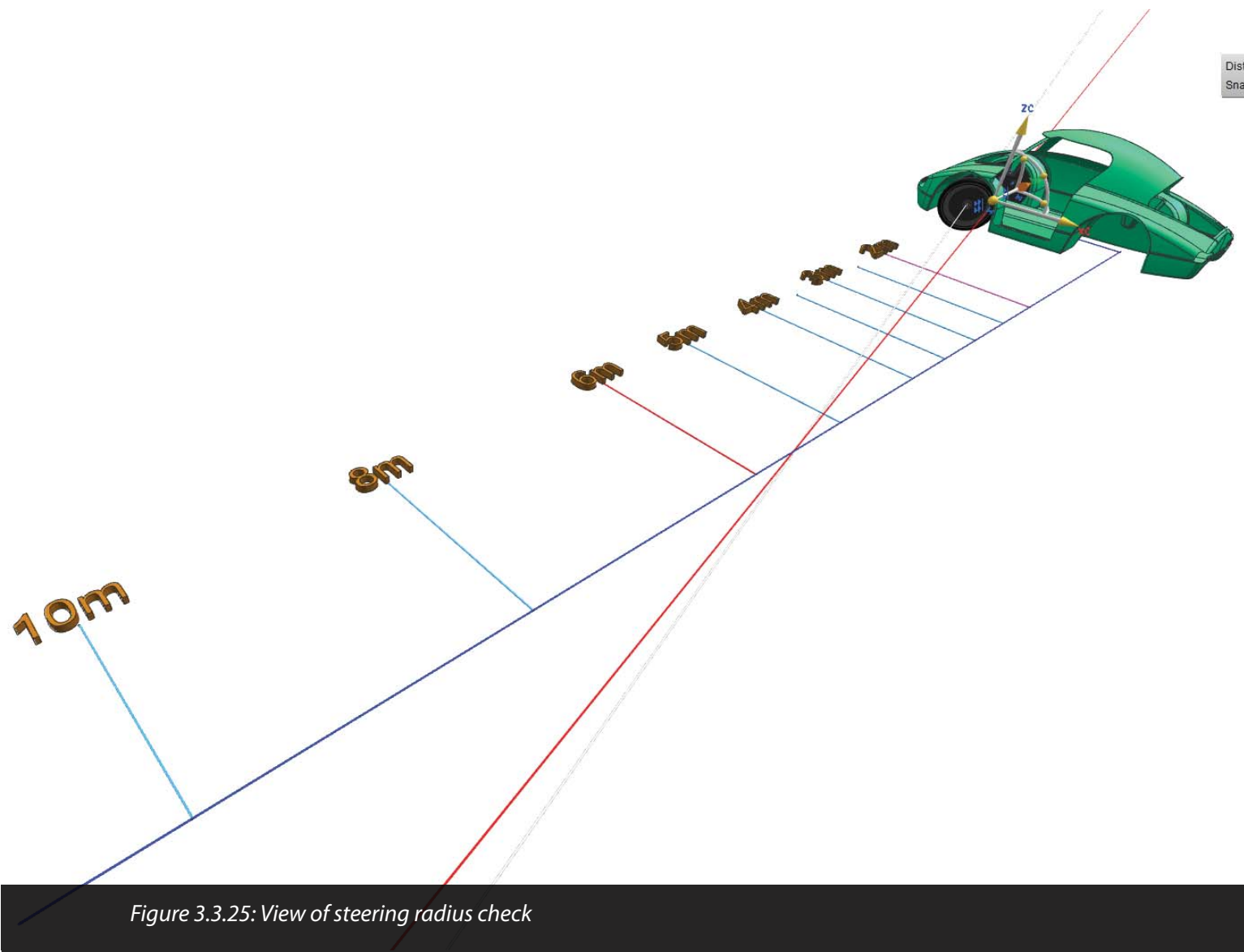


Figure 3.3.25: View of steering radius check

necessary: They discovered that in a Ferrari F40 only 40% of theoretical full ackerman was used.

With purely mechanical passive steering it is not possible to achieve full ackerman steering throughout all wanted turning radii. A test setup in NX showed that the steering appears fully ackerman compliant the first few degrees, and then the difference increases progressively until the inner wheel massively over-steers. This over steer of the inner wheel is thought to be good, since the lateral acceleration of the car (at higher speeds) transfers weight to the outer wheels, but as there will be some scrubbing it may waste energy. Still, given that we have been provided with a map of the race track with annotations of the corners, we know that the corners are no less than 15 m at

the sharpest, and 20 m in most other corners. The ackerman test model was thus used to optimize the position of the toes on the steering knuckles to achieve optimal ackerman on these curve radii.

As seen in figure 3.3.25, the grid marks the position of the different turning radii from 2 to 25 m, with the most important ones annotated. The red bar is an extension of the right axle, and the white of the left axle, so that the turning center can be observed as the drag link is moved in the CAD assembly, exploiting the constraints on all the suspension parts.



Figure 3.3.26: Verification of ackerman steering for 20 m turning radius

Figure 3.3.26 demonstrates the goal of satisfactory ackerman steering for cornering radii common on the race track. The testing showed that, as expected, the angles can be tuned by modifying the length of the drag link and tie rods, and the angle of the toes. Figure 3.3.27 and figure 3.3.28, shows the verification for smaller turning radii.

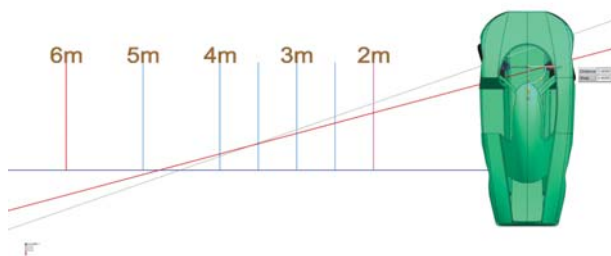


Figure 3.3.27: Verification of 6 m turning radius requirement

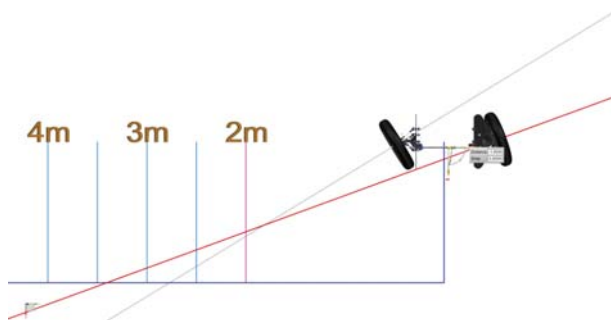


Figure 3.3.28: Finding the smallest possible turning radius, tilted view.

### Strength

The steering knuckles would be hard to analyze using shells and laminates. Instead, an isotropic model was analyzed for braking and cornering scenarios where the results can give an indication of the forces that must be absorbed by the massive laminate.

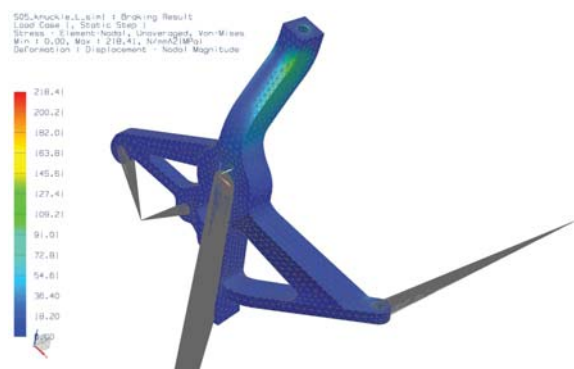


Figure 3.3.29: FEM analysis of knuckle during braking

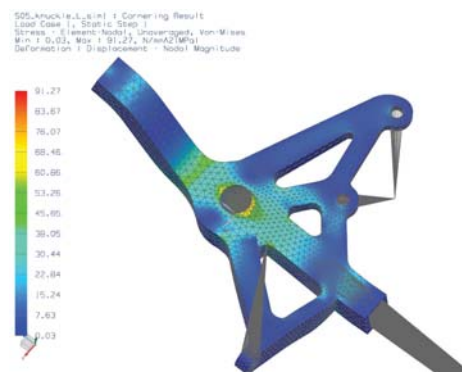


Figure 3.3.30: FEM analysis of knuckle during cornering

The stresses revealed by these simulations are far below the strength of the DB 420 carbon fiber.

HPC provided 15 mm thick samples of massive carbon fiber for testing. The tests revealed that the bolt connections would require reinforcement to avoid delamination. This reinforcement was made using unidirectional carbon fiber wrapping as illustrated in figure 3.3.31. Tests showed that a bolted connection could withstand as much as 9 kN, far exceeding the required 780 N.

### Production of Steering Knuckles

The knuckles were to be produced from the same material as the monocoque. Exact properties of this material were unfortunately not known; the theoretical properties are listed in Appendix B.

HPC suggested that they would cast and cure blocks of carbon fiber shaped by a mold, which would then be milled into the final shape. Figure 3.3.32 explains this production technique. The mold was machined from Ebaboard 60 in the Prototype lab and sent to HPC.

### Milling of Carbon Fiber

Based on Børge Holen's advise; diamond-coated end mills were used for machining the massive carbon fiber into the final shape of the steering knuckles. They were also used to mill out the monocoque's fire wall.

The milling was scheduled to be done by Bjarne Stolpnæssæter with the CNC mill in the Prototype lab. In addition to proper vacuuming and safety glasses, a set of double-layer coal-filter respirators were purchased from Clas Ohlson to protect the persons working with the machining. Protective gloves also had to be used.

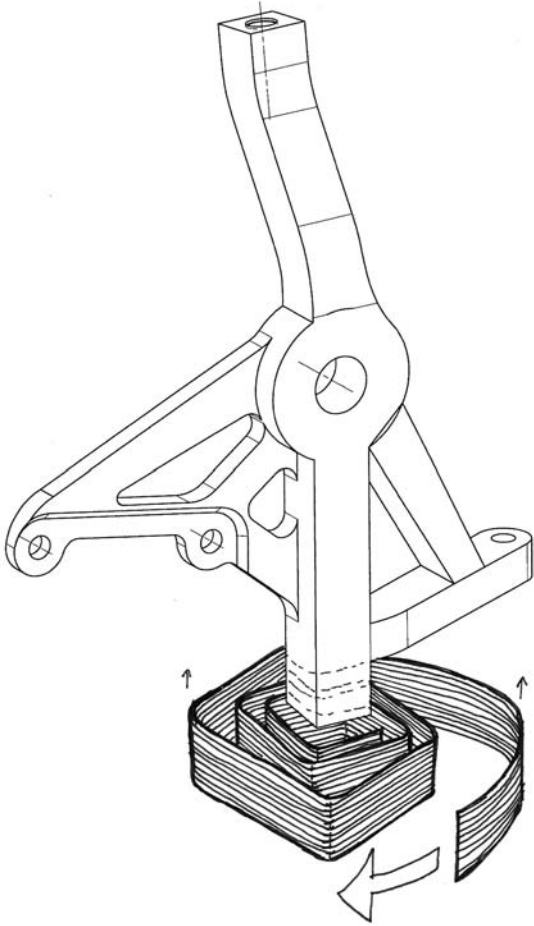


Figure 3.3.31: Unidirectional carbon fiber wrapping for reinforcement of bolted connections

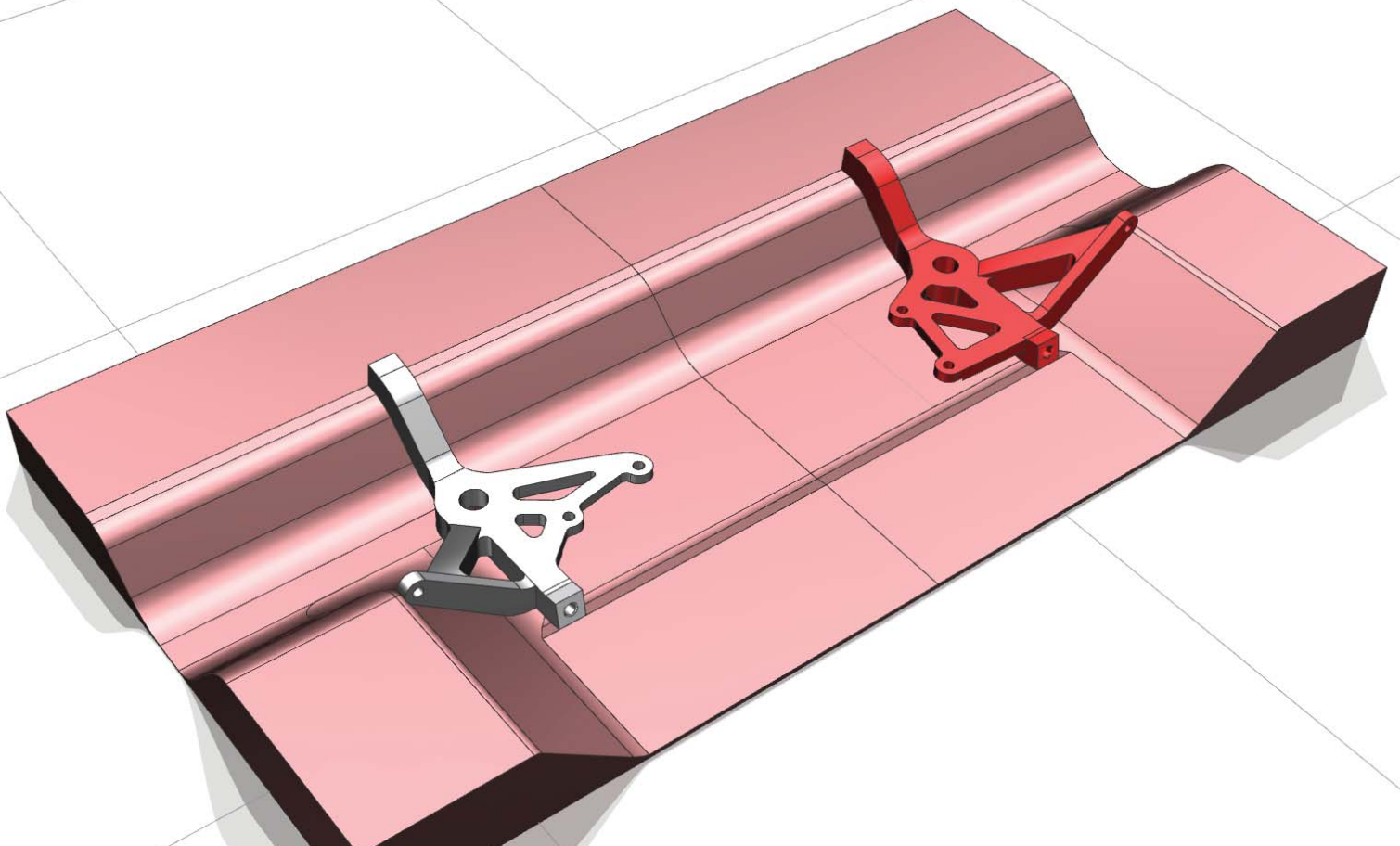


Figure 3.3.32: Mold for carbon fiber knuckles

### 3.3.1.4 Linkages

The easiest solution for linkages involved using standard parts. With the sponsorship agreement with SKF, and leftovers from earlier project teams, the required number of rod ends could be afforded. Similar types of rod ends are also commonly used on real cars.

Variations of male and female and mixed rod ends on the different links were considered. A link with external threads is the easiest to produce (figure 3.3.33) and therefore this approach was selected. The links' adjustability is obtained by using left hand threads in one end and right hand threads in the other. SKF offers rod ends with both right- and left-handed threads.

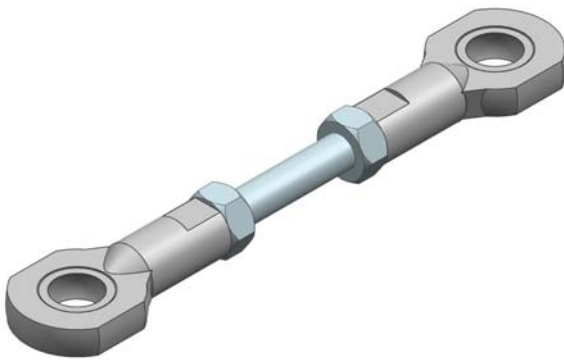


Figure 3.3.33: Link consisting of rod ends and nuts

#### Link Strength

The link rods are easily machined from round bars, and 24 meters of Ø10 mm Aluminum 6082 T6 were purchased from Smith Staal AS. It was decided to use Ø8 mm for the primary links and Ø6 mm for the tie rods. The strength of the rods is determined by the strain diameter from the thread size:

$$d_s = (d_2 + d_3) / 2$$

Where  $d_2$  and  $d_3$  are the pitch and minor diameter of the threads (Härkegård).

For external M8 and M6 these are (Fastener Thread Designations and Definitions Pitch, Minor, Major Diameters):

Thread size	M6 (mm)	M8 (mm)
$d_2$	5.212	7.212
$d_3$	4.596	6.596
$d_s$	4.904	6.904

Table 3.3.2: Table of minimum pitch and minor diameters of ISO M6 and M8

$$A_{\text{strain,M6}} = \pi r^2 = \frac{\pi d_s^2}{4} = \frac{\pi (4.904 \text{ mm})^2}{4} = 18.89 \text{ mm}^2$$

$$A_{\text{strain,M8}} = \pi r^2 = \frac{\pi d_s^2}{4} = \frac{\pi (6.904 \text{ mm})^2}{4} = 37.44 \text{ mm}^2$$

For wrought Aluminum 6082 T6, the fatigue strength is minimum 90 MPa (Granta Design Ltd. CES EduPack 2011). The fatigue limit of the links using M6 and M8 are thus:

$$F_{M6} = 90 \text{ MPa} \times 18.89 \text{ mm}^2 = 1700 \text{ N} = 1.7 \text{ kN}$$

$$F_{M8} = 90 \text{ MPa} \times 37.44 \text{ mm}^2 = 3370 \text{ N} \approx 3.4 \text{ kN}$$

This exceeds the max link force (1.4 kN for links, 0.53 kN for tie rods) by factors of 2.43 and 3.2, respectively. The safety factor criteria has thus been satisfied.

One other failure mode to be considered is buckling. The Euler buckling criterion for beams with plain joints that don't exert bending moment is given by:

$$P_B = \pi^2 EI / L^2$$

where L is the length, and E and I are Young's modulus and area moment of inertia. The modulus of elasticity for aluminium 6082 T6 is 70 GPa, The longest link is 116 mm and the tie rods are 108 mm long. Thus, the area moment of inertia for the tie rods and the longest link mm rods are:

$$I_{\text{polar}} = \pi d^4 / 32 \quad [3]$$

$$I_{\text{tie rod}} = \pi (6 \text{ mm})^4 / 32 = 127.24 \text{ mm}^4$$

$$I_{\text{link}} = \pi (8 \text{ mm})^4 / 32 = 402.12 \text{ mm}^4$$

$$P_{\text{tie rod}} = \pi^2 \times 70\,000 \text{ MPa} \times 127.24 \text{ mm}^4 / (108 \text{ mm})^2 \approx 814 \text{ kN}$$

$$P_{\text{link}} = \pi^2 \times 70\,000 \text{ MPa} \times 402.12 \text{ mm}^4 / (116 \text{ mm})^2 \approx 2400 \text{ kN}$$

These results were within the requirements, and the fatigue was the dimensioning criteria.

Maintenance-free rod ends with “steel/sinter bronze composite” were chosen for their accuracy and ability to run without lubrication. The other alternative was rod ends requiring maintenance. These have some play between the rod head and the ball which is undesirable. Analyses of the suspension setup show that as little as 0.5 mm elongation or contraction of a link affects the wheel angles.

The rod ends with 8 mm bore (SI 8 C), easily support up to 5.85 kN, and 3.6 kN for 6 mm bore rod ends (SI 6 C), which exceed the required loads calculated the previous sections.

Even though the double-wishbone concept was chosen for both the front and rear suspension, the end result was a variant of multi-link suspension. Only the lower swivel joints need a rigid part to connect the coilover, so the top swivel joint was made easier to manufacture by splitting it into two coaxial rod end joints located next to each other. The effect of two off-plane joints was found to be negligible and thus carried forward.



Figure 3.3.34: Single rod end on bottom, double rod ends on top

#### Wishbone Connectors

For the lower control arms, two solutions were considered. While a single-piece solid wishbone (figure 3.4.35) is simpler, it is not adjustable like the connector with rod links (figure 3.4.36). The connector solution is also easier to manufacture.

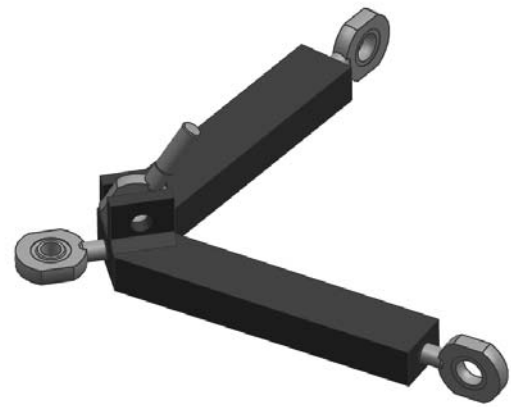


Figure 3.3.35: Solid lower wishbone

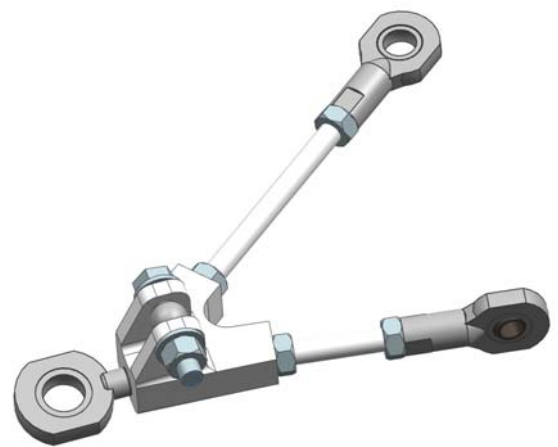


Figure 3.3.36: Connector and link rods

The lower control arms of the suspension can be made adjustable and lightweight by using a small “wishbone connector” that rigidly connects the lower swivel joint, the lower links and coilover.

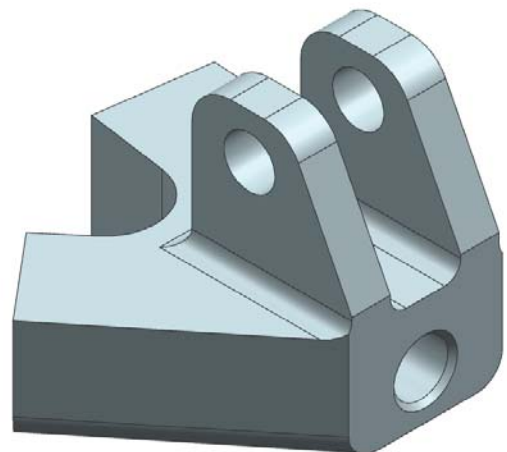


Figure 3.3.37: 3D view of the left wishbone connector

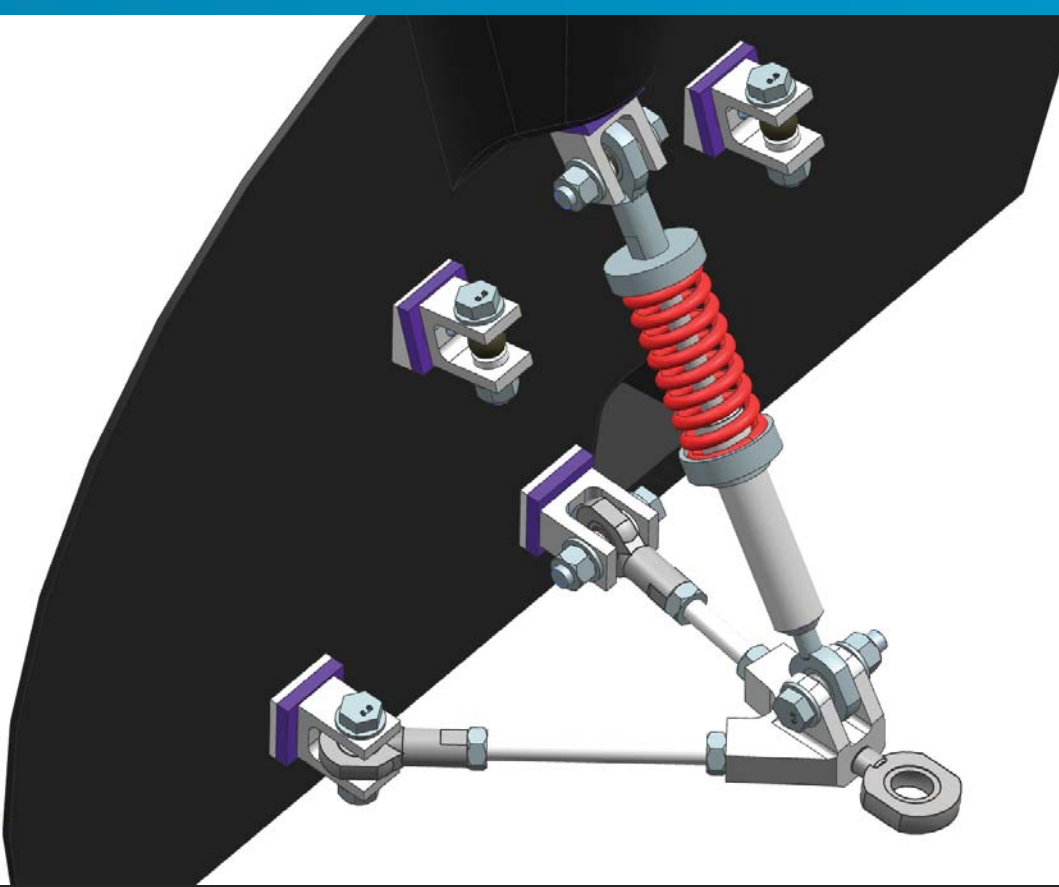


Figure 3.3.38: Left suspension with connector and coilover

The wishbones for the left and right sides are symmetrical.

Rod ends from SKF are primarily meant for radial loads (relative to the eye). The size of the lower rod ends was decided to be Ø10 mm.

The permissible load for rod ends is given by SKF as:

$$P_{\text{perm}} = C_0 b_2 b_6$$

where

- $C_0$  = static load rating [kN]
- $b_2$  = temperature factor (= 1.0 for temperatures below 120 °C)
- $b_6$  = load type factor (= 1 for constant, 0.5 for alternating)

Additionally, SKF states that "the load portion acting perpendicular to the direction of the shank axis should never exceed the value of  $0.1 C_0$ " (SKF) Thus the weight carrying capacity of SI 8 C and SI 10 C bearings are given by:

$$P_{\text{perm},8} = 12.9 \text{ kN} \times 1.0 \times 0.5 \times 0.1 = 645 \text{ N}$$

$$P_{\text{perm},10} = 18.3 \text{ kN} \times 1.0 \times 0.5 \times 0.1 = 915 \text{ N}$$

With an expected vertical load of 780 N it can be verified that 10 mm bore rod ends should be chosen over the other.

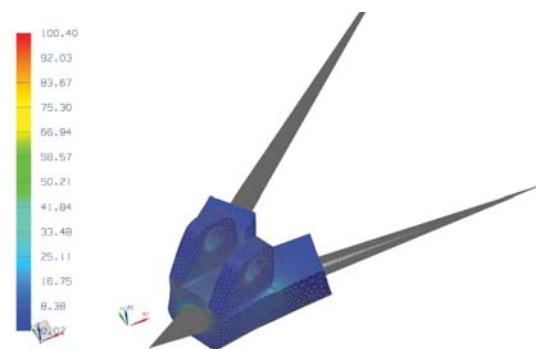


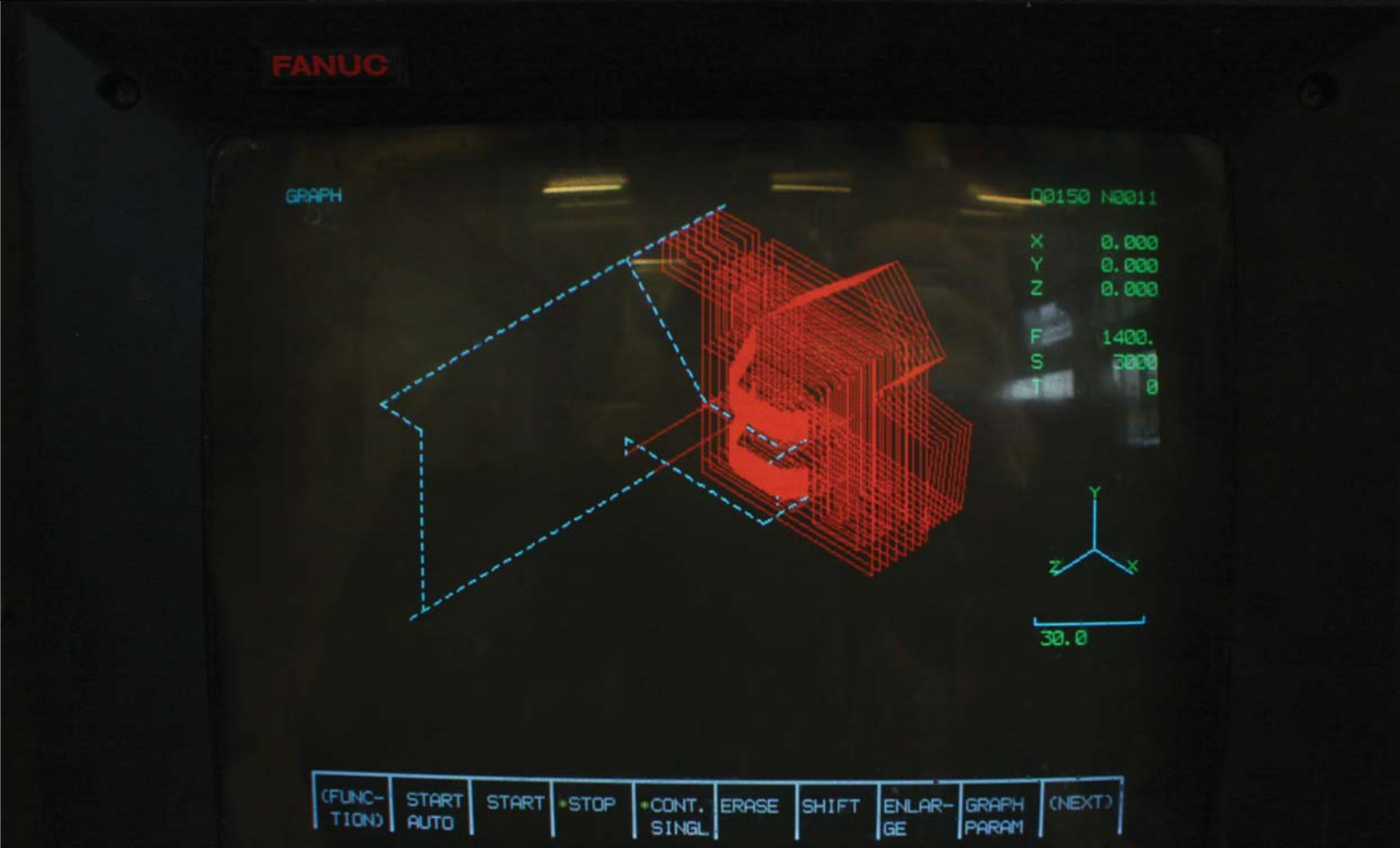
Figure 3.3.39: FEM analysis of wishbone connector during braking

Figure 3.3.39 shows the FEA of a connector during the hardest possible braking. The stress concentrations approach 100 MPa, which is at the limit of aluminum. Since this load scenario rarely will occur, the design is approved.

The wishbone connectors were milled from Alumecc 89 with the Makino CNC machine in IPM's workshop .



*Milling of connectors in the Makino milling machine*



*Verification of tool path using graph plot on the Fanuc computer*

### Tie Rods

The chosen solution was to use the same type of rods as elsewhere on the suspension, only smaller. The  $\text{\O}6$  mm rods with right-/left-hand threads in either end allowed for adjustability and unobstructed spring- and steering action of the front wheels.

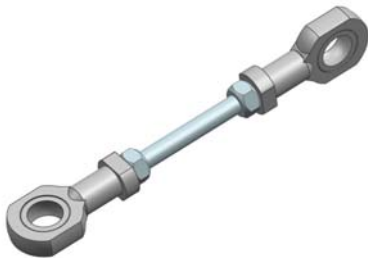


Figure 3.3.40: Tie rod assembly

### Roll- and Strut Bar

A roll bar was considered, but this would increase the weight (which was already a critical issue), and add a more complex joint mechanism for retaining the roll bar in the wheel wells made us avoid this feature. As roll bars affect the over/under steer factor, this is an option we retain as a backup solution in case the car should severely under- or over-steer.

Using a strut bar was also considered, but the stiffness of the monocoque was so high that this would be unnecessary weight.

### 3.3.1.5 Mounting Points

Each wheel requires five mounting points: Four for the links controlling the spring action motion, one for the coilover, and one extra for the tie rods. On the rear suspension the tie rods are connected directly to a sixth mounting point in the wheel well, while on the front they are connected to the drag link. The wheel wells were slanted to optimize for camber angle changes. HPC recommended to reshape the wells into something similar of the strut towers on real cars, to attach the coilovers.

An indent for the drag link was incorporated in the wheel well. To avoid bump steer while driving the drag-link tie rod-joint must lay in plane with the other mounting points.

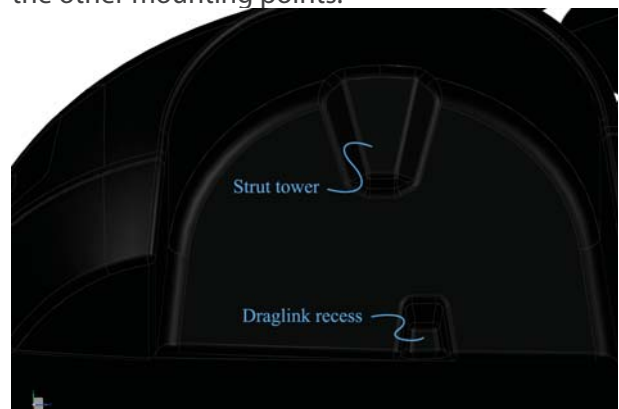


Figure 3.3.42: Front left wheel well on the final body shell

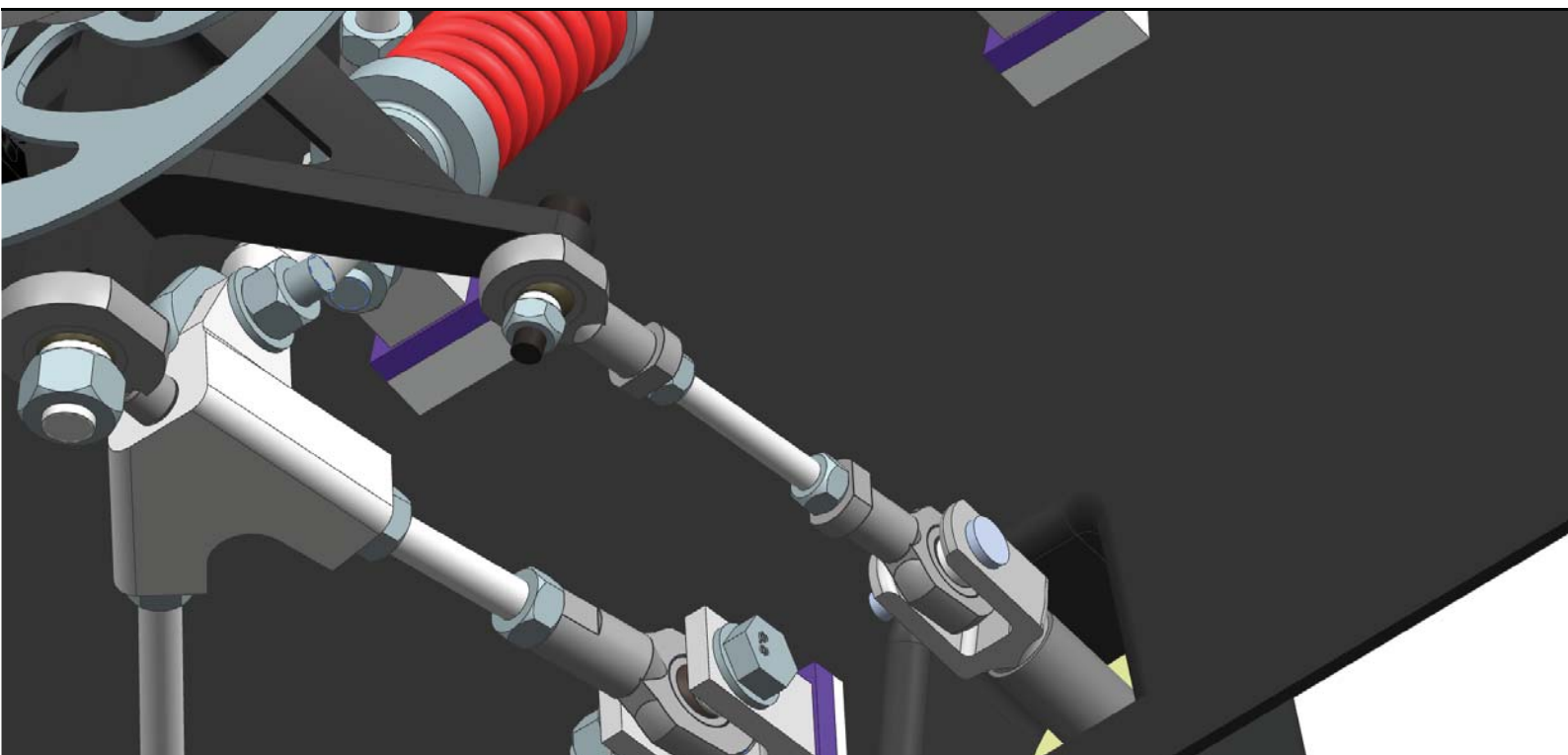


Figure 3.3.41: Left tie rod on suspension seen from beneath



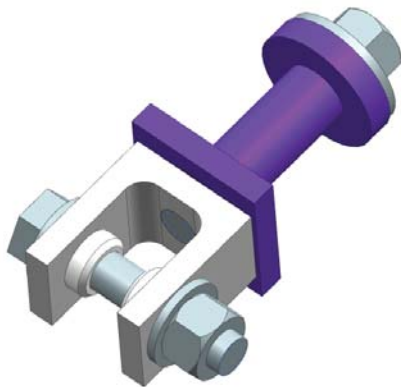
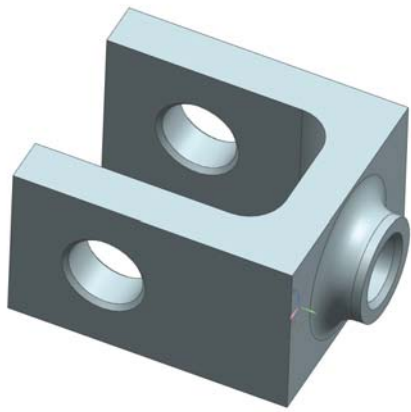


Figure 3.3.43: The final clevis design. Purple highlights the vibration damping bushings

Clevises were used to connect the suspension to the wheel well. These were designed to be lightweight, easily machined and allow maximum rod end tilt.

The bolt connecting the clevis to the body will be glued into the clevis.

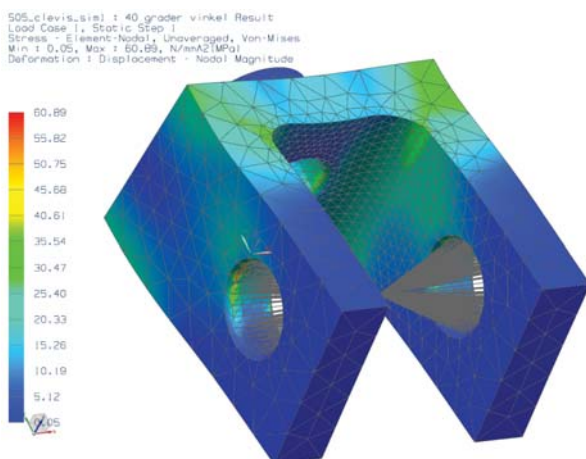


Figure 3.3.44: FEM analysis of clevis

Stress analysis shows that the maximum stress concentration is just 61 MPa, which gives a safety factor of 1.6 with regards to the fatigue limit.

Polymer wedges was produced to attach the clevises with the right angle.

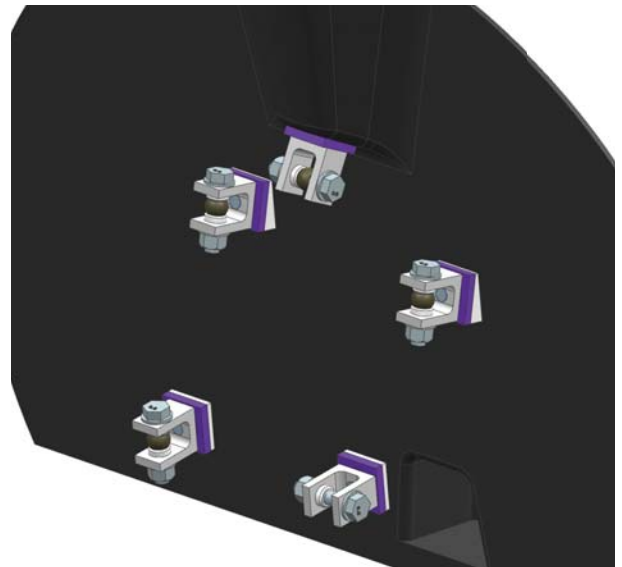


Figure 3.3.45: Clevises attached to wheel well using wedges and bushings

A casting resin, RenCast CW 2215 and hardener, with compressive strength 80-90 MPa was purchased from Lindberg & Lund. (Casting Resin RenCast). To reduce vibrations dampers were produced. For the vibration dampers, Flexane 60 was also purchased. The wedges and vibration dampers had to be cast in molds from Ebaboard 60.

### 3.3.1.6 Conclusion

The design of the front suspension has been very successful, but the final weight exceeds the weight goal slightly. Other strengths of the suspension, such as adjustability, spring/damper mechanism, high strength and vibration damping makes this an acceptable sacrifice.

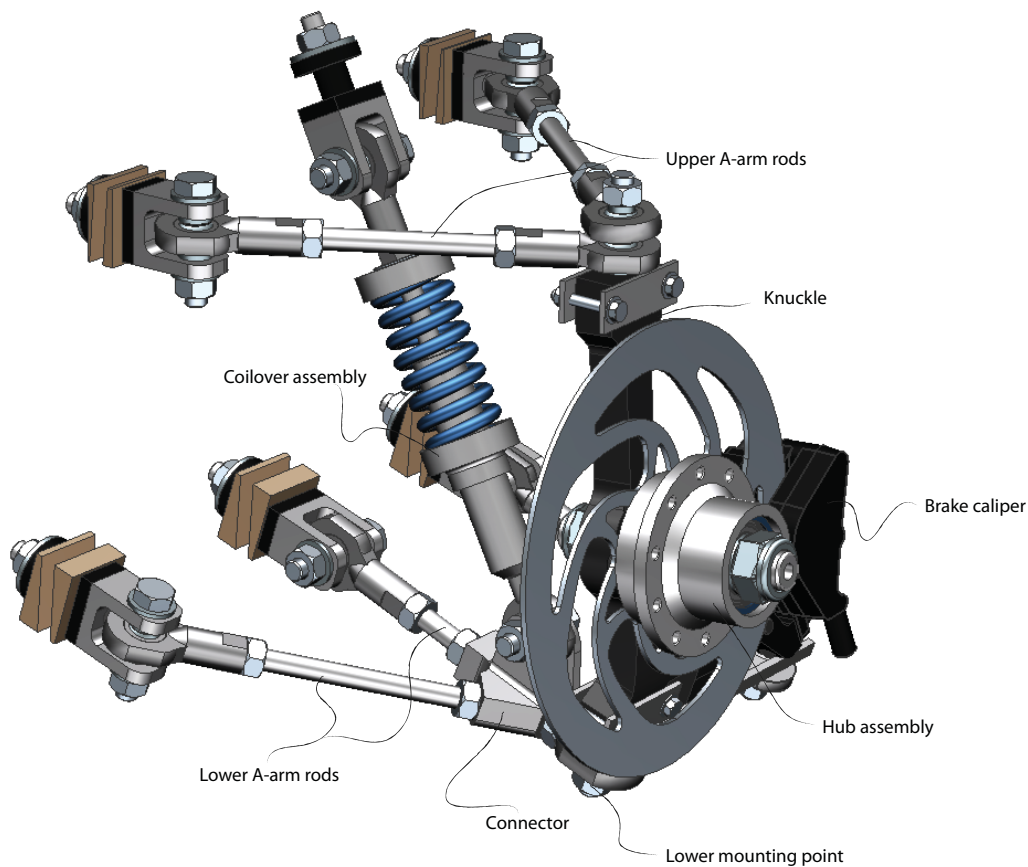


Figure 3.3.46: 3D CAD model of the rear suspension developed during the spring 2012

## 3.3.2 REAR SUSPENSION

### 3.3.2.1 Introduction

The most suitable solution for the rear suspension was the double wishbone. This would provide light weight, proper adjustability and a desirable change of camber angle during cornering. A suggestion for a fully damped rear suspension was presented in the project period (Endresen, et al., 2011), and was further developed during the Eco-marathon master project in the spring 2012.

### 3.3.2.2 Knuckle

The knuckle connects the axle, the hub and the wheel to the rest of the suspension. The forces acting on the wheel will be transmitted through the knuckle, to the rest of the suspension and to the monocoque. It needs to be designed to withstand the forces acting upon it, and provide sufficient ride qualities such as suitable camber change and optimal roll center height.

#### Geometric Optimization

The design developed during the project phase had a problem with the angular displacement of the rod ends being exceeded (Endresen, et al., 2011). This was due to changes done in the geometry of the monocoque at a late stage of the project phase.

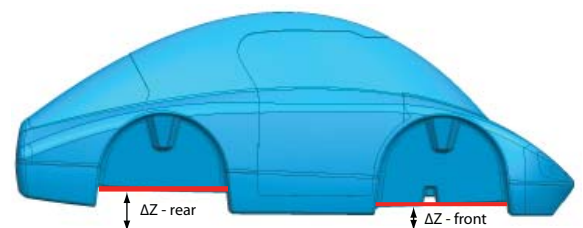


Figure 3.3.48: High vertical distance between the ground and the bottom of the rear wheel well wall

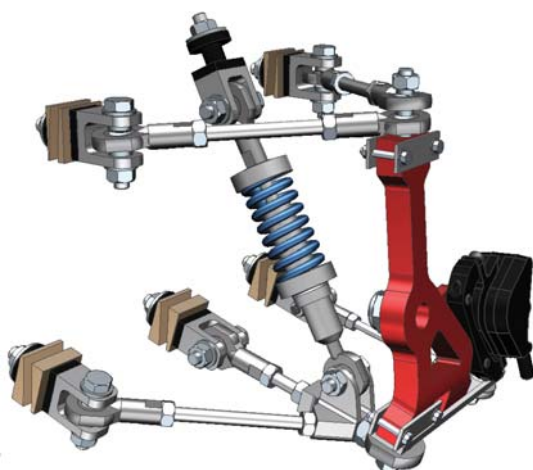


Figure 3.3.47: Knuckle

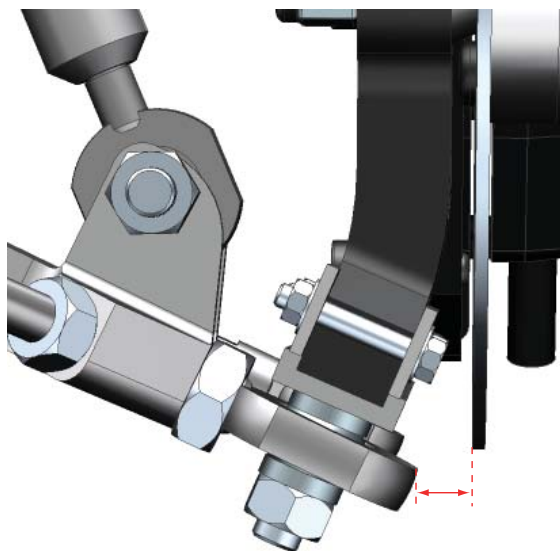
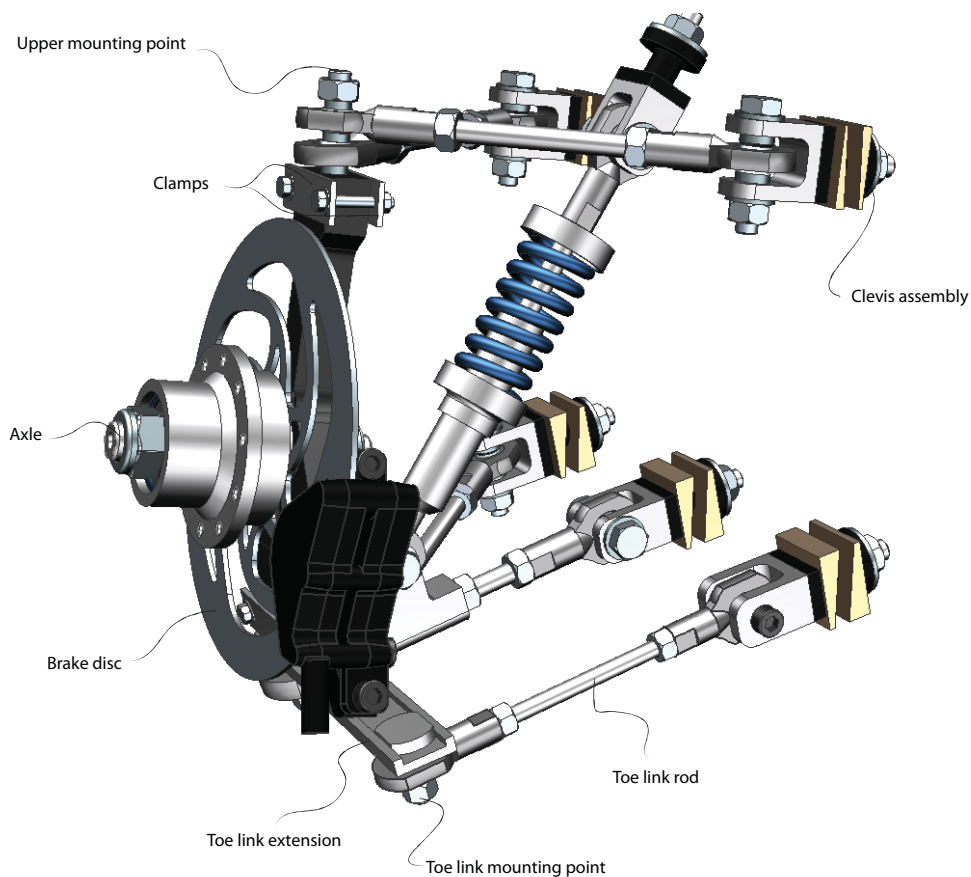


Figure 3.3.49: Distance between the lower rod ends and the brake disc increased on the new design

The geometric design of the knuckle was changed, tilting it 23° inwards at the bottom. This also increased the distance between the lower rod ends and the brake disc which was too short on the old design.

A 2D-model of the rear suspensions front-to-back view was made (figure 3.3.52). The geometry of the suspension as a whole was included when

optimizing the design of the knuckle.

The 2D-model was used to investigate the effect changes in the knuckle design would have on the cars roll center. The roll center affects the behavior of both the sprung- and the unsprung mass, and thus directly influences cornering. It is defined as a point in the transverse vertical plane through the wheel centers at which lateral forces may be applied to the sprung mass without producing suspension roll. The roll center is an instantaneous point which will move during cornering. The procedure for determining the roll center of a symmetric independent suspension is described below. See also figure 3.3.50.

- Find the virtual reaction point of the suspension links (A)
  - Draw a line from the tires contact patch with the ground (C) to the virtual reaction point
  - The roll center (R) is located where this line crosses the centerline of the body.
- (Gillespie, 1992)

The rear roll center is typically positioned 200-250 mm above the ground on a race car. On the DNVFF2 the rear roll center height is 293 mm when the suspension is in ride height, and 256 mm when it is fully compressed.

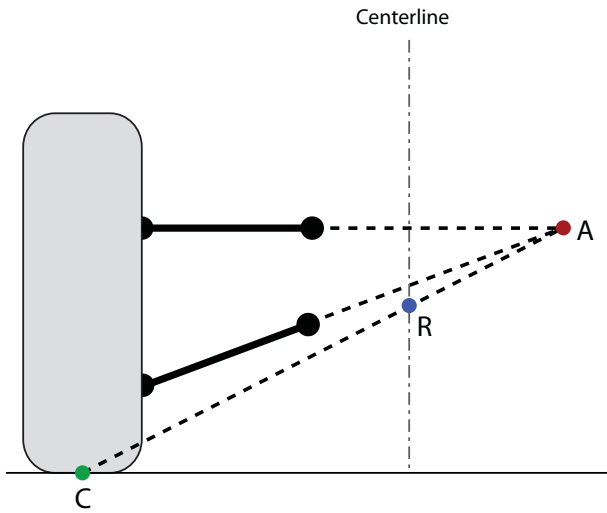


Figure 3.3.50: How to determine the roll center of an independent suspension

The geometry of the knuckle will also affect the bump- and roll steer, which are small changes in the suspension's toe angle when the wheel is moved relative to the body in bump and droop. Bump- and roll steer causes poor straight-line stability, unpleasant vehicle behavior and high energy losses on lighter cars (Dixon, 1996).

The change in camber angle during cornering is configured based on the wheels maximum vertical travel of  $\pm 20$  mm. Approximately it should be equal to the body roll to ensure good handling abilities.

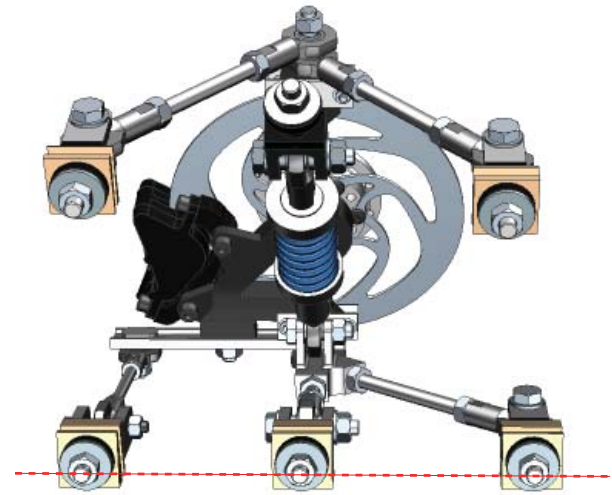


Figure 3.3.51: Mounting points for A-arm connector and toe link on the same horizontal line to prevent bump- and roll steer

$$\alpha_{\text{camber}} = \text{atan} \left( \frac{\text{vertical travel}}{\frac{\text{track width}}{2}} \right) \rightarrow \text{atan} \left( \frac{20}{400} \right) = 2.9^\circ$$

The change of camber angle for the rear suspension is  $2.1^\circ$  during compression. A larger camber angle change would lead to too much lateral movement between the tire and the ground. Then the wheel would be outside of the cars body during spring compression, violating the SEM rules.

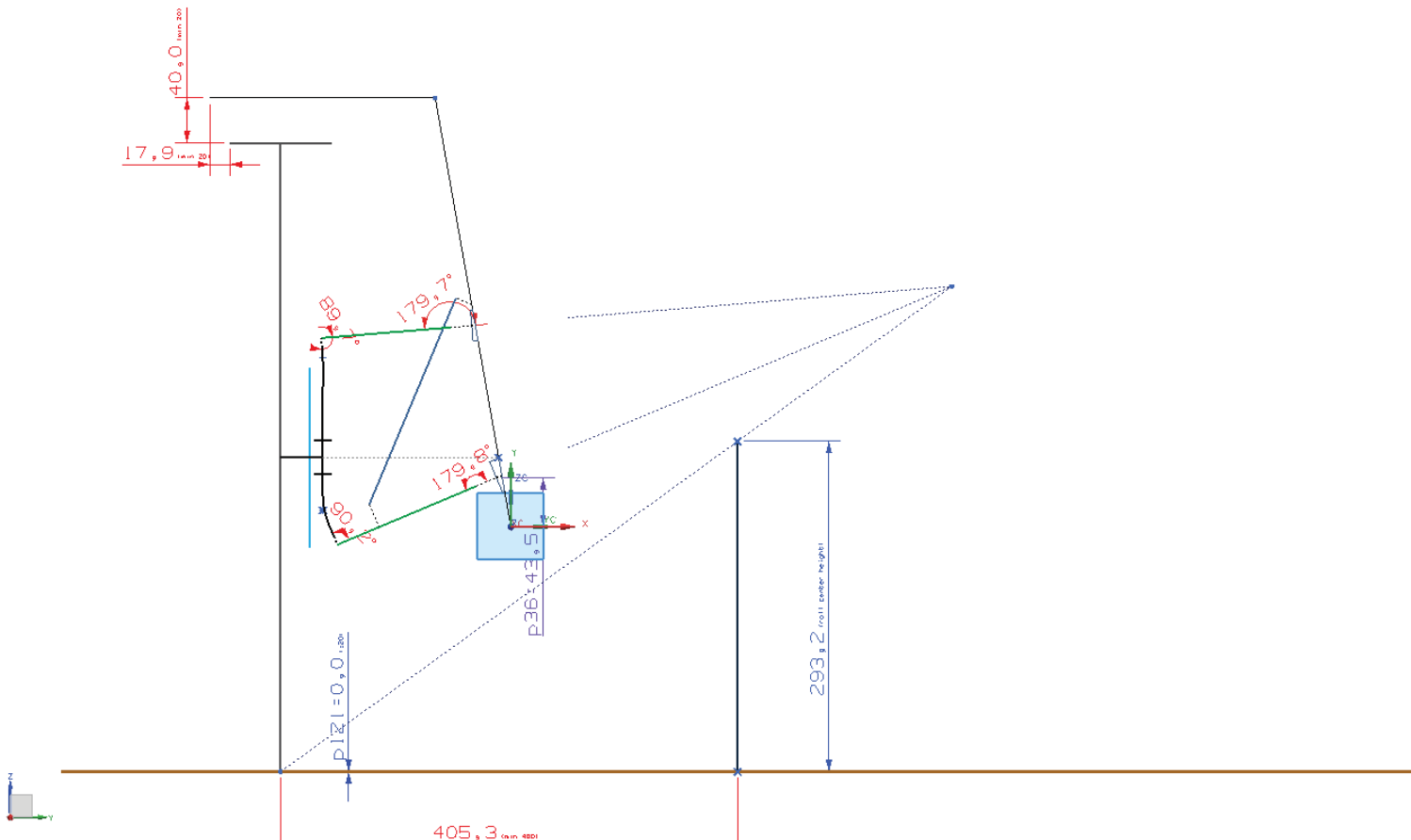


Figure 3.3.52: 2D-model of the suspensions front-to-back geometry in UGS NX 7.5. The most important dimensions are shown in the illustration.

### Weight Optimization and Strength Analysis

The knuckle was made in massive carbon fiber to save weight. A proper strength analysis of the knuckle was done in UGS NX 7.5 Advanced Simulation with estimated material properties for the carbon fiber Appendix B. The reader must be aware that the uncertainties regarding the material properties may have lead to small errors in the result.

1D RBE2 beam elements were used to make models of the axle and the wheel. This was done to apply the loads and constraints in the cor-

rect distance in relation to the knuckle. To apply constraints and forces as close to the reality as possible was emphasized, but the reader must be aware that some compromises have been made. The mounting points for the brake caliper have been neglected to simplify the simulations. This is assumed to have little influence on the final result. The forces applied are based on the calculations done in the project report from the autumn 2011 (Endresen, et al., 2011).

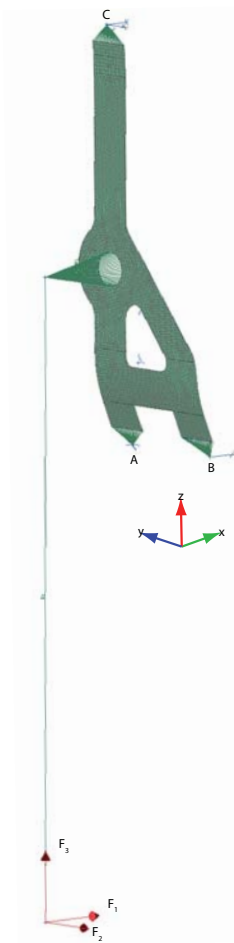


Figure 3.3.53: FE analysis setup for the knuckle

	A	B	C
DOF 1	1	1	1
DOF 2	1	0	1
DOF 3	1	0	0
DOF 4	0	0	0
DOF 5	0	0	0
DOF 6	0	0	0

Table 3.3.3: FE analysis set up for the knuckle. DOF 1-3 is displacement in x-, y-, and z-direction, respectively. DOF 4-6 is rotation about x-, y-, and z-axis, respectively

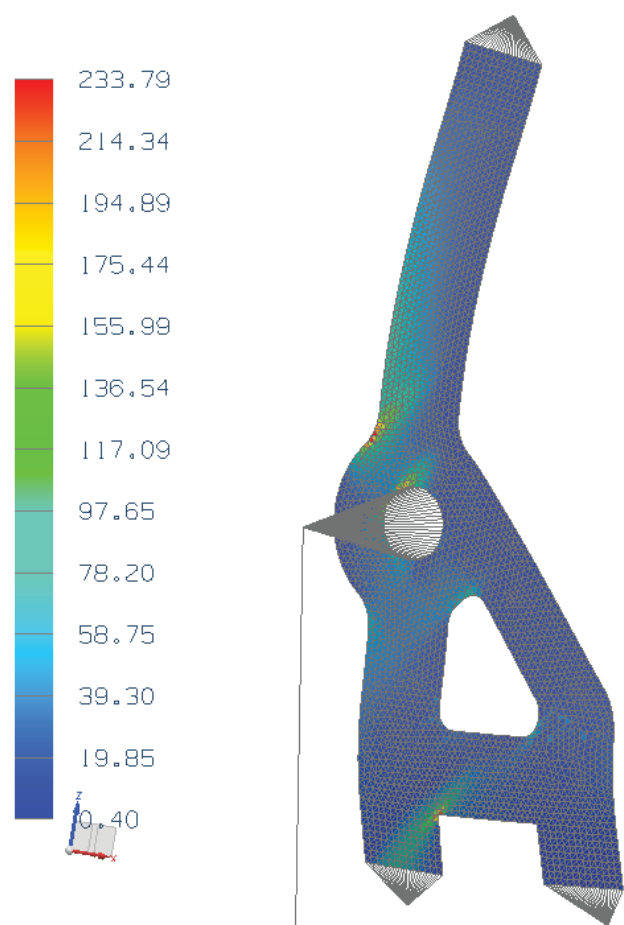


Figure 3.3.54: Test result from the final analysis of the knuckle

	Value	Unit
$F_1$	510	[N]
$F_2$	550	[N]
$F_3$	960	[N]
$\sigma_{max}$	233	[MPa]

Table 3.3.4: FE analysis set up and result for the knuckle

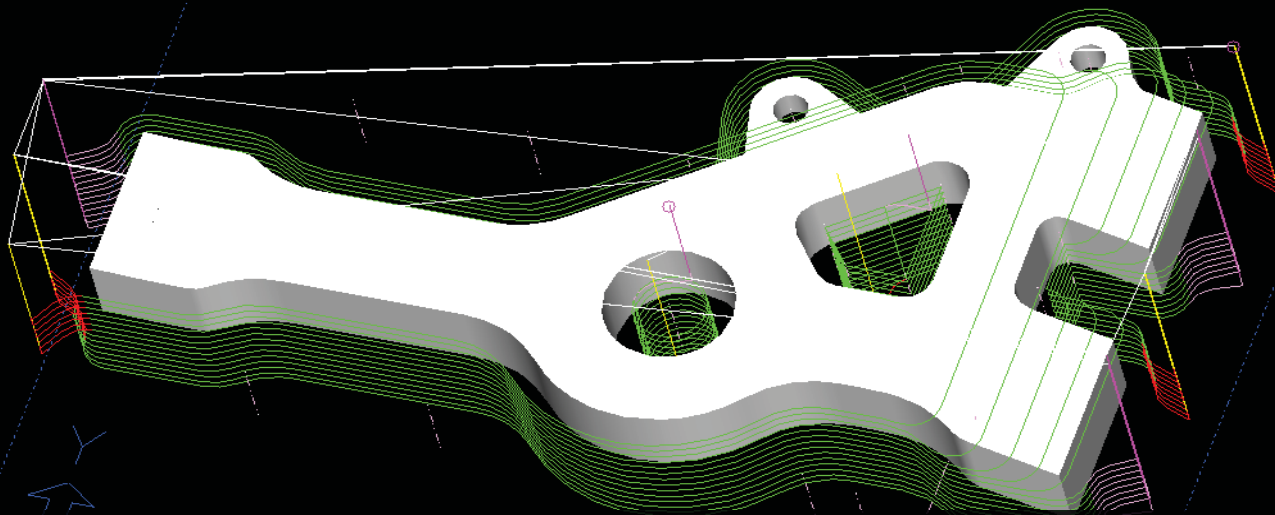


Figure 3.3.55: STEP - model of the knuckle imported into NX IDEAS 5.0. The coloured lines show the milling path

Several simulations were carried out and improvements were done until acceptable stress and strain values were achieved. The final design consisted of 32 layers of carbon fiber, giving an overall thickness of 16 mm.

#### Production

A mold for producing the knuckle was milled out from eboard at the IPM prototype lab. Bjarne Stolpnæssæter was very helpful during this process. The mold was sanded down and painted with polyurethane paint to ensure a smooth surface. The layup of the carbon fiber was done by HPC in Fredrikstad. Due to the asymmetric shape of the rear suspension system it was only necessary to produce one mold.

Three blocks of massive carbon fiber were ordered from HPC. The milling of the knuckles was done at the IPM prototype lab. A STEP - model of the knuckle was imported into NX IDEAS 5.0, which generated the code needed to mill the knuckle in the CNC milling machine. A diamond mill with high rotation speed was used to prevent delamination and splintering of the carbon fiber. One knuckle was kept as a spare.

The connection points between the knuckle and the rest of suspension system were constructed of threaded metal bars screwed into threaded holes in the carbon fiber. Araldite 2031 and aluminum clamps were added to ensure sufficient strength. For more detailed information, see Appendix F.

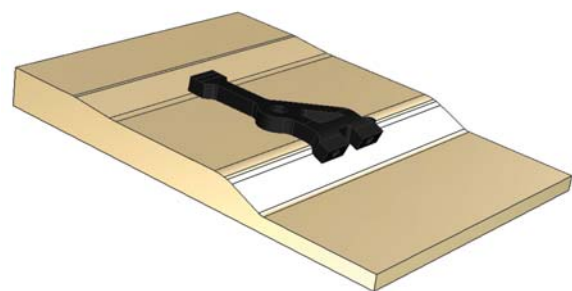


Figure 3.4.56: 3D model of the mold and the knuckle

The side of the carbon fiber that had been facing up from the mold during casting had an uneven surface; at most there was a variance of  $\pm 1.0$  mm in the thickness. The design of the knuckle required both sides to be perfectly even in order to achieve maximum stability between the axle and the knuckle. A 2.5 mm thick layer of Araldite 2031 glue was applied on this side and after hardening it was face milled down to create an even surface.

The engine knuckle was milled with a larger thorough hole for the axle due to the hexagonal shape of the engine axle. An additional insert was required to make it compatible with the engine axle. The insert was produced by Nomek in Alumecc 89 which is a type of aluminum that has excellent machinability, high strength, low weight and good stability during machining (Korea Nonferrous metals Co, 2005). It was glued to the knuckle with Araldite 2031.



*Milling of the knuckle from a massive carbon fiber plate*



*Glue applied on the knuckles uneven surfaces  
metal sheet formed to a tube to prevent glue from entering the axle hole*



*Face milling of the glue applied to the knuckles surface*

### 3.3.2.3 Lower A-arm connector

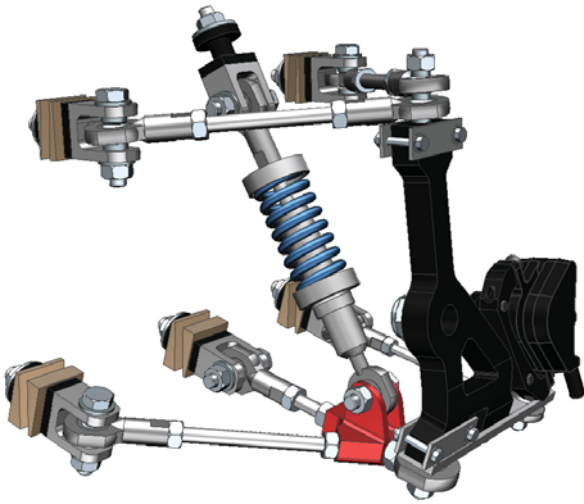


Figure 3.3.57: Lower A-arm connector

The lower A-arm connectors main purpose is to transfer the vertical forces that are acting on the wheel over to the coilover. It also keeps the knuckle steady in the lateral and longitudinal direction. This makes the connector one of the most important parts in the suspension systems, and also one of the most highly stressed. The connector acts as an extension to the rods that are going from the knuckle and into the wheel well. The angle between the rods is what determines the basic shape of the connector.

#### Weight Optimization and Strength Analysis of the Lower A-arm Connector

The connector was made in Alumecc 89. A lighter solution would be to make it in massive carbon fiber, but the complex geometric properties would not make this a suitable choice. The tension normal to the direction of the fibers could lead to delamination. A thorough FE-analysis was performed based on the calculation of the forces acting on the connector.

Forces acting on the connection joint between the knuckle and the lower A-arm generated by the vertical force  $F_4$  acting on the contact path between the tire and the ground:

$$\begin{aligned} \Sigma M_A &= 0 \\ F_1 \cdot L_1 - F_{5,1} \cdot L_3 &= 0 \\ F_{5,1} &= -\frac{F_1 \cdot L_1}{L_3} \end{aligned}$$

Forces acting on the connection joint between the knuckle and the lower A-arm generated by the lateral force  $F_1$  acting on the contact patch

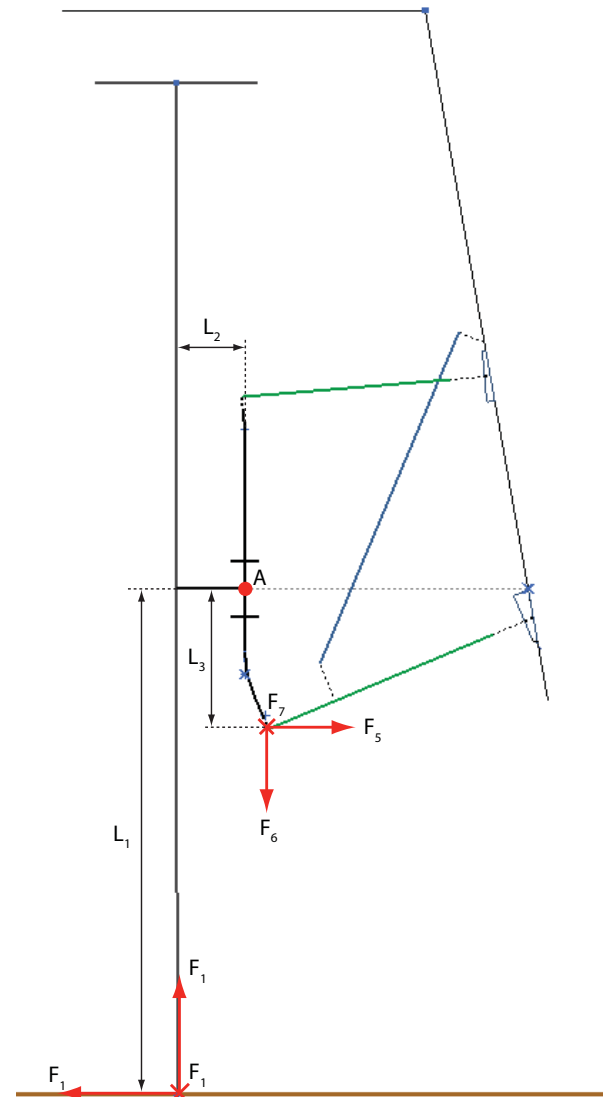


Figure 3.3.58: Forces acting on the suspension between the tire and the ground:

$$\begin{aligned} \Sigma M_A &= 0 \\ F_1 \cdot L_1 - F_{5,1} \cdot L_3 &= 0 \\ F_{5,1} &= -\frac{F_1 \cdot L_1}{L_3} \end{aligned}$$

It is assumed that the lateral force from cornering,  $F_1$ , is equally distributed over the upper and lower connection joints on the knuckle, hence:

$$F_{5,1} = \frac{F_1 \cdot L_1}{L_3} + \frac{F_1}{2}$$

This yield:

$$\begin{aligned} F_5 &= F_{5,4} + F_{5,1} = \frac{F_3 \cdot L_2}{L_3} + \frac{F_1 \cdot L_1}{L_3} + \frac{F_1}{2} \\ F_6 &= F_{6,4} = F_3 \\ F_7 &= F_2 \end{aligned}$$



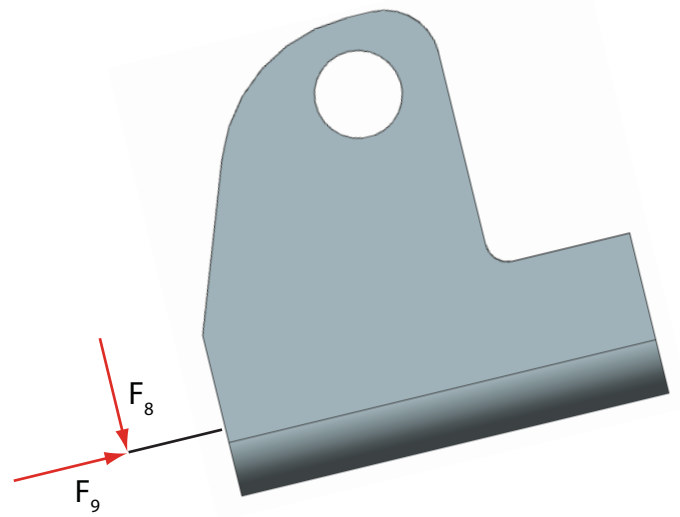
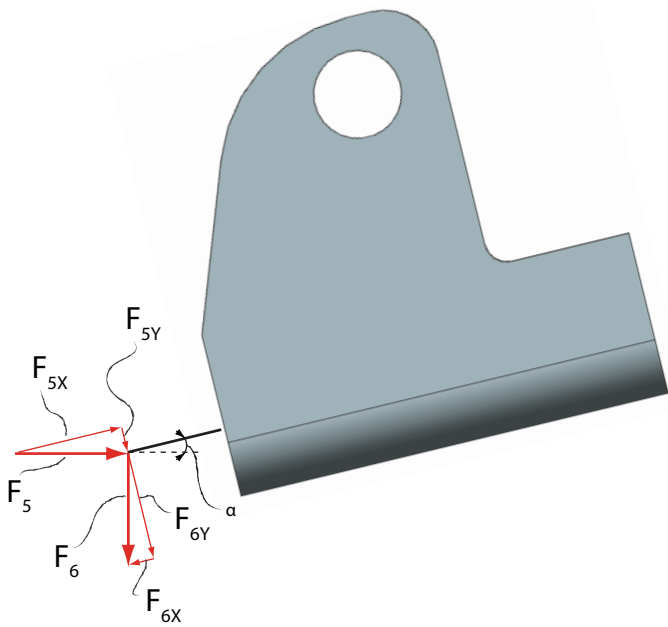


Figure 3.3.59: Forces acting on the connector

The forces are decomposed with respect to the connectors coordinate system (figure 3.4.59):

$$\begin{aligned} F_{5X} &= F_5 \cdot \cos(\alpha) \\ F_{5Y} &= F_5 \cdot \sin(\alpha) \\ F_{6X} &= F_6 \cdot \sin(\alpha) \\ F_{6Y} &= F_6 \cdot \cos(\alpha) \end{aligned}$$

If added up, this will yield:

$$\begin{aligned} F_8 &= F_{5Y} + F_{6Y} = F_5 \cdot \sin(\alpha) + F_6 \cdot \cos(\alpha) \\ F_9 &= F_{5X} - F_{6X} = F_5 \cdot \cos(\alpha) - F_6 \cdot \sin(\alpha) \end{aligned}$$

When substituted, this yield:

$$\begin{aligned} F_8 &= \left( \frac{F_3 \cdot L_2}{L_3} + \frac{F_1 \cdot L_1}{L_3} + \frac{F_1}{2} \right) \cdot \sin(\alpha) + F_3 \cdot \cos(\alpha) \\ F_9 &= -F_3 \cdot \sin(\alpha) + \left( \frac{F_3 \cdot L_2}{L_3} + \frac{F_1 \cdot L_1}{L_3} + \frac{F_1}{2} \right) \cdot \cos(\alpha) \end{aligned}$$

It is assumed that the longitudinal force, F2, generated by braking is equally distributed between the upper- and the lower A-arms, which gives:

$$F_{10} = \frac{F_2}{2}$$

Several FE-analyses were carried out, and the design was optimized with respect to stress and deflection.

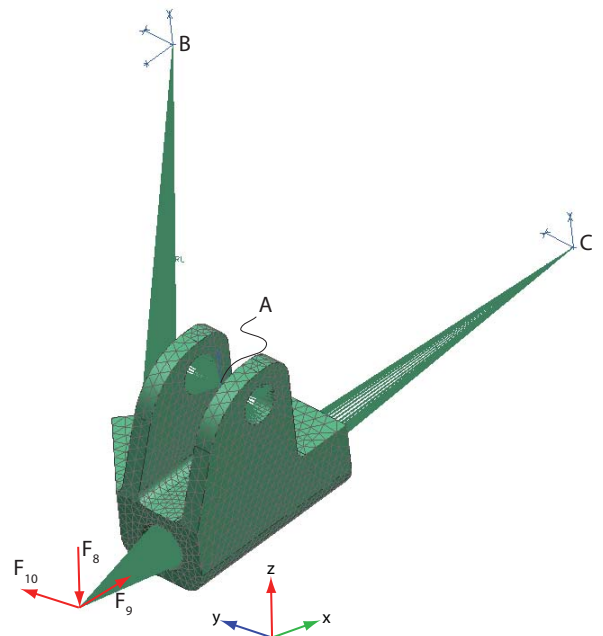


Figure 3.3.60: FE analysis setup for the connector

	A	B	C
DOF 1	0	1	1
DOF 2	0	1	1
DOF 3	1	1	1
DOF 4	0	0	0
DOF 5	0	0	0
DOF 6	0	0	0

Table 3.3.5: FE analysis set up for the knuckle

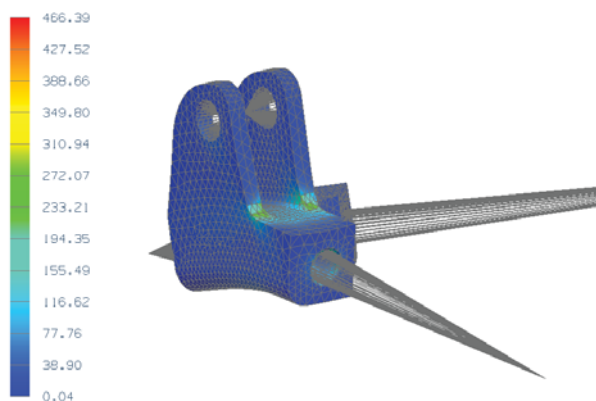


Figure 3.3.61: Test result from the final analysis of the knuckle

	Value	Unit
$F_8$	1900	[N]
$F_9$	2700	[N]
$F_{10}$	275	[N]
$\sigma_{max}$	467	[MPa]

Table 3.3.6: FE analysis set up and result for the connector

### 3.3.2.4 Coilover

Coilover is short for “coil over shock”, which means that the spring and the shock is combined in a single, compact package. The main purpose of the coilover is to absorb the vertical forces acting on the contact patch between the tire and the ground, ensuring a smooth ride and good handling abilities. The design of the coilover started very late in the autumn 2011, and a lot of changes were done during the spring 2012. See figure 3.3.62.

#### Theory

A coilover shock is a mono-tube shock with high quality that includes provisions to mount coil springs on the shock, which offers a number of advantages:

- Completely rebuildable.
- Good tune ability. The coilover allows the designer to choose between a vast array of spring lengths and spring rates. This makes it possible to select the perfect spring rate for a desired suspension frequency.
- The built in spring seat gives the designer the opportunity to adjust the suspension height, ride height and preload. It gives ability to vary between springs of different lengths, hence obtaining different amount of spring travel.

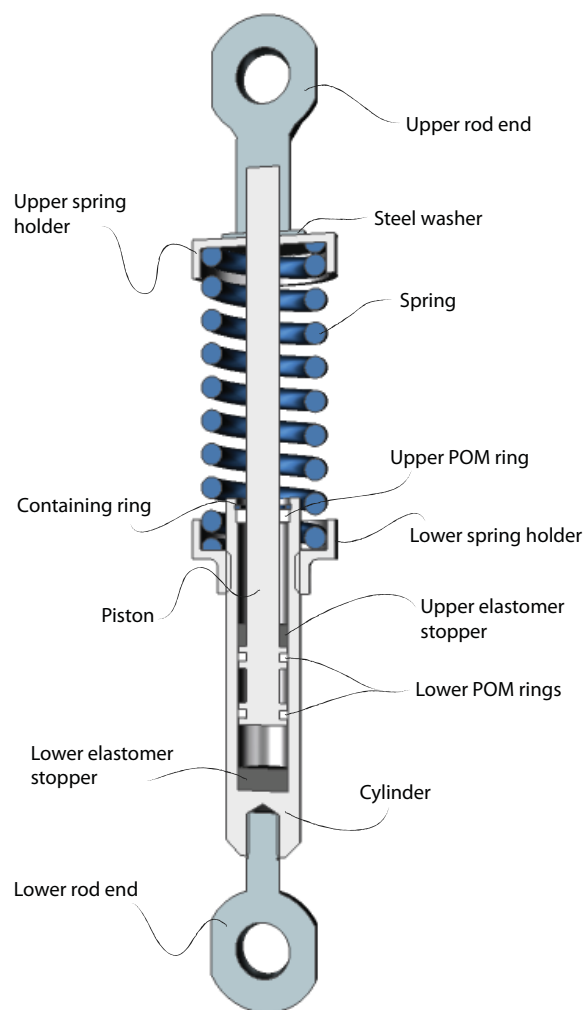


Figure 3.3.62: Coilover cross section overview

There are mainly three different types of coilovers, these are the “remote reservoir”, “piggyback” and “emulsion”. The most common type is the remote reservoir coilover shock, which is a mono-tube shock charged with nitrogen. The use of a remote reservoir to house the nitrogen and the floating piston allows the use of a shorter tube than would otherwise be necessary. The pressure tube is connected to the reservoir with a short flexible hydraulic hose.

A piggyback coilover shock is very similar to the remote reservoir, but instead of the reservoir being connected to the shock with a flexible hose, it is mounted directly on the shock with a bracket that incorporates the necessary hydraulic passage between the cylinder and the reservoir.

In an emulsion coilover shock there is no reservoir and no floating piston. The nitrogen charge is contained in the tube along with the oil in an emulsion. It is best suited to lightweight and/or low-speed use, and is also the most compact

type of coilover.

The most important part in the coilover is the spring, which is designed to carry a load by compressing. An easy way of describing the physical properties of a spring is by its spring rate, a description of how stiff it is, expressed in N/mm. The spring rate is defined by four properties:

- The spring material
- The diameter of the wire from which the spring is wound
- The coil mean diameter ( the diameter into which the coils are wound)
- The number of active coils

The effect of the different parameters is listed in table 3.3.7.

Parameter	Change	Effect on rate
Wire diameter	Increase	Increases
	Decrease	Decreases
Coil mean diameter	Increase	Decreases
	Decrease	Increases
Number of active coils	Increase	Decreases
	Decrease	Increases

Table 3.3.7: Changes in spring rate

(Ansell, 2008)

### Calculation of Spring Force and Spring Travel

The spring travel and spring force are both dependent on wheel travel, wheel force and the geometry of the suspension system.

It is further assumed that there will be no change in camber angle during the wheels vertical travel. The spring travel as a function of the wheel travel can then be determined. To simplify the calculations the distance  $L_3$  has been set equal to zero.

$$\begin{aligned}\Delta z_1 &= \Delta z \cdot \cos(\alpha) \\ \Delta z_2 &= \Delta z_1 \cdot \frac{L_2}{L_1 + L_2} \\ \Delta z_3 &= \Delta z_2 \cdot \cos(\beta)\end{aligned}$$

If substituted, this yields:

$$\Delta z_3 = \Delta z \cdot \cos(\alpha) \cdot \frac{L_2}{L_1 + L_2} \cdot \cos(\beta)$$

The spring force as a function of the force acting on the wheel is calculated based on the calculations from section 3.3.2.3. The value of the force  $F_z$  equals the value of the force  $F_8$  determined in the previous mentioned chapter.

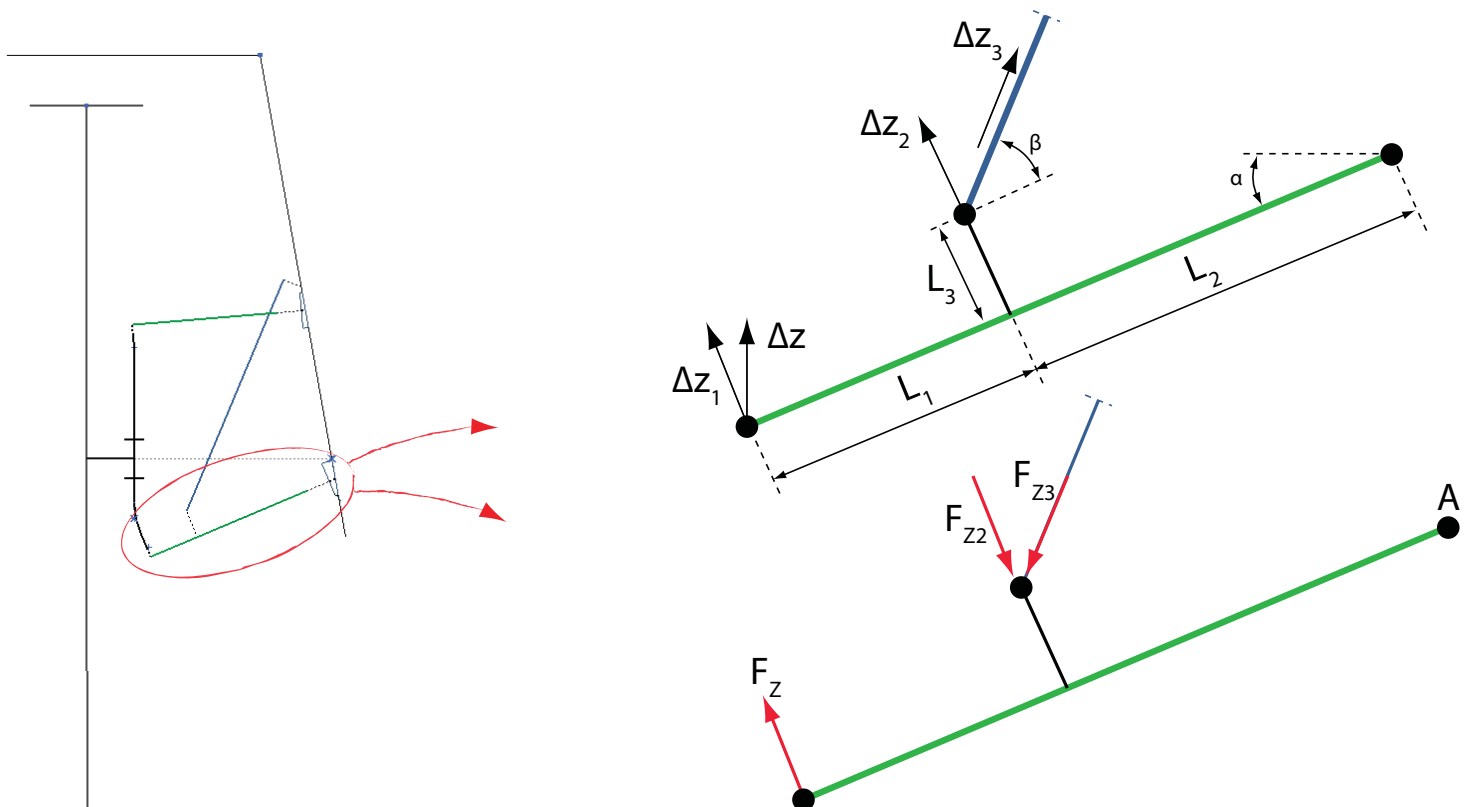


Figure 3.3.63: Determining spring travel and spring force

The distance  $L_3$  has been set equal to zero to simplify the calculations.

$$\begin{aligned} \Sigma M_A &= 0 \\ F_z \cdot (L_1 + L_2) - F_{z2} \cdot L_2 &= 0 \\ F_{z2} &= \frac{F_z \cdot (L_1 + L_2)}{L_2} \\ F_{z3} &= F_{z2} \cdot \cos(\beta) \end{aligned}$$

I substituted, this yields:

$$F_{z3} = \frac{F_z \cdot (L_1 + L_2)}{L_2} \cdot \cos(\beta)$$

A wheel travel of  $\pm 20$  mm implied a spring travel of  $\pm 9$  mm and the weight of the driver and car would result in a spring force of 390 N. This led to a required spring rate of 40 N/mm for the spring to be adequately compressed. The spring also had to be able to withstand the vertical force generated by the wheel driving over a bump (Endresen, et al., 2011) without hitting the top of the wheel well. This implied a necessary spring rate of 120 N/mm. A compromise was made to fulfill these properties. Elastomer dampers were added in the bottom of the coilover to help the spring absorb the shock if the compression force became too high, and a spring rate slightly higher than 40 N/mm was chosen.

Property	Value	Unit
Wire diameter	5	[mm]
Inner diameter	20	[mm]
Unloaded length	70	[mm]
Number of coils	9.8	[-]
Permitted loaded length for dynamic load	52.8	[mm]
Rate	47	[N/mm]

Table 3.3.8: Properties of the SF-TF 1901 compression spring ordered from Lesjöfors (Lesjöfors, 2012)

The static deflection rate of the suspension determines its natural frequency. This is the rate at which the suspension compresses in response to weight. The natural frequency can be determined by a simple formula:

$$N_F = \frac{188}{\sqrt{S_D}}$$

Where:

- $N_F$  = Natural frequency in cycles per minute (divided by 60=Hz)
- $S_D$  = Static deflection in inches

(Gillespie, 1992)

The chosen spring gave a frequency of 3.53 Hz, which is quite high and results in a harsh ride, but minimizes body roll during cornering. In comparison a high performance sport car has a natural frequency of 2 - 2.5 Hz.

### Strength Analysis

The most stressed components in the coilover are the upper and lower spring holder. They are transferring all the vertical force from the wheel to the spring. The design of the coilover requires the piston to be able to withstand the vertical forces from the wheel if the coilover is fully compressed.

A 2.0 mm thick steel washer was added to the upper spring holders design as reinforcement.

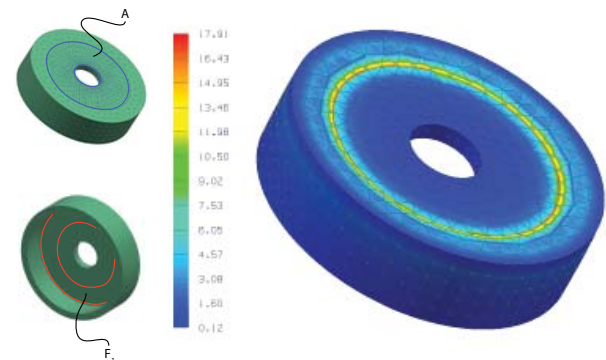


Figure 3.3.64: FE analysis of the upper spring holder

	A	Value	Unit
DOF 1	1	$F_1$	1200 [N]
DOF 2	1	$\delta_{max}$	9.3E-04 [mm]
DOF 3	1	$\sigma_{max}$	17 [MPa]
DOF 4	1		
DOF 5	1		
DOF 6	1		

Table 3.3.9: FE analysis of the upper spring holder

The force from the spring on the lower spring holder will be absorbed by the M18 threads connecting it to the cylinder. This was simulated as a plain inner cylinder wall to simplify the analysis.

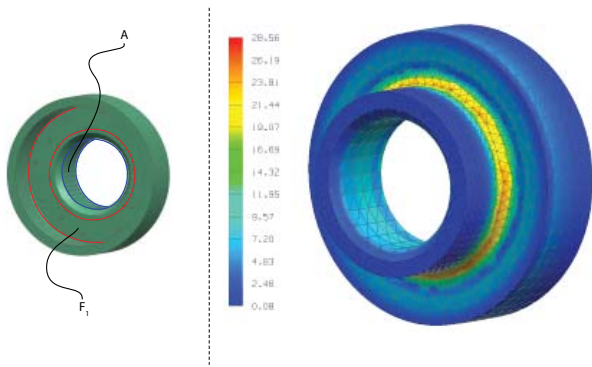


Figure 3.3.65: FE analysis of the lower spring holder

	A		Value	Unit
DOF 1	1	$F_1$	1200	[N]
DOF 2	1	$\delta_{\max}$	3.2E-03	[mm]
DOF 3	1	$\sigma_{\max}$	29	[MPa]
DOF 4	1			
DOF 5	1			
DOF 6	1			

Table 2.3.10: FE analysis of the lower spring holder.

The analysis of the piston was more complicated due to the pistons sliding properties inside the cylinder. There are three sliding connection areas between the piston and the cylinder when the coilover is operating. Only two of these were applied to simulate the worst case scenario.

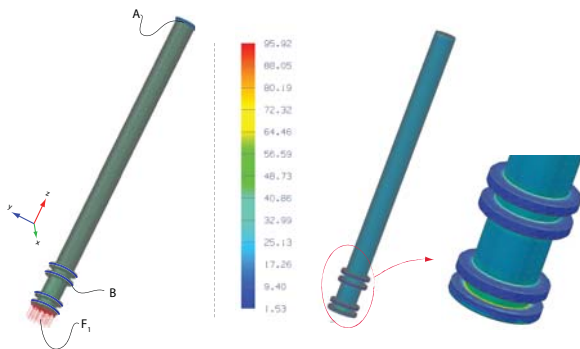


Figure 3.3.66: FE analysis of the piston

	A	B		Value	Unit
DOF 1	1	1	$F_1$	1200	[N]
DOF 2	1	1	$\delta_{\max}$	4.5E-02	[mm]
DOF 3	1	0	$\sigma_{\max}$	96	[MPa]
DOF 4	1	0			
DOF 5	1	0			
DOF 6	1	0			

Table 3.3.11: FE analysis of the piston

### Production

Most of the parts in the coilover were produced in Alumecc 89. The cylinders and the pistons were ordered from Nomek Maskinverksted due to time issues. The Upper and lower spring stoppers were produced by team members in the workshop at IPM. Springs were ordered from Lesjøfors, a Nordic spring company, and the Spirolox containing rings were ordered from Smalley, located in Chicago.

### 3.3.2.5 Toe Link Extension

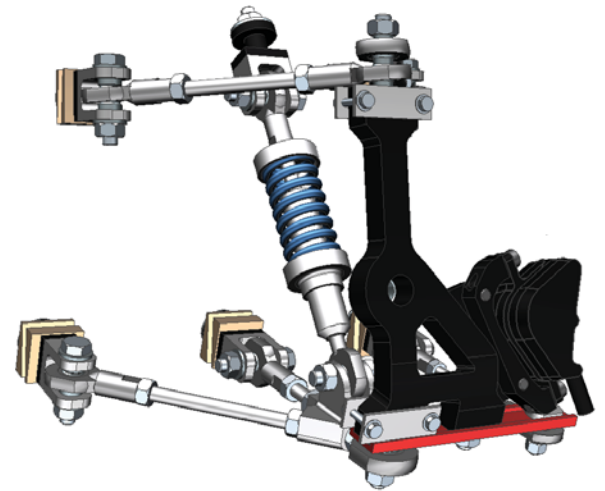


Figure 3.3.67: Toe link extension

The toe link extension is used to extend the distance between the lower A-arm connection point and the toe link connection point at the knuckle, hence obtaining better stability. The geometry of the knuckle is partly determined by the mounting points for the brake caliper. These are forcing the connection point for the toe link to be closer to the connection point for the lower A-arm than what is desirable. Any axial displacement of the toe link rod has a large impact on the toe angle. This is mainly a problem due to the 5 mm thick polyurethane (PUR) vibration dampers on the mounting points. It is assumed that the vibration dampers might compress or decompress with  $\pm 2.0$  mm. This gives a change in the toe angle of  $\pm 2.3^\circ$  without the toe link extension, compared to a change of  $\pm 1.1^\circ$  with the toe link extension installed. This is a total reduction of 52%.



Coilover assembled

### 3.3.2.6 Rods and Rod Ends

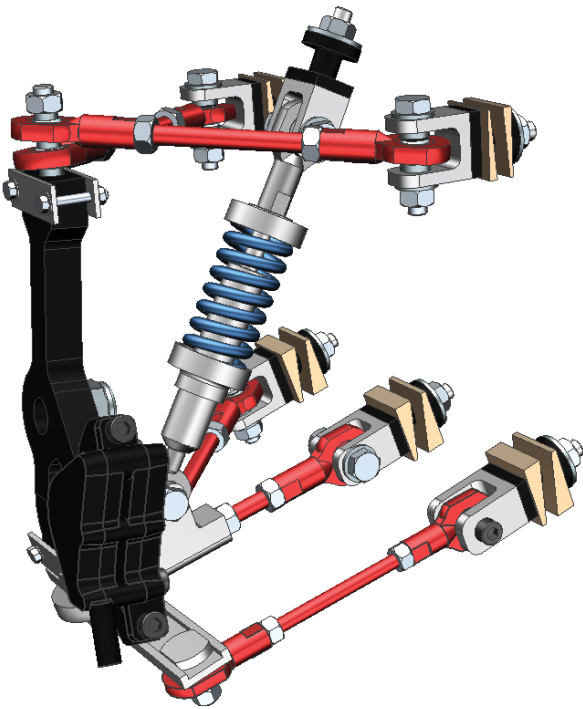


Figure 2.4.68: Rods and rod ends

Aluminum rods and rod ends were used to connect the suspension system to the wheel well wall. The rods were manufactured from aluminum bars (Aluminum 6082) at the IPM workshop. They were designed with left handed threads in one end and right handed threads in the other end. The total length could be adjusted by twisting the rods. The rod ends were ordered from SKF and the type was SIL 8 C and SI 8 C, left handed and right handed, respec-

tively.

For more detailed information about the rods and rod ends, see section 3.3.5.

### 3.3.2.7 Assembly

Holes were drilled for the mounting points in the rear wheel well wall. A printed template was used to find the exact placement of the holes. A special designed hole-tool was used to make sure the holes were drilled with the correct angle relative to the wheel well wall.

The rear suspension system is anti-symmetric. It means that the holes drilled for the rear suspension system in the cars body should also be so, but this was not the case. Due to uncertainties concerning whether the new motor would be finished in time or not, the old motor was used as a backup. It is a lot thicker than the new one, hence increasing the lateral distance between the knuckle and the wheel. The wheel would stick out from the wheel well if the old engine was used, violating the SEM rules. The design of the lower A-arm made it impossible to adjust the lateral distance between the lower A-arm connector and the wheel wells wall without decreasing the longitudinal distance between the connection points in the wheel well. The longitudinal distance between the connection points for the lower A-arm on the engine side was therefore decreased, and the holes were drilled slightly different than on the other side. The suspension system on the engine side was moved



*Paper template with the holes correct position in the rear wheel well*



*One of the lower A-arm connectors milled out in the Makino CNC milling machine*

further into the wheel well. One small block of aluminum was inserted behind each of the two suspension clevises in the mounting points for the lower A-arm to adjust the suspension system to fit the new motor. The engine was mounted on the left side of the body since most of the turns on the race track were left turns. Added weight on the left side would help preventing the car from rolling over.

The clevises with the belonging wedges and polyurethane vibration dampers were mounted

in the wheel wells. Following the lower A-arm, upper A-arm, coilover and the knuckle was mounted, respectively. After assembly the coilover needed to be adjusted. This meant adjusting the upper and lower stoppers inside the coilover so that the wheels vertical travel was restricted to  $\pm 20$  mm. A wheel made out of cardboard was used to do the final adjustments of the rear suspension before the axle, hub, brake discs and brake calipers were mounted.



*Clevises, lower A-arm, toe link, to link extensor and coilover mounted in the right wheel well*



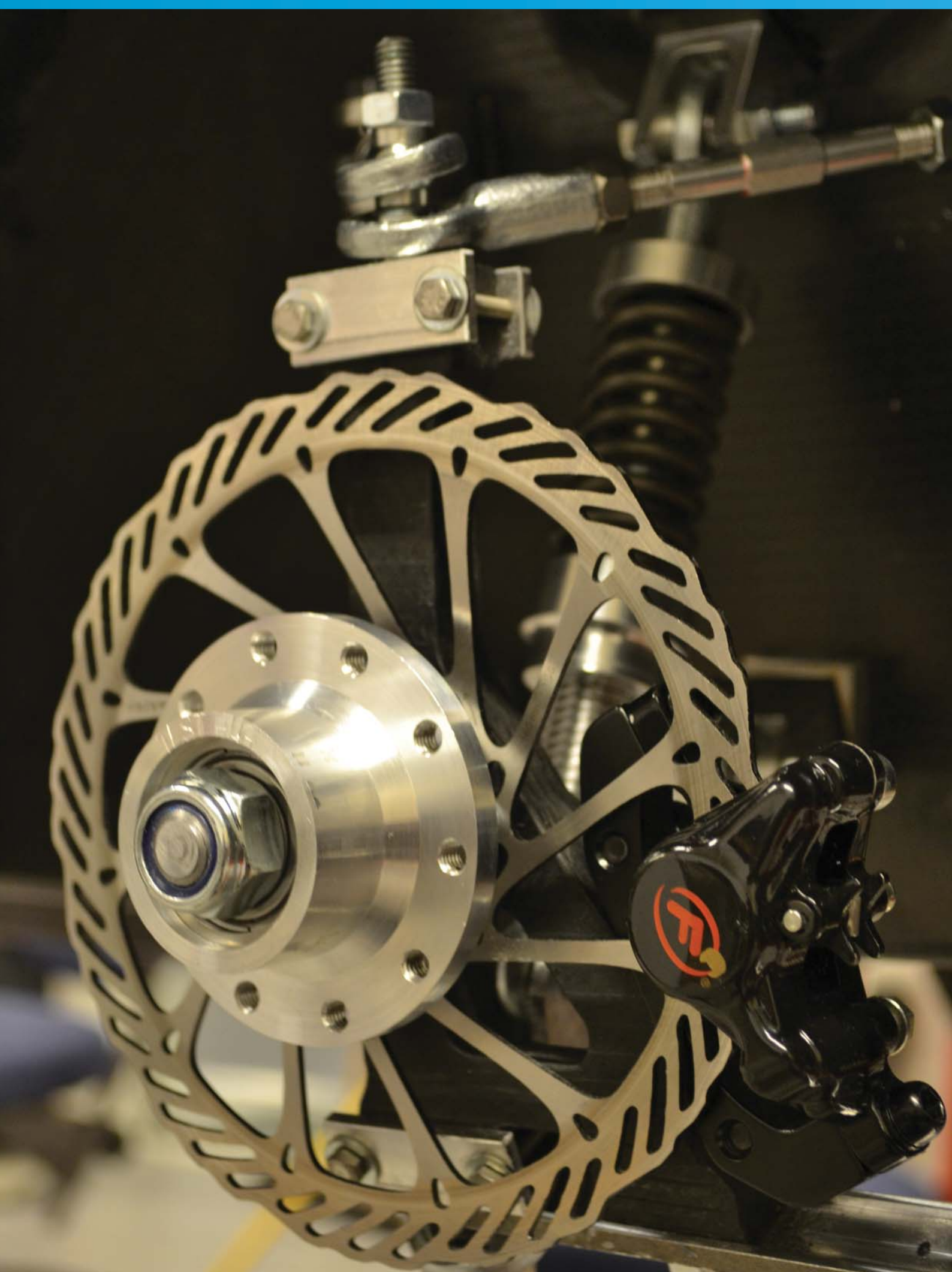
*From the left: Knuckle with hub assembly, lower A-arm assembly, coilover assembly*

### **3.3.2.8 Further Recommendations**

The rear suspension system worked perfect during testing and the race in Rotterdam. However, there is some play causing small misalignments in the toe angle while driving. Due to time issues the problem has not been further investigated, but it is believed the cause of the problem is play in the  $\text{\O}10$  mm rod end connecting the knuckle to the lower A-arm. If the suspension system is to be used next year, the team should find a solution to this problem

Next year's team should look into the possibility of making the suspension system as a flexible mechanism, as proposed in the Project Report from the autumn of 2011 (Endresen, et al., 2011). The coilover in the existing suspension system is heavy due to the weight of the steel spring. A flexible solution would decrease the weight and reduce the number of moving parts, hence decrease the mechanical complexity of the suspension system.



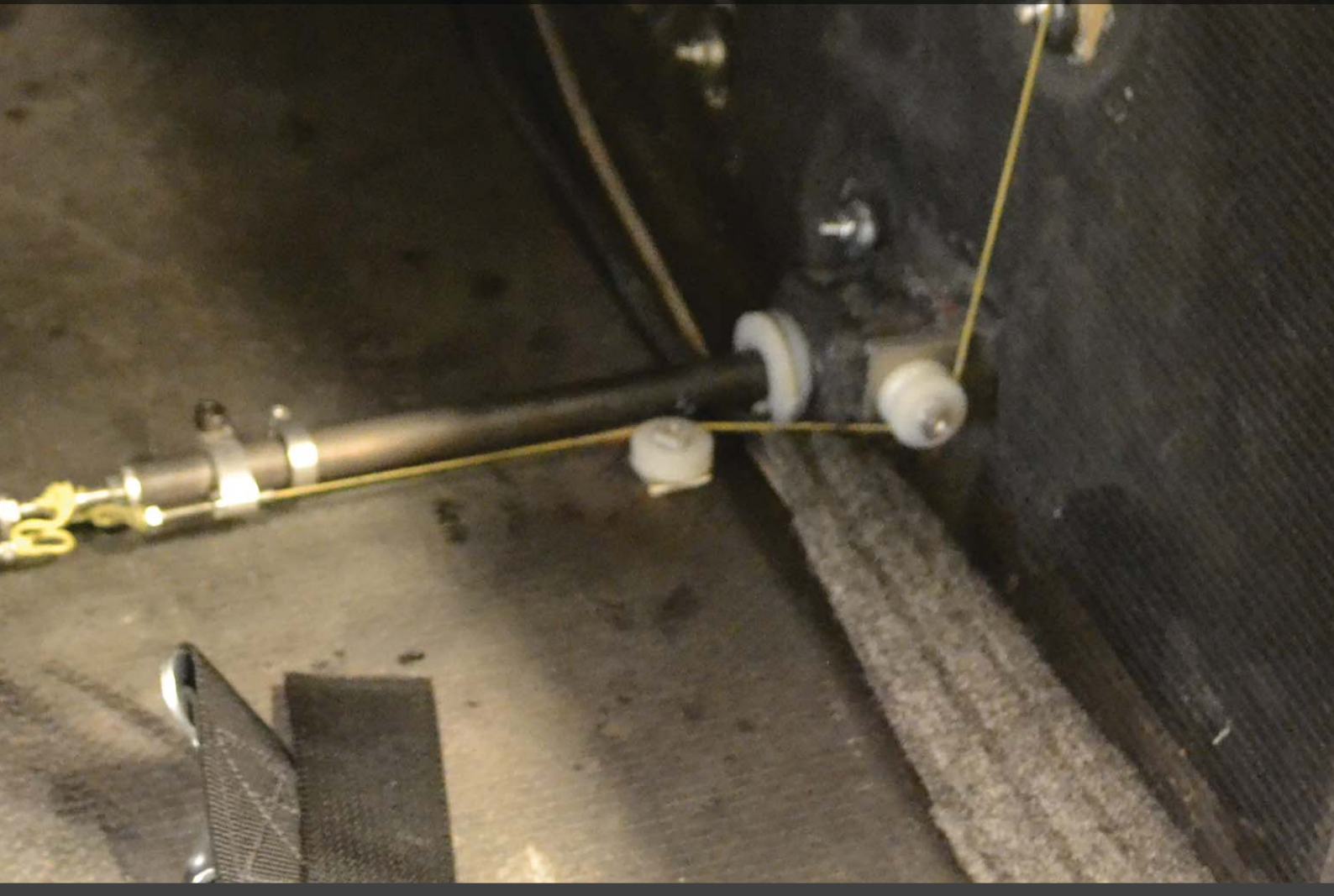


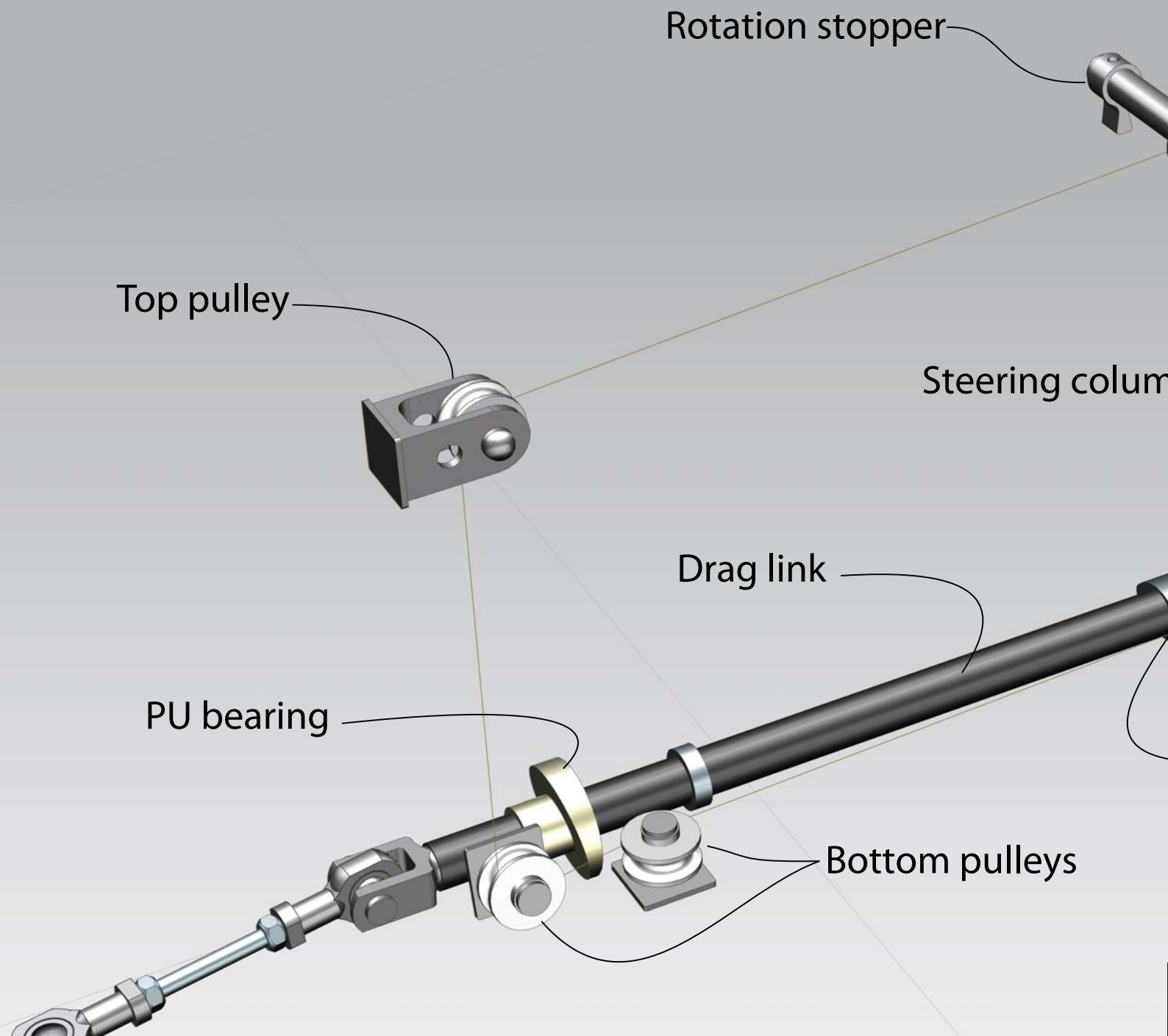
*Rear suspension with hub assembly and brake caliper*





# 3.4 STEERING





## 3.4 STEERING

This is a continuation of the work done on the steering in the autumn of 2011. A requirement had to be added to the requirements list from last semester. It was important to have the most amount of adjustability available for the front suspension and steering. This made it necessary to vary the length of the drag link in addition to having adjustable tie rods (Endresen, et al., 2011).

The chosen concept was a cable based system. When the steering column is rotated a cable that is spooled around it pulls the drag link. The chosen cable was made from Kevlar, as a backup solution this cable could be exchanged with one made from steel.

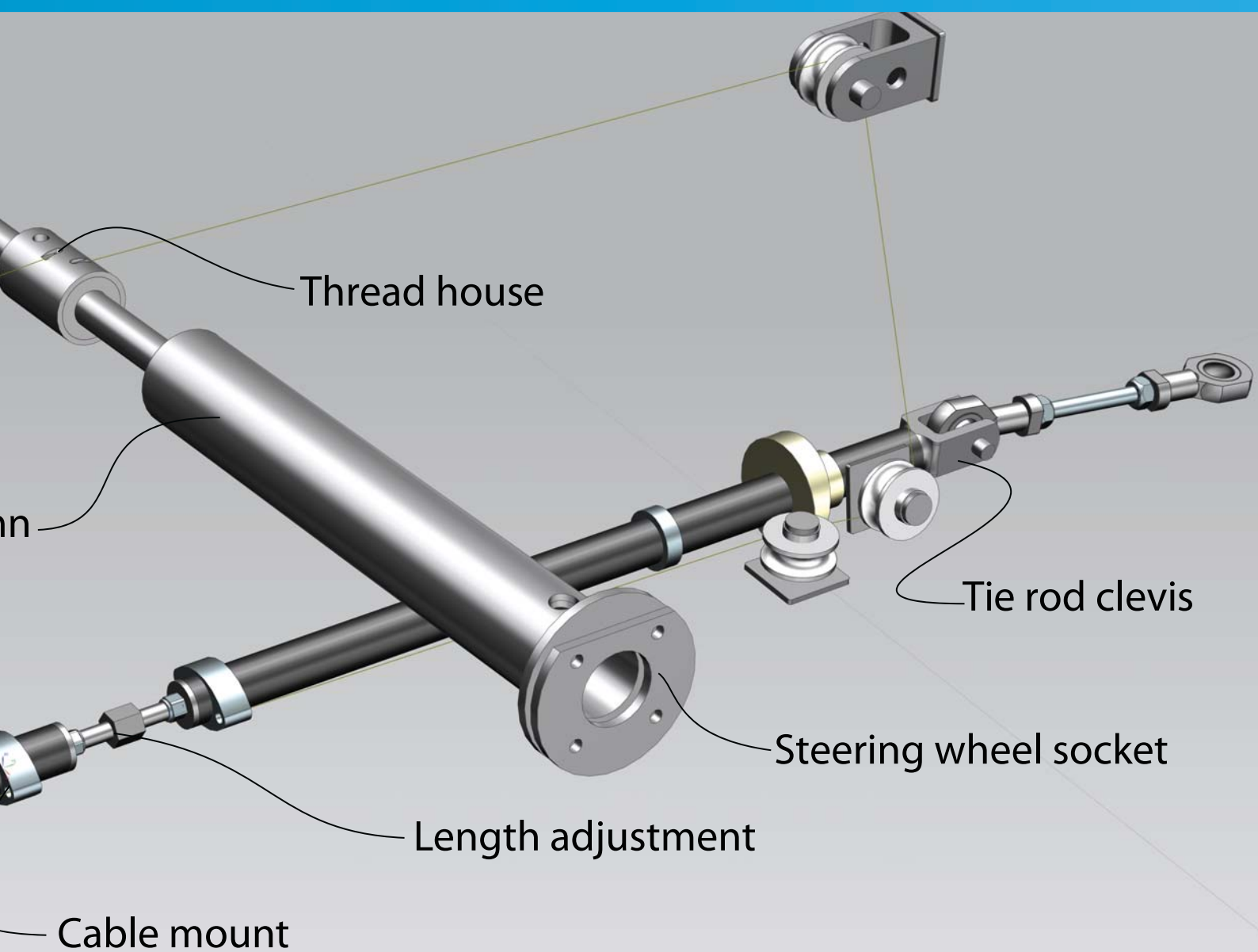


Figure 3.4.1: All steering components in the final assembly.

### 3.4.1 DRAG LINK

The overall specifications for the drag link were done early. They were needed for setting up the steering geometry in correlation with the front suspension. It was decided to mainly use carbon fiber in the drag link. A pair of LEKI Crosslite RS skiing rods were purchased, dismantled and stripped of paint. Their properties were well suited for this application. The decision was made to use a section of one of these as the main body for the drag link. Solid plugs are used to internally support areas where external force is applied.

#### 3.4.1.1 Length Adjustment

There were two fundamental ways of achieving a variable length: Varying the length of the drag link's main body, or adjustment on each side for the tie rod mounts. Length adjustments of suspension parts are often done by use of double threaded screws with locking nuts. This enables fine adjustments to be made.

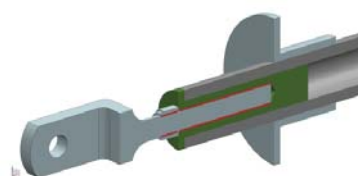


Figure 3.4.2: Length adjustment concept

Another possibility is to have a sliding mechanism, either be fastened by friction or secured with a locking pin. It is hard to achieve both accuracy and adjustability with such a setup. In a continuous friction based binding it is difficult to maintain a reference point when adjusting. With a locking pin it is necessary to have pre drilled holes with certain spacing.

Threaded bolts are a good solution, but they do have some weaknesses. Screws should not be subjected to shear stress. The drag link mainly experiences axial load, but some shear force can occur at the ends. Load acting on the drag link will not always be horizontal, but vary with the compression of the front suspension. Joints normally used in suspension applications have a limited angular displacement span. Due to these problems it was ultimately decided to have length adjustment of the drag link itself. The drag link was split in half and two aluminum plugs were produced. Each plug were manufactured with internal M6 threads, one of them left handed. These were glued in place in the drag link with a high strength adhesive. Along with a 6 mm double threaded aluminum bolt, the plugs made length adjustment possible.

### 3.4.1.2 Tie Rod Mount

The tie rods connect and transmit the movement of the drag link to the front suspension knuckle. Rotation about the x- and y axis needs to be allowed by the interface between the drag link and the tie rod.

The tie rod has to be able to move with the

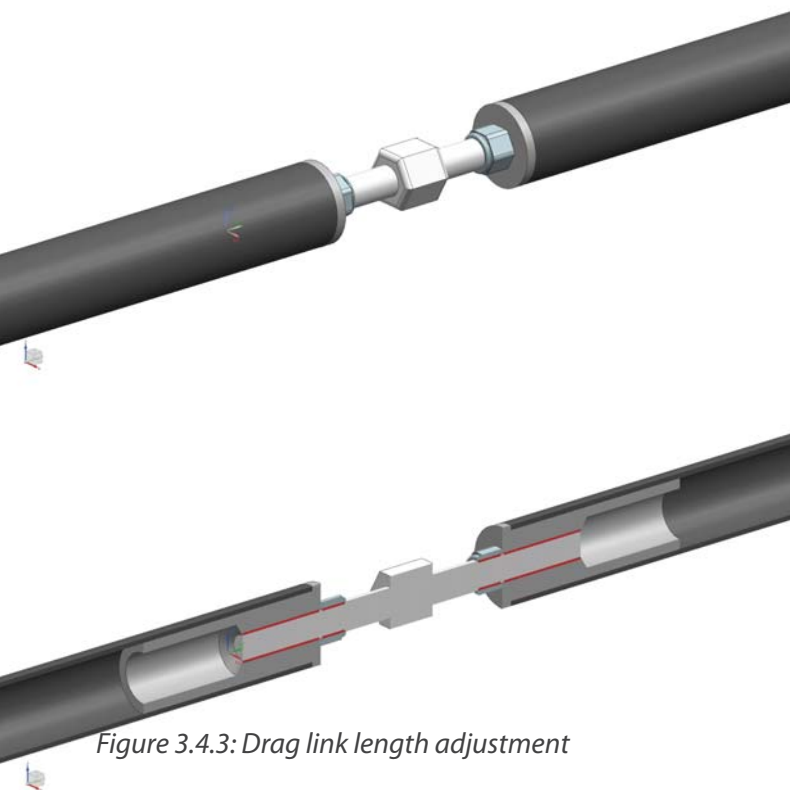


Figure 3.4.3: Drag link length adjustment

suspension. Rod ends, spherical ball bearings or ball joints are components that can achieve this. These parts usually have an angular displacement range of  $\pm 10-15$  degrees. For this solution the tie rod mount had to be designed with this in mind (SKF product catalog, 2012).

The solution from the old DNVFF consisted of a 5mm plain spherical bearing with a machined tie rod running through it. To secure the tie rod a nut was used on the other side of the bearing. The bearing was mounted in a socket that was fastened to the drag link with an M5 bolt. A casing was put onto the socket to secure the bearing in place. A similar solution was modeled in NX.

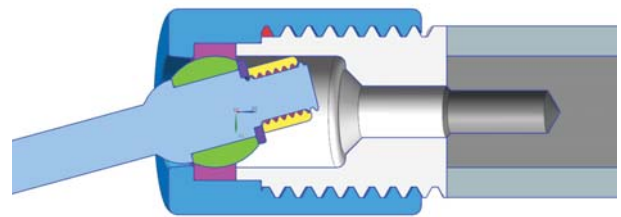


Figure 3.4.4: Old tie rod solution

The tie rod diameter was increased from 5mm to 6 mm in this recreation. The specifications for the 6 mm spherical plain bearing stated a maximum angular displacement of 13 degrees. This would not be enough.

As a alternative solution tie rod and mount could be split up into two simpler units. Four possible setups were created and compared to each other. A simple solution involving gluing a tie rod clevis in the drag link, as seen in figure 3.4.5.

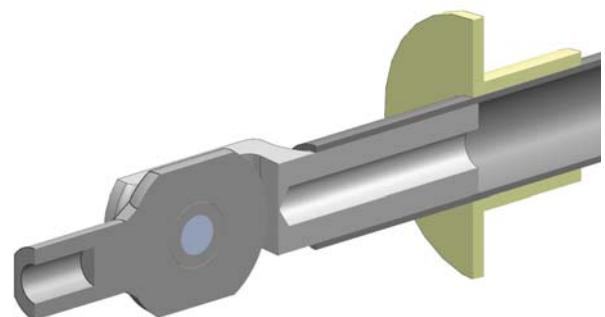


Figure 3.4.5: Tie rod solution chosen

### 3.4.1.3 Cable Mount

The steering solution needed two mounting points on the drag link for the cable. This enabled the drag link to be pulled from either side. The old cable mounts could be used, as the diameter of the new drag link was identical to the old.

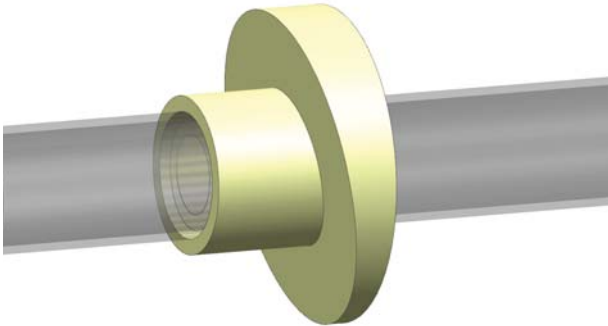


Figure 3.4.6: PU bearing, provides low friction for the drag link

### 3.4.1.4 Additional Drag Link Parts

When working on the front suspension geometry an issue regarding the drag link was identified. A critical angle could form between the steering knuckle toe and tie rod. This would happen if the drag link moved beyond a certain limit. To stop this from happening two physical stoppers were made for the drag link. These were set diameter clamps made from Alumec and were placed on the drag link to limit its axial movement. Bearings were produced to support the drag link going through the wheel well wall. Various solutions were considered and a simple plastic glide bearing was chosen. The bearings were produced from a 40 mm poly urethane (PU) bolt. The flange in connection with the wheel well wall was tilted 10 degrees to fit perfectly.

## 3.4.2 STEERING COLUMN

The steering column transfers driver input into steering motion. It is connected to the dash board with additional support. In addition to the dash board the steering column had the following interfaces: The steering wheel had to be mounted to the steering column, transferring torque. Electrical wires running to the steering wheel should be concealed for safety and vanity reasons. The Kevlar cable had to be attached to the column and spooled around it. The length spooled per degree of rotation determined the steering ratio, which had to be within a certain interval.

The main body of the steering column was from a 40 mm bolt of aluminum 6061. It was made with two different sections. The steering wheel section was made with a wide cross section of 26x30 mm to house the wires going to the steering wheel. The wires should not be seen from the outside of the car or when sitting in the normal driving position. With the wires running through the steering column there was no danger for something ripping them off. The other section of the steering column was made with a different cross section. A certain diameter was required to achieve the correct steering ratio. The driver should not have to change grip of the steering wheel when driving the car. This was achieved by limiting the angle required for full steering lock to  $\pm 120^\circ$ . The drag link had to move about  $\pm 25$  mm for the wheels to move from the straight ahead position to full steering lock. This meant that the following diameter  $d$  was needed:

$$\pi d * \frac{120^\circ}{360^\circ} = 25 \text{ mm}$$
$$d = \frac{25 \text{ mm}}{\pi} * \frac{360^\circ}{120^\circ} = 24 \text{ mm}$$

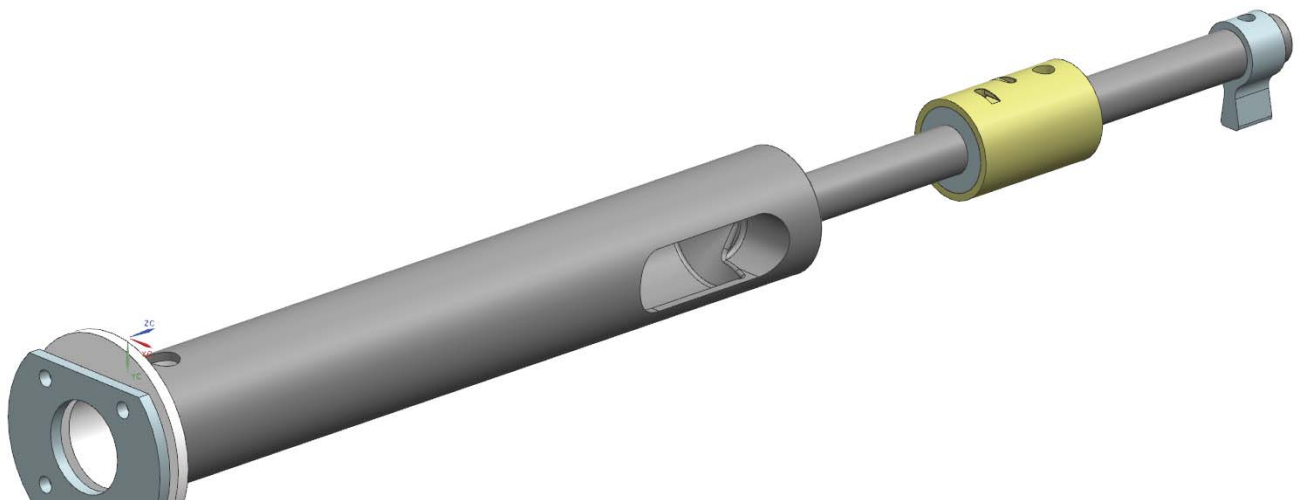


Figure 3.4.7: 3D model of the steering column, with sub parts assembled

The solution was to make the second section of the column quite small and slide a “thread house” onto it. This unit would be of the needed diameter and have two holes in which the cable could be threaded into. The housing had an open end that allowed access to the cable inside. The cable could be tied around the steering column and the housing could be slid over the knots. The housing was fastened with two M5 screws to the column. The cable would be in two lengths, one going to each side of the drag link. If one of the cables should snap it would still be possible to steer to one side and maintain some level of control.

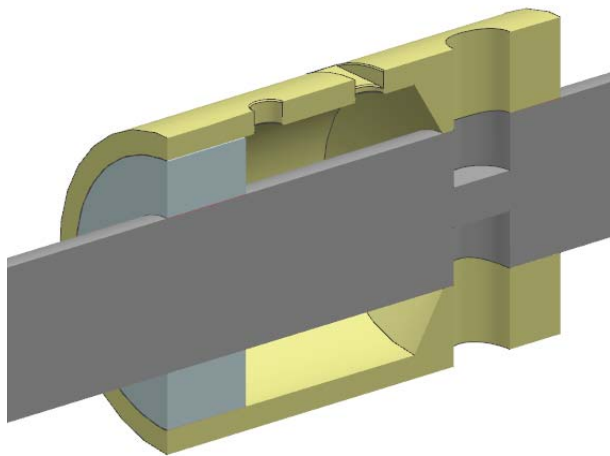


Figure 3.4.8: Thread house

For the steering wheel mount it was important to make a precise connection, to keep overall play in the steering low. This was done by making an aluminum socket that would fit perfectly into the steering column. The steering wheel was attached to this socket. A reinforcement ring was made to support the four attachment bolts on the inside of the steering wheel. The socket was secured to the column with an 8mm aluminum locking pin.

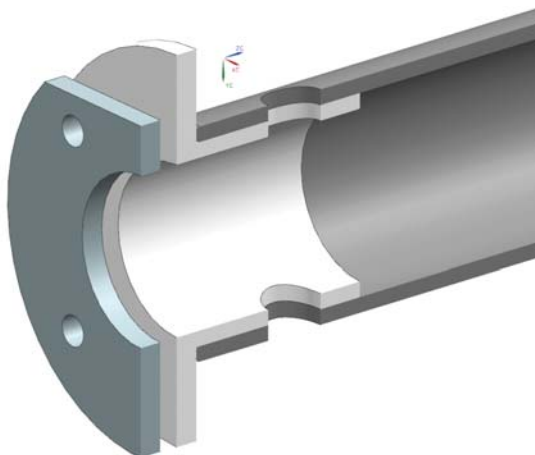


Figure 3.4.9: Steering wheel mounting socket

The dashboard and steering wheel mount consisted of two cross beams mounted between the wheel wells. Plastic cylinders were inserted in the core material of the cross beams during production. Holes could easily be cut out afterwards for the steering column. Another set of plastic bushings were inserted to form plastic glide bearings. The steering column was supported by these two bearings. Two aluminum stoppers were made for the column. These would press against the bearings and stop the column from moving in or out. One of the stoppers also limited the rotation to the 120° specified.

#### 3.4.2.1 Analysis

The maximum force exerted on the drag link by the front suspension would be 150 N. Friction in the steering system could double this force. The pre tensioning of the cable did not affect the steering column as the forces were in equilibrium.

The column was allowed to rotate and move to a certain extent in the bearing points. This is because the cross beams were not completely stiff and some elastic deformations were present. A load of 300 N was set in the mounting point for the thread house.

The results showed that the steering column would have no problems handling the 300N load. The maximum stress was 69 MPa and very small deformations.

### 3.4.3 PULLEYS AND KEVLAR CABLE

One of the goals for the new steering was to minimize friction to improve the feel of the steering, and enable self-centering. Pulleys would be used together with the Kevlar thread to achieve this.

In 2008 and 2009 the DNVFF used plastic pulleys with built in ball bearings in its steering system (Bjugstad, 2008). These pulleys were found in storage along with some other smaller plastic pulleys without bearings. The small pulleys were unused and weighed only 3 grams each. The larger, heavier ones had a weight of 21 grams and were in used condition. Both of them had an internal diameter of 8 mm.

The small pulleys were tested for friction on a machined aluminum bolt. With some lubrication, low friction was achieved, even for relatively high loads. There was no need to use the large pulleys with ball bearings.



To mount the pulleys to the body of the car brackets were produced. Aluminum plates with M5 bolts going through them were glued directly to the body as mounting points. Two different types of brackets were made for the top and bottom pulley mount point respectively.

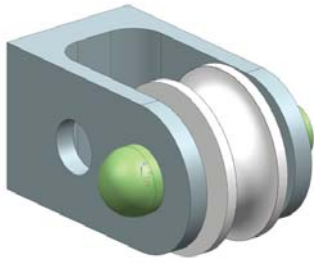


Figure 3.4.10: Pulley assembled on bracket

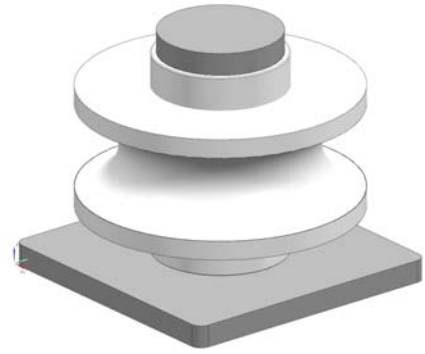


Figure 3.4.11: Pulley assembled on bracket

Stress - Element-Nodal, Unaveraged, Von-Mises  
 Min : 0.00, Max : 69.59, Units = N/mm<sup>2</sup>(MPa)  
 Deformation : Displacement - Nodal Magnitude

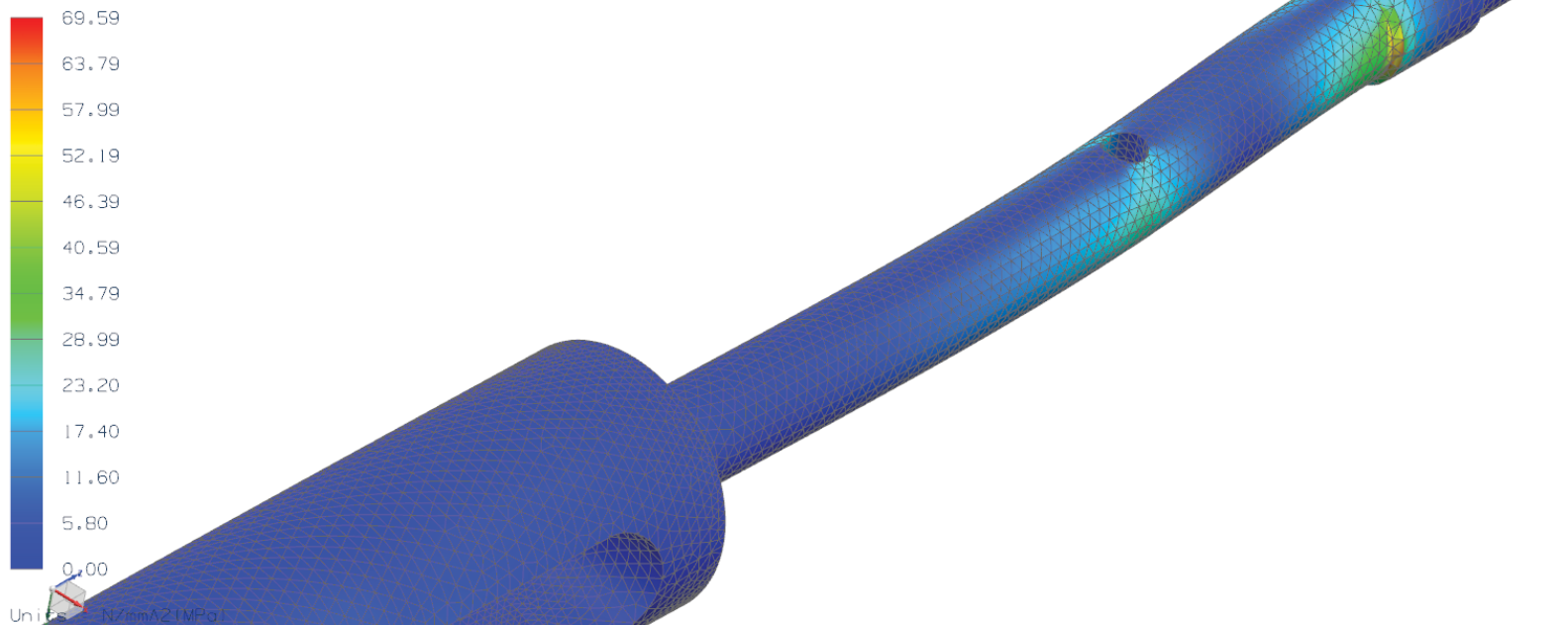
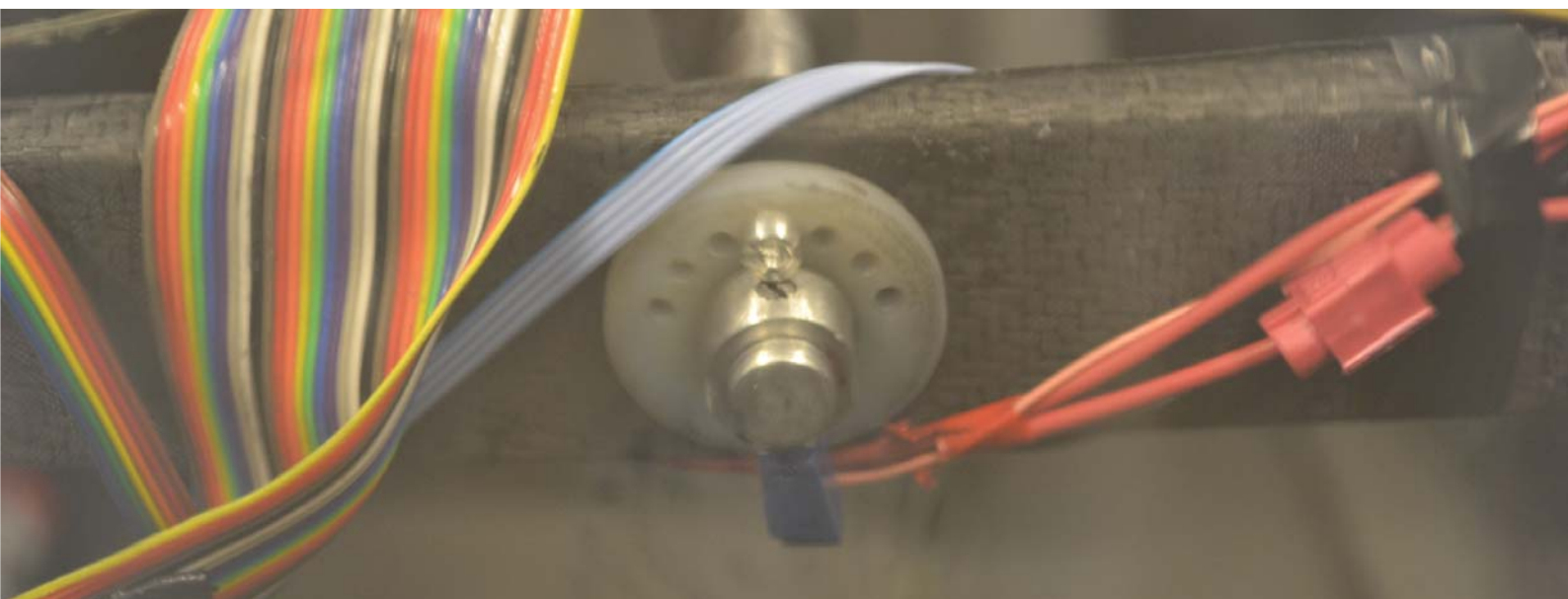


Figure 3.4.11: Strength analysis of the steering column, maximum stress of 69 MPa.



Physical stopper fo limit steering colum rotation to 120 degrees.



Kevlar has 5 times the tensile strength-to-weight ratio than steel. Because of its low bending resistance less tension was needed to achieve tight and precise steering. It could be used with the smaller pulleys without any negative impacts such as increased resistance or wear. Two Kevlar cables were purchased. One small rated at 200 lbs and a heavy duty spear gun rope rated at 400 lbs. The heavy duty rope was covered in wax to keep it from degrading.

Tests were conducted to discover the true strength of the cable. A weight scale was attached to one of the roof cranes in the IPM workshop. Weight was gradually added until the cable failed and the maximum load was recorded. Generally the cable failed in the knots, and at about 50-60% of its rated weight holding capabilities. This was around 50-60 kg for the small cable and over 100 kg for the heavy duty cable. A single strand of the heavy duty rope would be used in the steering.

The cable was tested for how much pre tension it would need to yield accurate steering. A length of rope was cut to the same length as the steering strands. At about 20 kg of load the cable was considered to be adequately tensioned. The knots used to secure the cable would begin to slip if the tension got too high, this was due to the wax coating.

### 3.4.4 ASSEMBLY AND TESTING

Holes were cut in the monocoque for the PU bearings. The holes had to be made 8 mm further

up than planned since the floor in the car was reinforced with 10 mm core material during production. This had not been accounted for in the design process. The consequence of this would be slight bump steer.

The physical stoppers and cable mounts were slid onto the drag link, the cable mounts had to be mounted such that their angle was in line with the lower pulley. The tie rod fork had to be pointing upwards when fastening the mounts. The entire drag link would rotate when the Kevlar cable pulled on it if this was not done. This would compromise the tie rod forks function in the wheel well. Grease was applied to the drag link to minimize friction.

When the first crossbar of the dashboard was in place the steering column could be inserted. The second crossbar was inserted onto the column and glued in place. Its final position turned out to be too low. This was because the dashboard was more flexible than previously assumed. This didn't affect the steering columns function, but it did add friction to the columns rotational movement.

Markings were made for the pulley mount points, using a dummy cable. The bottom pulley had to keep the cable lined up with the drag link. The pulley brackets were placed onto the mounting bolts and secured. The Kevlar cable was fastened using #8 knots at the cable mounts and bowties around the steering column. These were the two strongest knots found during research. The length adjustment of the drag link was used as the base tensioning for the cable. The cable mounts were used for fine tuning and adjusting

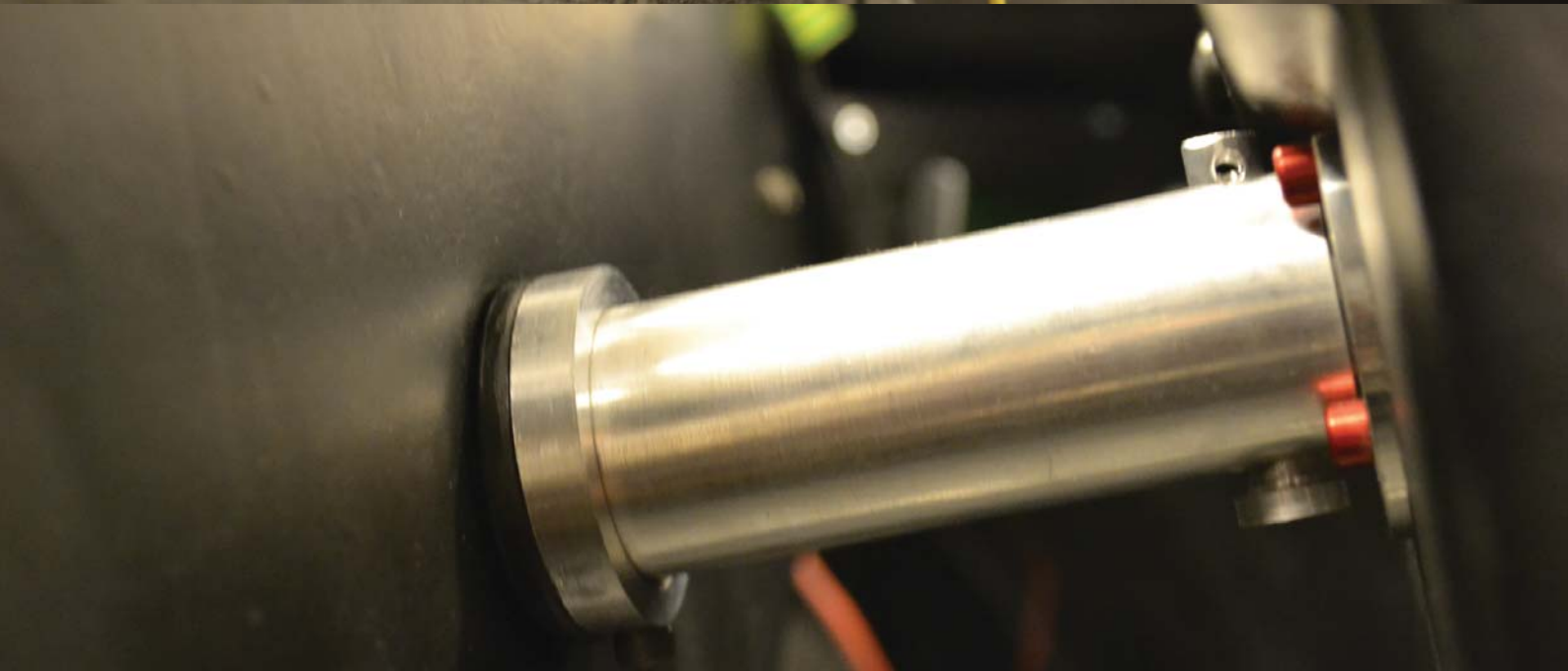
the center position of the steering.

During the first days of testing it became clear that the level of friction in the steering was too high. This was caused by the drag link bending from the forces from the Kevlar cable. There was a slight angle between the cable and drag link in the x-y plane. This caused a small force vector to act normally on the drag link. The length adjustment made the drag link more bendable than it otherwise would have been. To solve this a third pulley pair was introduced to the car. These were mounted on the floor near the bottom pulley. It made sure the cable was parallel to the drag link in all planes. After this addition the steering performed well. Tension decreased after some time due to creep in the #8 knots. By checking the tension and adjusting regularly the steering was kept fully functional.

### 3.4.5 RACE AND CONCLUSION

The steering met the SEM requirements by having a turning radius of 5 m and very little play in the steering wheel. The driver had no problems controlling the car during racing. Tension in the cable was kept at an acceptable level throughout the 40 minute runs. Between driving sessions the cable was checked for tension and wear.

On the first successful test run of the competition the left tie rod was damaged. This was due to the assembly problem with the drag link. The rod end at the steering knuckle end exceeded its angular displacement span. This caused the tie rod to bend. This was an unforeseen consequence of the increased height of the drag link. The tie rod was modified to stop this from happening again.



*Left: Drag link with length adjustment, cable mounts and physical stoppers. Kevlar thread in yellow.  
Right: Upper pulley assembly glued to the wheel well. Visible section of the steering column.*

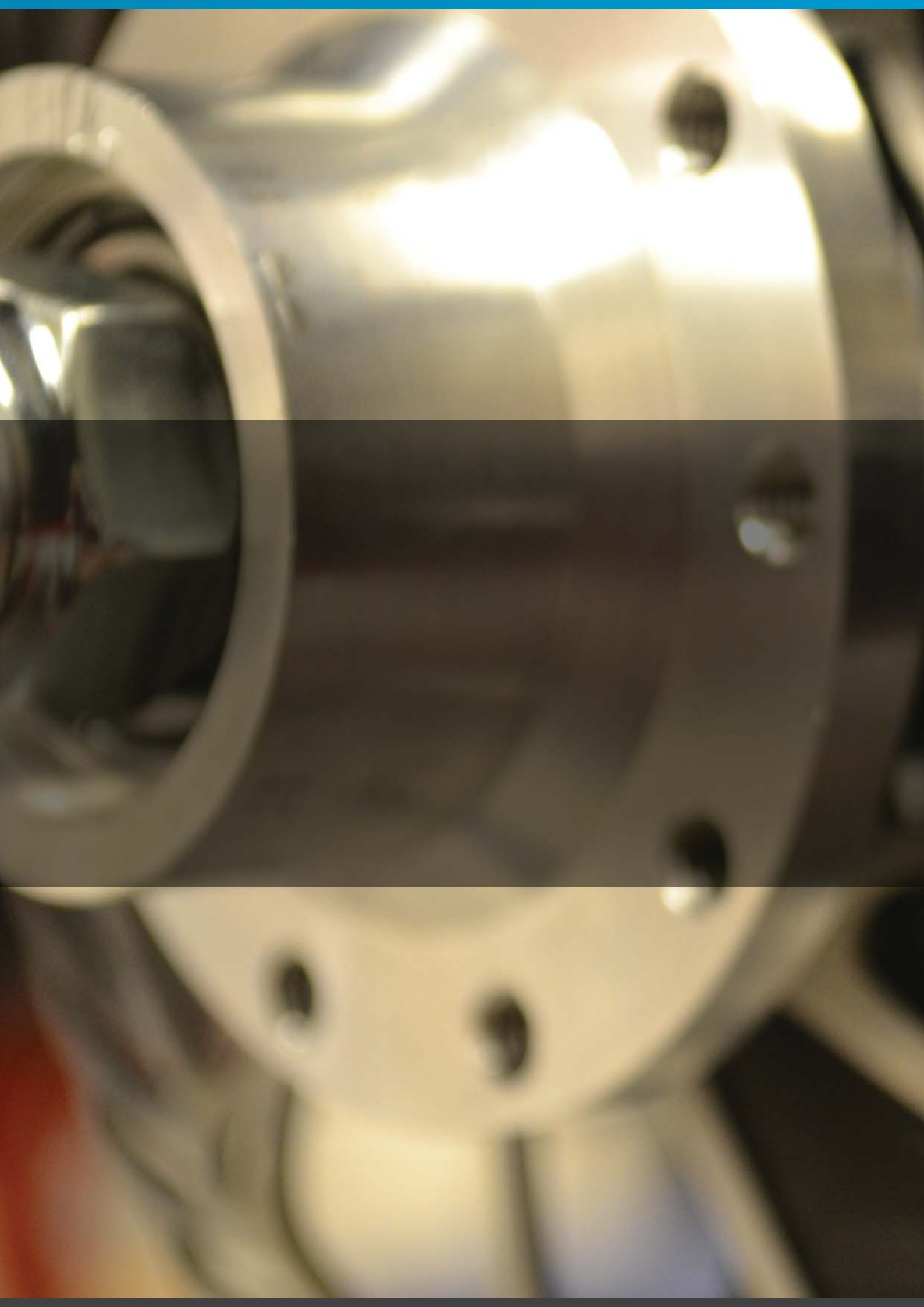
On the final attempt of the competition the steering failed. The car crashed into the barrier at the start/stop lane. This was right before the car should stop for the lap, so the speed was low. The car was returned to the paddock and inspected. It was discovered that the left cable had snapped at the exit of the thread house. The driver had complained during the run that the steering felt "hard". It was harder than usual to turn the steering wheel. Several things had been overlooked in the inter race checks that could have caused this. The track at Ahoy was very dusty. Filth had collected in the grease applied to the drag link during the competition. It made the drag link harder to move. The rear brake hose and electrical wires ran under the drag link on the right side of the car. They had changed position causing the physical stopper to catch hold of them. Straightening the car after a left turn would have been harder than usual. It is unknown how much strain this caused on the cable. The mechanism used to limit the steering columns rotation had come undone during the attempt. This meant that the steering column could be rotated further even though the drag link could not be moved. The last corner did not require full steering lock however, so this was probably not a contributing cause. Finally, the modification done to the tie rod had one serious side effect. When the left suspension was compressed the wheel would get a toe in angle. This would have made the car harder to steer. All these factors lead to the steering failure.

The overall result of the steering was good, and most importantly it satisfied the SEM rules. Its total weight was less than 1 kg. The complexity was kept low and it was easy to maintain. Only 1500 NOK were spent in total for the steering. There were a few goals not met in the requirements. The friction level in the steering was overall too high. The steering column had friction due to misalignment of the cross bars. The drag link bent slightly under load even with the third pulley pair. This caused added friction in the PU bearings. The high friction meant that no self centering of the steering was achieved. Despite the high friction level the driver had no problems controlling the car. The life span of the steering was lower than designed. It did last more than six hours, the time needed to complete the competition. However, this time was started during the test period and not at the start of the race. At the end of a run the tension in the cable was reduced. The requirement for less than 3° play in the steering was not met during the entire run.





*There was at times severe traffic conditions around the track. The driver maintained full control and regularly made spectacular overtaking moves.*



# 3.5 BRAKES

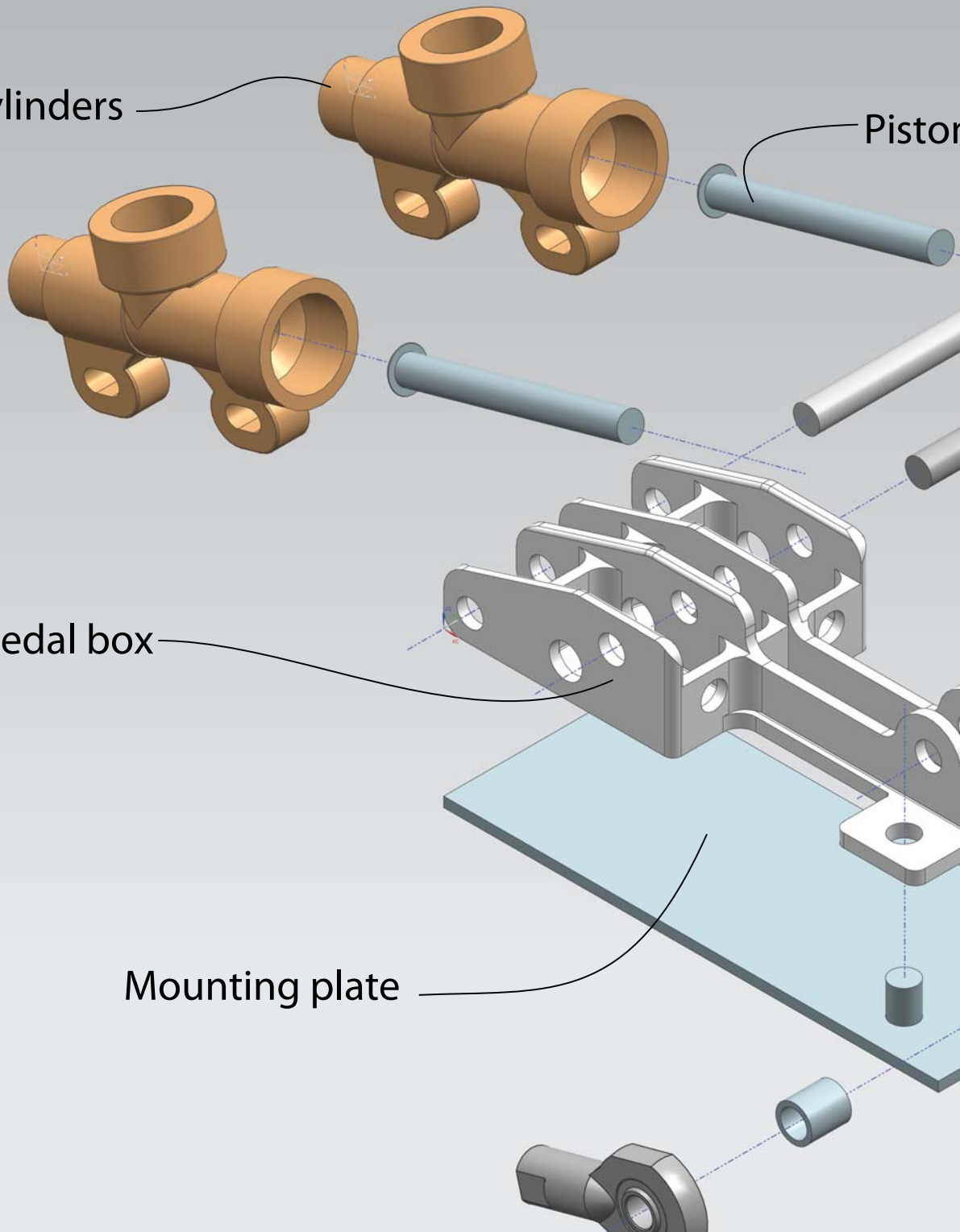


Master cylinders

Piston

Pedal box

Mounting plate



## 3.5 BRAKES

The work presented in this chapter is a continuation of the work done in the autumn of 2011 (Endresen et al, 2011). The main challenge for the brake system has been to design and produce a new pedal box and all its sub parts. The rest of the brake system is composed of standard, off-the-shelf parts (brakelines, calipers and discs).

The brake system is crucial for the safety of both

car and driver. Testing the driver's maximum strength would not necessarily reflect real force he or she would exert under emergency braking. A brake failure in an emergency situation could be very serious for the driver, car and other contenders. The brake system was therefore designed with a safety factor of 2 for worst case scenario.



n arm

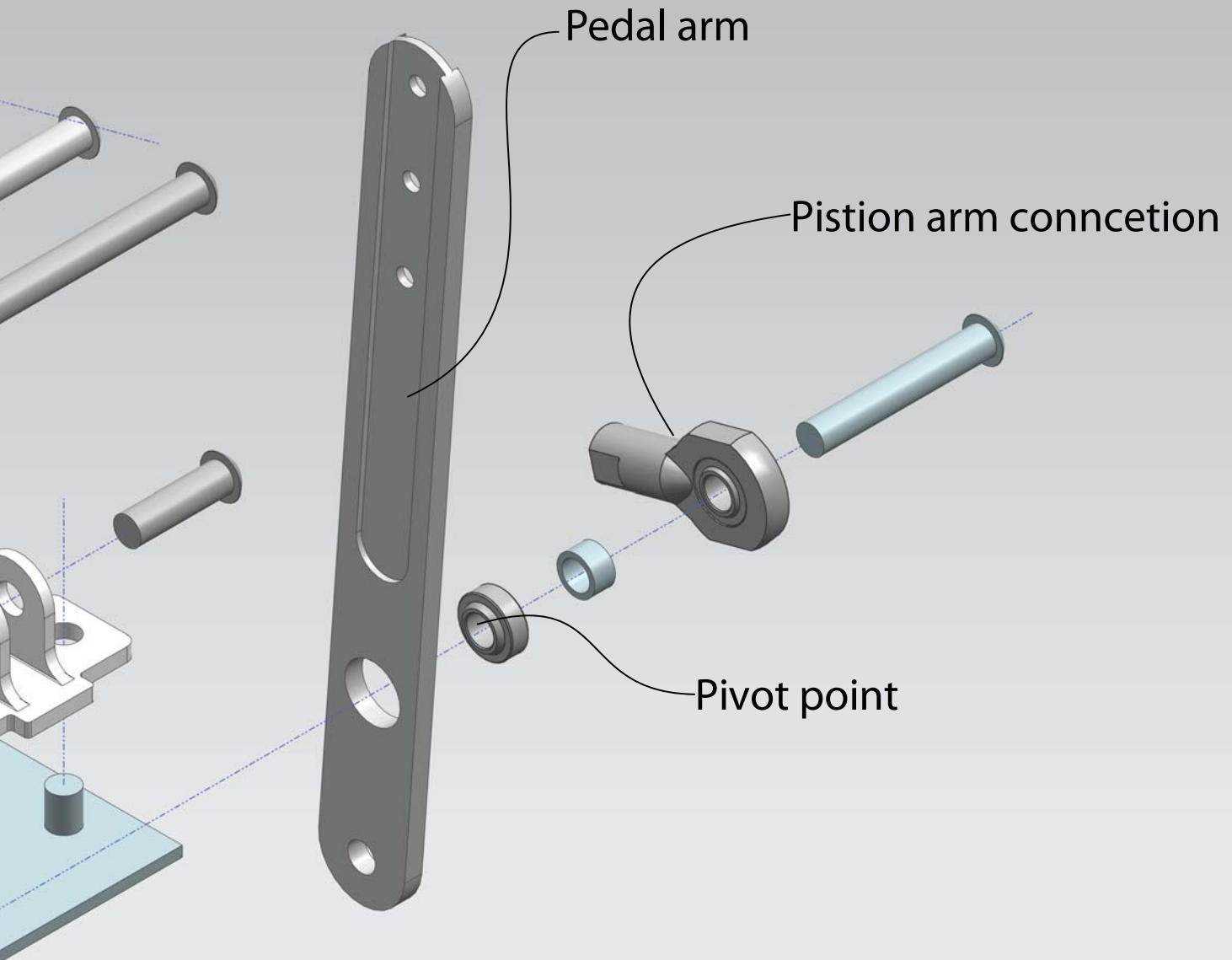


Figure 3.5.1: Exploded view of the brake pedal.

### 3.5.1 BRAKE PEDAL

The concept developed in the autumn semester could potentially have been used in the car, but there were some concerns. The two rods holding the two master cylinders were quite long and weak. They could potentially bend under load and deform the side walls in the process. Another problem with this concept was that it consisted of too many parts. This would make it complicated to assemble and maintain inside the car, the exact opposite of what was intended. It was decided to scrap the entire concept, except for

the pedal arm and pivot point.

The new concept implements more support for the rods holding the master cylinders. The number and size of parts had to be kept at a minimum to ensure a light weight construction. All the mounting points were integrated in the base plate. Small, identical brackets replaced the side walls. This new concept was eventually refined into the final design seen in figure 3.5.2.

#### 3.5.1.1 Pedal Arm

Design of the pedal arm directly affects pedal

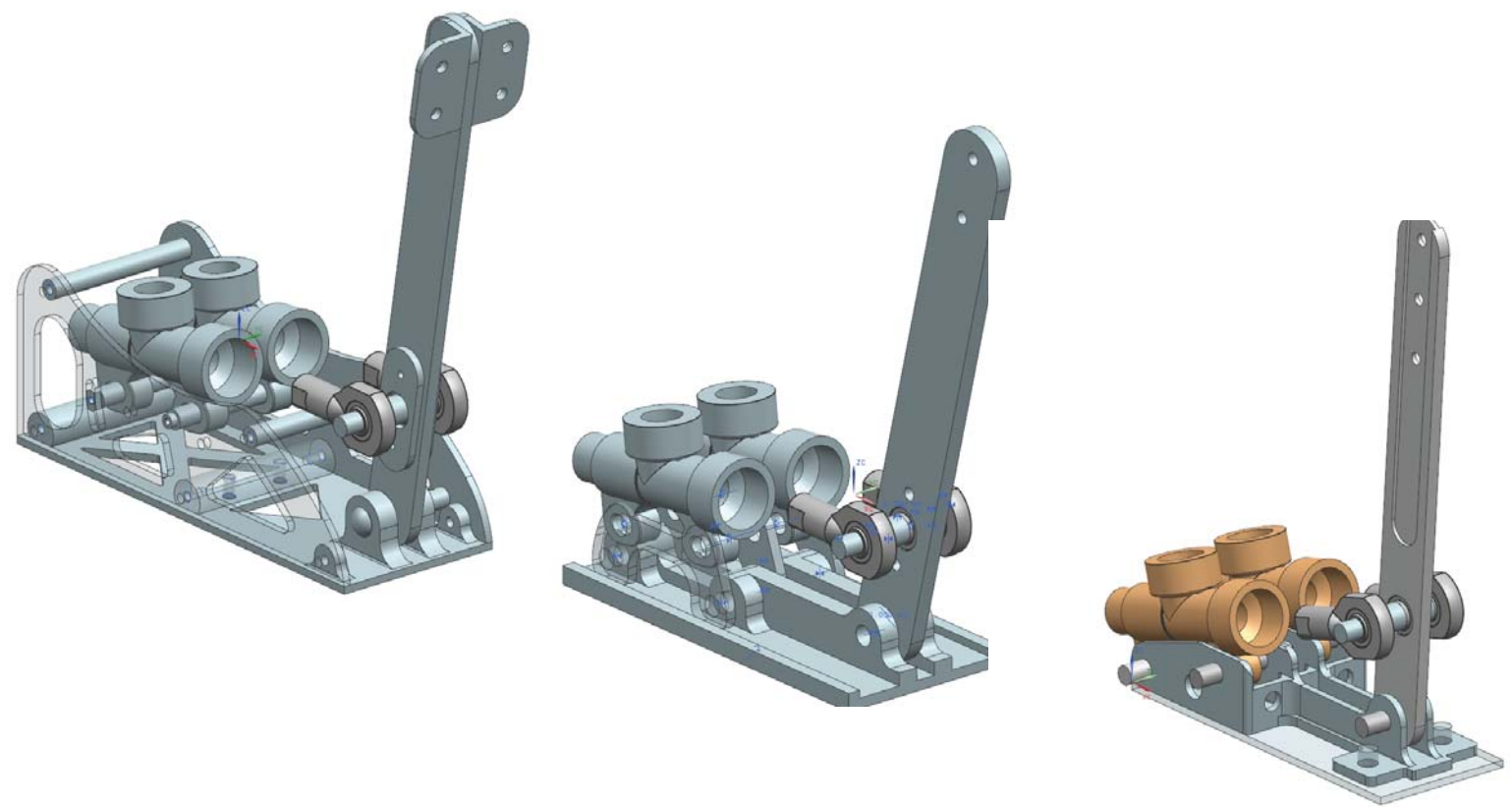


Figure 3.5.2: Stages of the brake pedal design, from early concept to final design

travel and how hard it is to operate the brakes. This component is experiencing the highest stress in the whole brake system. The master cylinders had to be pressed with a force of 360 N, to hold the car stationary on a 20 % slope. For a dynamic case with the car running in wet conditions, a higher force is needed to stop the vehicle safely. With a mechanical advantage of 4/1, 200 N input force from the driver would yield 800 N force to the cylinders. The final mechanical advantage achieved in the design was 4,4/1.

SEM rules states that the foot plate has to have a surface area of minimum 25 mm<sup>2</sup>. The old brake pedal had a foot plate made of wood with a surface area of 40 mm<sup>2</sup>. Producing a foot plate in carbon fiber would only save a few grams. The old foot plate was therefore refurbished and reused. A measurement of the driver's foot determined the maximum length of the pedal arm to be about 220 mm. To ensure that any driver can operate the brakes, the foot plate can be adjusted along the pedal arm. The mechanical advantage would however be affected by the placement of the foot plate.

The car should have more brake force on the front wheels to stop the back from sliding, (Endresen et al, 2011). By having a pivot point in the middle of the pedal arm, the master cylinders were given different mechanical advantages.

Arms of different lengths were connected to the piston arm of each cylinder. The cylinder attached to the shortest arm would receive a higher force due to force equilibrium (see picture). The brake balance could easily be fine tuned between the front and rear circuit by altering the length of the pivot arms.

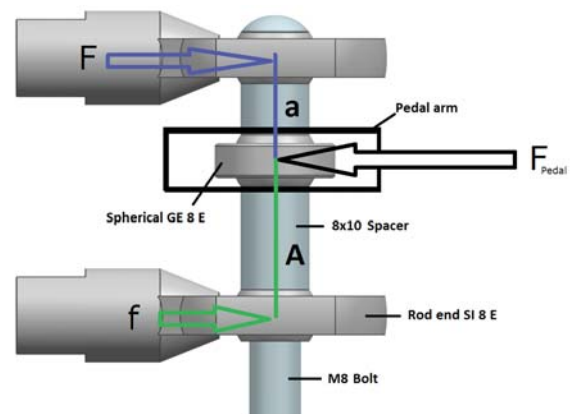
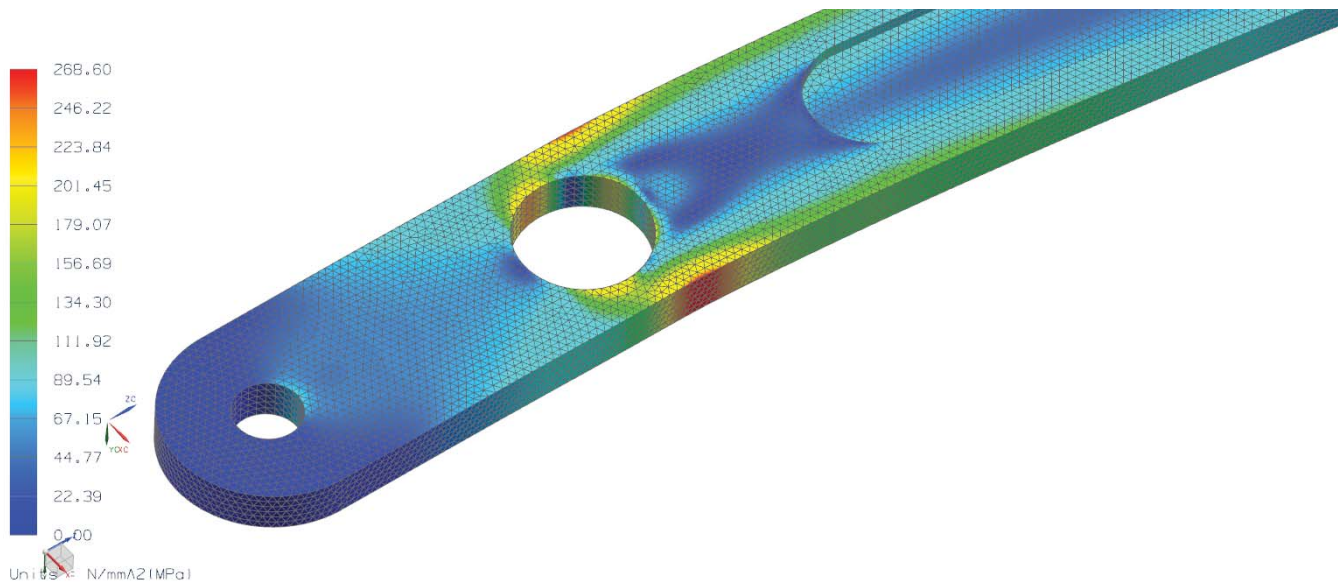


Figure 3.5.3: Pivot point force sketch

$$A * f = a * F$$

$$F + f = F_{Pedal}$$

For the strenght analysis, NX7.5 was used. The material properties were set to aluminum 6061, as Alumec was not available. A force of 600N (emergency braking) and constrains was applied in the mounting points.



*Figure 3.5.4: The maximum stress of 268 MPa was located around the pivot point hole, which yields a safety factor of 2. The analysis showed a deflection of 2.5 mm, which will be a conservative results due to the material data.*

The pedal arm was produced from a 10mm thick Alumec plate. Due to problems fastening the work piece in the hydraulic press, the part moved slightly during production. This resulted in a difference in thickness of 0.4mm over the pedal arm. The performance of the pedal arm will not be affected by this unevenness. Holes for the pivot point, mount and foot plate were drilled out. The hole for the pivot was made to a H7 fit specification. This way the GE 8 spherical bearing would not need any external support after being inserted. 8x10mm aluminum spacers mounted on a M8 steel bolt were used to adjust the force arm for each master cylinder. SI 8 E rod ends were used to connect the cylinders and pivot point arms. Spacers and rod ends were secured in place by fitting a nut to the end of the bolt.

### 3.5.1.2 Brake Pedal Box

The brake pedal box has to withstand the opposing forces of the brake pedal arm and master cylinders. In addition to being strong, it needed to be securely fastened to the car. It is the most complex sub-part of the brake pedal and required the most attention.

It was decided to go for a simple, light and strong design for the pedal box. The pedal box needs to accommodate adjustments of the master cylinders, due to variable length of the pivot point. In addition required piston travel had to be achieved. The pedal arm needs to stop normally to the piston arm of the master cylinder when pressed. This will maximize the mechanical advantage during braking. The pedal arm should

be as upright as possible in its resting position. This minimizes vertical travel of the pedal, which could lead to the driver's foot slipping off.

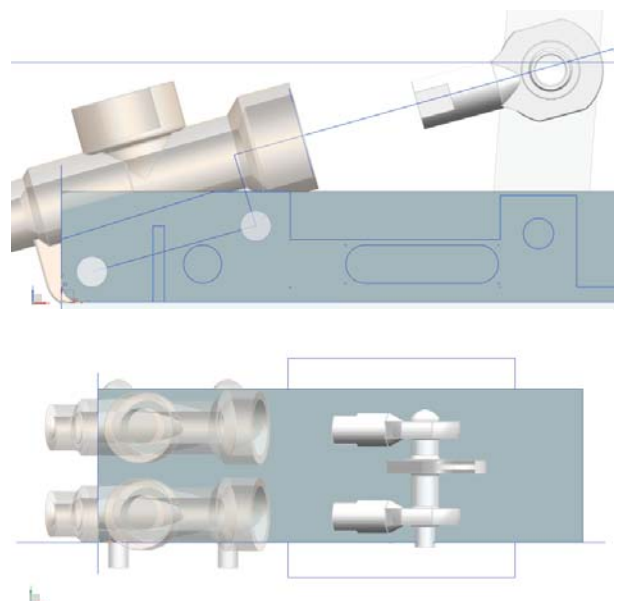


*Figure 3.5.5: Placing of master cylinders and pedal arm. From this the minimum distance between components was determined.*

The design process continued with removing material from a rectangular slab of 145x60x30 mm, just as one would in a milling machine. Because of the high forces involved it was desirable to have the cylinder piston arms as straight as possible towards the pivot. Some cross bracers were left between the walls to keep the 'box' rigid. Edge blends were applied to avoid any stress concentrations. The bracers made sure that the part was not damaged when it was fastened in the milling machine's hydraulic press.

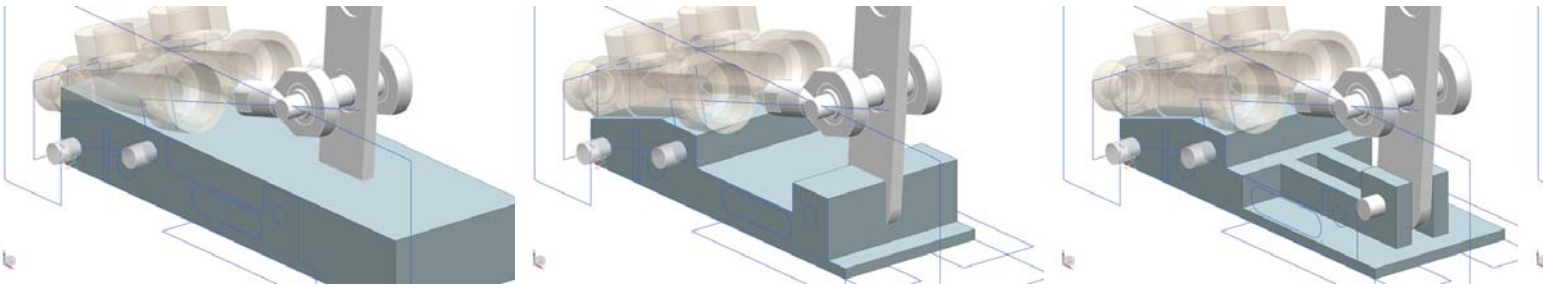


Figure 3.5.6: Grooves removed from block and final piece

Underneath the box 2 mm deep grooves similar to those on top were subtracted to reduce weight. Two 6 mm bolts going across all four walls would hold the master cylinders in place. The pedal arm was held in place with an 8 mm steel locking pin. Two mount points were left in the floor of the box near the pedal mount. Two bolts would be used in these points to fix the box to the car.

The analysis was performed on an earlier revision of the part. Another brace would be added to the design before production. The results of the analysis were conservative and still valid. Aluminum 6061 was assigned as the material. Forces acting on the master cylinder does not act directly on the holes supporting the cylinder cross bolts. This was simulated by adding 1D connectors, as seen in figure xx. To simulate brake balance, 1700 N and 900 N force vectors were set on the two master cylinder points. For the pedal arm supports the reaction forces were simulated by bearing forces of 2000 N. The pedal box was held in place by a fixed constraint on the contact area of the two mounting bolts. A simple support from below simulated the floor of the car.

The brake pedal box was machined out from a single block of AlumeC, in the Makino milling machine at IPM. According to volume calculations done in NX the finished part would weigh approximately 120 g. The AlumeC block had a mass of 1 kg before production started. Holes for the master cylinders and pedal arm were made with H7 specifications. The front most bolt would carry most of the load from the master cylinders. A steel bolt was used for the front mount, while an aluminum bolt would suffice for the rear. The pedal arm locking pin was made from steel in the turning machine. The final piece had a weight of 116 g (without bolts), a very satisfactory result.

### 3.5.1.3 Master Cylinders

More detailed descriptions and calculations performed on the new master cylinders can be found in the autumn report (Endresen et al,

2011). Alterations had to be made to the master cylinders for them to be compatible with the rest of the system. An adapter solution was made for the hydraulic hoses going to the calipers. Bicycles use 6 mm hoses and banjo plugs for the brake system, while motorcycles use 10 mm. The solution was to produce a M10 bolt with internal M6 threads. This bolt could be secured and sealed with a gasket in the master cylinder. The original 6 mm banjo screws could then be used without modifications. To reduce weight the M10 screw was machined out of aluminum, and the piston arms were cut to half their original length.

To further reduce weight the cylinders were fastened in the milling machine and excess material was removed. This saved 35 g per cylinder, but it was discovered that they had been damaged by the hydraulic press. Some deformation and cracks had occurred on top of the cylinder at the connection of the brake fluid reservoir. The cylinders were fixed by filling the cracks with Araldite and machining the hole circular. After the repairs the cylinders were tested and found to be in working order. The other area for potential weight savings was exchanging steel parts with aluminum. Both the piston arms and hydraulic connection bolts were made from steel. Remaking these parts in aluminum saved about 100 g. A total of 170 g was trimmed from the master cylinders.

## 3.5.2 OTHER BRAKE CIRCUIT PARTS

The rest of the brake system consisted of standardized, off the shelves parts. Some were purchased and some were reused from the old car. As the products for bicycle brakes already have a low weight, very little can be gained by making custom parts. The only area where a significant weight reduction could have been made was the steel brake discs. These could have been replaced with discs of carbon fiber, but this was not prioritized.

The hoses reused from the old car were of a steel

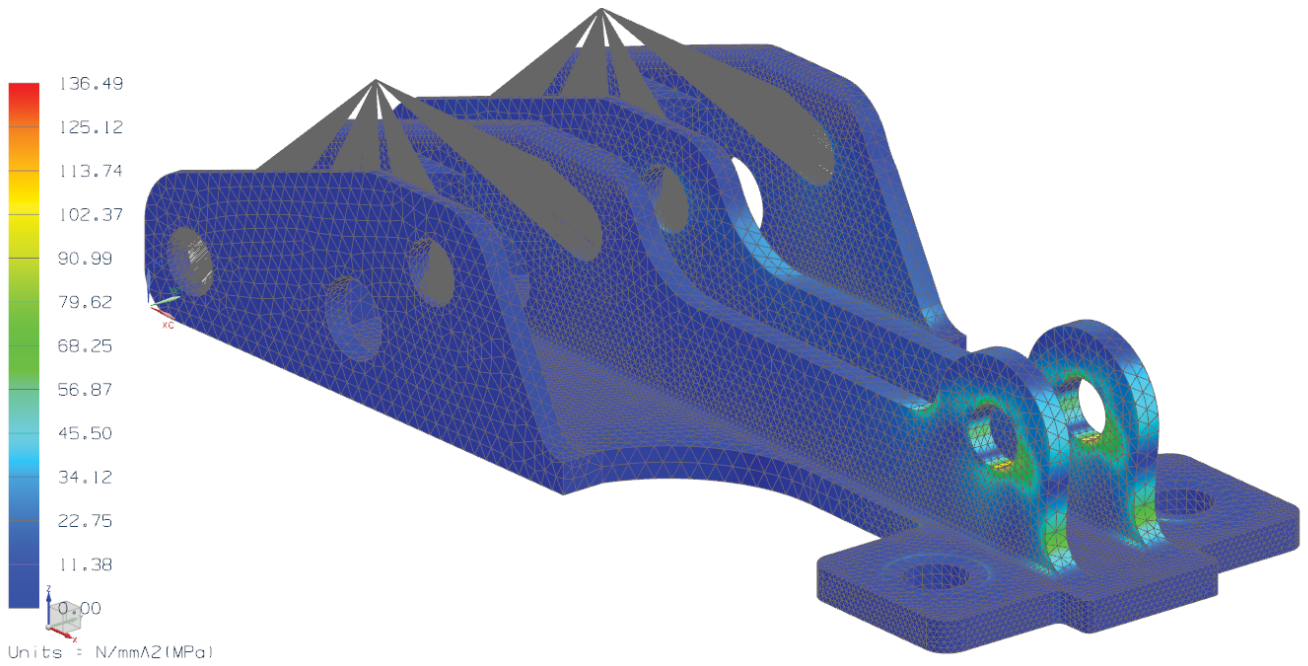
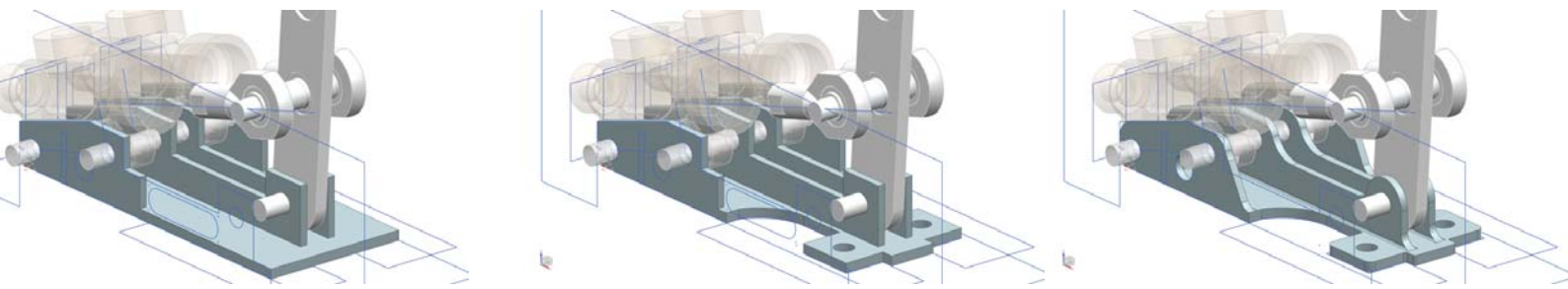


Figure 3.5.7: The maximum stress was 136 MPa, giving a safety factor of 4. This stress occurred at the pedal arm support. There were no significantly deformations in the pedal box

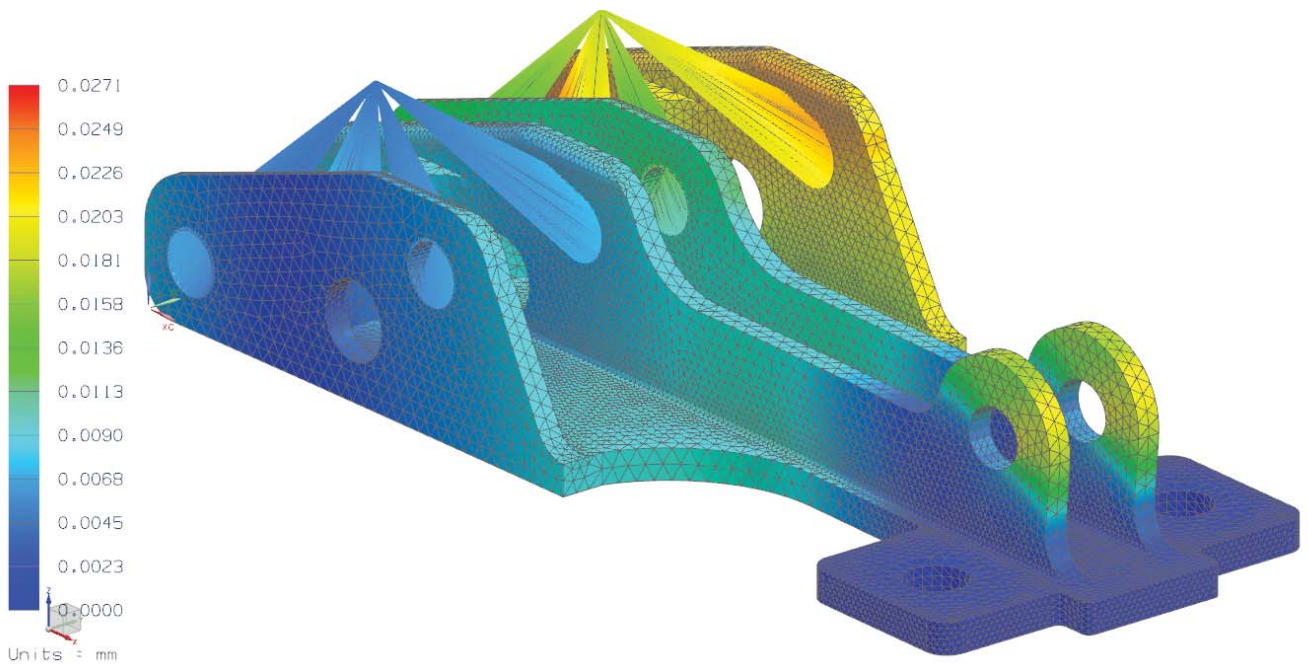
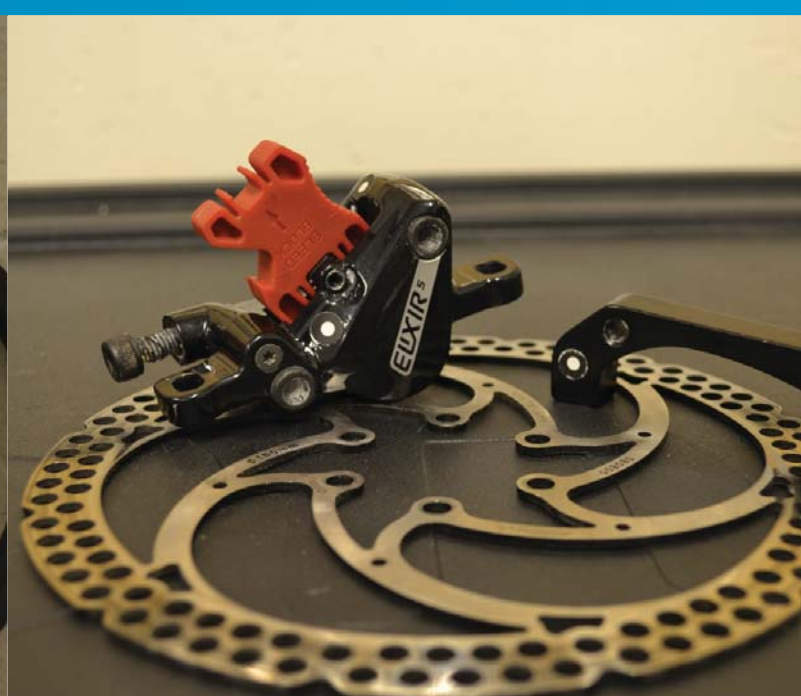


Figure 3.5.8: Displacements in the pedal box



*Left: Master cylinder with piston arm and hose connecting the fluid reservoir  
Right: Avid Elixir 5 brake caliper, 160 mm rear post mount adapter and brake disk*

reinforced type. This reinforcement stops them expanding under load, giving a firmer feel to the brakes. DOT fluid used in the brake circuit required o-rings made from a special rubber. The reused calipers were from two different brands, Formula Oro and Avid Elixir 5. The Formula calipers were the lighter of the two, and therefore placed in the back. They both had the same piston size of 22 mm.

A more detailed description about the status of the parts reused can be found the report from previous semester (Endresen et al, 2011).

### 3.5.3 ASSEMBLY AND TESTING

After the brakes had been assembled a quick function test was performed. Because the mounting holes on the master cylinders were elongated they could be moved back and forth about 5mm. This presented a solution for the brake sensor for the electrical system. A bracket for the sensor was made and fastened using a hole made for weight savings. This positioned the sensor directly in front of the cylinder mount. By fitting the pedal arm with a powerful spring it would pull both master cylinders towards it, thus triggering the sensor.

When mounting the calipers and discs a problem was discovered. The wheel hubs were not designed big enough in the axial direction. This was exaggerated by the fact that the backside of the rims was rough and uneven, so the wheels touched the brake calipers. The hubs had to be

spaced out to solve this problem. Because the discs are attached to the hub they had to be spaced an equal amount. Spacing the discs was done by stacking three M5 washers per bolt (each disc had six bolts). To do this accurately a micrometer had to be used.

Hydraulic hoses were connected from the calipers to the master cylinders and the system was filled with DOT 5.1 brake fluid. Bleeding the brakes was a simple process that could be performed by two people. One had to actuate the fluid syringe connected to the brake caliper. The other would tell when the level in the fluid reservoirs started to rise. When this happened the circuit should be air free and full of fluid. The bleed kit was purchased by an earlier SEM team.

When working on the suspension the calipers were often taken off. To stop any fluid leaking they were fitted with bleed stoppers. These stoppers compress the caliper piston fully, to stop movement if the brake pedal is pressed. The calipers needed to be fine adjusted to stop the discs from rubbing the brake pads. Using a bright light underneath the suspension made fine tuning easier. It was possible to visually determine which way the caliper had to be moved in order for the disc to rotate freely. Two of the discs were slightly bent making it impossible to eliminate scrubbing completely. This was only crucial for the race, so the old discs were used in the testing period.

During the test day at Dragvoll several test were done on the brake system. Two team members were needed to test the car. One person pushed

the car up to a certain speed and the driver applied the brakes. This speed was gradually increased from run to run. The brakes stopped the car every time in a very short distance. As a final test the brakes were 'slammed on', which resulted in the rear tires actually locking up. The brake balance at this point was 66/33% (front/rear). The conclusion of the test was that the braking systems performed quite well. After adjusting the brake balance forward to stop the rear wheels from locking up, the performance was excellent. Several more tests were conducted with no further issues.

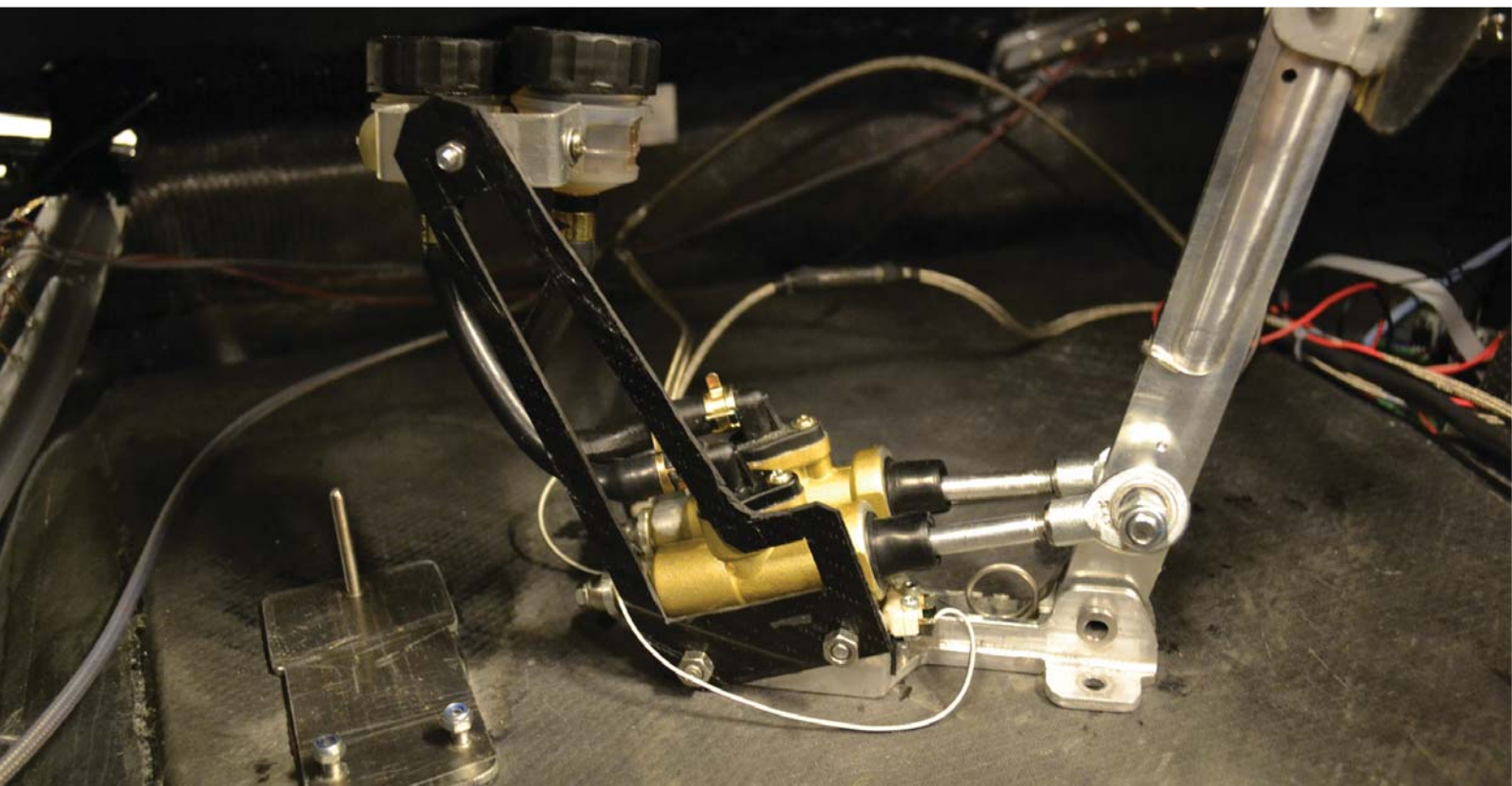
When working on the car in the workshop, two of the brake discs were damaged. One case involved the engine wheel, where the disc is directly attached to the rim. When taking the wheel off the car, the brake caliper first needs to be detached. This was forgotten and one of the good discs was bent. Dymo notes with warnings were put in positions where they could be seen when working on the suspension. No more incidents occurred after this. New brake discs would not be installed until the car had reached Rotterdam as a precaution. The system was otherwise ready for competition.

### 3.5.4 RACE AND CONCLUSION

For the race attempts the new brake discs were mounted. The calipers could now be adjusted

so no scrubbing occurred. Some deformation of the discs will occur during operation. After the discs had been used for a run the calipers needed to be readjusted. Some spillage was detected around the brake pedal. It was discovered that back pressure will build up in the fluid reservoirs. The seals around the cylinder pistons are not completely tight. Some fluid will escape the pressure circuit every time the brake is pressed. This leakage is very minute and did not affect the performance of the brakes. Some problems with the brake sensor were also detected. The spring pushing back the pedal arm was worn and not as stiff as when first installed. To trigger the sensor, the brakes needed to be released abruptly. This was more a source of annoyance than an actual problem on track. The driver had no problem operating it.

All obligatory requirements were fulfilled. The exchange time for the parts worked on was less than 30min. Total cost for the brake system was 6000 NOK. The total weight of the system was less than 2kg. A 50% weight reduction was achieved for the brake pedal compared to previous year. The new brake pedal had a final weight of 750g. Total number of parts far exceeds 50, though the number of major parts is below 50.



*Brake pedal assembly with reservoir holder and brake sensor. Mounting plate glued to the floor of the car.*





# 3.6 WHEELS

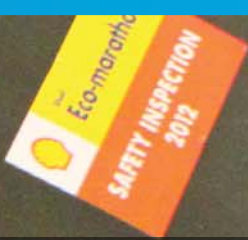




Figure 3.6.1: Exploded 3D CAD model of the rims produced in 2012

## 3.6 WHEELS

The development of the rim design started in the project phase executed in the autumn 2011. It was finalized during the spring 2012.

### 3.6.1 STRENGTH ANALYSIS

The strength analysis of the carbon fiber layup was performed in UGS NX Nastran. The carbon fiber type used was DB 420.

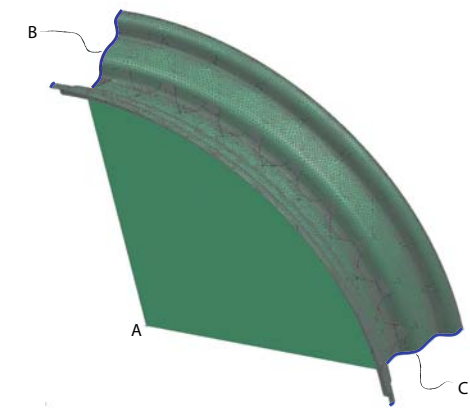


Figure 3.6.2: FE analysis set up of the rims.

At point B and C symmetry planes were applied.

An internal pressure of 5 bars was applied on the rim rings surface.

	A
DOF 1	1
DOF 2	1
DOF 3	1
DOF 4	1
DOF 5	1
DOF 6	1

Table 3.6.1: FE analysis set up for the rims.

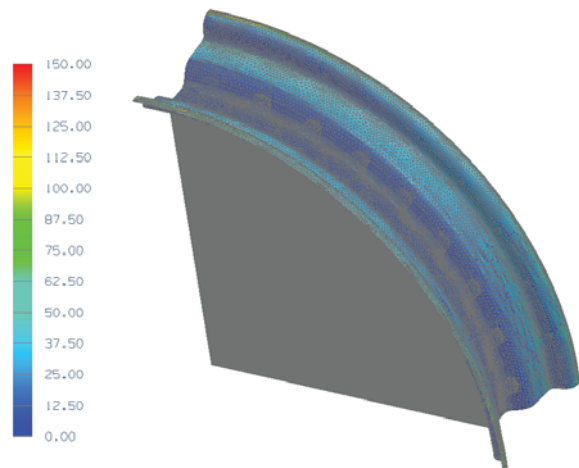


Figure 3.6.3: FE analysis results of the rims.

### 3.6.2 PRODUCTION

The mold in eboard was milled at To-mo Modeller og Interiør AS in Fredrikstad. This was a positive plug which was used to produce a negative mold in fiberglass. The result was an accurate and durable negative mold that could be used to produce a large amount of rims before its condition would be exacerbated.

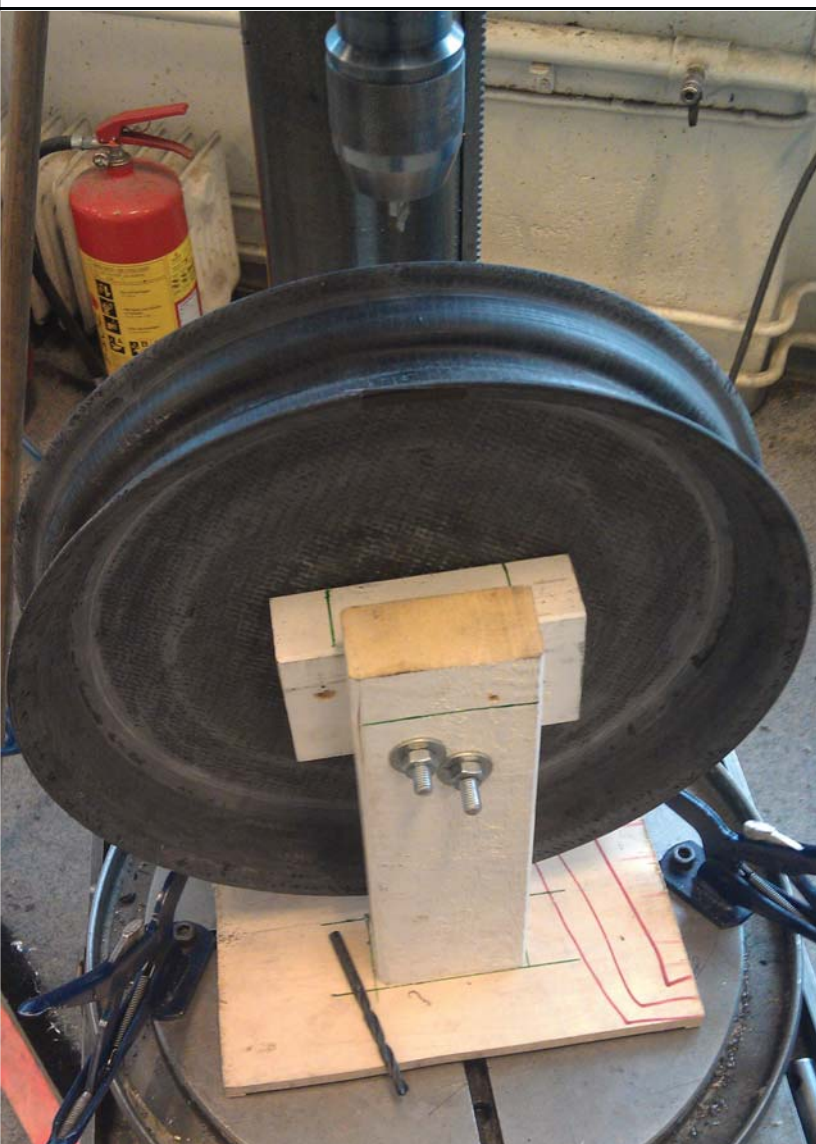
The rims were produced at HPC by using the same layup method as in 2011 (Qviller, Stockfleth, Bleie, & Hoel, 2011). 8 layers were applied, giving the rim an overall thickness of 4.0 mm. Three regular rims and one engine rim was made, plus one spare of each.

The center hole and the bolt circle on the regular rims were made by HPC, but the 45° chamfer around the center hole had been left out from the production. This was a crucial part of the rims design, and without it the rims would not fit onto the hubs. The chamfer was made by Finmekanisk

verksted at NTNU.

The hole for the valve was drilled on the rim rings inner surface, which had the most free space due to the rims asymmetric shape. It was placed there to prevent the valve from coming in conflict with the tire. A special jig was made to secure the rim while the hole for the valve was made in the drill press, and to make sure the hole was drilled with the correct angle relative to the rim rings surface. The hole was drilled with a  $\text{Ø}4.0$  mm bore, followed by  $\text{Ø}8.0$ ,  $\text{Ø}10.0$  and  $\text{Ø}11.5$  mm which is the specified bore size for the valve. This was done to avoid delamination and rough edges in the carbon fiber.

Small cracks and irregularities in the rim rings inner surface were filled with Araldite 2031. After applying the glue and sanding it down with fine sand paper the rim rings inner surface was smooth and without any visible cracks or irregularities.



Drilling of hole in the rim ring for the TR-414 tubeless snap in valve



Left: Araldite 2031 to cover up small cracks and irregularities on the rim rings inner surface  
Right: Sikaflex and PVC tape to prevent leakage



*The crack in the broken rim after testing at Dragvoll*

Testing showed that the rims were not airtight, losing pressure over time. A closer investigation revealed that air was leaking through the carbon fiber in the rim ring. This could cause the rim ring to delaminate. Air could also penetrate into the rim's center plate and cause a delamination between the carbon fiber and the foam core, causing severe damage to the rims. A thin layer of Sikaflex was added on the rim rings' inner surface. This created an airtight membrane and stopped the air from leaking through the carbon fiber. A protective layer of PVC tape was applied to prevent the Sikaflex from being damaged and further testing showed that the rims were performing well and without any leakage.

### 3.6.3 PERFORMANCE

Testing revealed that the rims were not as good as first predicted. The unevenness on the rim ring was the main problem, causing the wheel to wobble in the lateral direction when rotated. This led to reduced handling abilities and loss of energy while driving.

One rim cracked after the first outdoor testing day at Dragvoll. It happened after the car had been transported back to the workshop, and the tire had an internal pressure of 5 bars. It was reason to believe that something had gone wrong during the production process of this rim since the rim did not explode, but air was leaking slowly through a visible crack in the rim ring. The damaged rim was sent to Paal Fediuk at HPC who repaired it for

free. Testing showed that the rim was able to hold a pressure of 5 bars after the repair, but it was not used during the competition.

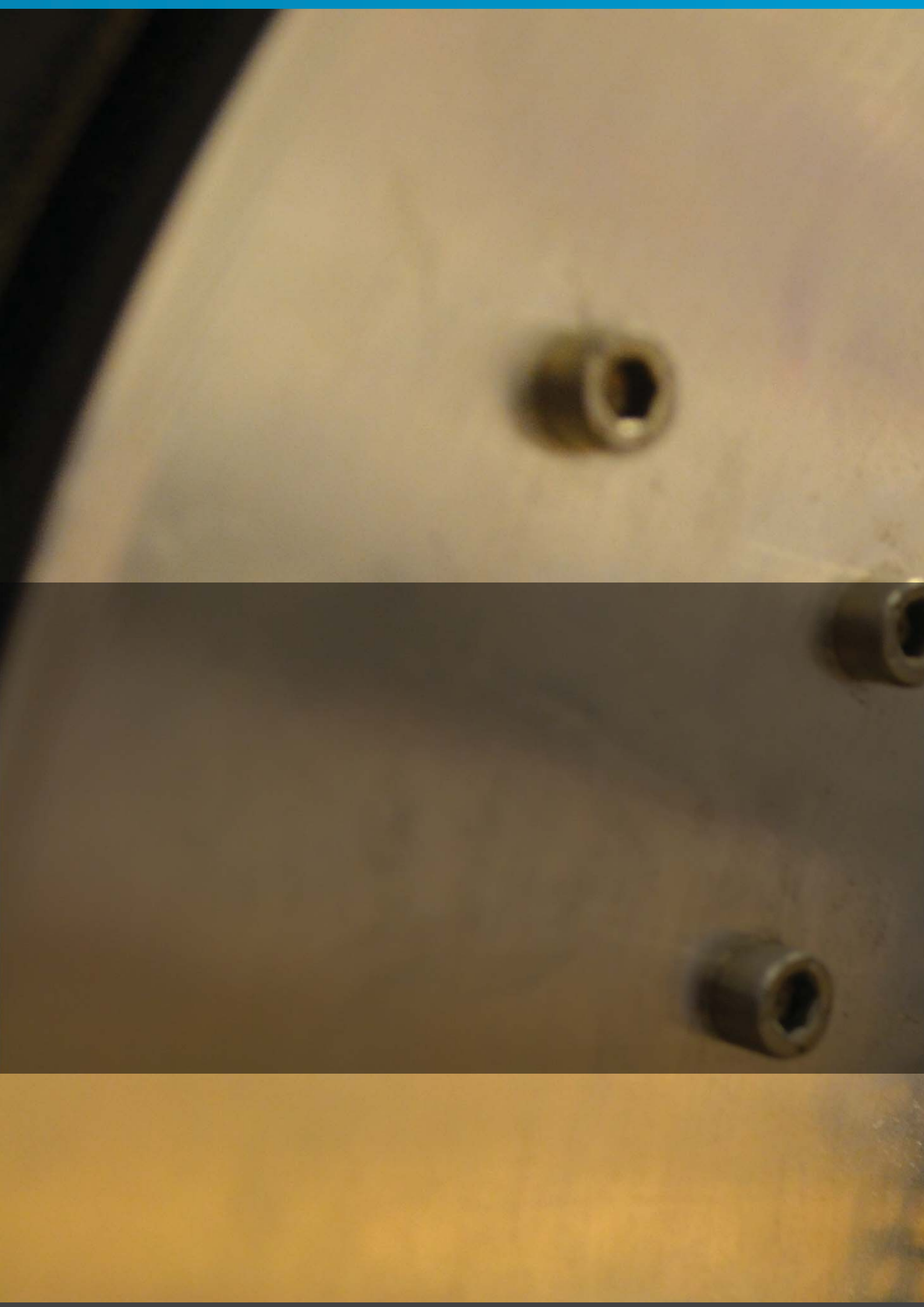
The front left rim exploded on the way back from Rotterdam. The incident happened after the car had been standing outdoors in the sun, and it is reason to believe that the energy from the sunlight had heated up the air inside the tire. The internal pressure was initially 5 bars and the heated air may have generated a high enough internal pressure to destroy the rim. Next year's team should be aware of this and not place the car in the sun without first decreasing the tire pressure. The rim has not yet been repaired.


The rims produced in 2011 are each 200 grams lighter than the ones produced in 2012. Therefore the rims from 2011 were modified to fit the new hubs, and were used on the two last attempts in Rotterdam. They performed well and could also be used next year. However, it is recommended to use them as spare rims only.

### 3.6.4 FURTHER RECOMMENDATIONS

Next year's team should make new rims. It is highly recommended to produce them in another material than carbon fiber. Several of the teams in Rotterdam had rims milled out of aluminum. Producing rims in carbon fiber is a complicated job and several risks will be eliminated by producing them in a more durable material.





A close-up photograph of a mechanical assembly. The background is a light-colored metal plate with several small, cylindrical protrusions. In the foreground, a large, curved metal ring with a series of small, semi-circular perforations is visible. Below the ring, a rectangular metal block is partially shown. The text "3.7 PROPULSION" is overlaid in white on a dark semi-transparent background.

# 3.7 PROPULSION

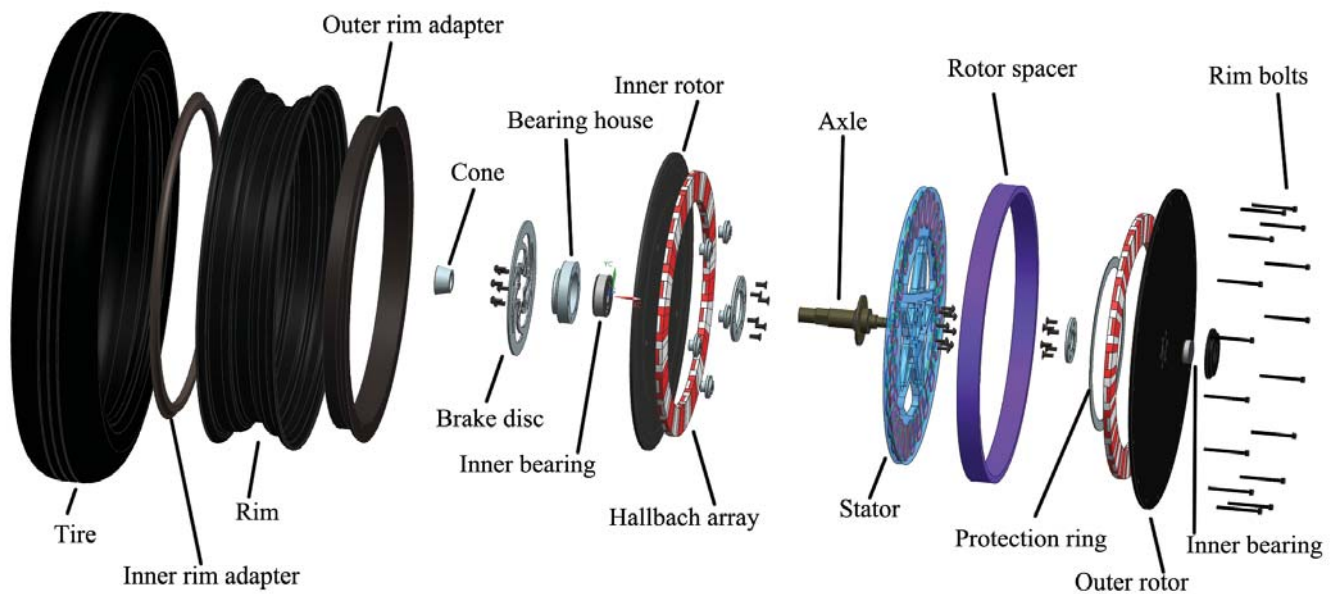


Figure 3.7.1: Exploded view of completed motor assembly

## 3.7 PROPULSION

### 3.7.1 MOTOR DESIGN

This section summarizes the work done on the motor parts. It is an improvement of last year's motor based on the specifications from last semester (Endresen, 2011).

#### 3.7.1.1 Requirements

The motor was given a budget of 100 000 NOK. In addition to service hours, SmartMotor sponsored the purchase of the magnets, which were expensive and had a lead time of many months. A significant improvement over the previous iron ring motor is the use of a Hallbach array which eliminates the need for steel cores to conduct the magnetic flux and reduces the weight of the engine considerably – if the magnets are glued directly onto the rotors.

Due to the efficiency of the motor, combined with the low nominal output (around 100 W) alleviates the need for cooling, it is therefore not a requirement.

#### 3.7.1.2 Concept Description

In general the Hallbach array motor is an incremental improvement of last year's motor, and its concept is therefore largely already determined.

Design of the stator, magnet arrays and air gaps are based on project report of Endresen (2011). The stator is a resin cast with Litz wire windings cast inside. Torque is transferred to the rim through the rotors.

#### 3.7.1.3 Hub and Axle

The new magnet array, with the removal of the iron core rings used in previous years, the motor can be made much more compact.

The diameter of the axle is designed to accommodate easy insertion of wires for the three-phase drive current. It is, however, kept reasonably thin to avoid oversized and heavy bearings.

Larger diameters enables a octagonal section that mates with the suspension. This will make it simpler to attach the motor wheel to the car as it does away with the key that easily fell out (Bleie et al., 2011).



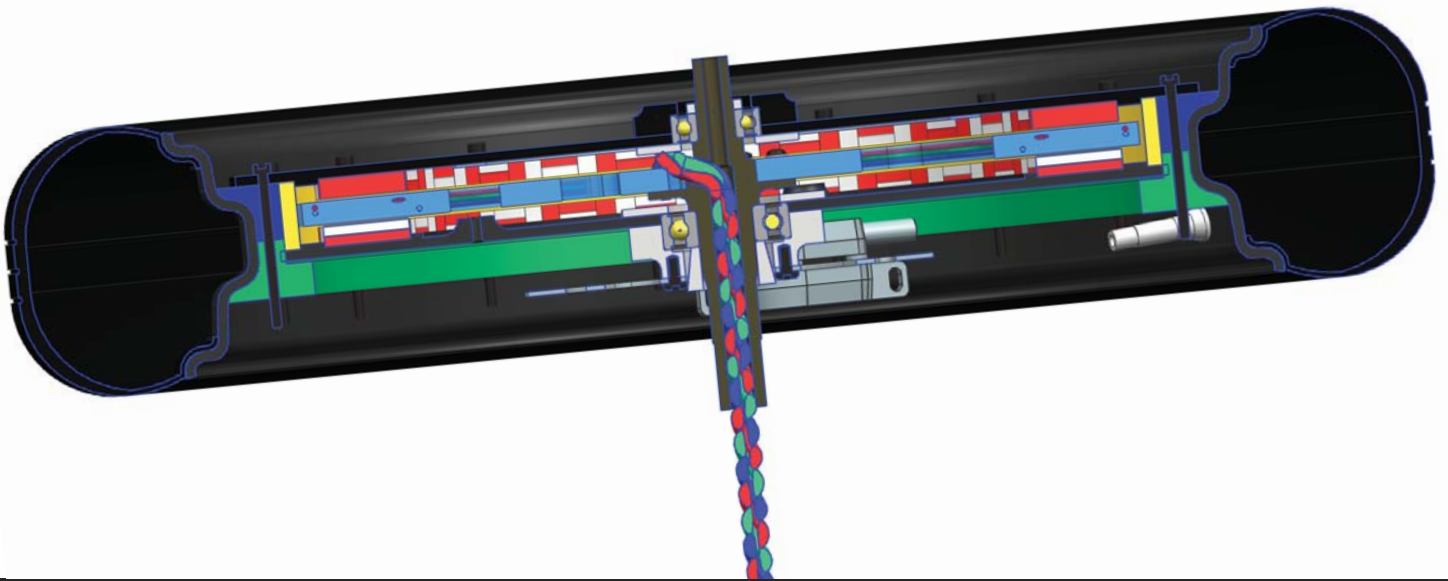


Figure 3.8.2: Cross section of motor

Requirement	Value	Must	Should
Withstand lateral force caused by cornering	$F_1$	X	
Withstand longitudinal force caused by braking	$F_2$	X	
Withstand vertical force caused by weight of car plus driver, and g-forces	$F_4$	X	
Withstand torque from braking		X	
Fit the engine rim		X	
Allow space for the three wires for the drive current		X	
Adjustable magnet air gap		X	
Non-magnetic material		X	
Support the strong magnet array	4000 N	X	
No parts interfere during rotation		X	
Separable		X	
Weight	< 10 kg	X	
Weight	< 7 kg		X

Table 3.7.1: Requirements specification for mechanical motor parts

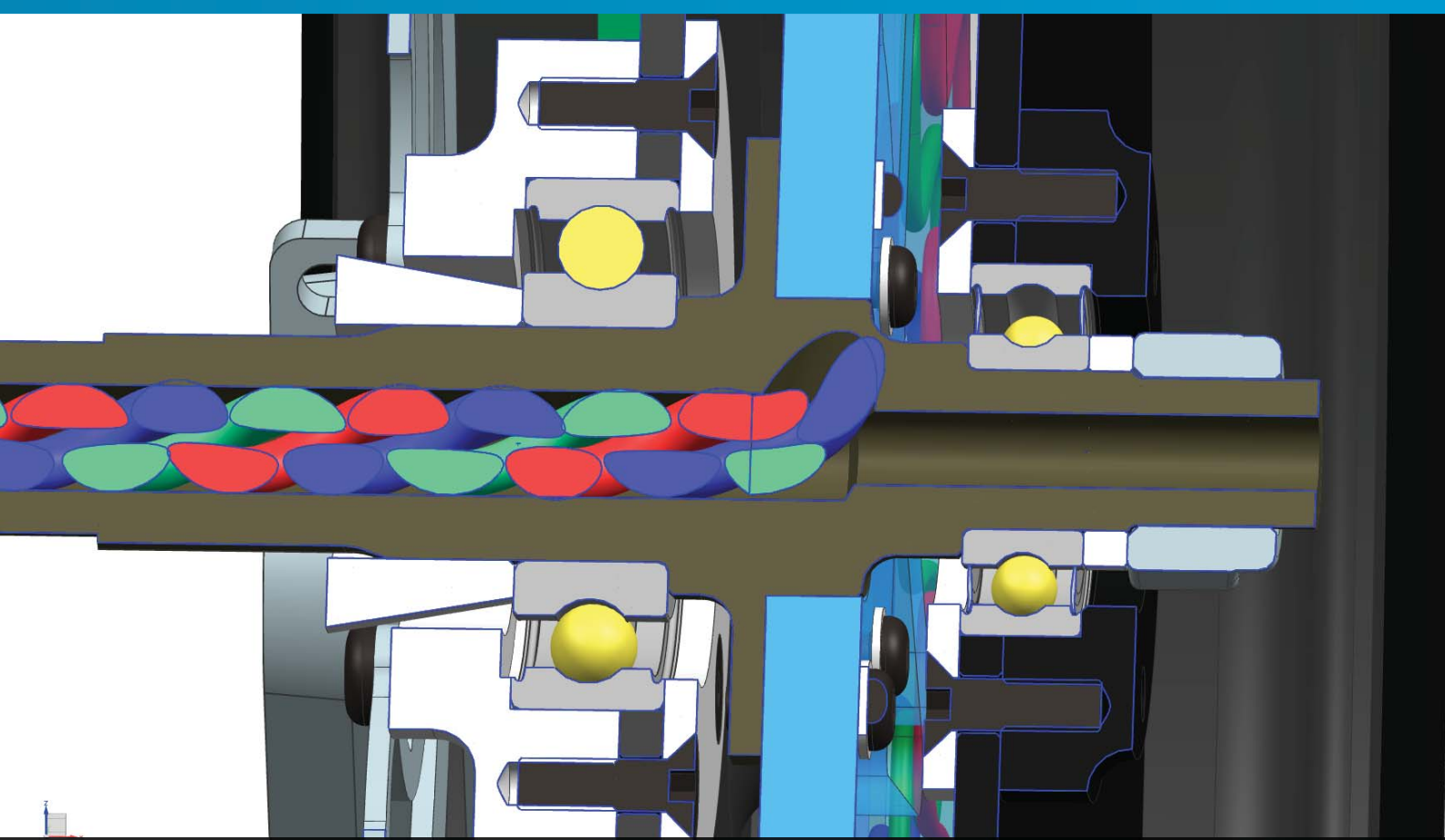


Figure 3.7.3: Close up of the motor hub

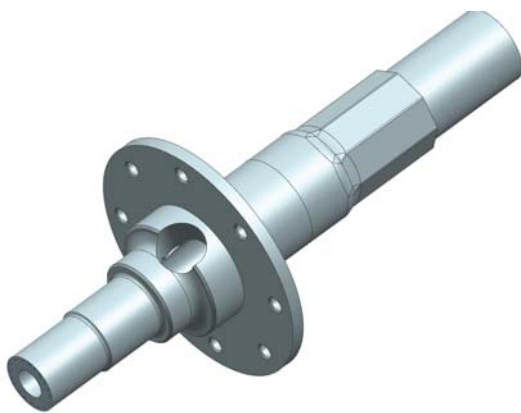


Figure 3.7.4: 3D view of the new motor axle

The motor axle will be used on the left side of the car, and as the sharpest turns go to the left, the motor axle will rarely undergo the extreme loads of hard cornering. The spreadsheet shown in appendix E was used to determine the forces applied to the inner or outer wheel of a typical curve. This is important because the lateral force developed in the contact patch is low when it acts to further bend the axle. When the force is high due to turning in the other direction, the force pushes the car up and the bending moment decrease (see figure 3.7.5).

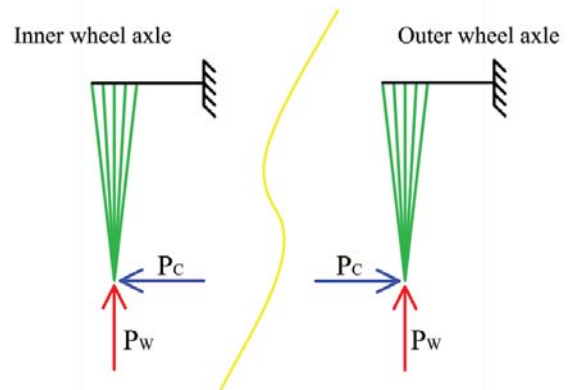


Figure 3.7.5: Load cases for an axle during cornering

S11.3\_motor\_axle\_sim1 : Bump on braking Result  
Load Case 1, Static Step 1  
Stress - Element Nodal - Unaveraged, Von-Mises  
Min : 0.00, Max : 190.16, N/mm<sup>2</sup>(MPa)  
Deformation : Displacement - Nodal Magnitude



Figure 3.7.6: FEM analysis of motor axle subject to a hard bump

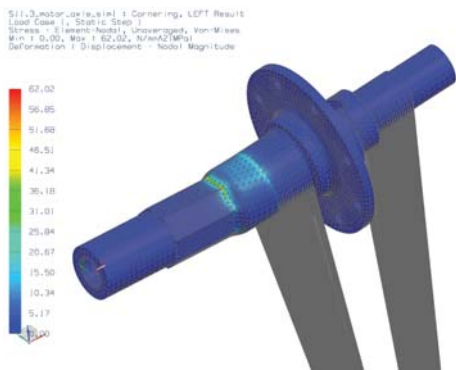


Figure 3.7.7: FEM analysis of motor axle on inner wheel of a typical, sharp curve

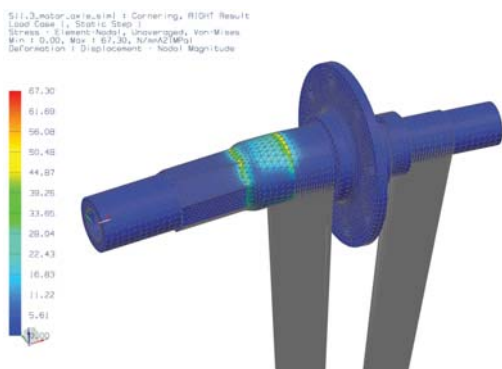


Figure 3.7.8: FEM analysis of motor axle on outer wheel of a typical, sharp curve

The simulations of the motor axle were performed without the support of the cone (figure 3.7.1) as the conditions were difficult to reproduce in NX. With the cone in place the stresses of 190 MPa from the bump simulation will be drastically reduced.

The axle was machined by Finmekanisk for 5 400 NOK, using Aluminium 7075 provided by the department.

#### 3.7.1.4 Rotors

The rotors consist of circular plates with magnets glued on. Bearing with bearing housings is placed on both plates. Due to the axles geometry, a smaller bearing is used on the outer plate to reduce friction and weight.

Figure 3.8.9 shows the rotor plates. The outer rotor (top), shows a protection ring which will be used since the rotor is made from carbon fiber, to protect the carbon fiber from the bolts used to separate the motor. The three holes (bottom plate) are threaded with M10 to allow the bolts to be inserted and force the rotors apart. Because of the strong magnets it is not possible to separate the motor otherwise. Since the plates are made in carbon fiber the three holes for separation would be made by threaded inserts.

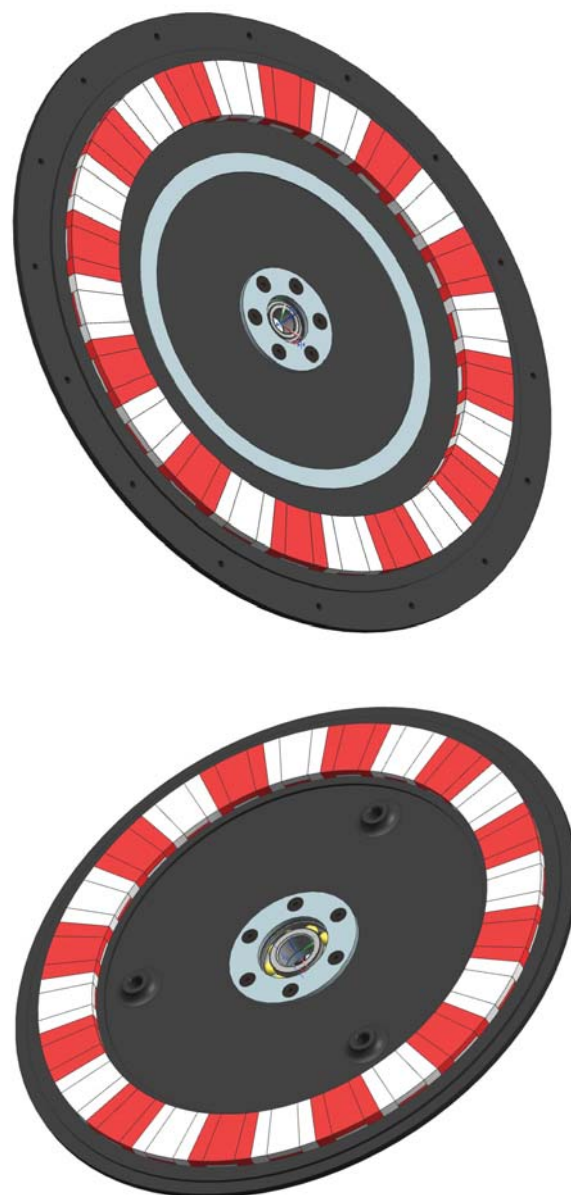


Figure 3.7.9: Outer and inner rotor with colored magnet arrays

#### 3.7.1.5 Rim Adapters

The rim adapters allow the motor to be mounted non-permanently into the rim ring. Design of the array motor is smaller in diameter than the previous iron ring motor. This allows two conical rings to be inserted from each side of the rim, and 16 M4 bolts keep the motor in place.

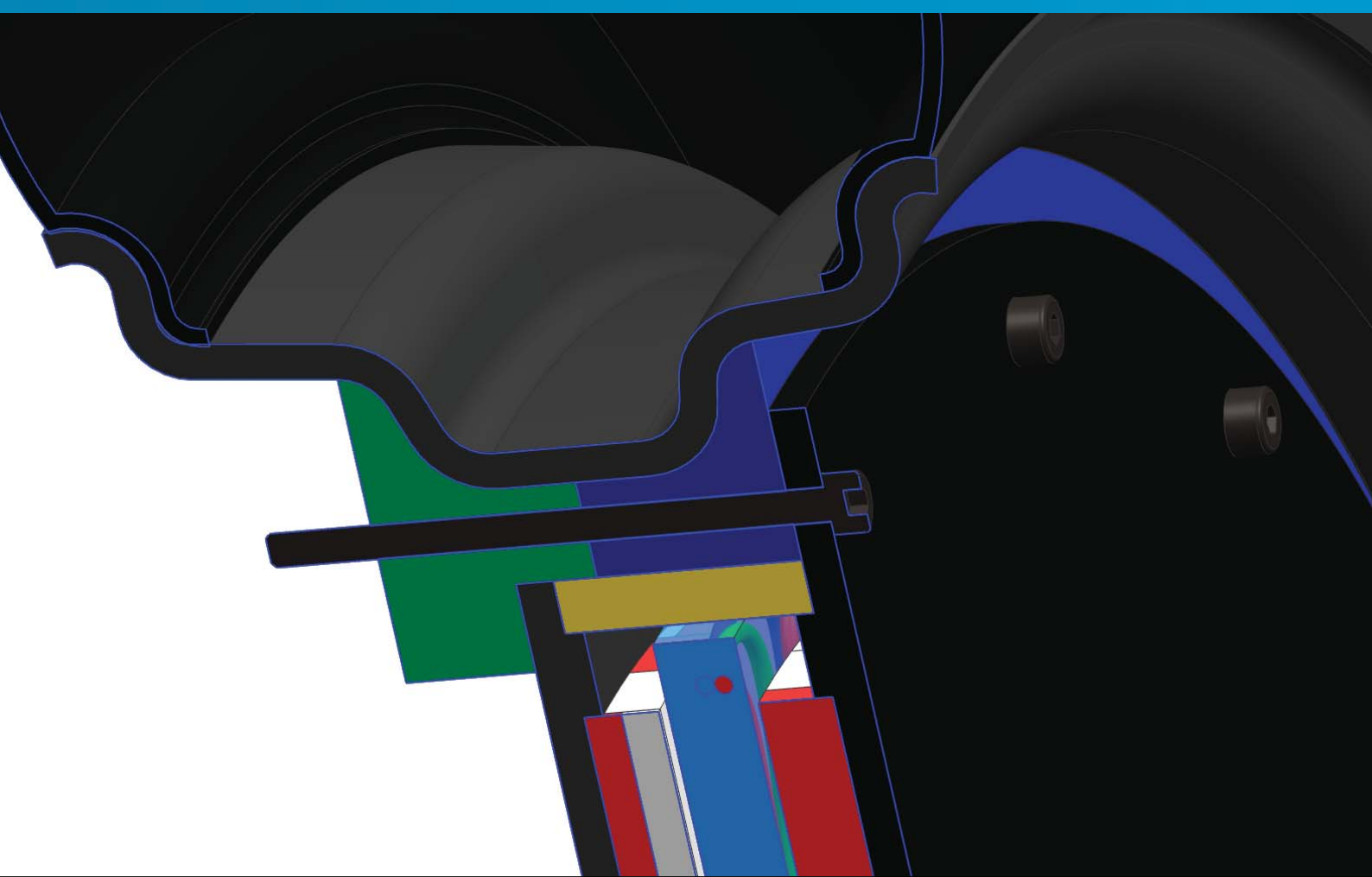


Figure 3.7.10: Close up of rim adapters, in green and blue. The yellow section is the rotor spacer

Since the outer rim adapter will be exposed to sunlight, it must be from a UV-resistant polymer, or else be coated with a UV-blocking paint. During competition the rear wheels will be occluded by aerodynamic covers anyway, but experience from testing shows that the car is tested a lot without wheel covers.

### 3.7.1.6 Test Rig and SM-Adapter

Testing the motor thoroughly is important, and SmartMotor's laboratory offers a test bench and virtually unlimited service hours. To be able to test the motor, an adapter must be produced. An aluminum adapter was produced to fit the existing test bench configuration at SmartMotors.

The adapter allows the motor to transfer torque to an opposing motor which can be used to either drive the motor or measure the energy output.

Experience from the SEM team of 2011 revealed the need to drive the motor at cruise RPM to measure the back-induced voltage during competition. The adapter is equipped with a end

tip, which can be inserted into a normal power drill.

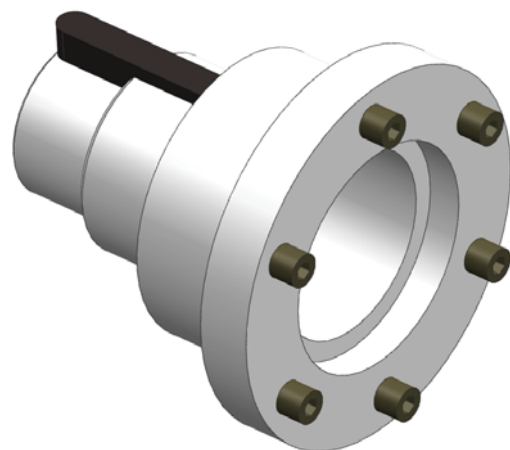
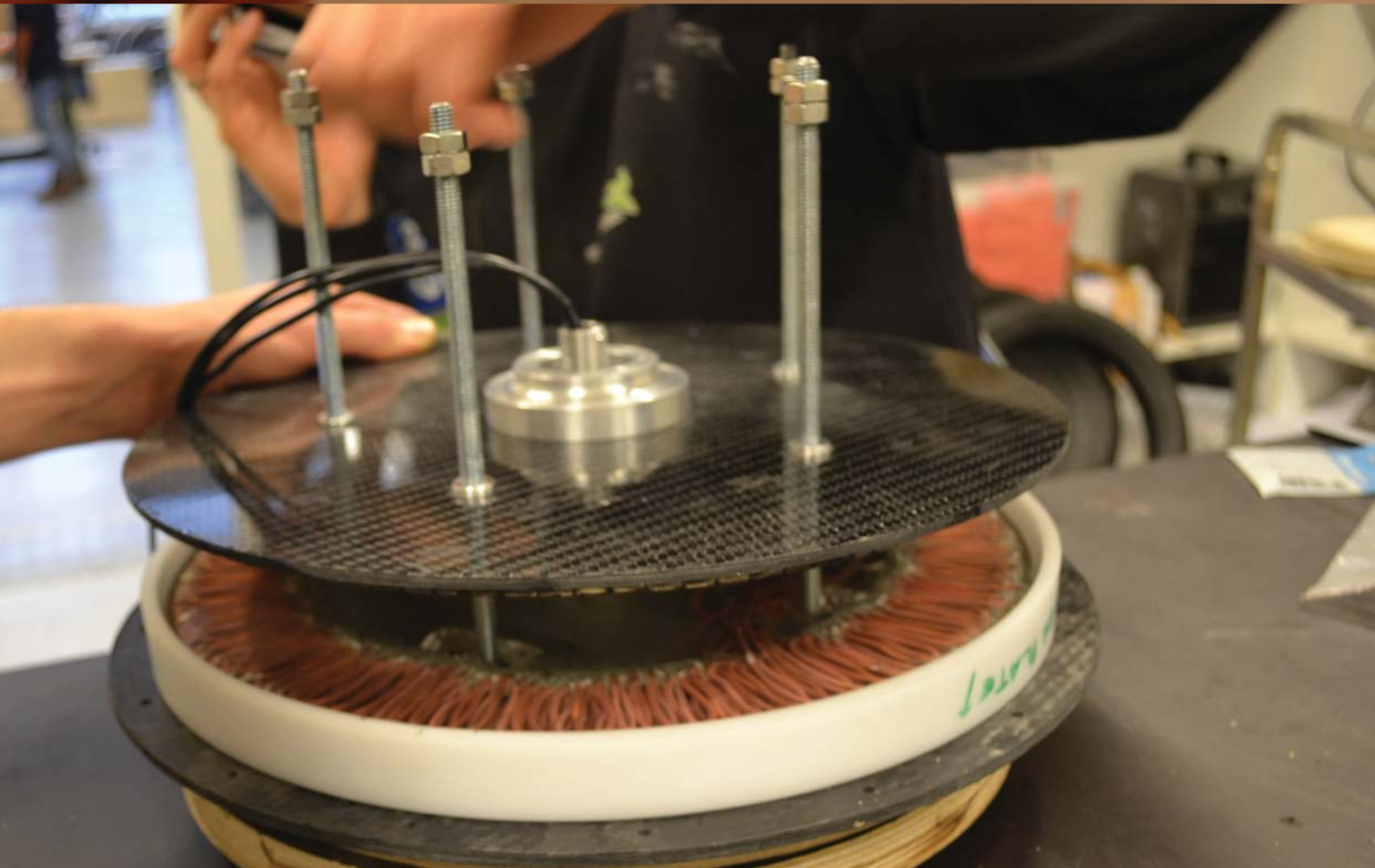
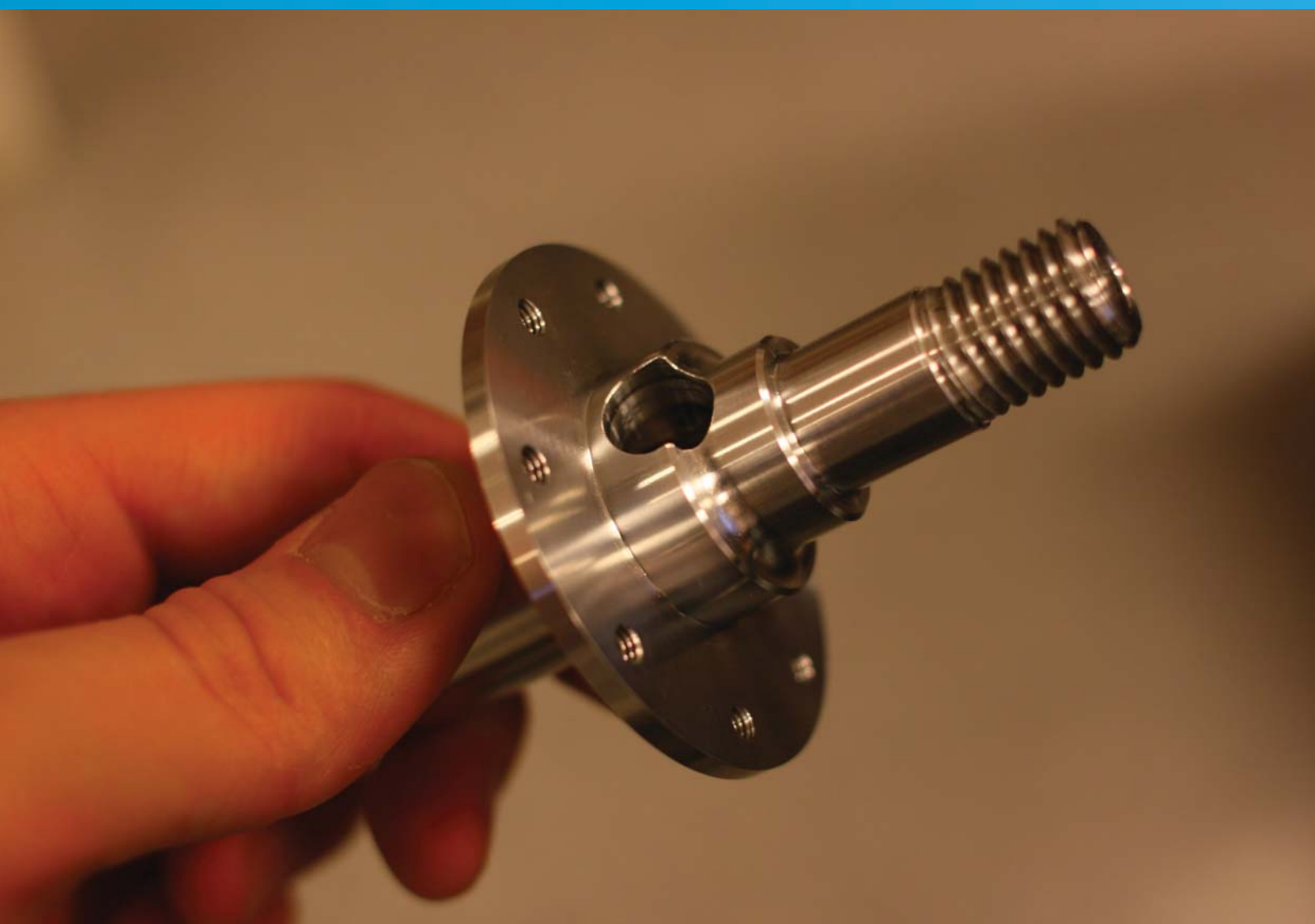


Figure 3.7.11: The new test adapter



Top: New motor axle  
Bottom: Assembling the new motor

### 3.7.2 MOTOR DEVELOPMENT

Both the motors are axial flux, permanent magnet motors with no iron in the stators. The principal difference is to use a magnet arrangement called Hallback array instead of iron rings to lead the magnetic field. A benefit of Hallback array is that the flux lines are more concentrated giving a higher flux density. Also the iron ring motor has a stator with single layer distributed windings made of enameled copper wire. The Hallback array motor has a double layer wave winding made with litz wire. There is however a great difference in size and weight. The iron ring motor has a weight of 17 kg, compared to the Hallback array motor that weighs 7 kg. Large amount of iron in the motor is the biggest contributor to the large difference. The rings location leads to a high moment of inertia.

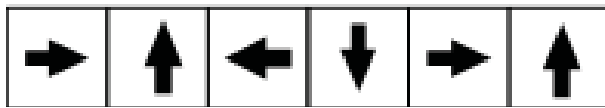


Figure 3.7.12: Magnets in a Hallback array, arrows showing direction of magnetization

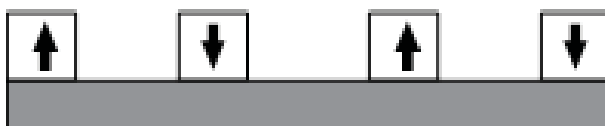


Figure 3.7.13: Magnets and iron ring, arrows showing direction of magnetization

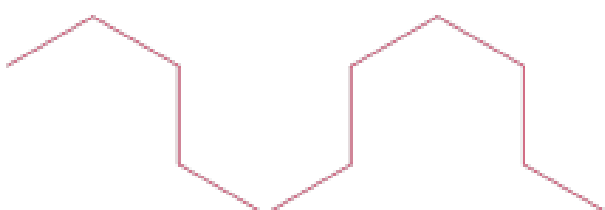


Figure 3.7.14: Single phase single layer wave winding



Figure 3.8.15: Three phase single layer wave winding

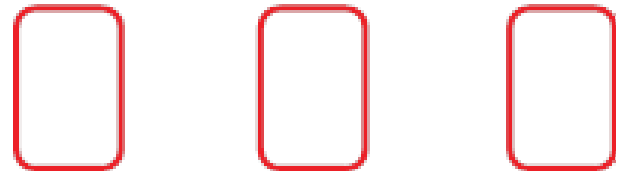


Figure 3.8.16: Single phase distributed winding



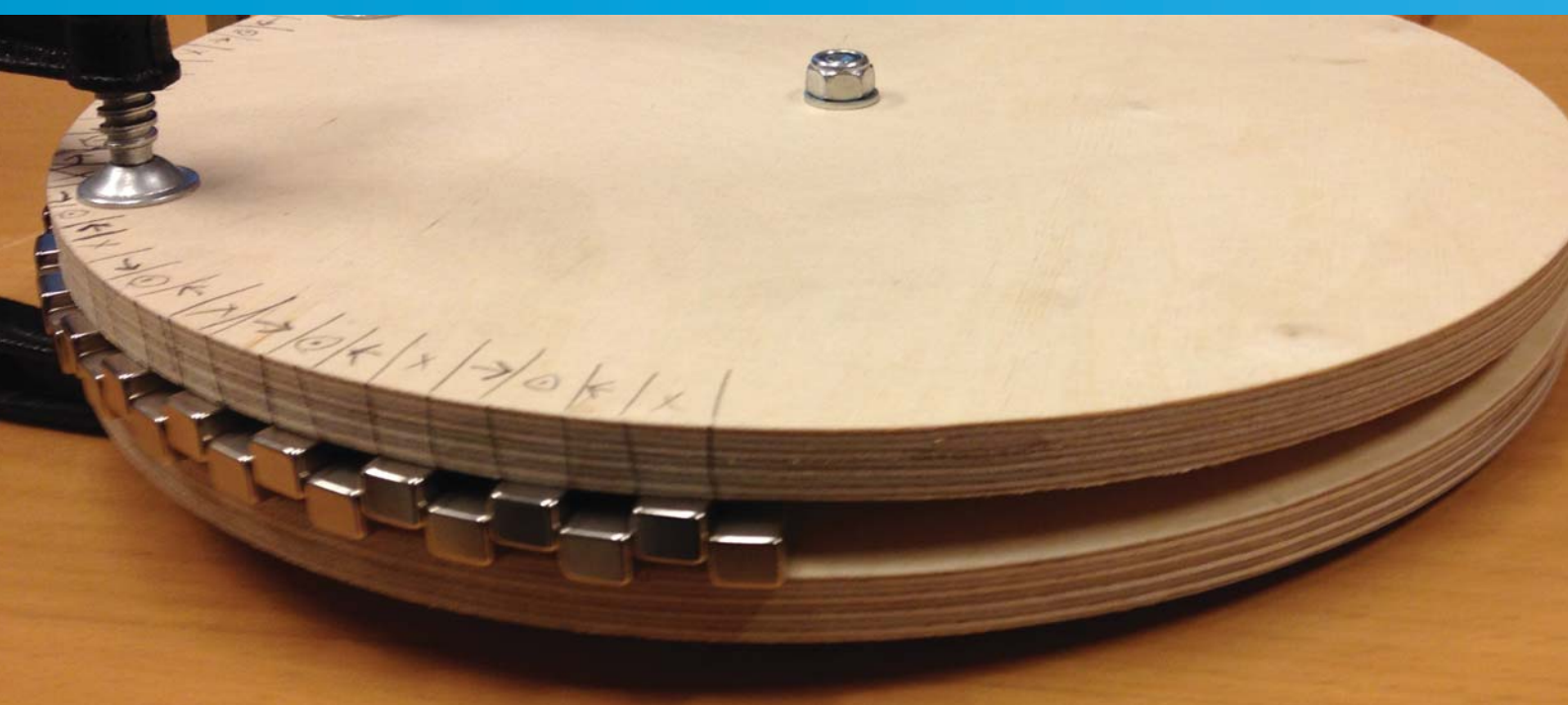
Figure 3.7.17: Three phase distributed winding

#### 3.7.2.1 Rotor

The rotor consists of carbon fiber plates and permanent magnets. Magnets were glued on with a two component Araldite. The glue was recommended by one of our major sponsors with a wide experience within composites. Before the magnets were glued, the Araldite was tested for tensile strength. Four tests were performed. Three of these showed acceptable results, the last showed insufficient glue in the necessary area. The successful tests showed that the carbon fiber delaminated before the glue failed. This makes the carbon fiber the limiting factor.

The magnets used were NdFeB N42 magnets. These were selected because of their magnetic strength and their thermal abilities. The magnets were assembled in a Hallback array before they were attached to the rotor plates. Several attempts were made in order to find the right technique for doing this. The first attempt was to use a circular wooden plate with another wooden plate of a smaller diameter centered on top of the first. Shape and diameter of the array can be controlled this way. This procedure was however unsuccessful as the magnetic field caused the magnets to turn out of position. By adding a third wooden plate on top of the center plate, the problem was fixed.

The plates were made of wood since wood is not magnetically conductive. When the magnets were arranged in the Hallback array they kept themselves in position. The magnet arrangement collapsed several times due to disturbances. An



*Assembly of Hallbach array*

important challenge was to keep all metals in a safe distance. Since the plates were fastened with a bolt and nut, wrenches were necessary. Careless handling of these caused the magnet arrangement to collapse.

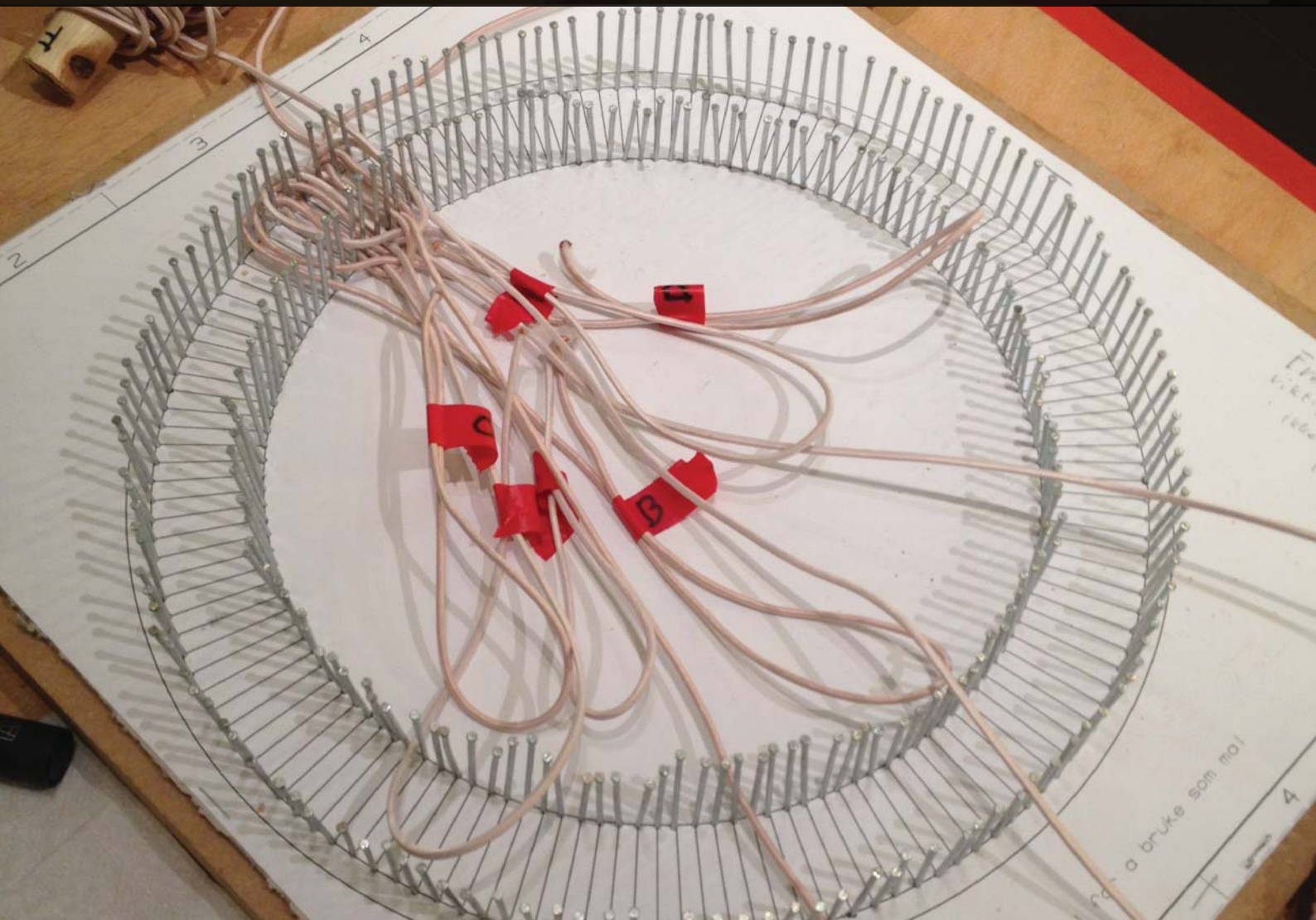
The rotor plates were made of carbon fiber. These were milled out to the correct thickness and with the proper flange to support the spacer ring and magnets. The necessary thickness was found by first calculating the forces that the plates would be exposed to. HPC suggested a thickness of 2 mm would be sufficient. To increase safety, a thickness of 4 mm was chosen.

To assemble the rotors properly, special equip-

ment had to be constructed. This was particularly important when gluing the magnets as the forces here would be especially high. When the magnets were assembled in the Hallbach array, glue was put on the carbon fiber plates. The plates were then lowered onto the Hallbach arrays. In order to get the magnets centered on the rotor plates, wide shafts were designed to exactly match the attachment holes in the rotor plates. These shafts were then put on the bolts in the center of the wooden plates used for the magnet assembly. This ensured a right position of the magnets. In addition it kept the carbon fiber plates horizontal while lowering. This led to a successful distribution of Araldite 2021 glue.



Assembly of Hallbach array



Rotor production





*Welding of stator mold*

### 3.7.2.2 Stator Production

The stator consists of litz wire and epoxy. The wire was wound on a wooden board. To ensure a clear layout of the wires a technical drawing was printed and stapled onto the wooden board. Nails were used to keep the wires in place. With three phases and 24 pole pairs, 288 nails were needed. Another wooden board was used to make an outer radius guideline. This was necessary to ensure the correct size of the coils. A margin of 1 mm was added to the diameter. Six wires were then wound in a double layer wave winding. The winding was then tied up with 288 knots to replace the nails. Cotton string was used to tie the winding as this is not magnetically conductive. Steel wire was also considered as this would have an easier assembly but this was discarded as it would lead to a higher leakage flux. The nails were then removed.

When the wires were wound, tied and properly fitted in the circumference ring, the wires were placed in the mold.

### 3.7.2.3 Mold Production

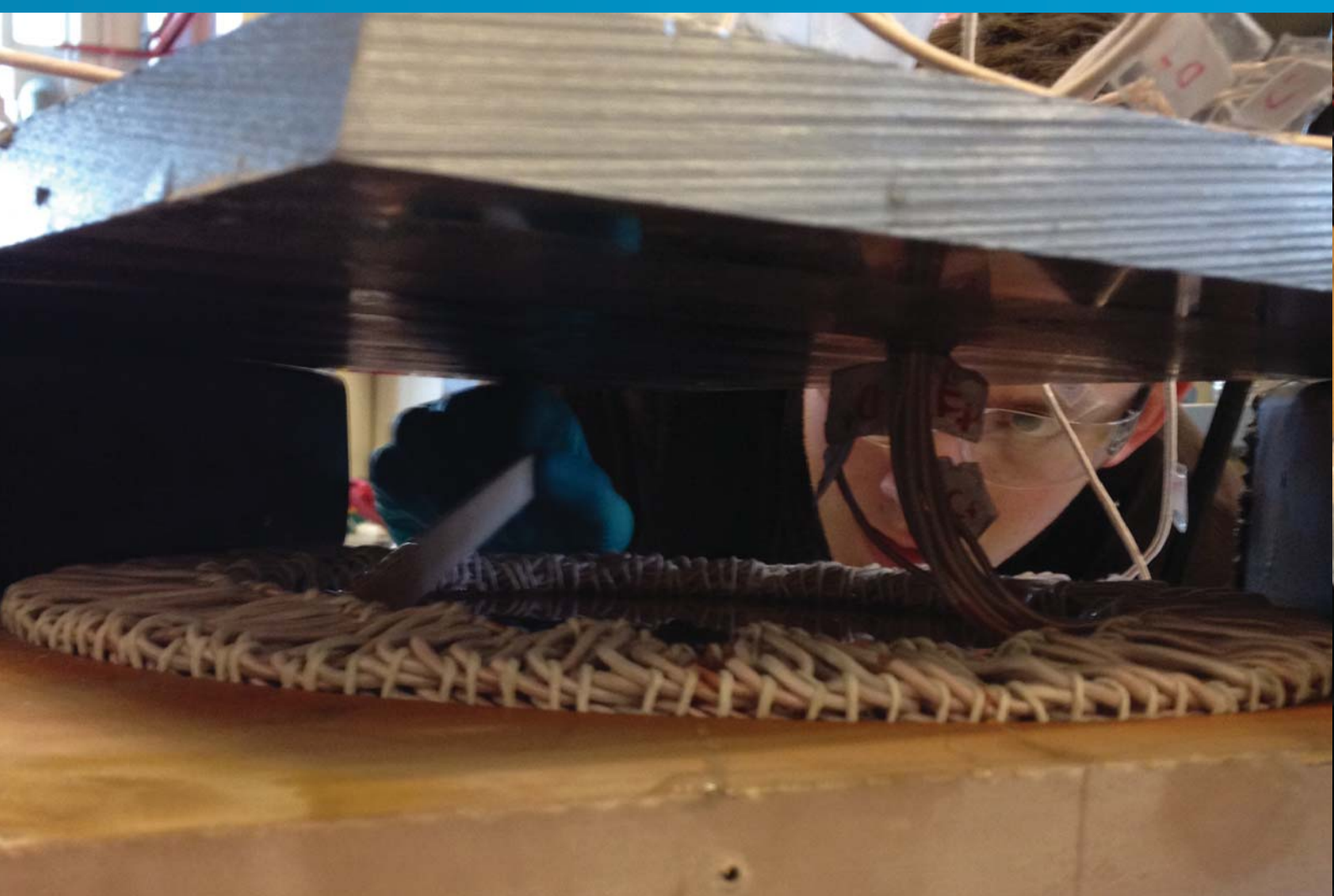
For the different stators two different molds were made. The first mold was made for vacuum casting. This was a four piece mold made of steel. The mold consisted of a plane bottom plate with an entry hole for the epoxy, two semi-circle shaped side plates and a plane top lid with exit hole for

air, epoxy and wires. In the bottom plate, four bolts were attached. These ran through holes in the remaining pieces. Bolts were intended for tightening the plates together during the vacuum process. In order to get the cast out of the mold after casting the mold needed to be covered with release agent. This was smeared on the pieces which were then baked at curing temperature for 10 minutes, three times. The pieces were baked so the release agent would set properly to the steel and to prevent it from reacting with the epoxy.

The second mold was of a simpler design, consisting of Ebaboard with a stator sized hole milled out. This was then covered with spray paint and wax. Spray paint was used to fill the pores in the material and the wax was a release agent suitable for low temperatures. The same lid was used for this mold to squeeze the wires.

### 3.7.2.4 Open Casting

The open casting technique used the ebaboard mold. Windings is placed in the mold with wire ends coming out of the top lid. Epoxy is poured in and the lid is pressed down. This causes some of the epoxy to overflow the mold. Before production, too little epoxy was prepared, resulting in shortage of epoxy. Still, this stator had many of the desired properties.



*Open casting of the second stator*

### **3.7.2.5 Vacuum Casting**

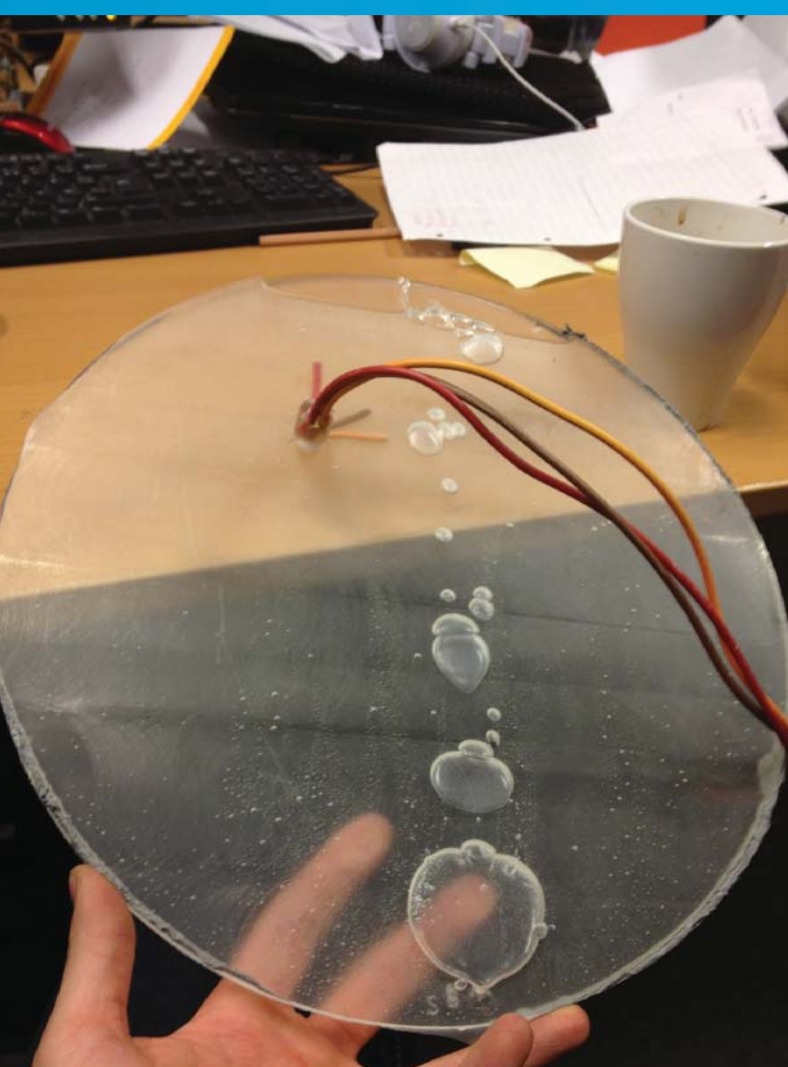
The method of vacuum casting was recommended by professor Nils Petter Vedvik at IPM, as a casting method suitable for electrical equipment. This method will, if performed successfully, give great dielectric properties and prevent partial discharges. In this design partial discharges is not an issue and it would therefore be acceptable with minor imperfections in the cast. However, casting the stator was quite challenging.

A vacuum pump was connected with tubes to two safety chambers in series, before it was connected to the topside of the mold. The mold was slanted so the outlet tube was positioned higher than the inlet tube. This configuration enabled the mold to be filled with epoxy in a controlled manner. The epoxy would flow into the mold and it was easy to see when the epoxy would come out of the topside. When this happened the outlet tube was blocked and the epoxy would continue to fill the mold until the pressure inside the mold was equal to the atmospheric pressure. One major challenge here was to keep all interfaces airtight. All connections were covered

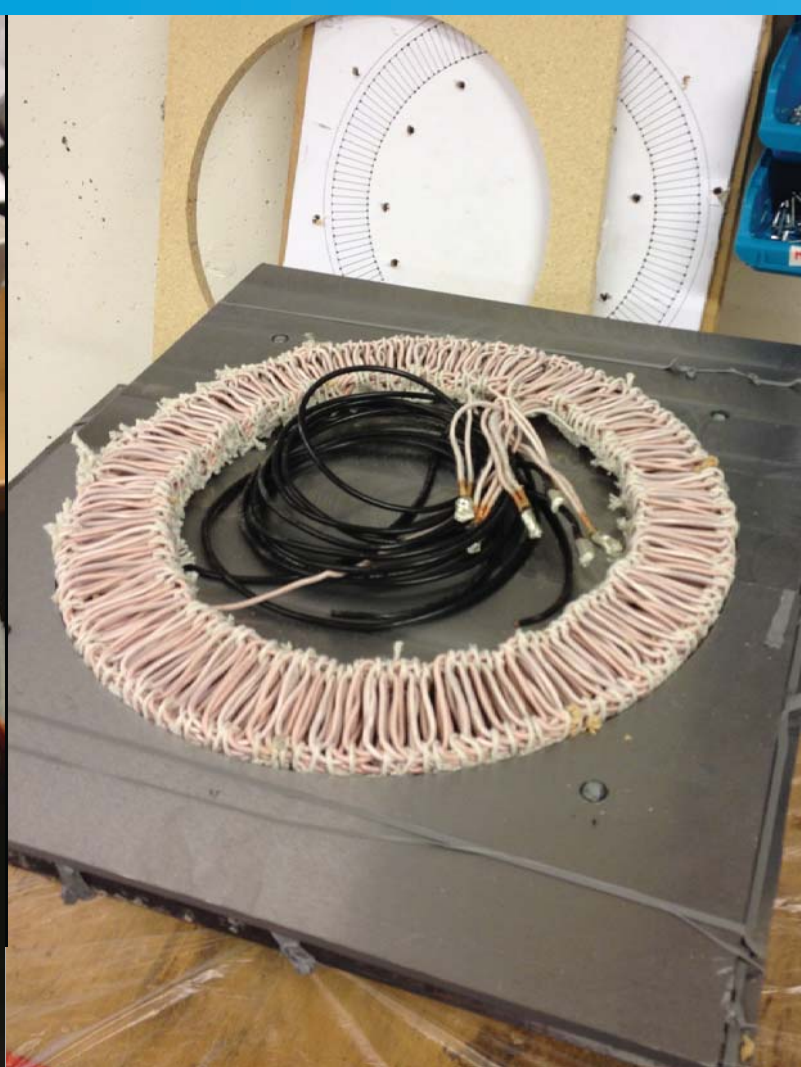
with sealing tape, but the mold was particularly challenging to seal. This might have been due to the welding done when making the mold, as this may have created an air canal from the side of the mold. The distance between the pressure bolts was too long for supplying the right pressure in between the bolts. This problem was solved using clamps along the circumference of the mold. In order to check the cast procedure several test stators were made. When the first test stator was made it included three wires coming out of the mold for simulating the power cables and a bundle of litz wire was also tied tightly and put in the mold. This was done in order to examine how the epoxy would surround the litz wire.

### **3.7.2.6 Spacer Ring**

To keep the rotor discs at a desired distance, a spacer ring was constructed. The ring was supported by a flange in the rotor discs. In order to achieve the right mechanical strength polyoxymethylene (POM) was selected as material. The flanges in the rotor discs were highly necessary as there was a very small margin for misplacement. Any misplacement of the spacer ring would



*Left: Air bubbles in the first test stator produced with vacuum casting  
Right: Preparing the vacuum casting of the first stator*



lead to rubbing between the spacer ring and stator.

### 3.7.2.7 Assembly of the Motor

The stator was to be fitted on an aluminum axle made especially for this project. Necessary holes needed for fitting and securing the stator on the axle were milled out.

The stator was mounted on the axle and the three power wires were lead through the hollow axle. Wires would then come out on the inner side of the engine, the side facing the car. Rotor plates were fitted with ball bearings in the center holes. The axle was then put through the ball bearing in the outer plate and the spacer ring was then put on, surrounding the stator. Last, the inner rotor plate was to be lowered onto the remaining parts. Since the magnetic forces are very strong, this process needed special tools. Five holes were made in the inner rotor plate and fitted with threaded inserts of aluminum. These inserts would allow assembly of the motor plates with threaded rods. The rods went through holes in the stator and down to the outer rotor plate. To

reduce the wear on the outer plate, an aluminum ring was glued to the outer plate where the rods would come in contact. With all this equipment in place the inner plate could be lowered onto the rest of the motor.

### 3.7.2.8 Problems Regarding the Construction

When the motor was assembled the axle was spun. Clear cogging force was experienced, similar to that one may find in iron based machines. Since the motor is completely ironless, this indicated a short circuit in the stator. The motor was then brought to Smart Motor for testing. Using a separate engine, the motor was spun as a generator and torque was measured. Even with open wires the machine still needed 7 Nm just to spin at rated speed. Since there was no mechanical issue regarding the motor, the motor was disassembled and the stator removed. The motor now spun freely. This showed that the problem was stator related. The stator was inspected visually and by loading it with a high current while examining it with a thermal camera. Still, no problem were found.



*Thermal camera used to examine the first stator when it was exposed to high current*

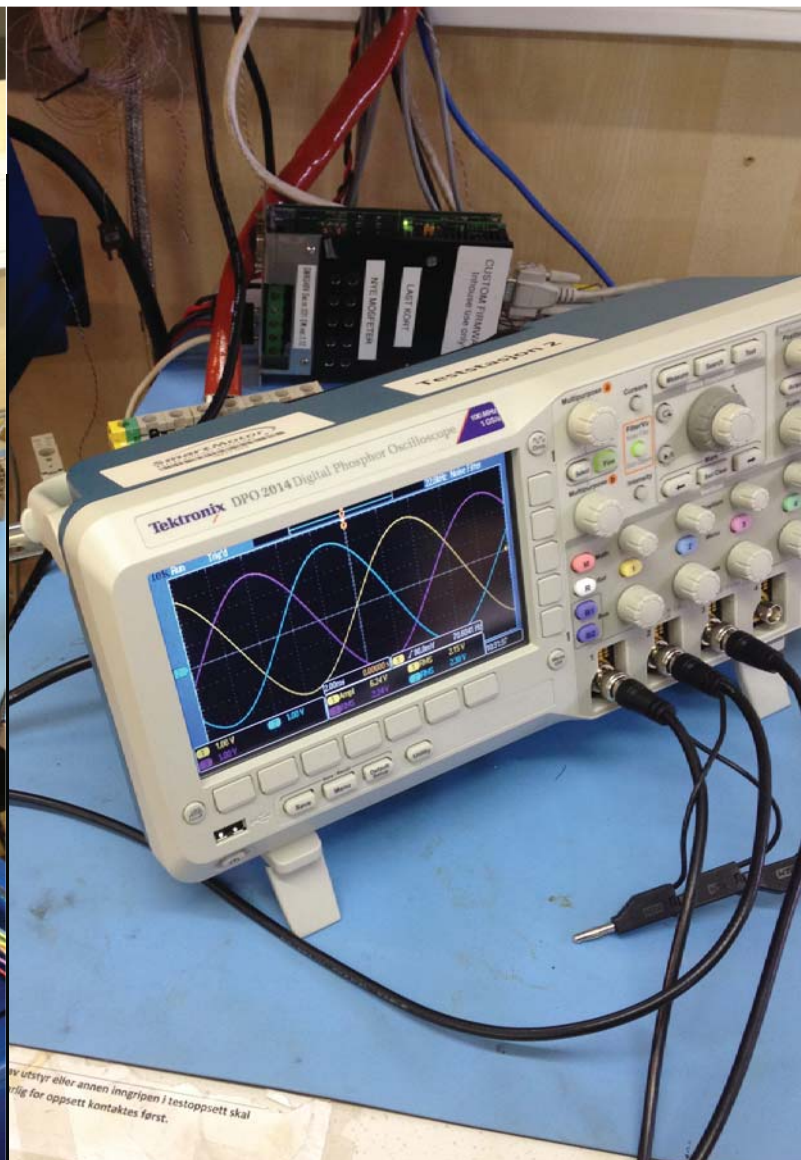
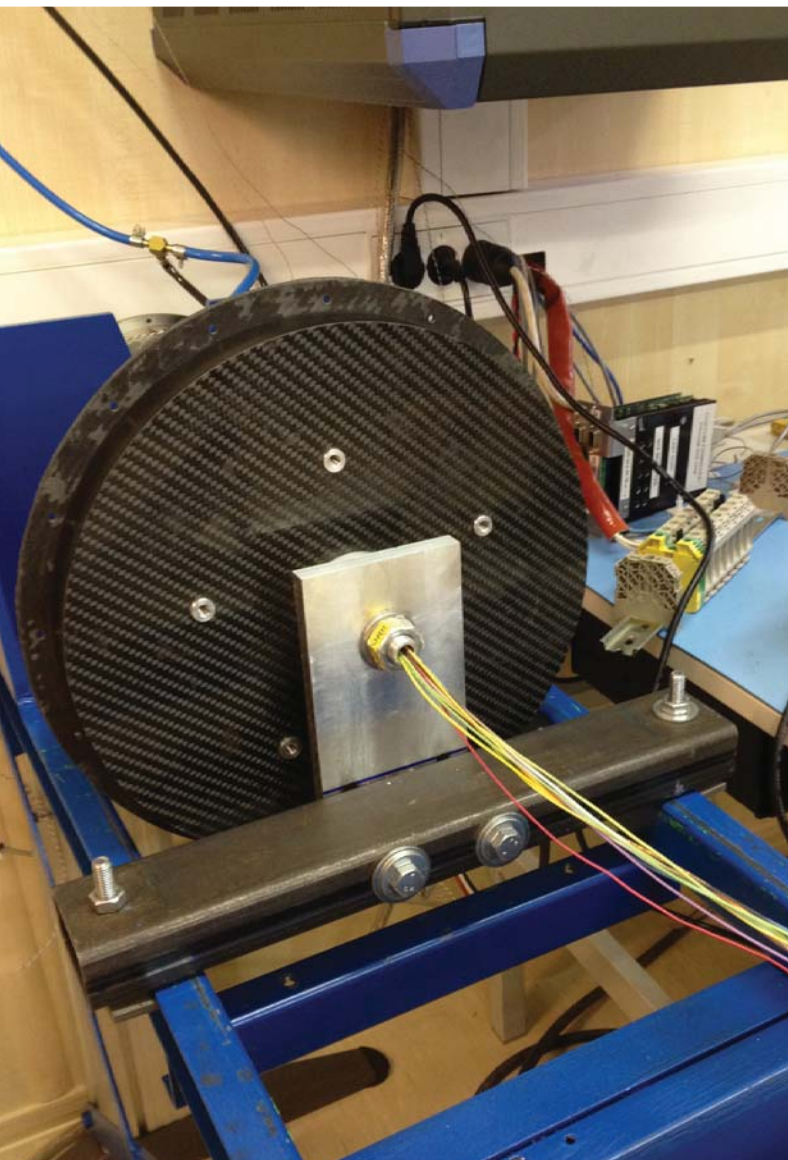
After this a new stator was constructed. Due to the problems with the first stator it was a high priority to keep all connection points out of the epoxy.

Since the outer shielding of the litz wire was made of silk and nylon, it was not airtight. It would therefore be difficult to use vacuum casting and get the wire ends out of the mold. Therefore, the production method was changed to open casting. After the new stator was casted, it was assembled and tested. Tests showed an induced voltage much lower than anticipated. The connections were then opened and each wire end was connected to thinner wires which were lead through the axle. This enabled monitoring of the voltage induced in each winding. All the induced voltages were as expected. This concluded that the wires had originally been connected so the induced voltages counteracted each other.

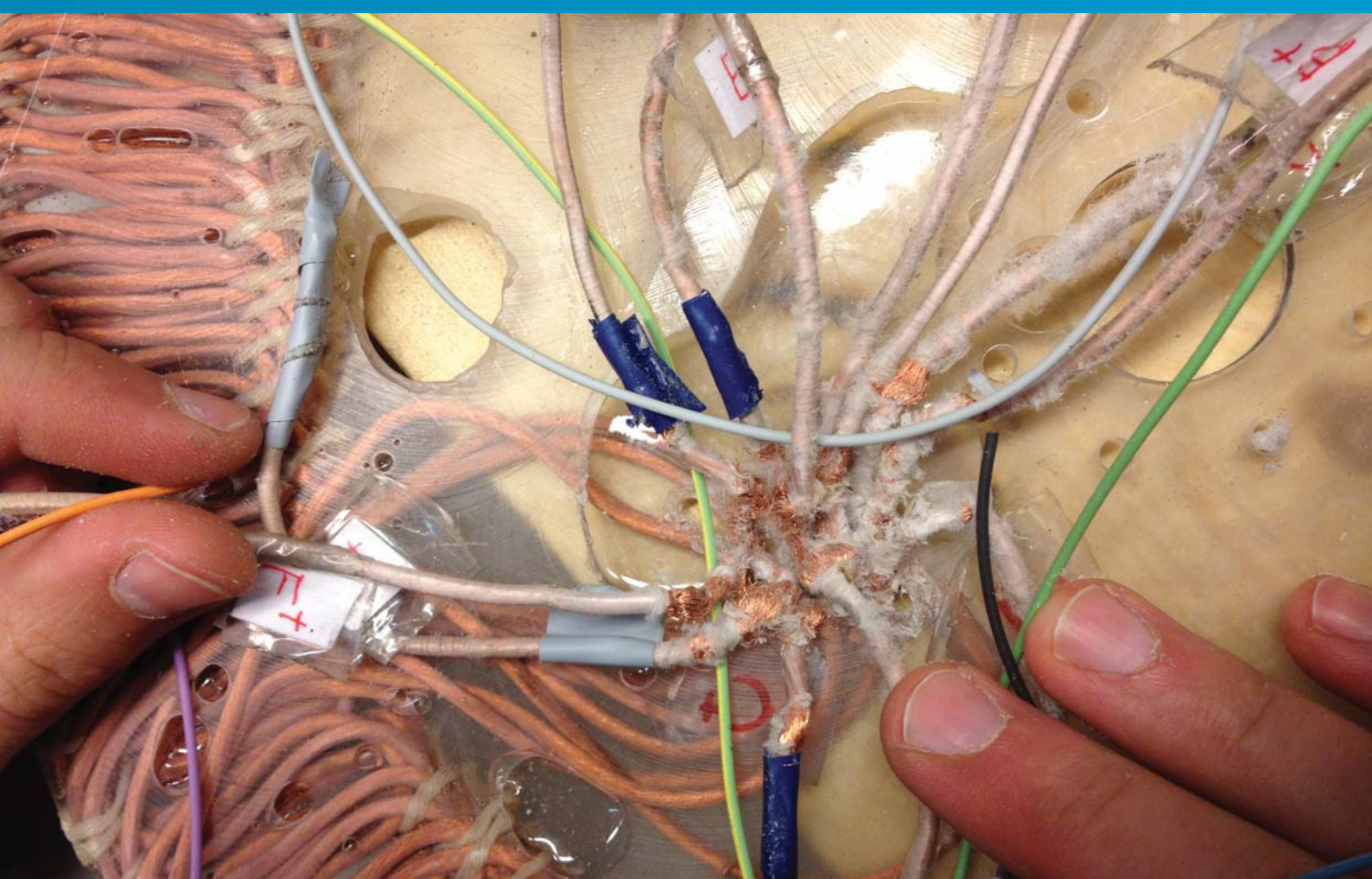
When the measurement was done the windings were reconnected in the correct order.

One severe problem with this stator was that since all twelve wire ends needed to come out of the cast, the wires needed a lot of space in the axial direction. This led to a bigger air gap than what the engine was designed for. Since the torque is  $\tau = B \times l$ , more current is needed to achieve the same torque. The loss is dependent on the current  $P_{\text{loss}} = R \times I^2$ . A bigger air gap lowers the motors efficiency.

Due to limited time, the Hallback array motor was not finalized, there was therefore decided to continue using the iron ring motor. Further testing and optimization was therefor initiated at SmartMotors.



Left: Engine with all wire ends accesable  
Right: Induced vltages in the new engines final winding setup



Damaged litz wire

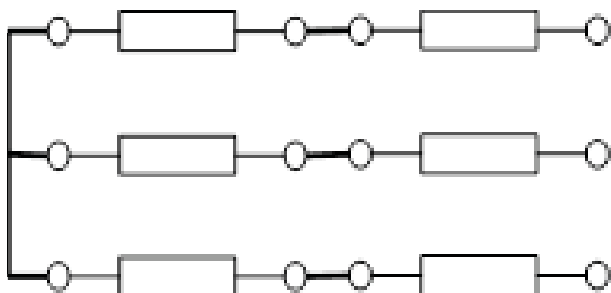


Figure 3.7.18: Winding connection

### 3.7.2.9 Testing the Existing Motor

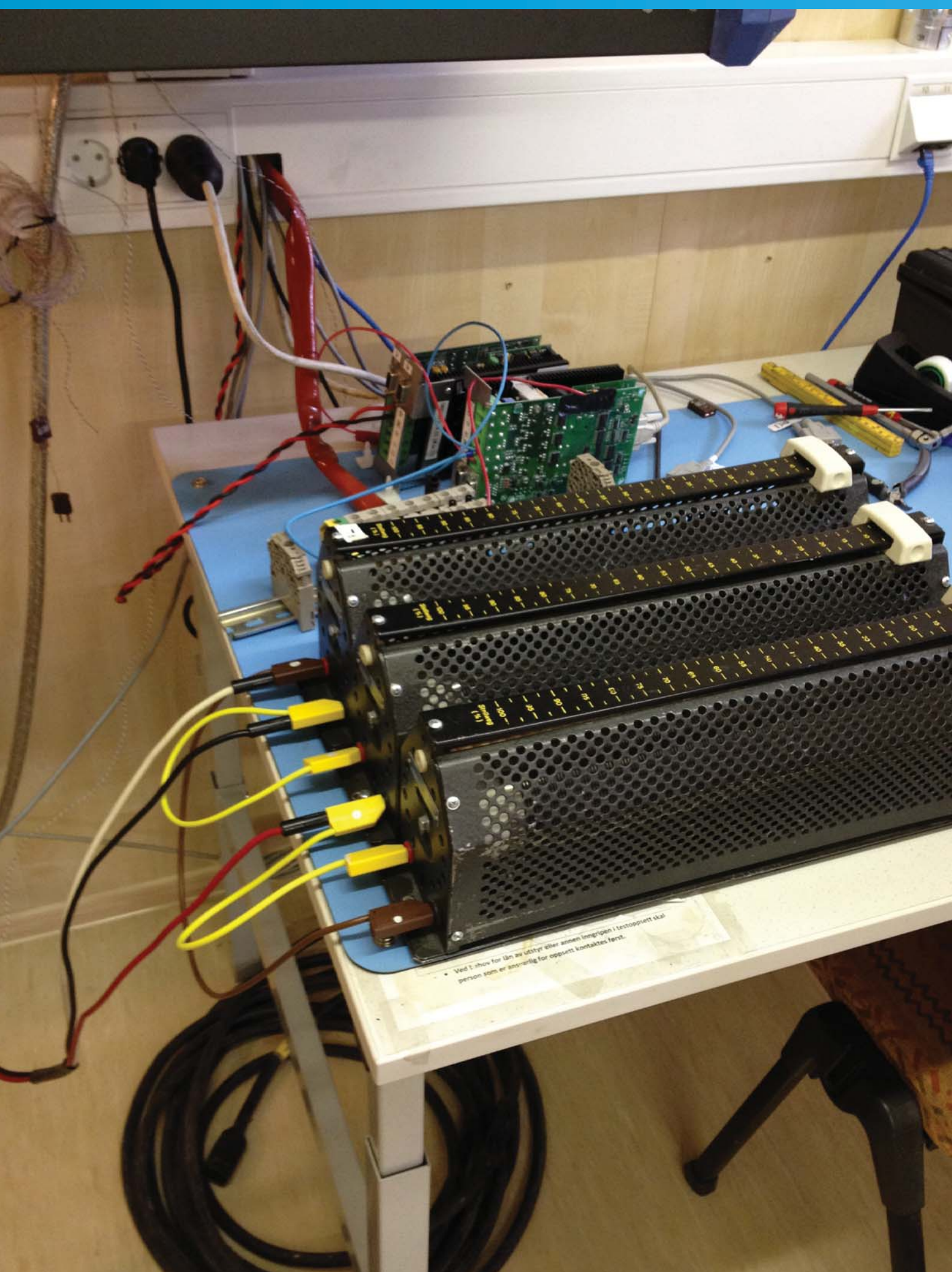
The tests were performed using the battery intended on board the car. The air gap of the iron ring motor was decreased as planned (Endresen, et al., 2011). The project is sponsored by two suppliers of different batteries. It turned out that the battery pack with the highest number of Ampere hours had a significant voltage drop. It was chosen to increase the air gap as a middle ground and this seemed to work. It was later discovered that the other battery pack had a much lower voltage drop. Unfortunately this battery pack had a lower energy capacity than the first battery. A third battery pack was therefore ordered which had twice the capacity of the second.

In order to burn off the power supplied by the engine from the battery, three resistors were connected in a delta-connection. These were then connected to the terminals of a load engine. This was done because the electronics normally used to drive the test engine were not able to receive the induced power.

In between the motor and the test motor a torque meter was connected. The torque was controlled by adjusting the resistors. This solution supplied constant torque for all steady states, but changed with the speed. This is due to the fact that the induced voltage is proportional to the speed, while the counter torque is proportional to the current. The current is a function of voltage and resistance. Therefore it was impossible to check the transition between operating points.

$$V \sim \omega \quad I = \frac{V}{R}$$

$$T \sim I \quad T \sim \frac{\omega}{R}$$



Ved t. show for lån av utstyr eller annen innrigning i testoppsett skal person som er ansvarlig for oppsett kontaktes først.

Resistor setup

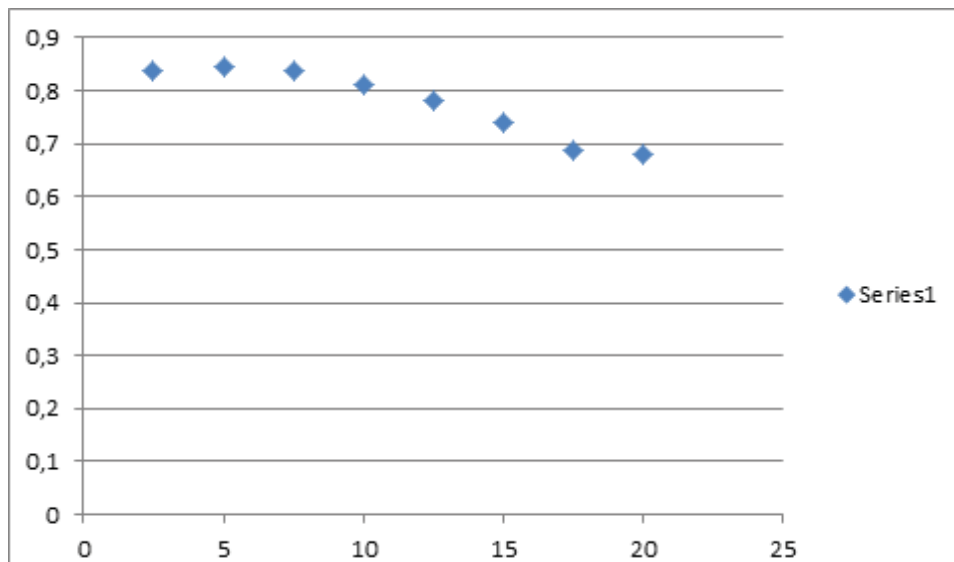


Figure 3.7.19: Efficiency as a function of torque of the old engine at 300 rpm, 31,55 km/h as it was in 2011

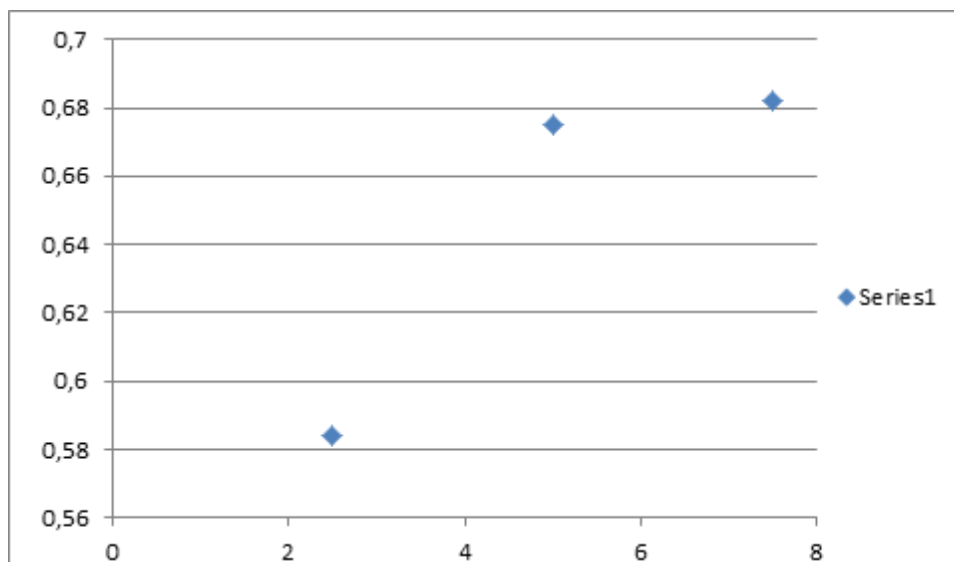


Figure 3.7.20: Efficiency as a function of torque of the new engine at 257,5 rpm, 26 km/h with the smallest obtainable air gap

The efficiency of the drive train is limited by two factors, air gap and back induced voltage. Lowering the maximum speed will increase total efficiency.

### 3.7.2.10 Conclusion

The car had not been tested under windy conditions. When the car was accelerating facing the wind, this required more current than the battery was able to deliver. The battery management system shut down and the car stopped. This was solved by rewriting the code in the acceleration program to have a lower acceleration.

The engine was also modified. Since the engine

had an air gap adjusted for the first battery pack with a high voltage drop, the air gap was reduced to better match the second battery pack with a more stable voltage. This was done by first reducing the air gap, then using a drill to spin the engine at nominal speed, measure the back induced voltage and implement the new parameters in the engine controller. No more changes were made to the engine for the rest of the competition.

The Hallback array motor is operational but it is not as energy efficient as it should. This could be greatly improved by making a new stator. Experience shows that the stator width could probably



be reduced from 8.7 mm to about 6 mm. The wires should not be taken out of the stator cast. Instead the wires should be soldered onto connection rings that are casted into the mold. When the cast has cured, one can drill away the epoxy to free these rings and thereby connect the windings without using too much space in the axial direction. It is also recommended to keep all twelve wire ends available for connections as this makes it easier to make changes if mistakes are made. Another advantage of this is that the windings can be connected in parallel instead of series as they are now. This would allow a higher current and thereby a higher torque. This could be useful during acceleration.

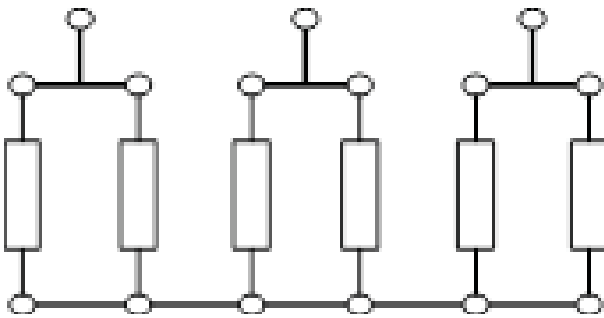


Figure 3.7.21: Possible winding arrangement

Soldering the wires to connection rings also

makes it easier to perform tests on the windings. One test that is interesting is the Megger test. Here a high voltage is applied across two windings that are not connected and measure if there is any current flowing. This is interesting when working with litz wire since partial short circuit may occur.

One severe issue with the existing drive train is the moment of inertia of the motor. The old motor consists of big magnets and a heavy iron ring placed far away from the axle. This makes it easy for the engine to create a high torque but it also gives a high moment of inertia. The new engine has a lower total mass with smaller magnets and no iron. This gives a lower moment of inertia but it should be considered if a new engine setup could be preferable. The problem with having a high moment of inertia is that it requires a lot of energy during acceleration. In 2012 the competition had a shorter track than before and the driver had to do more laps with a complete stop in between in each lap. This made it more necessary than ever to reduce the needed energy for the acceleration process. Also the engine controller draws a large current at slow speeds, typically less than 0,2 per unit.





Med

Low

R28

R31

R26

R29

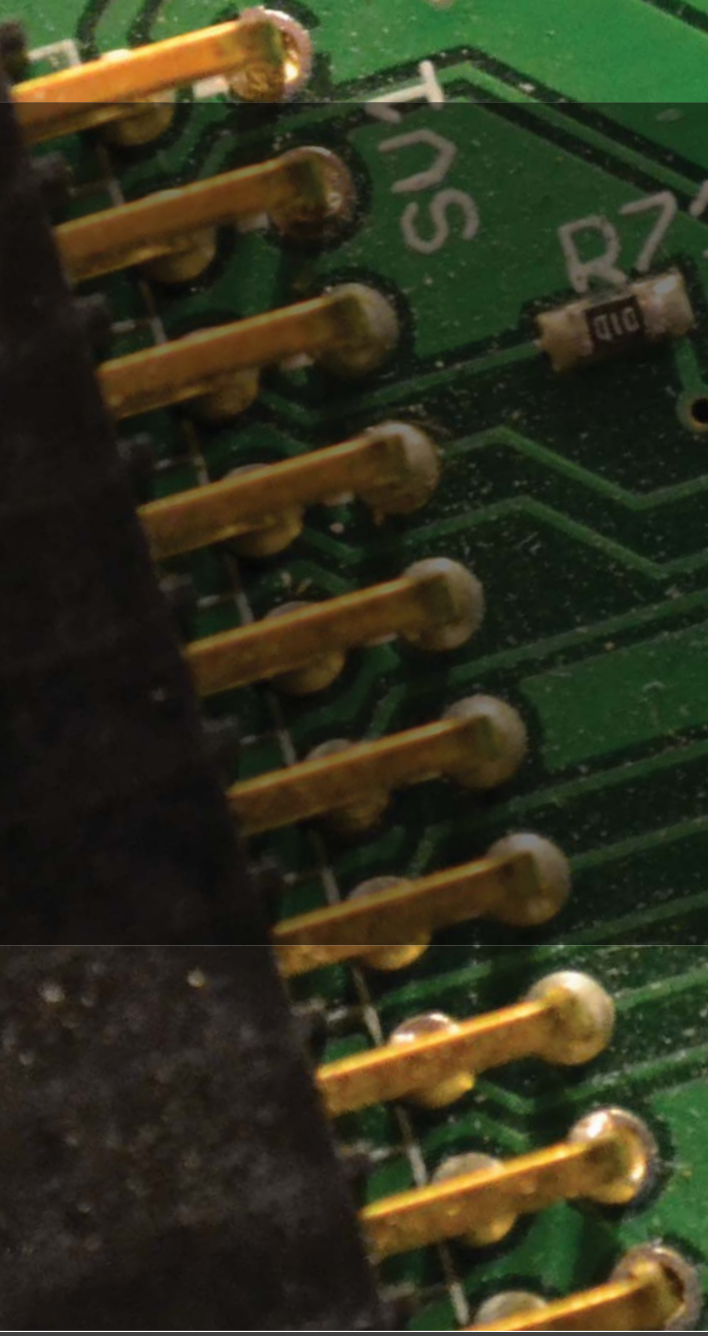
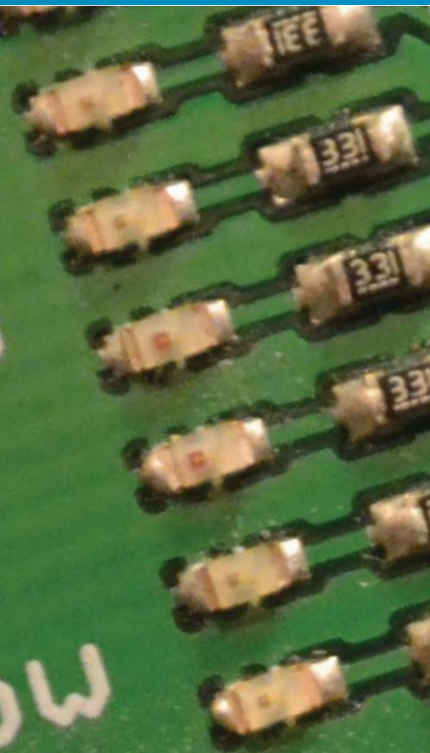
R30

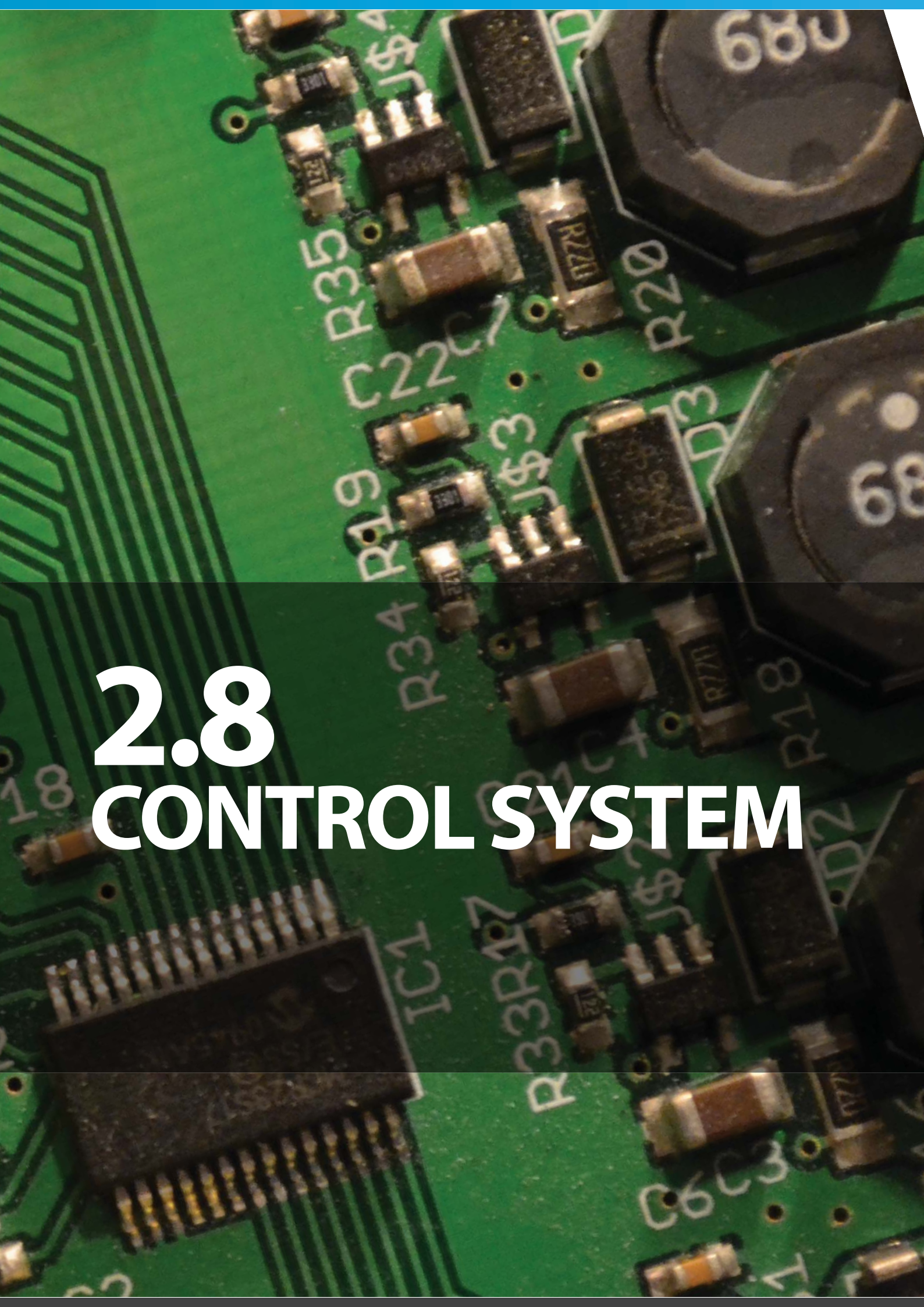
S

R71

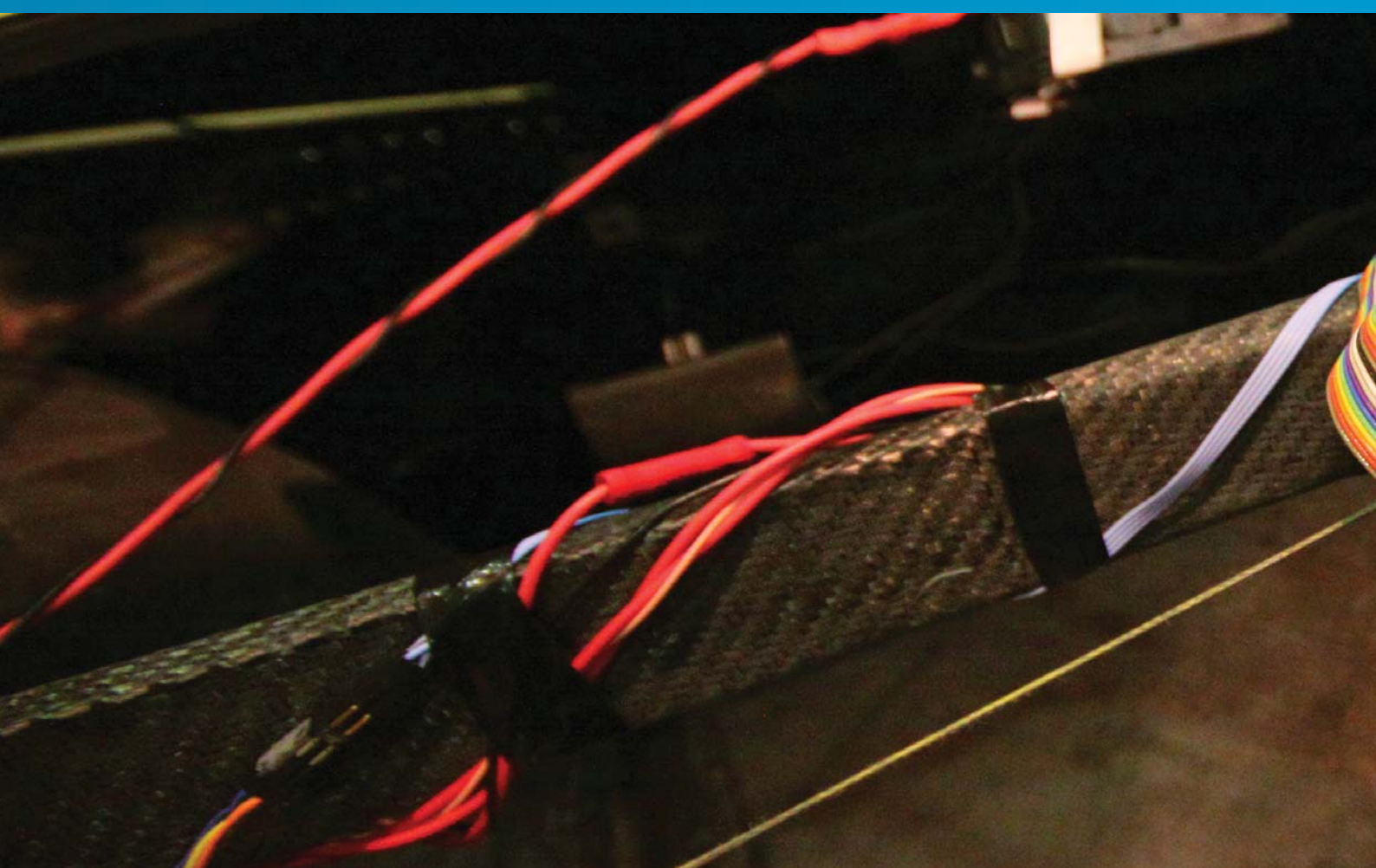
R72

R25





# 2.8 CONTROL SYSTEM



## 2.8 CONTROL SYSTEM

### 2.8.1 CAR CONTROL SYSTEM

#### 2.8.1.1 Characteristics

The car control system, CCS was designed in 2009/2010 by Gunhndal (2010). It is a modular CAN-Bus based system. Different modules can be easily added to or removed from the the system due to CAN-Bus technology.

For the DNVFF in 2010 several modules was designed to provide a broad range of functionality. Some of the modules however were either not functional or not nessesary for competing in the battery electric class.

The DNVFF2 CCS uses a total of three modules. The front module handles the brake pedal sensor input and operates the horn and front lights. The driver interface is managed by the dashboard module. This module operates all button inputs and button LEDs as well as the driver display. The engine module operates the rear lights and communicates with the engine controller via RS-232. It is the interface between the CCS and the propulsional control system.

#### 2.8.1.2 Changes to the Car Control System in 2012

Based on the old teams experience and due to the goal of a more energy efficient way of driving, several changes have been done to the 2011 CCS. Changes in the 2012 race requirments made additional changes nessesary too. All changes can be distinguished by the topics below.

##### *Windshield Wiper*

The 2012 rules required a functionable electric windshield wiper. A windshield wiper was designed by using a commercial front light wiper engine that included a gearbox. This engine operates using 12V and 3A. Since the accessory circuit uses a 24V battery an additional buck-converter circuit was nessesary in order to make the wiper engine run. Unfortunately there was no free pin on the front module to include the wiper functionality in the CCS. The buck-converter circuit was instead connected to be operated by a hardware switch totally independent of the CCS.



### *Two-Way-Communication*

Based on last years experience it was crucial to get a working two way communication with the SmartMotorController through the RS-232 interface. With this in place the effects of all planned CCS changes and optimizations could be monitored. The 2011 team put some effort into this already but wasn't able to make it work in 2011. Starting off with the results achieved in 2011 a two-way-communication was established. Reading controller variables and parameters online made a controller state observation possible. The communication rate between the engine controller and the engine module was not sufficient to use the signals for any further online optimization. Also a velocity integration in order to know the distance traveled was impossible. By observing the engine controllers internal signals at high refresh rate using DSPComm a great measurement inaccuracy was discovered. It can be stated that these measurements can not be used for any online optimization. Especially the DCLink power signal shows a big variance. Therefore all optimization had to be done offline.

A better understanding of the RS-232 communication lead to a more advanced communication from the engine module to the engine controller. For instance not just the speed reference variable was changed while driving, but also variables

setting the acceleration (speed ramp) and the starting routine were adjusted online.

### *Automated Section Controlled Drive ASCD*

The biggest change in the CCS was the idea of having a optimized driving strategy for the Rotterdam race track. This idea included an pre race track analysis to determine an optimized velocity and torque profile around the track. The track was divided into 4 different sections, each starting after a 90° turn. The optimization was done by modelling the car and the track in MATLAB and varying the speed, acceleration and coasting times for each section. Wind and track inclination were assumed to be zero (testing and racing showed that these influences must be considered for a more accurate optimization). The optimization result was hardcoded in the CCS.

The hardcoding of the optimization made CCS hardware changes necessary. For each of the four sections a dedicated button was included in the CCS. Whenever a section button was pressed a hardcoded velocity profile was run. Therefore the two-way communication was necessary. Changing the old parameters for current speed

reference, the acceleration and the time when the car should coast determine the cars behavior till the next turn. This strategy of driving adds a optimality criteria and gives the driver the possibility to focus on other aspects of driving.

Since there are other cars racing on the track at the same time, the hardcoded sections would have to be ended prematurely in certain cases. Therefore a coast button was included in the CCS. Whenever the driver senses a traffic jam situation the coast button is supposed to be pressed. Also if wind pushes the car the driver can save energy by using this button.

To give feedback of the current engine controller state, information such as the current speed and the current speed reference is shown on the drivers display at all times while driving.

As a backup solution for racing and to make testing more efficient, a cruise control was implemented in the CCS as well. The cruise control can be enabled by pressing the cruise control button on the steering wheel. Pressing this button disables the ASCD section buttons by changing their functionality. The two section control buttons on the right now increase the current speed reference. The two section control buttons on the left decrease the current speed reference. To be able to change the speed reference quickly, the upper buttons increase or decrease the speed refernece in steps of 5 km/h respectively whereas the lower buttons are changing the speed reference by steps of 1 km/h. The coast button does not change in functionality whenever the cruise control is enabled.

Using buttons for velocity changes made a gas pedal obsolete. The advantage of not having a gas pedal is a weight reduction and the fact that it simplifies a energy efficient way of driving.

## 2.8.2 PROPULSIONAL CONTROL SYSTEM

### 2.8.2.1 Characteristics

The propulsional control system defines the control system of the cars drive train. The main drive train components are the battery, the load relay, the engine controller and the electric engine.

The engine controller is sponsored by SmartMo-

tor. The software running on the controller is also provided by the same sponsor. This means that the team is not able to change the controller code or to compile new code. However there are some parameters that can be changed via the RS-232 interface. Since SmartMotor is a extraordinary cooperative sponsor, code changes have been done by them even in last minute. Compiled code can be flashed on the controller by the team. The engine controller is a cascade linear controller for speed and torque.

As discribed in the CCS description parameters and variables can be changed and read via the RS-232 interface by the CCSs engine module. This gives the possibility to change the controllers behavior in different situations.

The engine used for racing was the same engine as used in 2011. This engine has been designed by Dahl-Jacobsen (2010). The batteries were sponsored by Altitec and Gylling. For the batteries charakteristics, see K-Brief Batteries.

### 2.8.2.2 Changes to the Car Control System in 2012

Using a testbench at SmartMotor the drive trains properties were determined especially for worst case scenarios such as high load and low battery capacity. It became obvious that a under voltage limit is nessesary due to a high voltage drop for low battery capacities. The testing also resulted in a adjustment of the engines airgap to prevent controller shut down due to a high back induced voltage.

To prevent the battery or the controller to shut down due to over load a torque reference limit was set including an anti wind up after the speed controller.

In order to coast the contoller was set up with a flystart routine that can be called via the RS-232 interface.



*Smart motor controller (SMC) converts DC-input to a three phase AC-signal driving the motor.*



4





# CONCLUSION

## CAR PERFORMANCE

The team is very satisfied with the finished product. The goal of a more robust, high quality and efficient car was achieved.

The carbon fiber monocoque is very good with respect to weight, strength and aerodynamics. A new independent and fully damped suspension system worked as intended and together with the strong monocoque enabled the driver to take the turns at full speed. A lot of effort was put into the suspension geometry to eliminate misalignments and scrubbing of the wheels. Actually implementing this designed proved to be difficult. Laser equipment is needed to accurately align and adjust the suspension.

Brakes are good and reliable, but lighter brake discs can be looked into. Also the number of degrees of freedom in the pivot point should be reduced. New hubs or improved spacers to eliminate play and brake disc scrubbing.

Interior in general satisfied both driver comfort and ergonomics, and looked pleasing for displaying the car. The steering wheel has good ergonomics, functionality and strength. Due to the ASCS the driver was able to focus on positioning the car on track and taking the turns in an optimal way.

The extensive use of carbon fiber lead to challenges regarding load transfer and assembly. The super adhesive Araldite allowed us to secure parts of different materials to the carbon fiber parts. However, the use of carbon fiber has some limitations and challenges. The rims is an example of this and should be produced in another material.

The production of the windows was very difficult. Proper molds should be made out of a material that can handle high temperatures. Next years

team should contact professional manufacturers early in the project regarding both molds and production. A windshield wiper was successfully designed and implemented to satisfy the new SEM rule. The material used for the windshields was easily scratched and a different material should be used.

The change in power source from hydrogen to battery was successful. The battery packs from Gylling are very good and reliable. They deliver a very stable voltage all the way up to 17A which is important for the SMC to work properly. They will last several years if maintained properly and can be used for testing without wearing them out. The battery pack from Altitec can deliver a lot of power before shutting down (~35A), but will display a significant voltage drop when taken to the limit.

The car control system (CCS) has a lot of helpful functions for the driver, eliminating the need to focus on smooth acceleration.

Propulsion system needs to be totally re-thought. The winning teams used separate motors for coasting and acceleration. For startup it is better to use smaller motors running at higher RPMs. In 2008 and 2009 the NTNU team used a single small motor with good results. A hybrid between the current- and old solution could be worth looking into. The motors efficiency is highly influenced by the level of precision achieved during production. It is therefore highly recommended to purchase the motors from a professional supplier.

The SMC driving the motors worked satisfactory. SmartMotor finally released the source code making it easier for next years team to perform optimizations. It is worth noting that the efficiency of the SMC is only about 90% and that more efficient controllers can be acquired.



## EXPERIENCES MADE DURING THE COMPETITION

During the competition in Rotterdam the team had some organizational problems. This made it obvious that all team members should have clearly defined tasks. For test and race attempts everyone needs to know where everyone else is, who to contact, whom to not let out of sight etc. A dedicated communication system should be acquired and tested before going to the race. This would be very valuable to have, especially in case of emergency.

Maintenance routines should be made for critical parts/systems. These need to be run through before every run, whether testing or racing. A proper maintenance plan could have prevented the steering from failing on the last attempt in Rotterdam. It was lucky that the previous attempt was successful and nearly perfect. Kevlar in steering should be replaced to improve safety and shorten maintenance intervals. Another principal solution should be looked into. All lubricated parts that are exposed to the elements should be sealed or otherwise protected.

The black theme of the car and trailer caused several problems. The matt black surface made the inside of the car very hot which puts strain on the driver. When presenting the project at DNV in Høvik the car was put on display outside. The heat from the sun made the back hatch, windows and windshiled wiper loose their shape. Additionally, the increase in pressure in the front left tire caused the rim to explode.

## GENERAL

The PR and media effort did not live up to the teams expectations. The media responsible needs to be a member of the core team in order to motivate the rest of the team.

The systems engineers have developed a knowledge transfer system that will greatly aid next years team. A3 sheets for each subsystem contains information necessary for next years team members to get a complete understanding of the car.



5



# REFERENCES



# REFERENCES

- Alcoa. (2011). Fatigue Properties (confidential text on Alumec fatigue properties obtained from Alcoa).
- Beckman, B. (2008). *The Physics of Racing*. USA: Burbank.
- (n.d.). *Casting Resin RenCast*. Solutions RenShape.
- Chapman, C. B. (2002). *A Risk Engineering Approach to Project Risk Management*. International Journal of Project Management , 5-16.
- Chapman, R. J. (1998). *The Effectiveness of Working Group Risk Identification and Assessment Techniques*. International Journal of Project Management , 333-343.
- Dahl-Jacobsen, A. (2010). *Energy Efficient Motor for Shell Eco-marathon*. Trondheim, Norway: Norwegian University of Science and Technology.
- Eikeland, H. A. & Lien, M. S. (2010). *Aerodynamic Development and Construction of a Car for Participation in the Eco-marathon Competition*. Trondheim, Norway: Norwegian University of Science and Technology.
- Endresen, F. V., Garmendia, I. Y., Gudvangen, H., Heidarloo, F. A., Larsen, P. T., Qviller, A., et al. (2011). *Eco-marathon 2012 Project Report*. Trondheim, Norway: Norwegian University of Science and Technology.
- Fastener Thread Designations and Definitions Pitch, Minor, Major Diameters*. (n.d.). Retrieved February 2012, from <http://www.engineersedge.com/hardware/metric-external-thread-sizes1.htm>
- García-Fornieles, J. M., Fan, I. S., Perez, A., Wainwright, C., & Sehdev, K. (2003). *A Work Breakdown Structure that Integrates Different Views in Aircraft Modification Projects*. Concurrent Engineering , 47-54.
- Gillespie, T. (1992). *Fundamentals of Vehicle Dynamics*. USA: Society of Automotive Engineers, Inc.
- Granta Design Ltd. CES EduPack 2011. (n.d.).
- Gudem, M. (2006). *Design and evaluation of sports car suspension system*. Trondheim: Norwegian University of Science and Technology.
- Guhndal, A. (2010). *Styre- og overvåkningssystem for Shell Eco-Marathon kjøretøy*. Trondheim, Norway: Norwegian University of Science and Technology.
- Härkegård, G. (n.d.). *Dimensjonering av maskindeler*. Trondheim: Tapir Akademiske Forlag.
- Irgens, F. (1999). *Formelsamling mekanikk: statikk, fasthetslære, dynamikk, fluidmekanikk (3 ed.)*. Trondheim: Tapir.
- Herroelen, W., & Leus, R. (2005). *Project Scheduling Under Uncertainty: Survey and Research Potentials*. European Journal of Operational Research , 289-306.
- Herroelen, W., Demeulemeester, E., & Reyck, B. D. (1997). *A Classification Scheme for Project Scheduling Problems*. Leuven: K.U.Leuven - Departement Toegepaste Economische Wetenschappen.
- Huang, H., & Xu, C. (1998). *Soft Budget Constraint and the Optimal Choices of Research and Development Projects Financing*. Journal of Comparative Economics , 62-79.
- Jung, Y., & Woo, S. (2004). *Flexible Work Breakdown Structure for Integrated Cost and Schedule Control*. Journal of Construction Engineering and Management , 616-625.
- Kaplan, S., & Garrick, B. J. (1981). *On The Quantitative Definition of Risk*. Risk Analysis , 11-27.
- Kolisch, R., & Padman, R. (2001). *An Integrated Survey of Deterministic Project Scheduling*. Omega-The International Journal of Science , 249-272.
- Tonning, O. (2012). *Implementing Lean System Engineering in the DNV Fuel Fighter project*. Trondheim, Norway: Norwegian University of Science and Technology.
- PMI. (2008). *A Guide to the Project Management*

*Body of Knowledge*. Project Management Institute, Inc.

*Proceedings of the Institution of Mechanical Engineers: Vehicle Ride and Handling*. (n.d.). Qviller, A., Stockfleth, T., Bleie, S., & Hoel, M. (2011). Shell Eco-marathon, DNV Fuel Fighter 2011. Trondheim: NTNU.

Rølvåg, T. (2008). *Design and Optimization of Suspension Systems and Component*. Trondheim: Department of Machine Design and Materials Technology, Norwegian University of Science and Technology.

SAE. (2012). *Bosch Automotive Handbook*.

Shell. (n.d.). *Ahoy race track map*. Retrieved November 2011, from [http://www.shell.com/home/content/ecomarathon/europe/2012\\_rotterdam/competition\\_structure](http://www.shell.com/home/content/ecomarathon/europe/2012_rotterdam/competition_structure)

Shell. (n.d.). *Chapter I Official Rules*. Retrieved November 2011, from Chapter I Official Rules: [http://www.shell.com/home/content/ecomarathon/europe/for\\_participants/europe\\_rules/](http://www.shell.com/home/content/ecomarathon/europe/for_participants/europe_rules/)

SKF. (n.d.). *Selection of bearing size*. Retrieved February 2012, from Selection of bearing size.

Tatikonda, M. V., & Rosenthal, S. R. (2000). *Technology Novelty, Project Complexity, and Product Development Project Execution Success: A Deeper Look at Task Uncertainty in Product Innovation*. IEEE Transactions on Engineering Management, 74-87.

Vedvik, N. (2011). *Composite Materials*. Trondheim: Norwegian University of Science and Technology.

Venkataraman, R. R., & Pinto, J. K. (2008). *Cost and Value Management in Projects*. John Wiley & Sons, Inc.

Yuguero-Garmendia, I. (2012). *Verification, Validation and Testing Activities of the DNV Fuel Figheter 2*. Trondheim, Norway: Norwegian University of Science and Technology.

# LIST OF FIGURES

Figure 2.1.1	Work breakdown structure	23
Figure 2.1.2	Milestones arranged in the schedule	25
Figure 2.1.3	Planned S-curve of the project	26
Figure 2.1.4	Detailed budget	29
Figure 2.2.1	The template uses a Plan-Do-Check-Act approach, meaning the problem is solved through analysis, testing, verification and then implemented	36
Figure 2.2.2	The front page is dedicated to listing components, interface diagrams, describing major decisions and the manufacturing process. The components are categorized as 'New Product Development' (NPD) meaning designed by this year's team, 'Reused' (R) meaning an unaltered design or 'Purchased' (P) meaning bought from a manufacturer. Also, the components are rated for satisfaction stating how well the component behaved relative to its expected behaviour	37
Figure 2.2.3	Page 2 is dedicated to the 3D-models, simulations and analyzes	38
Figure 2.2.4	Page 3 is dedicated to perceived risks, a description of problems and how they were solved, and proposed future work	39
Figure 2.2.5	The sub-system "Wheel" broken down into its components	40
Figure 2.2.6	The elements that make up the wheel are positioned along the diagonal. Lines between the elements show interfaces between them (emphasized by diamonds). The Hub is the part that links the sub-system to the rest of the system	40
Figure 2.2.8	VPB for DNVFF2. Tasks are numbered on the right-hand side. The Gantt-diagram in the middle shows what day a certain task is due. Colors tell whether a task has slipped or not. The left-hand side is for information and exchanging messages	41
Figure 2.2.9	Risk cube display	42
Figure 2.2.10	Curve showing how average risk level developed through the project	42
Figure 2.2.11	Variation of program risk and effort throughout system development (Kosia-koff et al, 2011)	43
Figure 2.2.12	Template for the Timeline	43
Figure 2.2.13	Template for the Wall-Architecture. Orange means "in production", red is "critical", yellow is "pending", green is "produced" and blue is "assembled"	44
Figure 2.4.1	Map of the Ahoj. The track is highlighted in red. The numbers indicate corners and driving direction	59
Figure 3.1.1	Suspension system modeled with RB2 elements, loads and moments are applied in the wheel center and transferred into the body through the stiff suspension system.	73
Figure 3.1.2	Displacement due to loads during race conditions	74
Figure 3.1.3	Displacement due to loads during testing	74
Figure 3.1.4	Layup for the car, placement of 4 layers (top), core reinforcement (middle) and 2 layers (bottom)	75
Figure 3.1.5	Stresses in the most highly stressed carbon fiber ply	76
Figure 3.1.6	A draft angle analysis done in Catia to discover what needed to be improved before the production	78
Figure 3.1.7	3D model of molds	79
Figure 3.1.8	Overlay in a corner, two layer layup leads to four layers in the splice area	86
Figure 3.1.9	Overview of the final layup of the car	89
Figure 3.1.10	Arrangement of the windows	108
Figure 3.1.11	The holes for the lights needed to be planned before the production of the monocoque started, and therefore also before the inside of the lights were designed	113
Figure 3.1.12	Different combinations of light placement were tested in SolidWorks	115
Figure 3.1.13	The final front light and rear light concepts	116
Figure 3.1.14	Different placements of the hinges	120
Figure 3.1.15	Different door opening solutions	120
Figure 3.1.16	Idea generation of different hinge concepts	121
Figure 3.1.17	Idea generation of different door handle concepts	123
Figure 3.1.18	Principle drawing of the hinge showing the opening motion	122



Figure 3.1.19	Door handle in the open position	123
Figure 3.1.20	Idea generation of windshield wiper	124
Figure 3.1.21	Different wiper motions	124
Figure 3.1.22	Idea generation for mounting the back hatch	129
Figure 3.1.23	Idea generation for mounting the side covers	130
Figure 3.1.24	Idea generation for the towing hook	132
Figure 3.1.25	Strength analysis of the towing hook. The 2000 N load yield maximum stress of 110 MPa	132
Figure 3.2.1	Before the design of the interior could start, one needed to establish a layout of the cockpit, and in that way set an outline for the size of each component	152
Figure 3.2.2	An 3D-model with the outlines for the dashboard were given to group working with idea generation	154
Figure 3.2.3	Concept 1 had a removable top cover to provide easy access	156
Figure 3.2.4	Concept 2 consisted of a light construction attached to both the monocoque shell and the floor. It had no removeable parts	156
Figure 3.2.5	3D-model of front beam mold ready for milling. The mold is milled in two parts and then glued together later	157
Figure 3.2.6	Sketching was done to explore ideas, but most of the ideation process was done with physical models and 3D-models	166
Figure 3.2.7	Concept 1	168
Figure 3.2.8	Concept 2	169
Figure 3.2.9	Concept 3	170
Figure 3.2.10	Criteria matrix	171
Figure 3.2.11	The molds for the vacuum forming was first designed in SolidWorks and then milled out in a CNC milling machine	172
Figure 3.2.12	Seat Interfaces	177
Figure 3.2.13	Basic Ergonomics	178
Figure 3.2.14	A lot of explorative sketching was done to generate as many ideas as possible	180
Figure 3.2.15	3D-modelling was used to test different ideas and to decide on different dimensions in a fast way	181
Figure 3.2.16	Idea 1	182
Figure 3.2.17	Idea 2	183
Figure 3.2.18	Idea 3	184
Figure 3.2.19	All the different seat ideas, where idea number 2 was selected for further development	185
Figure 3.2.20	Details of the final concept , cushions added	186
Figure 3.2.21	Detailed model of the interior without mirrors	190
Figure 3.2.22	Explorative sketching was done to generate ideas	191
Figure 3.2.23	The three different concepts seen from the drivers view. Closeup of the different concepts are shown below	192
Figure 3.2.24	The main part for the mirrors designed in SolidWorks. The model was planned in a way that made it easy to mill	193
Figure 3.3.1	Typical steering knuckle concept	196
Figure 3.3.2	Double wishbone system, parts annotated	197
Figure 3.3.3	Camber angle change during spring action	198
Figure 3.3.4	Top view front view of front left suspension links	198
Figure 3.3.5	Viewed from beneath, front right suspensions	198
Figure 3.3.6	Rear view of front left suspension links	198
Figure 3.3.7	Rigid body model of front suspension, where $P_B$ and $P_C$ are the braking and cornering forces, and $C_{1,2,3,4}$ are the support forces acting through the wishbone links	199
Figure 3.3.8	Force and constraints on the knuckle	199
Figure 3.3.9	Simplified force and torque on knuckle	199
Figure 3.3.10	Steering knuckle modeled as a beam with load and reaction forces	200
Figure 3.3.11	Constraint model for top arms during braking	200
Figure 3.3.12	Constraint model for lower arms during braking	200

Figure 3.3.13	Constraint model for top arms during cornering	201
Figure 3.3.14	Constraint model for lower arms during cornering	201
Figure 3.3.15	Diagram of weight force and link geometry view from behind the car, where $P_w$ is the weight on the wheel and $C_s$ is the coilover's reaction force	202
Figure 3.3.16	Sketch setup in NX to obtain measurements for anti-dive calculations	202
Figure 3.3.17	Force diagram of dive/anti-dive contributing forces	203
Figure 3.3.18	Front and back view of the hub	204
Figure 3.3.19	View of hub assembly	204
Figure 3.3.20	FEM analysis of hub during braking	204
Figure 3.3.21	FEM analysis of hub during cornering	204
Figure 3.3.22	CAD model of axle	205
Figure 3.3.23	FEM analysis of axle during braking	205
Figure 3.3.24	Ackerman steering based on sketch in the PD-journal, wheels and angles annotated. $\alpha$ is the typical toe-angle when driving straight ahead.	206
Figure 3.3.25	View of steering radius check	207
Figure 3.3.26	Verification of ackerman steering for 20 m turning radius	207
Figure 3.3.27	Verification of 6 m turning radius requirement	208
Figure 3.3.28	Finding the smallest possible turning radius, tilted view	208
Figure 3.3.29	FEM analysis of knuckle during braking	208
Figure 3.3.30	FEM analysis of knuckle during cornering	208
Figure 3.3.31	Unidirectional carbon fiber wrapping for reinforcement of bolted connections	209
Figure 3.3.32	Mold for carbon fiber knuckles	209
Figure 3.3.33	Link consisting of rod ends and nuts	210
Figure 3.3.34	Single rod end on bottom, double rod ends on top	211
Figure 3.3.35	Solid lower wishbone	211
Figure 3.3.36	Connector and link rods	211
Figure 3.3.37	3D view of the left wishbone connector	211
Figure 3.3.38	Left suspension with connector and coilover	212
Figure 3.3.39	FEM analysis of wishbone connector during braking	212
Figure 3.3.40	Tie rod assembly	214
Figure 3.3.41	Left tie rod on suspension seen from beneath	214
Figure 3.3.42	Front left wheel well on the final body shell	214
Figure 3.3.43	The final clevis design. Purple highlights the vibration damping bushings	215
Figure 3.3.44	FEM analysis of clevis	215
Figure 3.3.45	Clevises attached to wheel well using wedges and bushings	215
Figure 3.3.46	3D CAD model of the rear suspension developed during the spring 2012	216
Figure 3.3.47	Knuckle	216
Figure 3.3.48	High vertical distance between the ground and the bottom of the rear wheel well wall	216
Figure 3.3.49	Distance between the lower rod ends and the brake disc increased on the new design	217
Figure 3.3.50	How to determine the roll center of an independent suspension	218
Figure 3.3.51	Mounting points for A-arm connector and toe link on the same horizontal line to prevent bump- and roll steer	218
Figure 3.3.52	2D-model of the suspensions front-to-back geometry in UGS NX 7.5. The most important dimensions are shown in the illustration.	219
Figure 3.3.53	FE analysis setup for the knuckle	219
Figure 3.3.54	Test result from the final analysis of the knuckle	219
Figure 3.3.55	STEP - model of the knuckle imported into NX IDEAS 5.0. The coloured lines show the milling path	220
Figure 3.3.56	3D model of the mold and the knuckle	220
Figure 3.3.57	Lower A-arm connector	222
Figure 3.3.58	Forces acting on the suspension	222
Figure 3.3.59	Forces acting on the connector	223
Figure 3.3.60	FE analysis setup for the connector	223

Figure 3.3.61	Test result from the final analysis of the knuckle	224
Figure 3.3.62	Coilover cross section overview	224
Figure 3.3.63	Determining spring travel and spring force	225
Figure 3.3.64	FE analysis of the upper spring holder	226
Figure 3.3.65	FE analysis of the lower spring holder	227
Figure 3.3.66	FE analysis of the piston	227
Figure 3.3.67	Toe link extension	227
Figure 3.3.68	Rods and rod ends	228
Figure 3.4.1	All steering components in the final assembly	235
Figure 3.4.2	Length adjustment concept	235
Figure 3.4.3	Drag link length adjustment	236
Figure 3.4.4	Old tie rod solution	236
Figure 3.4.5	Tie rod solution chosen	236
Figure 3.4.6	PU bearing, provides low friction for the drag link	237
Figure 3.4.7	3D model of the steering column, with sub parts assembled	237
Figure 3.4.8	Thread house	238
Figure 3.4.9	Steering wheel mounting socket	238
Figure 3.4.10	Pulley assembled on bracket	239
Figure 3.4.11	Pulley assembled on bracket	239
Figure 3.4.12	Strength analysis of the steering column, maximum stress of 69 MPa	239
Figure 3.5.1	Exploded view of the brake pedal	247
Figure 3.5.2	Stages of the brake pedal design, from early concept to final design	248
Figure 3.5.3	Pivot point force sketch	248
Figure 3.5.4	The maximum stress of 268 MPa was located around the pivot point hole, which yields a safety factor of 2. The analysis showed a deflection of 2.5 mm, which will be a conservative results due to the material data	249
Figure 3.5.5	Placing of master cylinders and pedal arm. From this the minimum distance between components was determined	249
Figure 3.5.6	Grooves removed from block and final piece	250
Figure 3.5.7	The maximum stress was 136 MPa, giving a safety factor of 4. This stress occurred at the pedal arm support. There were no significantly deformations in the pedal box	251
Figure 3.5.8	Displacements in the pedal box	251
Figure 3.6.1	Exploded 3D CAD model of the rims produced in 2012	256
Figure 3.6.2	FE analysis set up of the rims	256
Figure 3.6.3	FE analysis results of the rims	256
Figure 3.7.1	Exploded view of completed motor assembly	262
Figure 3.7.2	Cross section of motor	263
Figure 3.7.3	Close up of the motor hub	264
Figure 3.7.4	3D view of the new motor axle	264
Figure 3.7.5	Load cases for an axle during cornering	264
Figure 3.7.6	FEM analysis of motor axle subject to a hard bump	264
Figure 3.7.7	FEM analysis of motor axle on inner wheel of a typical, sharp curve	265
Figure 3.7.8	FEM analysis of motor axle on outer wheel of a typical, sharp curve	265
Figure 3.7.9	Outer and inner rotor with colorized magnet arrays	265
Figure 3.7.10	Close up of rim adapters, in green and blue. The yellow section is the rotor spacer	266
Figure 3.7.11	The new test adapter	266
Figure 3.7.12	Magnets in a Hallbach array, arrows showing direction of magnetization	268
Figure 3.7.13	Magnets and iron ring, arrows showing direction of magnetization	268
Figure 3.7.14	Single phase single layer wave winding	268
Figure 3.7.15	Three phase single layer wave winding	268
Figure 3.7.16	Single phase distributed winding	268
Figure 3.7.17	Three phase distributed winding	268
Figure 3.7.18	Winding connection	276

Figure 3.7.19	Efficiency as a function of torque of the old engine at 300 rpm, 35, 55 km/h as it was in 2011	278
Figure 3.7.20	Efficiency as a function of torque of the new engine at 257,5 rpm, 26 km/h with the smallest obtainable air gap	278
Figure 3.7.21	Possible winding arrangement	279

# LIST OF TABLES

Table 2.1.1	Improvement points for developing a new vehicle	20
Table 2.1.2	Weighting of different elements	26
Table 2.1.3	Detailed budget	29
Table 2.1.4	Definition of rating system	31
Table 3.1.1	Input data for calculations of lift and drag	143
Table 3.1.2	Results from wind tunnel testing	143
Table 3.3.1	Trade-off matrix for steering knuckle material selection	206
Table 3.3.2	Table of minimum pitch and minor diameters of ISO M6 and M8	210
Table 3.3.3	FE analysis set up for the knuckle. DOF 1-3 is displacement in x-, y-, and z-direction, respectively. DOF 4-6 is rotation about x-, y-, and z-axis, respectively	219
Table 3.3.4	FE analysis set up and result for the knuckle	219
Table 3.3.5	FE analysis set up for the knuckle	223
Table 3.3.6	FE analysis set up and result for the connector	224
Table 3.3.7	Changes in spring rate	225
Table 3.3.8	Properties of the SF-TF 1901 compression spring ordered from Lesjöfors (Lesjöfors, 2012)	226
Table 3.3.9	FE analysis of the upper spring holder	226
Table 3.3.10	FE analysis of the lower spring holder	227
Table 3.3.11	FE analysis of the piston	227
Table 3.6.1	FE analysis set up for the rims	256
Table 3.7.1	Requirements specification for mechanical motor parts	263



**DNV FUEL**



# APPENDIX

L FIGHTER 2

## Appendix A: Acknowledgments

I would like to thank the following people for their support, either directly or indirectly, to the progress and success of this project:

- Knut Einar Aasland  
IPM staff, NTNU  
Supervisor
- Kristina Dalberg  
Det Norske Veritas (DNV)  
Main sponsor contact person
- Bjarne Stolpnæssæter  
IPM staff, NTNU  
For all the CNC milling of moulds, suspension knuckles and a lot more, for always being open to new machining requests and short delivery times
- Per Øystein Nortug  
IPM workshop, NTNU  
For machining assistance and staying late nights, even weekends, so we could work in the workshop
- Børge Holen  
IPM workshop, NTNU  
For machining assistance
- Office Administration  
IPM staff, NTNU  
For handling all the purchasing orders and payments
- Arne Gellein  
SINTEF Materialer og Kjemi  
For free metal cutting
- Jan Erik Molde  
Elkraft, NTNU  
For machining of motor hub



## Appendix B: Estimated material data for DB420

Material type: Orthotropic

		Min	Max	Units
Youngs modulus	E1	110	140	GPa
	E2	5	8	GPa
	E3			GPa
Poissons ratio	NU12	0.25	0.30	-
	NU23	0.50	0.60	-
	NU13			-
Shear modulus	G12	3	5	GPa
	G23			GPa
	G13			GPa
Tensile stress	ST1	1500	2000	MPa
	ST2			MPa
	ST3	20	50	MPa
Compressive stress	SC1	800	1200	MPa
	SC2			MPa
	SC3	100	200	MPa
Shear stress	S12	40	80	MPa
	S23			MPa
	S13			MPa
Density		420		g/m <sup>2</sup>
Density, cured		1.5		g/cm <sup>3</sup>
Thickness		0.8		mm
Thickness, cured		0.5		mm

NB: DB420 er en strikket armering bestående av 2 distinkte lag, det er IKKE en vev. Altså gir en armering en layup [45/-45]. Tykkelse på hvert lag er jo gitt av tettheter og volumfraksjoner, så det finner du greit. Angående volumfraksjon, vil en rimelig range være 0.50-0.55 med godt vakuum. Slurv og fanteri forøvrig kan gi lavere, f.eks. 0.45.

## Appendix C: Program listing

### Program: Main

O0150 ;	Main program for milling front left wishbone
S3000 M03 F1400 G17 G90 ;	
M08 ;	Coolant on
M21 ;	Optional: Mirror X-axis, for right wishbone
M22 ;	Optional: Mirror Y-axis, for right wishbone
M23 ;	Optional: Mirror OFF
G00 X-15. Y0. ;	Move outside material block
Z-90. ;	
G01 Z-103. ;	Prepare cut depth for first cut
M98 P151 L7 ;	Cut seven times with 3mm cuts
G90 ;	Switch back to absolute coordinates just in case
G01 Z-123. ;	Prepare height for final planar cut
M98 P151 L1 ;	Last planar cut
N11 G90 ;	Labeled for graph plot
G01 X-15. ;	
G00 Z-90. ;	
X40. Y-28.8 ;	
G01 Z-106. ;	
X35. ;	
M98 P152 L21 ;	Mill north ear profile
G90 ;	
G00 Z-90. ;	
X40. Y-45.8 ;	
G01 Z-106. ;	
X35. ;	
M98 P152 L21 ;	Mill south ear profile
G90 ;	
G00 Z-90. ;	
X-15. ;	
Y-59.1 ;	
G01 Z-125. ;	
M98 P153 L8 ;	Cut out the bottom angles
G90 ;	
G01 Z-90. ;	Begin safe return to origin
M09 ;	Coolant off
M05 ;	Spindle stop
G00 Z0. ;	To origin
X0. Y0. ;	
M30 ;	Program end/all reset
%	

**Program: Rough cut**

```
O0151 ;           Program for milling around ears until Z-middle of the wishbone
                   Assumes starting in position X-15. Y0.

G17 G90 ;
G01 X0. ;
Y-41.9 ;
X30. ;
G03 X35. Y-36.9 R5. ;
G01 Y-30.9 ;
G03 X30. Y-25.9 R5. ;
G01 X0. ;
Y-58.9 ;
X30. ;
G03 X35. Y-53.9 R5. ;
G01 Y-47.9 ;
G03 X30. Y-42.9 R5. ;
G01 X0. ;
Y-63.1 ;         To south edge
X61.3 ;          To south-east vertex
Y0. ;           To north-east vertex
X5. ;           To second west edge
Y-20.9 ;        To second north edge of north ear
X40. ;          To second east edge of both ears
Y-58.1 ;        To second south edge
X56.3 ;         To second east edge
Y-5. ;          To second north edge
X10. ;          To third west edge
Y-15.9 ;        To third north edge of north ear
X45. ;
Y-53.1 ;
X50. ;
Y-10. ;
X-15. ;
Y0. ;
G91 ;
G01 Z-3. ;       Lower for next cut
G90 ;
M99 ;
%
```



## Appendix D: Program listing

### Program: Main

O0150 ;	Main program for milling front left wishbone
S3000 M03 F1400 G17 G90 ;	
M08 ;	Coolant on
M21 ;	Optional: Mirror X-axis, for right wishbone
M22 ;	Optional: Mirror Y-axis, for right wishbone
M23 ;	Optional: Mirror OFF
G00 X-15. Y0. ;	Move outside material block
Z-90. ;	
G01 Z-103. ;	Prepare cut depth for first cut
M98 P151 L7 ;	Cut seven times with 3mm cuts
G90 ;	Switch back to absolute coordinates just in case
G01 Z-123. ;	Prepare height for final planar cut
M98 P151 L1 ;	Last planar cut
N11 G90 ;	Labeled for graph plot
G01 X-15. ;	
G00 Z-90. ;	
X40. Y-28.8 ;	
G01 Z-106. ;	
X35. ;	
M98 P152 L21 ;	Mill north ear profile
G90 ;	
G00 Z-90. ;	
X40. Y-45.8 ;	
G01 Z-106. ;	
X35. ;	
M98 P152 L21 ;	Mill south ear profile
G90 ;	
G00 Z-90. ;	
X-15. ;	
Y-59.1 ;	
G01 Z-125. ;	
M98 P153 L8 ;	Cut out the bottom angles
G90 ;	
G01 Z-90. ;	Begin safe return to origin
M09 ;	Coolant off
M05 ;	Spindle stop
G00 Z0. ;	To origin
X0. Y0. ;	
M30 ;	Program end/all reset
%	

# Appendix E: Spreadsheet for simplified vehicle dynamics

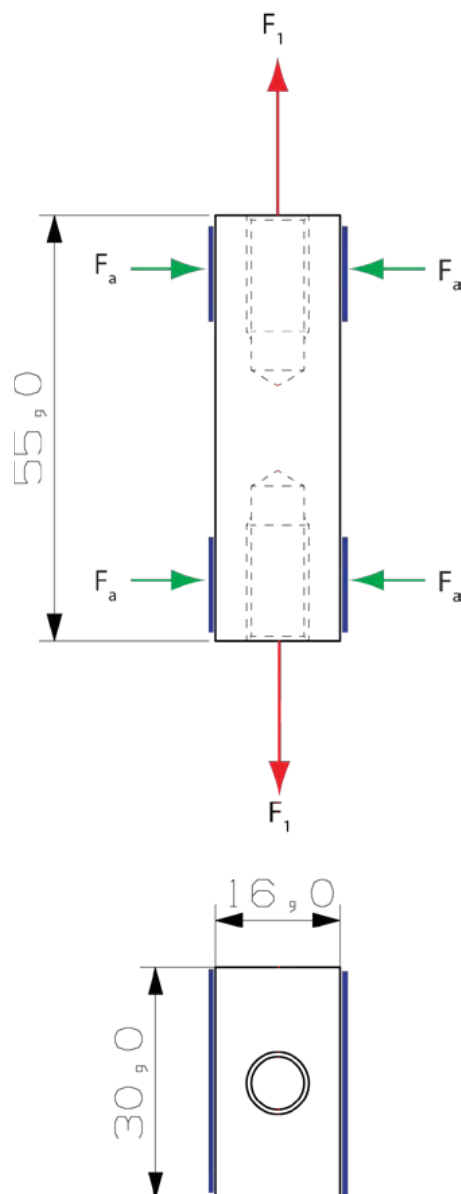
## Quasi-dynamic vehicle calculations for steering

<b>Coordinate system</b>		<b>XY-plane reaction unit vectors</b>		<b>Ackerman steering angles</b>	
X	Right/lateral	Fmt left	4.11	Turn radius *	m
Y	Forwards/heading	Fmt right	3.90	Fmt left	°
Z	Upwards	Centript fce	2.00	Fmt right	°
All turns left/counter-clockwise, thus the vectors		Fmt left (X,Y)	-0.997429	-0.071665	L - R
All turn radii calculated from differential		Fmt right (X,Y)	-0.997680	-0.068084	°
		Rear left (X,Y)	-1.000000	0.000000	L/R
		Rear right (X,Y)	-1.000000	0.000000	%
<b>User input in yellow cells :</b>					
<b>Invariants</b>		<b>Per-wheel turn radii and speeds</b>			
Wheel base	1.40 m	Fmt left radius	19.54 m	6.0	14.32
Front track width	1.03 m	Fmt right radius	20.56 m	5.0	17.34
Rear track width	0.80 m	Rear left radius	19.49 m	4.0	21.89
Car base mass	70.00 kg	Rear right radius	20.52 m	3.0	29.40
Driver weight	75.00 kg	Fmt left speed	6.78 m/s	2.0	43.31
Static mass	145.00 kg	Fmt right speed	7.14 m/s		
Center of mass X	0.00 m	Rear left speed	6.77 m/s		
Center of mass Y	-1.00 m	Rear right speed	7.12 m/s		
Center of mass Z	0.70 m				
Gravity	9.81 m/s <sup>2</sup>				
<b>Case/LCP setup</b>		<b>Center of mass turn radii and acceleration</b>			
Turn radius *	20 m	Cm turn radius	20.00 m	Adjusted for Cm to diff	
Speed	25 km/h	Diffrntial arc spd	6.94 m/s	@diff	
		Cm arc speed	6.95 m/s	@Cm	
		Angular speed	0.35 rad/s	@Cm	
		Angular speed	19.90 °/s	@Cm	
		Centriptl accelr	2.41 m/s <sup>2</sup>	@Cm	
		Centriptl force	349.67 N	@Cm	
		Centriptl fce (X,Y)	349.46	12.23	@Cm
		<b>Intermediate calculations</b>			
		P_w	1,422.45 N	Static weight force	
		M_x	-8.56 N m	Moment backwards from centripetal force	
		M_y	244.62 N m	Moment laterally from centripetal force	
		P_o_z	1,245.92 N	Outer wheels up reaction force	
		P_i_z	176.53 N	Inner wheels up reaction force	
		Stability	Stable	Unstable => tips over	
		P_o_z_clamp	1,245.92 N	Ugly clamping of outer wheels reaction force	
		P_i_z_clamp	176.53 N	Ugly clamping of inner wheels reaction force	
		<b>Approximate contact patch reaction forces</b>			
		WheelForce dir	Lateral	Up/weight	
		Fmt left	21.80	90.79 N	
		Fmt right	150.21	625.48 N	
		Rear left	24.62	102.54 N	
		Rear right	153.03	637.23 N	
		Check sum	349.67	1,456.03 N	

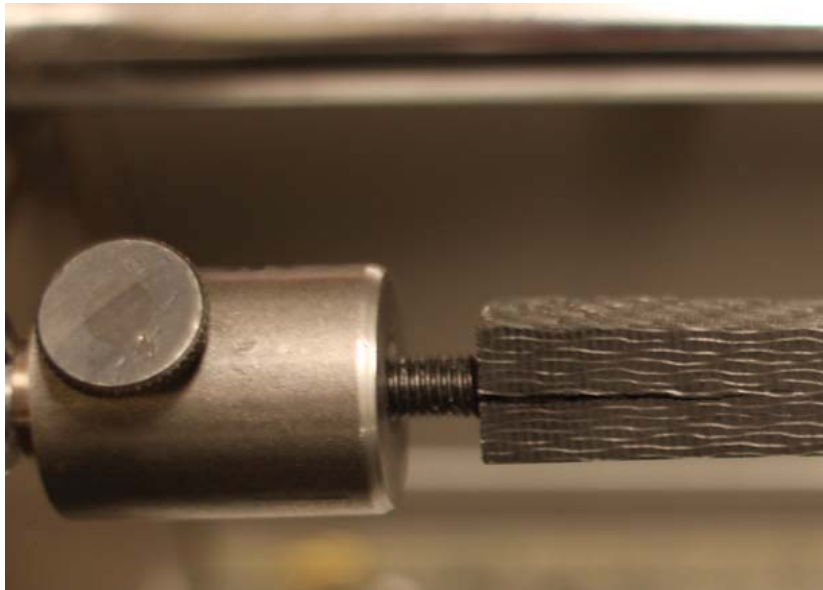
## Bolt-carbon fiber tensile tests

NTNU  
Hans Gudvangen  
Aksel Qviller  
February 2012

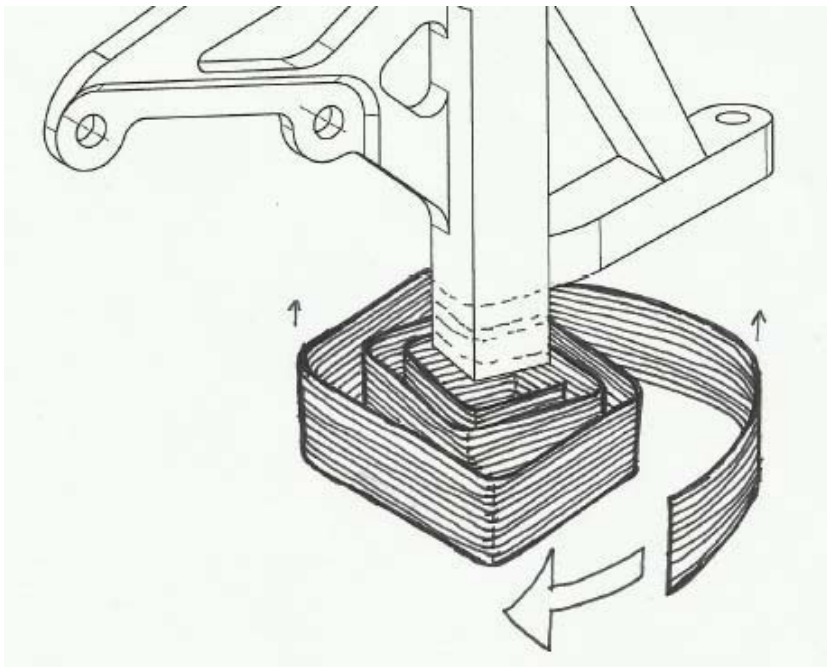
The goal of the testing was to verify the viability of using a bolted connection to massive carbon fiber for our car's suspension. The size of the bolt was dictated by the size of the end rods that we were aiming to use. The test setup therefore consisted of a short rod of massive carbon fiber with two M8 bolts inserted into either end. The end holes were carefully drilled to  $\text{Ø}6.8$  mm and thread-tapped to M8. Two bolts were inserted through connectors and screwed into the CF test piece, then pulled until failure in a tensile testing machine.



The CF rods were sawed off from a larger piece of massive CF. The first tests quickly revealed that the CF would delaminate around one of the bolt holes.



We proposed to reinforce the ends with layers of CF UD wrapped around. For these tests, this would be unpractical, so we used two clamps from aluminum and M4 bolts. These were tightened to simulate the additional stiffness provided by wrapping UD layers around the ends of the CF rod.



Additionally, we tried to glue the bolts into the holes using Araldite 2031, both with and without threads in the hole of the CF piece.



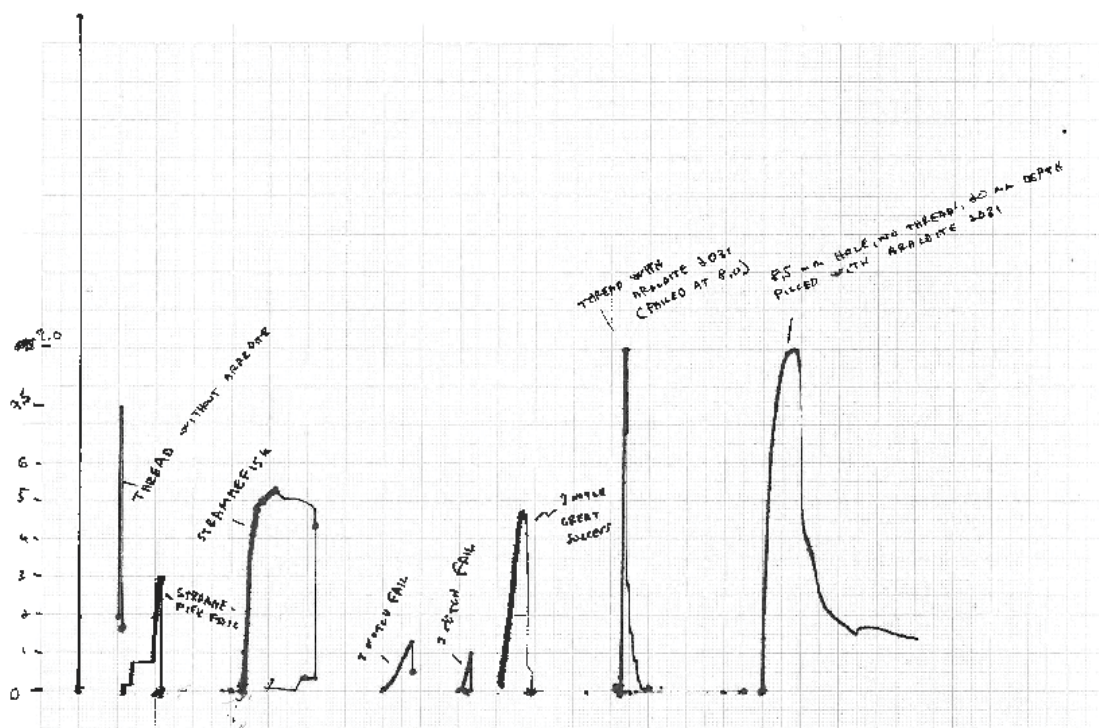
The actual test setup is illustrated below:



The results from the different tests, although few, were consistent and is summarized as follows:

Thread dimension	M8x1,25
Hole depth	20 mm
Thread depth	15 mm

	Result ( $F_{1\max}$ )
Test 1 – threads without glue	7,5 [kN]
Test 2 – threads with Araldite 2031	9,0 [kN]
Test 3 – 8,5 mm hole 20 mm deep with Araldite 2031	9,0 [kN]



BLUE BATTERY



- Specifications:
- sponsor: Alritec
  - battery charger included
  - nom voltage 48V
  - nom discharge current 24A
  - capacity 5800mAh

Problems :

- for power drawing >300W depending on discharge capacity very high voltage drop
- voltage drop often triggers the BMSs under voltage protection and shuts down battery
- battery is likely to get warm which triggered BMSs temperature protection one time while testing

Conclusion:

- battery is not suitable for race conditions in combination with the 2012 drive drain

Charger:



WHITE BATTERY



Specifications:

- sponsor: Gylling
- battery charger NOT included
- nom voltage 46,2V
- max discharge current 19A
- capacity 4400mAh

Battery is charged by a power source (rating: 60V/10A) from the Electrical department.

Problems:

- limited current discharge ability
- BMS over current protection triggers latest at 19A
- SmartMotor engine controllers fly start routine at high torque (>12Nm) not possible
- Limited torque for drive train due to limited current

Conclusion:

- battery is of limited suitability for the 2012 drive drain

## Appendix G: Assembly test example

### ASSEMBLY TEST:

Subsystem: **S.8 Brake circuit** Responsible: H.J.S Test Date: 19.04.2012 Place: Dragvoll Sport center

Test no.	Test ID.	Procedure	Requirement for passing the test	Personnel	Material/ Tools	Performance (measures)	Comments	Status Pass/No pass	Correcting actions
1	Effectiveness of the braking circuit	Place the car on a 20% slope.	The vehicle must remain stationary.	Driver and team member pushing the car		The car must remain stationary	The car remained stationary and then it was also pushed while the braking.	Pass	
2	Braking capabilities	Move the vehicle and test the brakes	Enough brake force	Driver and team member pushing the car				Pass	
3	Leaks	Press hard on brake pedal	No visible leaks	Driver and team member to check if there are some leaks	Entire Brake system	No visible leaks have to appear		Pass	
4	Brake pedal dimensions	Measure the dimensions	Minimum surface area of brake pedal: 25 cm <sup>2</sup> .	One team member to measure it			The Brake pedal is approximately 49 cm <sup>2</sup>	Pass	
5	Braking effectiveness	Combinations of weak, gradual, hard and instant braking with low and higher speed, as well as during turning at different radius.	The brakes must be strong enough and have to stop the car as soon as the driver steps on the pedal	Driver and another team member to push the car and to measure the distance		The brake systems must be reliable and able to perform		Pass	

#### Braking:

Initial braking should be cautious to listen to how the brake pads attack the discs, and the vibrations that are transferred to the chassis and amplified. We should try combinations of weak, gradual, hard and instant braking with low and higher speed, as well as during turning at different radius. We will also need to check whether the rear wheels begin to skid (if allowed by the gym center) - if they do, too much force is routed to the rear brakes.